RISK BASED NETWORK PLANNING: PROBABILISTIC ASSET INTERVENTION ANALYSIS USING MONTE CARLO SIMULATION

A thesis submitted to The University of Manchester for the degree of

Doctor of Philosophy

in the Faculty of Science and Engineering

2022

YUE WANG

School of Engineering

Department of Electrical & Electronic Engineering

The University of Manchester

CONTENTS

Word Count: 39397

LIST OF TABLES

LIST OF FIGURES

ABSTRACT

Modern power networks are characterised by, among others, the following two features: a) Large amounts of low carbon technologies (LCTs) have been connected to both transmission and distribution networks; and b) In mature systems, power components are quite old and their ageing needs to be considered. LCTs have introduced new uncertainties and consequently operational issues in transmission networks. One important aspect, which needs to be addressed both in planning and operation, is the correlation between uncertain phenomena, such as wind speed, load fluctuations, etc. On the other hand, ageing of power system components can significantly affect network reliability performance, which, in turn, can have a negative impact on the asset "health".

In this research, sequential Monte Carlo simulation is developed to analyse operation and reliability of transmission networks. The above-mentioned phenomena, correlation between stochastic processes and asset ageing, are modelled and integrated into the sequential Monte Carlo simulation procedure. The correlation is modelled using Nataf transformation in conjunction with Cholesky decomposition and the technique is applied to both wind power and load since correlation between them has a significant impact on transmission networks. Asset ageing condition is also integrated into the SMC algorithm.

The probabilistic expansion planning methodology under development shall model both component reinforcement and replacement. In the UK, transmission and distribution companies use methodologies for asset replacement based on asset Health Indices (HIs) which are used to describe asset conditions. In this research, two Monte Carlo procedures are developed to model the reliability of individual component. The first is deterministic approach, which is developed from the UK guide for distribution companies "DNO Common Network Asset Indices Methodology". The second is a proposed probabilistic approach, which makes use of proportional hazards models and Kijima II virtual age model. The outputs for these two approaches are system-wide and nodal reliability indices, as well as asset interventions and asset profiles. The proposed probabilistic HI methodology is tested on IEEE RTS-96, and then compared to the deterministic HI method. Advantages of the transition to any HI approach are finally pointed out.

DECLARATION

No portion of the work referred to in this thesis has been submitted in support of an application for another degree of qualification of this or any other university, or other institution of learning.

COPYRIGHT STATEMENT

ACKNOWLEDGEMENTS

First and foremost, I would like to express sincere thanks and respect to my supervisor, Dr. Victor Levi, for his professional guidance, constructive advice, continuous support, kind encouragement and understanding during my PhD. He has been a role model and inspires me to follow in his footsteps as a researcher. It has always been a great honour for me to do research with him.

I would like to extend my great appreciation to National Grid for their financial support for part of my PhD research and Dr. Qiang Liu for his insightful and helpful advice during my transfer viva.

I would also like to heartily acknowledge all my colleagues working in Ferranti Building, Yue Feng and Jaime Trivino, for their generous help with my research. And I am deeply grateful to my dear friends, Ziye Guo, Qinghua Han, Wenyuan Li, Dr. Chengxing Lian, Dr. Zongwen Yan, Dr. Xiaohan Li, Yiyuan Sun, Dr. Xu Zhang and his wife Rongrong Wang, Hang Xu and his wife Shuyang Shen, for their invaluable support and warm encouragement.

Last but not least, I wish to express my deepest thanks to my parents, Xiuxiang Song and Xijun Wang, for bringing me to this wonderful world, teaching me to speak, raising me up and now giving me this opportunity to pursue a PhD. Thanks for everything I could imagine.

CHAPTER 1 INTRODUCTION

1.1 Background

1.1.1 Probability Analysis

There are rapid changes in the way of electricity generation and consumption, leading to a transition of the current power system to a new low-carbon power system which is guided by continuous innovation, efficiency and policy enhancement. With the integration of low carbon technologies, uncertainties and risks are introduced to the power system, which brings loads of challenges in the decision making of the power system operation and investment [1].

In general, the uncertainties can be divided into two types: uncertainties from technical level and uncertainties from economic level [2]. The technical level involves both topological and operational perspectives. The topology group represents failures or interruptions of any component in the power network, such as generator, transformer, transmission line, etc.; the operation group represents the change of load demand, load growth, new load (such as electric vehicle and heat pump), the output from renewable sources (such as wind, solar, etc.) and fluctuations (voltage and frequency). The economic level involves the price variations of electricity market.

In this research, the focus is put on the technical level in transmission network. The analysis of these uncertainties allows flexibility in power system investments and provides a guide to an optimal reinforcement/replacement planning of assets. Therefore, an analysing tool with the feasibility to incorporate uncertainties into the power system operation and planning is required. The probability analysis is done by using a probability density function (PDF) identified for the input variables. Two approaches are mainly used for probability analysis: analytical approach and simulation approach [3]. In brief, analytical approach can reflect the relationship between input data and results. But due to its simplified assumptions, this approach is limited when chorological features of the system are focused. It is usually applied to calculate the approximated average values of the system performance. The simulation approach can incorporate complex systems and reflect the frequency and duration characteristics as it is based on random sampling. It is usually used to calculate detailed values with the related probability distribution. The details for probability analysis approaches are discussed in Chapter 2.2.2.

1.1.2 Low Carbon Technologies

Low carbon technologies (LCTs) are utilized to generate electricity with a low level of greenhouse gas emissions. Typical LCTs are hydroelectric power, nuclear power, wind power, solar power, geothermal power, tidal power and carbon capture and storage [4].

The immoderate carbon emission has been recognized as a paramount reason for climate change. Furthermore, it poses a threat to natural carbon cycle and human society [5]. The energy industry is acknowledged as the primary source of carbon emissions. In 2019, it emitted more than 41.7% of overall carbon emissions, wherein nearly 39.4% came from the combustion of fossil fuels in thermal power plants [6]. In 2020, the emission reduced because of the applied restrictions during the pandemic. The impact, however, was still modest [7].

Hence, to deal with this problem, the reduction of carbon emissions becomes inevitable. Many governments have taken endeavours to target this issue in the past decade. For example, the EU has committed that 20% of its energy needs to be provided from renewables by 2020 [8]. Following the EU directives, the UK has set a legally binding target of 15% energy from renewable energy by 2020 [9]. In 2021, the UK announced a new legal target to cut emissions by 78% by 2035 compared to 1990 levels [10]. Later in 2021, the 26th meeting of the Conference Parties (COP26) was held in Glasgow, UK. Several goals were set targeting climate change and several approaches were urged to deliver on the goals such as speeding up of the phase-out of coal, acceleration of shift to electric vehicles and encouragement of renewable energy investment [11].

As a result, power network transformation has become an inevitable trend. In the meantime, this transformation brings problems. On the supply side, the retirement of traditional coal-fired power plants (CFPPs) is an essential factor as most carbon emissions in the power industry are from thermal generators. However, the replacement of CFPPs with renewable generations usually takes years as the whole process needs to consider various aspects such as selection of site location, resource assessment, and installation. Besides, the integration of renewables poses uncertainties due to the intermittent and “uncontrollable” mode of operation. Moreover, with the incessantly growing demand in the future, the transmission network, generation capacity, and energy storage are required to be expanded [12]. On the demand side, domestic customers are encouraged to adopt low carbon technologies (LCTs). These are related to distributed generation such as photovoltaic systems (PV), transport electrification such as electric vehicles (EV) and electro-thermal technologies such as heat pumps (HP) that bring uncertainties [13]. Several studies have been carried out to tackle the problems of this transformation [12]-[15].

From the perspective of network planning, the changes introduced by LCTs contain the intermittent output of renewables, the varying output from other alternative energy sources and consequently the increasing difficulty for maintaining the instant generation-demand balance (i.e. system frequency). These features need to be taken into account in network planning. Therefore, in both operational and planning time scales, uncertainties related to the integrated renewables need to be appropriately treated. Specifically, these uncertainties are [16]:

- In operational time scales, the forecast of renewable generation contains an inevitable forecast error which needs to be integrated with other uncertainties;
- In planning time scales, network planning needs to design the connection of renewable sources to the current network and consider the uncertainties related to the location (which is related to the values of wind speed, solar radiation, etc.) and capacity (i.e. the proper design of volume which is cost-related) of the renewables.

1.1.3 Ageing Assets

Many electric utilities in Europe, the United States and other countries around the world are having difficulties satisfying the customer service quality. A main reason is that large portions of their power networks consist of ageing assets. Several factors affecting ageing are discussed in [17]:

- Ageing equipment
  Ageing equipment (specifically in [17], the equipment was installed prior to the 1970s) has an increasing failure rate and customer interruption rate, which may have an impact on the system security and national economy. Ageing assets also

cause higher costs for maintenance and lead to further refurbishment and replacement.

- Outdated system layout

  Old areas need additional supply capacity via supplementary substations. However, these regions are forced to use the existing and inadequate assets due to the problems related to obtaining permissions for new right-of-ways.

- Obsolete planning

  Conventional power transmission planning and engineering tools cannot effectively address current problems such as ageing equipment, outdated system layouts, and new types of generations and demands.

- Old cultural value

  Using planning and operational concepts and procedures to inform the vertically integrated power industries can be inadequate in the deregulated power industry.

Challenges posed by ageing assets and their rising failure rates are one of the most contentious topics in modern power systems [18]. UK regulator, Ofgem, has pointed out that the ageing assets are not just in UK gas and electricity networks, but also other sectors such as power generation, water, rail, etc.; Europe faces similar issues [19]. To address these challenges, asset risk management technique has been widely employed, which contains three aspects [20]:

- Gathering essential information such as asset conditions, failure mechanisms and failure effects;
- Alignment of business and asset investment policies and strategies;
- Development of a systematic and documented process for asset management.

In literature, due to different dominant failure mechanisms, different approaches have been developed in terms of asset types. For example, in high voltage transformer, oil impregnated paper insulation is subjected to more failures [21]; in cable, cable joints are more likely to fail [22]; whilst for overhead line, failures are closely related to environment [23].

1.1.4 Regulatory Aspects

Regulations at different levels provide guidance and reference covering corresponding responsibilities.

Regulatory Requirements for LCTs

With the threat posed by climate change, there has been a transition in power networks from coal-based generation to renewable generation. Regulators are supposed to contain all the changes introduced by power network transition. In the US, some essential regulations were passed to force the energy industry to focus on electricity generation sources other than coal. In China, the commitment to green energy has been made based on Paris Agreement. In this country, 104 coal-based power plants have been suspended. In the EU, the recently launched European Green Deal is a guideline for fulfilling climate neutrality in members by 2050. In the UK, Brexit is expected to be a significant factor impacting the energy market; some rules and regulations introduced by the EU would be revoked, such as [8]. The UK has introduced its own plan to decarbonise power system by 2035 which focuses on the establishment of a secure and home-grown electricity sector. The scheme supports the UK in proceeding with the power transition [26].

Regulatory Requirements for GB Power Network

Currently, the general energy system in the UK is confronting challenges from ageing assets and the changing energy structure which incorporates a rising proportion of renewable generation. The regulators need to make adjustments to the changes while preserving security of supply and protect interests of consumers, which may trigger substantial investments for expansion, reinforcement and replacement in transmission networks. Ofgem has introduced the Integrated Transmission Planning and Regulation (ITPR) project to evaluate if the current regulatory regimes are sufficient for the planning and development of the future transmission system in an efficient and coordinated manner [27][28].

Beside ITPR, Ofgem also updated their regulations towards GB energy network companies to enable them to provide the networks with a sustainable, low carbon energy sector. It is known as the RIIO model (Revenue = Incentives + Innovation + Outputs), which encourages network owners to provide long-term value-for-money energy services with sufficient security, reliability and sustainability to consumers. RIIO is used by Ofgem to develop price controls for GB gas and electricity companies, in both distribution and transmission industries. These price controls include RIIO-ED1 (which is for electricity distribution network; runs from 2015 to 2023 and follows by RIIO-ED2), RIIO-T1 (which is for transmission network; runs from 2013 to 2021 and follows by RIIO-T2) and RIIO-GD1 (which is for gas distribution network; runs from 2013 to 2021 and follows by RIIO-GD2) [29].

Ofgem requires the annual reports from the network owners on their performance against the price control. For example, National Grid, published their yearly results against the categories: safety, reliability, environmental impact, customer and stakeholder satisfaction and quick and efficient connect to customers, etc. [30]

1.2 Research Aims and Objectives

The ultimate aim of this research is to develop a probabilistic aggregated methodology for asset intervention planning that encompasses both reinforcement and replacement aspects. The following objectives are assigned to support the aim. All developed models are tested on the IEEE RTS-96 test system. Models and simulations are carried out using the codes developed in MATLAB/MATPOWER.

1. Development of simulation methodology where temporal models describe asset health:
    - Modelling of load on an hourly basis;
    - Modelling of component operating state in normal operating stage via exponential distribution and ageing stage via modified Weibull distribution within developed sequential Monte Carlo simulation;
    - Modelling of renewable generations (wind power generation);
    - Modelling of spatial correlation between wind speeds and between nodal loads using Cholesky decomposition technique with the aid of Nataf transformation;
    - Assessment of network reliability via the calculated reliability indices using optimal power flow model.
2. Development of simulation methodology where asset health is modelled with deterministic asset health approach:
    - Specification of asset categories;

- Development of the calculation process of deterministic asset health approach based on DNO documents (the use of distribution asset health approach on the developed transmission network model);
- Incorporation of the deterministic health indices into the asset reliability models that are used within the developed sequential Monte Carlo simulation;
- Assessment of network reliability via optimal power flow model.

3. Development of simulation methodology where asset health is modelled with the proposed probabilistic asset health approach:
   - Specification of asset Health Index categories;
   - Assumptions on appropriate hazard functions for different Health Index categories;
   - Modelling of the “forward” transitions (deterioration) between asset Health Indices using a “queueing type” transition model;
   - Specification of repair types;
   - Modelling of “backward” transitions (repair process) using Kijima II virtual age model;
   - Incorporation of the probabilistic asset health approach into the asset reliability models that are used within the developed sequential Monte Carlo simulation;
   - Assessment of network reliability via optimal power flow model.
4. Comparison of the developed models

1.3 Research Contributions

The contributions of the entire research are summarized as follows:

- All real-life development planning stages are integrated within a single integrated planning methodology that consists of four stages: reinforcement, quality-of-supply investment optimization, optimal asset intervention planning and probabilistic simulation methodology for decision verification.
- The thesis presents in-detail development of the last stage, probabilistic simulation methodology for decision verification.
- The first version of the probabilistic simulation methodology is based on the *temporal* “asset health” models. The simulation methodology models nodal loads on an hourly basis, component operating states, uncertain renewable

generations, spatial correlation and optimal power flow model, which are all built into the developed sequential Monte Carlo simulation. Asset in-service time is sampled from exponential distribution for assets in normal operating stage, and modified Weibull distribution for ageing assets; out-of-service time is sampled from exponential distribution. The impacts of ageing assets as well as correlation between wind speeds and nodal load are studied.

- The second version of the probabilistic simulation methodology is based on the *deterministic* asset health models; this approach is developed to address the impact of several (exogenous) influence factors on different asset types. Within the sequential Monte Carlo simulation, asset in-service time is sampled from hazard functions based on deterministic functions of asset scores for different asset types (cable, transformer and overhead line); out-of-service times are sampled from exponential distributions. The impacts of asset initial age, location and duty factor, and health score factor are also studied.
- The most important contribution is the third version of the probabilistic simulation methodology that is based on the *probabilistic* asset health modelling. Probabilistic asset health approach is proposed to consider uncertainties in determining the asset health scores in real-life. In the developed methodology, asset degradation towards worse asset Health Indices (asset HIs) is modelled using a "queueing type" transition model, whilst asset improvement towards better HIs is modelled using a set of rules and processes. In this approach, asset in-service time is sampled using a proportional hazard model (PHM) in combination with the Kijima II model; out-of-service time is determined by random sampling from the uniform distribution. The impacts of asset initial age, exogenous factors and reduced set of repairs are also studied.

1.4 Papers from the Dissertation

The following paper has been submitted and is under review:

1. Y. Wang, V. Levi, D. Cetenovic; "Probabilistic Health Index Based Methodology for Asset Intervention Planning", *IEEE Trans. On Power Systems,* 2022.

The following paper is to be submitted:

1. Y. Wang, V. Levi, M. Osborne; “Bringing Asset Interventions and Reinforcement Together: Probabilistic Asset Intervention Planning”, *IET*, 2022.

1.5 Thesis Outline

This thesis is organised into seven chapters:

Chapter 1: Introduction

This chapter gives an overall research background involving probability analysis, low carbon technologies, ageing assets and regulatory aspects. Aims and objectives, as well as main contributions of the research are also summarized.

Chapter 2: Literature Review

This chapter introduces power system planning and related concepts. Reliability evaluation techniques and quantitative expressions are also reviewed. The development and presentation of the IEEE reliability test network are given in this chapter.

Chapter 3: Aggregated Network Planning

This chapter provides an overview of the higher level aggregated network planning which consists of reinforcement and quality-of-supply investment optimization, optimal asset intervention planning and probabilistic simulation methodology for decision verification.

Chapter 4: Modelling of Blocks in Reliability Analysis

This chapter presents the modelling techniques involved in network reliability assessment. These include modelling of hourly load, component operating state, renewable generation and spatial correlation, as well as optimal power flow model.

Chapter 5: Asset Health Condition

This chapter introduces the concept of asset health condition and presents the methodologies of deterministic approach and probabilistic approach.

Chapter 6: Probabilistic Asset Intervention Planning – Results

This chapter presents the reliability results obtained by the three developed models. Impacts of ageing assets, spatial correlation and generation reliability are discussed within temporal model. Impacts of asset initial age and some influence factors in deterministic function, as well as generation reliability are studied with deterministic approach. In probabilistic approach, impacts of asset initial age and some influence factors are analysed; asset repairs and trajectories are also given.

Chapter 7: Conclusions and Future Works

This chapter summarizes the main findings and conclusions of the research. Potential opportunities and further works are also identified.

CHAPTER 2 LITERATURE REVIEW

This chapter provides a general review of power system planning and basic concepts of power system reliability. Essential aspects, for example, uncertainties from new generations and loads, investments and system reliability, are focused on within power system development planning. Reliability is one of the most significant criteria that must be considered at every stage of power system planning, design and operation. An insightful and comprehensive outline of the power system reliability, which includes the evaluation techniques and quantitative expressions, is presented. Furthermore, in order to provide a basis for comparing the results calculated from different methodologies, IEEE has developed a reference or “test” system, which is called “IEEE Reliability Test System”.

2.1 Power System Planning

2.1.1 Overview of Power System Planning

Power system planning is a prediction of the system performance in a specific period of time, with the premise of certain assumptions and determinations applied for future loads, generation capacity and the scale of transmission equipment investment such as reinforcement [31].

Planning for power system involves operational and development planning [32]. IET published a technical report of the "Electric Power Network Joint Vision" group, in which the extensive regulatory and commercial environment of investment planning for UK power system networks are presented [33]. It emphasised some key challenges of future network planning, such as:

- For generation network planning, renewable generation such as wind and solar generation, by its nature, is intermittent. These generators are uncontrollable and unscheduled, therefore unable to support the balance between demand and supply.
- For transmission network planning, the change of net demand at supply side is a result of the change of system demand and the growth and DG. Transmission planners do not expect the demand to grow extensively due to measurement

efficiency and cost efficiency, but do expect the growth of DG to ensure the net demand can be met. The growth of DG can cause the substantial change of power flows in the network, which needs to be accommodated.

- As more uncertainties are encountered and new planning options are considered, network planning is facing multiple analytical challenges. To manage network planning effectively, a system-wide approach is required, which should incorporate transmission and distribution for planning and operation purposes.

Due to multiple objectives, numerous variables and the dynamic nature of the network, complexity planning is introduced. The development of new technologies provides more opportunities to improve network operation. At the same time, however, it complicates the planning process. Fig. 2-1 indicates the objectives of network planning [34]. In general, three factors need to be optimized:

- Expenditure

  The calculation of the investment costs is the sum of the (annual) costs of all reinforcements, replacements and other asset interventions during the planning period. Operation and maintenance (O&M) costs can be included.
- Reliability

  In general, reliability is looked at the system basis and at the nodal, or customer level. Depending on the planning task and information available, different reliability indices are used to describe the network reliability (for example, transmission and distribution networks). Reliability indices can be used as an investment planning criterion (e.g. generation development planning in vertically integrated systems).
- Power Losses

  Power losses are usually included in the case of vertically integrated systems. The cost of power losses needs to be calculated throughout the entire planning period.

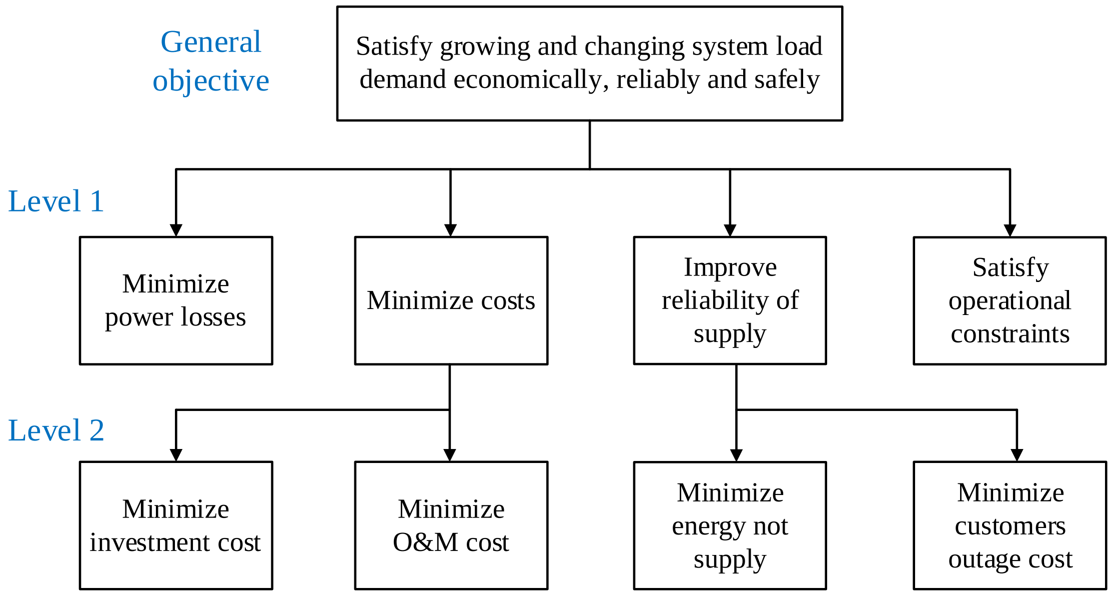

Figure 2-1: Objectives of network planning [34]

During the entire planning period, a certain number of security and configuration constraints must be satisfied. The constraints are generally presented in equality or inequality form and usually include [35]:

- Generation constraints

  The generation constraints include the lower and upper limits for generator active and reactive power.
- Transmission constraints

  The transmission constraints represent all system operational constraints, including loading constraints, voltage constraints and power flow constraints.
- Contingency (or, security) constraints

  The contingency constraints are in regards to all operational aspects when a disturbance occurs on any component in the system, and also related to the associated operating state of the failed component.
- Operational policy based constraints

  It represents the limits of human-operation based system control. For example, it is unrealistic for a system operator to change numerous controls during a given period. The constraints help avoid the non-practical results.

The main responsibilities of network planning are to inspect the load, voltage regulation, power quality, operating facilities, power supply security, system reliability, environmental impact and overall efficiency (losses included). This requires a considerable planning effort which is able to provide asset replacement, network reinforcement, improvement of supply quality and system flexibility and efficiency, in order to avoid an unacceptable deterioration in system security or performance. Therefore, it is crucial to build a network planning scheme from both a long-term and short-term perspective, while considering the overall development of the network. The following aspects should be considered during the design of planning scheme:

- Systematic and accurate load forecast;
- Asset condition information and network performance data;
- Prospective new connections, including DG developments, such as solar panels, wind farms and energy storage schemes;
- Any cost-effective opportunities to improve long-term efficiency (e.g. reduce demand and electrical losses) or network performance (e.g. active network management, enhanced protection, etc.).

The network planning aims to minimise the total cost of the network in order to make the network service most effective. The total cost of the power system network contains three parts [36][37]:

- The cost of network infrastructure;
- The cost of operating the system;
- The impact of the unreliable supply on consumers.

Planners need to make appropriate investments for the management of these three parts, and must deliver a network with adequate security. This planning process is guided by planning standards. Fig. 2-2 shows the context of network planning associated with the timescales of system operational processes, rules and standards, and disturbances and uncertainties. In the timescales of investment planning, the background conditions for applying security standards are more uncertain than in the operational planning (i.e. all the uncertainties given in the top of Fig. 2-2 have an impact on system planning). Therefore, planning standards need to specify the operational conditions, quality of supply, and a set of security events, and align with the security standards utilized in timescale of operation. Specific planning standards are introduced in Chapter 2.1.2.

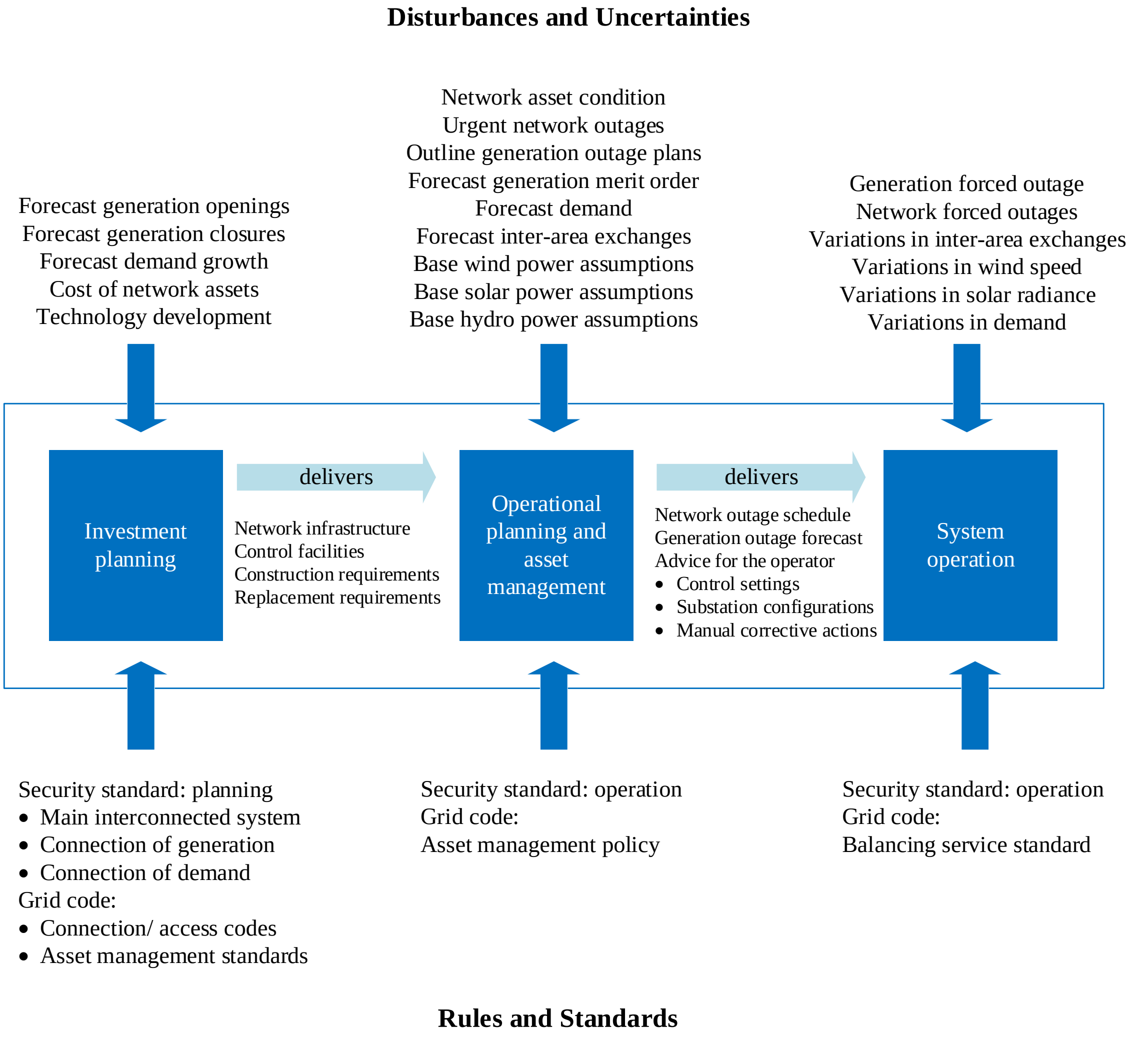

Figure 2-2: The context of network planning [37]

In current literature, a number of studies has been carried out in the area of network planning. Reference [38] studied generation and transmission planning. It pointed out that generation expansion planning involves the decision of size, location and time for construction/installation and meanwhile, the minimization of total cost over the planning period; the transmission expansion planning includes the establishment of new transmission lines and/or the expansion of current transmission lines. Reference [39] proposed a new methodology for transmission expansion planning with N-1 contingency, aiming to minimize investment cost. It also considered the integration of wind power. References [40] and [41] studied distribution network planning with integration of wind power and DG plants, respectively. And reference [42] studied distribution network planning by dividing the distribution network into three levels: power supply functional area, mesh and unit.

2.1.2 Planning Categories

Fundamental planning categories are planning of reinforcements (so-called load-related planning) and planning of asset interventions (including replacement, repair and maintenance).

2.1.2.1 Reinforcement

One of the critical issues for power transmission and distribution utilities is to develop an optimal reinforcement strategy to support and maintain reliable and economical service to customers. Planning of reinforcement is always based on loading of power components and associated network constraints, and should suggest, exhaustively, each compulsory modification in the network. For example, system capacity should have the ability to satisfy the needs from the consumer side when load reaches a certain level. In this case, possible reinforcement options to support load range from traditional approaches such as upgrade of asset, feeder reinforcement and substation, to installation of distributed generation (DG) [43]-[45].

In multiple regulatory environments, Transmission Network Owners (TNOs) and Distribution Network Operators (DNOs) are responsible for planning of network reinforcements in such a way to comply with national planning standards set by the national regulator. Thus, TNOs and DNOs should develop reinforcement plans which should be consistent with planning standards and avoid overloaded branches or substations under pre-defined conditions. There are several studies focusing on network reinforcement strategies using different algorithms [46]-[49].

When utilities carry out reinforcement planning, the process follows specified planning standards. In the UK at transmission level, Security and Quality of Supply Standard (SQSS) [50] sets out the criteria for planning as the minimum requirements for power supply quality and security. At distribution level, Engineering Recommendation P2/7 [51] defines the standard of power supply security [52].

2.1.2.2 Replacement

Decisions for replacement are generally based on three criteria: a) asset age; b) asset condition; and c) asset performance [53]. These criteria are directly related to reality. The economic aspects sometimes also need to be considered, which means replacement is required when it is more economical compared to frequent repairs. In practice, there are different replacement strategies for different types of assets. For example, overhead lines are refurbished/replaced when frequent failures are experienced (i.e. based on asset performance). In HVDC systems, ageing components are usually continuously monitored and replaced when failures of major components are observed (i.e. based on asset condition). Finally, assets can be replaced when they reach their expected lifetime age [54].

In the UK, regulator Ofgem has introduced an age-based model to assess asset replacement in RIIO-T1 Electricity Transmission Price Control Review [55] and distribution price control review (DPCR5) [56], which considers asset age profile, unit costs and asset condition (associated with asset age).

2.1.2.3 Repair and Maintenance

Repair and maintenance are essential to the security, reliability and environmental performance in network planning. The planning of repair and maintenance contains the understanding of asset reliability under certain failure modes, consideration of rising operating costs between repair and maintenance activities and identification of asset performance changes. These activities enable the discovery of developing defects and corrections of failures. Precisely, through repair and maintenance, the asset conditions can be monitored, and subsequently, the reduction in degradation of asset conditions can be achieved [28].

For a repairable and maintainable system, the most common models are renewal process (RP, also called perfect repair/maintenance), which brings asset to an as-good-as-new state, and Non-Homogeneous Poisson Processes (NHPP, also called minimal repair/maintenance), which brings asset to a same-as-old state [57][58]. In practice, however, repair/maintenance may lead asset to another state between as-good-as-new state and same-as-old state. Hence, imperfect repair/maintenance is introduced in order to model the repair/maintenance more generally, where perfect repair/maintenance and minimal repair/maintenance can be treated as special cases [59]. In current studies, virtual age model is an essential tool to model imperfect repairs/maintenances; asset age is described by virtual age rather than “real” age [59]-[61]. Kijima I and Kijima II models are the fundamental virtual age models, which use a constant parameter to accommodate the repair degree [62][63]. Details are given in Chapter 5.3.2.

Moreover, repair and maintenance actions may cause failure or reduction in reliability. The common reasons include: a) the technician's operation directly results in the failure due to poorly written manual or human error such as lack of training; b) the access to the component which needs repair/maintenance is blocked; c) certain parts of the component are difficult to conduct preventive maintenance without broken, such as fittings [64]. Maintenance-induced failure has been studied in some literature. For example, references [65] quantified post-maintenance failure rate and analysed the network reliability. Reference [66] used the imperfect repair model (as reviewed in [59]) to analyse the impact of maintenance-induced failures.

2.2 Power System Reliability Concepts

2.2.1 Reliability and Planning: Higher Level Story

2.2.1.1 Overview of Reliability and Planning

Reliability generally represents durability, dependability and system performance. In the engineering area, reliability of the system needs to be considered in planning, design and operation stages. In power systems, reliability refers to the capability of a system, within its expected lifetime, to perform the designed functions under the given operating conditions. Reliability is usually addressed at three levels [67]:

- Generation system,
- Transmission (and generation) system,
- Distribution system.

From consumers' perspective, power system reliability ideally means a constant supply of electricity from the above three systems. In practice, the most important reliability indicators for customers are duration and frequency of outages.

The aim of power system is to maintain uninterrupted electricity supply to consumers safely, reliably and economically. The assessment of power system reliability is crucial to achieving this aim. The methodologies for reliability assessment continually evolve in order to accommodate the technical changes in power system configuration and operation.

Currently, the main changes are introduced by the renewables as they significantly affect the operations of generation, transmission and distribution networks. Apart from renewable energy sources, another outstanding challenge for energy companies is to boost the market value of their services with proper reliability level, while reducing costs for construction, operation and maintenance. With these concerns, power companies expect the optimal power system planning with the appropriate reliability value leading to the lowest combined costs [67].

2.2.1.2 Generation System Reliability

A commonly accepted indicator for generation system reliability is Loss of Load, an event caused by the lack of generation capacity. Generation system reliability is defined by Loss of Load Probability (LOLP) in p.u. over a given time duration, or Loss of Load Expectation (LOLE) in days over a year. When a loss of load occurs, due to scheduled intervention and/or forced outages of other generators, the system capacity drops below the system demand [67].

Both LOLP and LOLE have been widely used to quantify the amount of time that load exceeds generation capacity and, consequently, indicate the generation system reliability. These are the fundamental indicators for which the constraint is imposed in generation development planning. Numerous researches have been carried out to develop the evaluation tools and models with LOLP and LOLE as the main planning criterion [68]-[73].

On the other hand, to assess the cost of unreliably, which is the financial damage to customers due to supply interruption, another reliability indicator is used. This is the Expected Energy not Served (EENS) which gives non-delivered energy in MWh/year. Specific unreliability costs, often called Value of Lost Load (VOLL) in £/kWh, is then used to calculate reliability (or, outage) costs in £/year.

An example of applied generation reliability can be found in the worldwide known methodology for generation expansion planning “Wien Automatic System Planning” (WASP). The global flowchart is shown in Fig. 2-3 [74]. In expansion stage, several feasible configurations of existing and new units are established. Each feasible configuration has technical and non-technical constraints, such as limitations on the number and capacity of new units, and is characterised by the total investment costs of new units. Here, LOLP index is calculated in an approximate way and any feasible configuration must satisfy a constraint on it. In operation stage, detailed reliability assessment of each configuration is done and each configuration not satisfying LOLP constraint is dropped. Generation cost and reliability cost based on EENS are then calculated for all configurations that satisfy the reliability requirements. In optimization stage, the optimum development strategy is determined from the "minimum cost path" across the decision tree in which investment, operation and reliability costs are associated with branches.

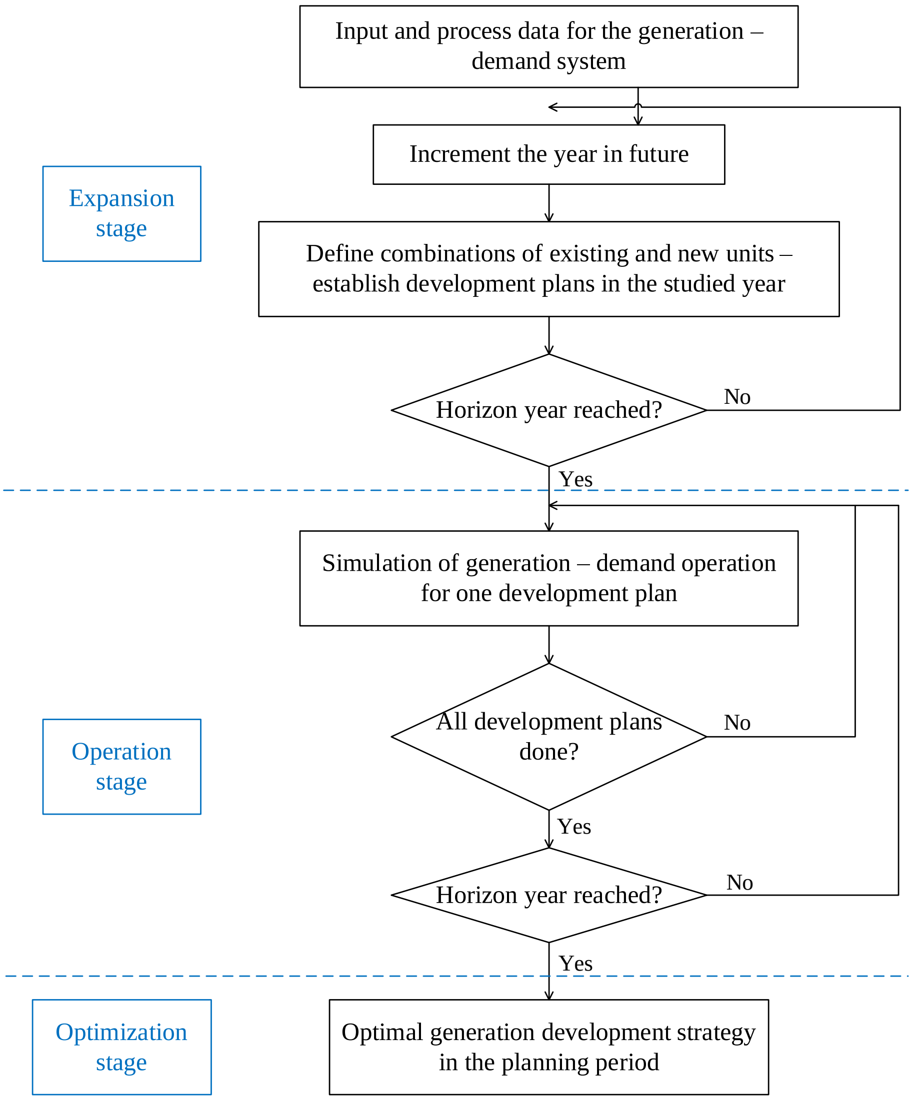

Figure 2-3: Global flowchart for generation expansion planning [74]

2.2.1.3 Transmission System Reliability

Transmission system contains transmission lines and substations which consist of different assets such as overhead lines, transformers and circuit breakers. The system performance – reliability depends on each component reliability. However, the reliability is not only influenced by different assets, but environmental factors and system configuration. Environment has an impact on the asset constraints and consequently system operation. For instance, severe weather such as lightning, heavy winds and snow may most likely cause failures of outdoor components. Beyond that, failures of assets in transmission system are not always independent, i.e. failure in one asset may increase the likelihood of failure in other assets. On the other hand, failure in one asset may not necessarily contribute to system failure due to the redundancy in other sections of transmission system [67].

Various studies have been done regarding different assets [75]-[78] and weather conditions [79]-[83]. References [75] and [76] present statistical analysis of different transmission assets such as transmission lines, cables, circuit breakers and transformers; while in [77] and [78], reliability models were developed and reliability indices were allocated to each asset to describe the reliability level. The impact of extreme weather is studied through weather state models. Two-state weather model was introduced in [79], which divides the entire weather conditions into normal state and adverse state. Based on two-state model, three-state weather model subdivides the adverse state, where the state groups become normal, adverse and major adverse weather [79]-[81]. References [82] and [83] specifically discussed the icing conditions. A climate-dependent failure rate was utilized for the reliability assessment of transmission lines.

An essential planning concept that defines transmission system reliability is the contingency criterion. The commonly used criterion is N-1 contingency, which means the ability of the system to withstand a single asset outage. This type of contingency only guarantees the normal system operation under the condition of one single component failure. When two or more failures occur, this contingency will contribute to system unreliability. Therefore, other types of criteria, for example, N-1-1/N-2 contingency, which require the system to accommodate new operating conditions with two sequential/simultaneous asset outages, are established [84][85]. Then N-k contingency criterion is the general concept for k simultaneous component failures [86]. After having built the network that satisfies one of the above security criterion, the transmission system reliability can be assessed using the estimated probabilities of component failures.

2.2.1.4 Distribution System Reliability

Distribution system in England and Wales usually starts at 132kV busbars of Grid Supply Points and goes down to low voltage of 0.4 kV over 33 kV and 11 kV (or, 6.6 kV) voltage levels. The 132 kV and 33 kV networks are called primary distribution system, they are meshed, and "similar" to transmission networks.

Secondary distribution system starts at 11 kV (or, 6.6 kV) side of primary substations. In the most of cases, the 11 kV (or, 6.6 kV) network is constructed as a meshed network but operated radially with normally open points. LV networks have some connections between individual radial feeders via link boxes, and are almost always operated as radial networks. Secondary distribution network is illustrated in Fig. 2-4.

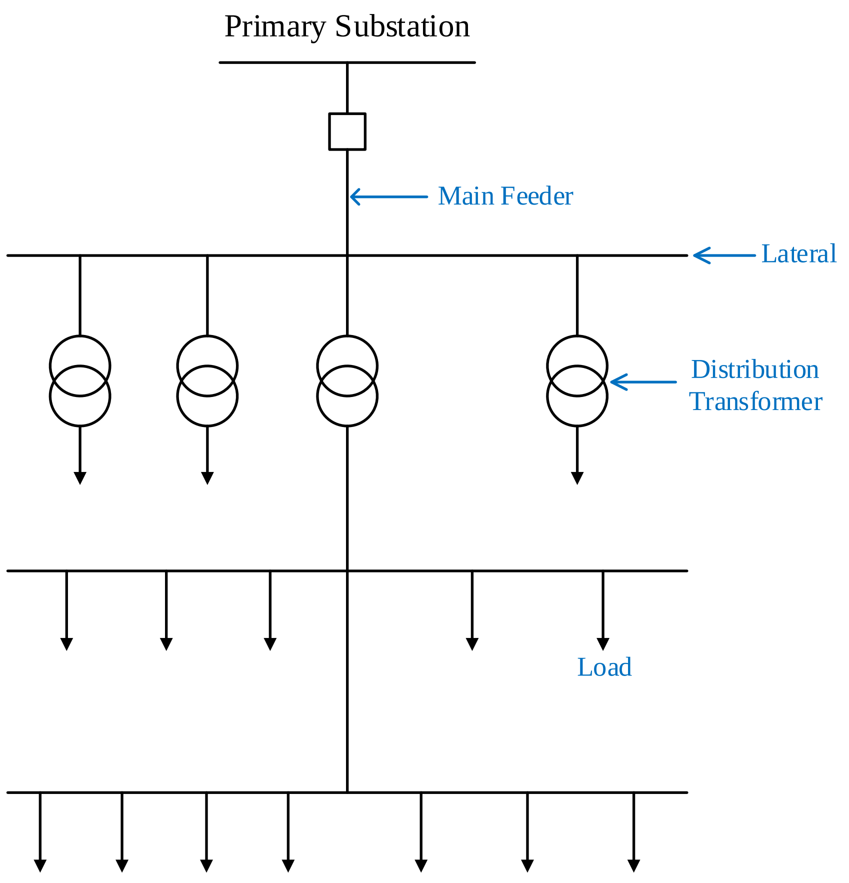

Figure 2-4: Line diagram of secondary distribution system [87]

Distribution system reliability is more consumer side oriented and only considers the local distribution system whilst neglecting generation and transmission assets. Along with transmission reliability, it also considers network capacity and quantifies network reliability via different indicators [67].

In the past, compared to generation and transmission system, less attention was paid to distribution system in terms of reliability assessment. This is because failures of generation and transmission can lead to extensive disastrous economic impacts on society. However, most outages on consumer side occur due to failures in distribution system. Moreover, due to the radial operation topology of the secondary system, a single outage can easily result in power interruption to consumers. Therefore, distribution feeders are recognized as the most vulnerable segment between supply side and customer side [88]-[90].

The distribution system reliability level is usually determined by the calculation of interruption frequency and duration indices. IEEE has introduced a guide for indices and factors that are involved in the calculation of distribution reliability [91]. Apart from the system-oriented indices such as Energy Not Suppled (ENS), Expected Energy Not Suppled (EENS), Loss of Load Probability (LOLP) and Loss of Load Expectation (LOLE), customer/load-oriented indices, namely System Average Interruption Frequency Index (SAIFI), System Average Interruption Duration Index (SAIDI), Customers Average Interruption Duration Index (CAIDI) and Average Service Availability Index (ASAI) are also defined. In the UK, distribution network performance is measured in terms of SAIFI and SAIDI indices, which are simply called, respectively, "Customer Interruptions" and "Customer Minutes Lost".

Several studies have been carried out to analyse distribution system reliability. The conventional assessment method consists of three parts: establishing asset-level and system-level reliability model, and evaluating the reliability by reliability indices. Reference [92] pointed out that the traditional evaluation method may not be sufficient for systems with partial redundancy, especially for converters. Therefore, improvements targeted at component failure rate and system-level model were proposed; focus is put on the modification of component failure rate, which was related to asset operating conditions such as asset loading, cable length and cable joints. Reference [93] considered customers' view against interruptions and defined Customer Dissatisfaction as a reliability index. There are some studies related to assets. For example, reference [94] discussed the reliability of DC distribution network. The assessment model differed from the common-used model in electronic devices, and redundant components were also studied. Reference [95] integrated the identification and analysis method of key assets into the reliability study, whilst reference [96] studied the effect of reclosing devices and distribution generation in order to improve reliability indices in radial distribution lines. Finally, some studies conducted a statistical analysis historical/observed data using proper models [97][98].

2.2.2 Reliability Assessment Aspects and Techniques

Power system reliability refers to the probability that, at any given time, the power system will remain sufficient under a given series of disturbances, while maintaining to supply power demand for a given operational duration. The way to make the power system reliable is a combination of solutions which take both the external and internal effects of factors into account. The external factors are environmental-related failures, whilst internal factors contain failures associated with power generation, transmission and protection components [99].

Power system reliability can be categorized into adequacy and security. System adequacy evaluates the adequacy of the present system assets to meet the needs of customer side and/or satisfy the system operational constraints. This includes the necessity of the assets to produce adequate energy and the requirement of transmission and distribution assets to deliver the energy to demand points. System security evaluates the performance of the power system in the event of disturbances. This includes local and extensive disturbances and sudden interruptions of primary generation or transmission [100][101].

In the field of system security, disturbances include overloading, voltage and dynamic instability, as shown in Fig. 2-5 [102]. Several studies have been carried out to evaluate power system security. These studies have pointed out that advanced analysis tools, for instance, Dynamic Security Assessment (DSA), which are capable of comprehensive static and dynamic security evaluation, are necessary. They must be able to model the system properly and compute security limits accurately and fast [103]. Regarding adequacy, the concerns are system generating units and load demand. There is a broad range of evaluation techniques and tools which can be commonly categorized as analytical and simulation techniques [104].

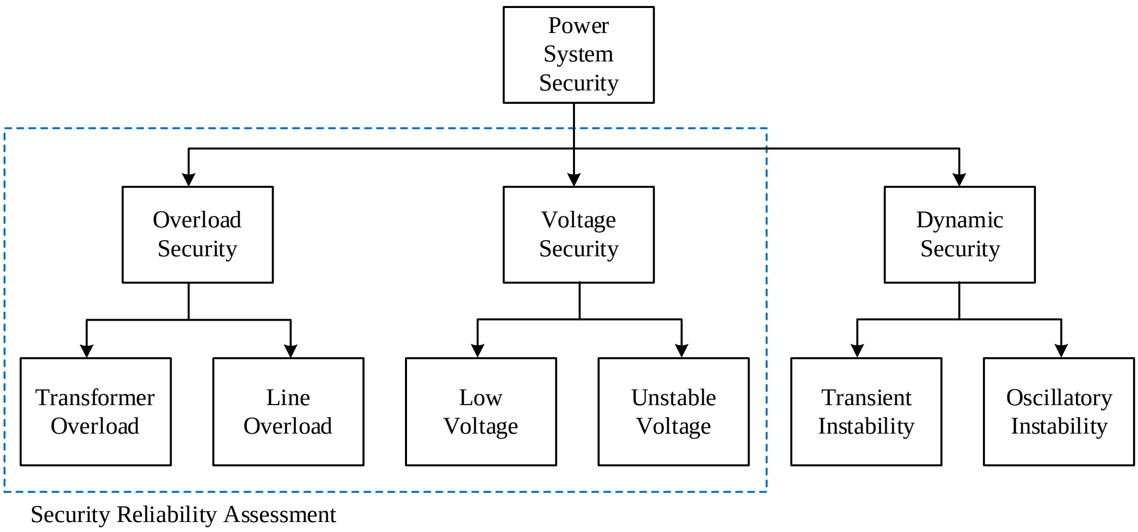

Figure 2-5: Security Reliability Assessment [102]

Various reliability assessment techniques have been developed over the past. Analytical techniques evaluate the system reliability indices based on an appropriate model through mathematical approaches. There are some studies using the analytical technique to assess system adequacy. State enumeration is a commonly used analytical technique for systems with a small scale or low failure rate [105][106]. System states are enumerated until a given failure sequence or pre-set probability threshold is met [107]. Then, an impact increment-based state enumeration method is developed for the reliability evaluation of composite generation and transmission systems, which has higher efficiency than the traditional state enumeration method. Apart from state enumeration, reference [108] proposed an analytical method for flexible resource adequacy assessment of power system with renewable generations. The proposed method is based on a net-load duration curve and is capable of evaluating reliability indices and a trade-off between reliability and generation cost. Reference [109] introduced supplied demand algorithm to calculate reliability indices, mainly for generation systems. In summary, however, accurate mathematical equations can be very complicated for large and complex systems and may require approximations when modelling complex operating procedures.

Simulation techniques, such as Monte Carlo simulation, simulate the random behaviour of the system to evaluate the reliability indices. This technique is more flexible in modelling and can be more easily carried out using computers [110]. It has been widely used in various systems. For example, reference [111] analysed the reliability of distribution network with solar generation and DG by using Monte Carlo simulation. Reference [112] applied Monte Carlo simulation to forecast the failure rate based on temperature and humidity distributions; reference [113] discussed the reliability of reactor protection system using the Monte Carlo simulation. Moreover, there are also some researches that combine analytical and simulation methods to analyse the reliability of power systems [114][115]. The application of Monte Carlo has been introduced in [110], which will be presented in later chapters.

2.2.2.1 State Enumeration

State enumeration method (also called contingency enumeration method) is a common numerical method [116]. The reliability of the network is evaluated by calculating reliability of each network state. The network state is based on the load level, as well as network structure defined by first-order independent failures and/or second-order independent failures. Since all events in the power system are considered independent, the system state probability can be obtained by multiplying the probability of each element, such as load level, overhead lines, transformers, etc. The equation is given by Eq. (2-1).

$$p_s = \prod\nolimits_{c \in C} p_c \cdot p_l \tag{2-1}$$

where p_{sys} is the probability of system state s; p_c is the probability of component state (represented by unavailability of failed components times availability of the in-service comments); p_l is the probability of load level; C represents the set of all components in the network. The number of system states is determined by the order of contingencies, such as first order, second order, etc. In each system state, reliability indices are calculated, multiplied by system probability, and added up to find their expectations.

2.2.2.2 Monte Carlo Simulation

Monte Carlo Simulation is a traditional simulation method. It is a stochastic procedure which is suitable for the analysis of large and complex systems. The method is based on stochastic selection of system states (as opposed to enumeration) by using random numbers. The random numbers, in other words, directly simulate the stochastic behaviours of the studied system. The random numbers in Monte Carlo simulation have the following characteristics [117]:

- Uniformity: The random numbers should be uniformly distributed between 0 and 1.
- Independence: The random numbers should be independent from each other.
- Random numbers are generated use pseudo-random algorithms, which are the mathematical models that satisfy certain randomness criteria.

Monte Carlo Simulation method is categorized as sequential and non-sequential simulation.

I) Sequential Monte Carlo Simulation

Sequential Monte Carlo (SMC) can be applied to simulate the chronological operation of the power system network. The procedure for analysing system reliability by using SMC is summarized as follows:

1. Define the set of possible stochastic events;
2. In in each time interval, randomly sample all stochastic events and generate system model;
3. In each time interval, apply power system analysis and find reliability indices;
4. Aggregate the reliability indicators within the studied period.

The main advantage of sequential Monte Carlo simulation is that it is mathematically simple to implement, it can model chronological phenomena like wind, hydro and storage, and can be applied to estimate frequency and duration reliability indices. Also, it has the ability to correlate time-dependent uncertainties. The main drawback is the need for a long computational time, especially when all chronological behaviours in the network are modelled.

II) Non-Sequential Monte Carlo Simulation

Compared to sequential Monte Carlo simulation, there is no temporal modelling of physical phenomena and the generated system states are mutually independent. In particular, each system state is determined by the combination of states of all components. System state sampling method is adopted in non-sequential Monte Carlo simulation technique. Given that each system state is independent, this method cannot be used to record and assess frequency and duration indices, and is unable to correlate the chronological phenomena.

In particular, each network component may reside in one of several discrete states. In the two-state representation, a component can be in the up-state and down-state, and the corresponding probabilities (i.e. availability and unavailability) are defined via failure rate λ and repair rate μ. The state space diagram is presented in Fig. 2-6 [118]. When modelling the states by non-sequential Monte Carlo simulation technique, a random number *U* in uniform distribution between (0, 1) is generated. The component state is determined by comparing *U* and the component availability, or forced outage rate (*FOR*). The calculation of *FOR* is given in Eq. (2-2):

$$FOR = \frac{\lambda}{\lambda + \mu} \tag{2-2}$$

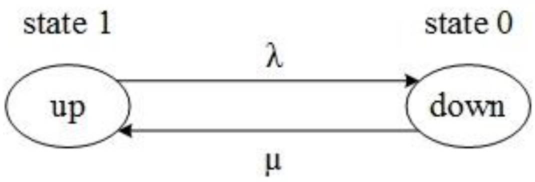

Figure 2-6: Two-state representation [118]

For each component [118],

- if $U \leq FOR$, the component is in down state;
- if $U > FOR$, the component is in up state.

The system state is the combination of all individual component states and the system probability is calculated accordingly.

Large generators can often be operated at a reduced MW output, which is a so-called derated state. Assuming there is only one derated state, the state space diagram is presented in the Fig. 2-7 [119]. It should be noted that large generating units may have more than one derated state and the transitions between states need to be specified based on real-life experience.

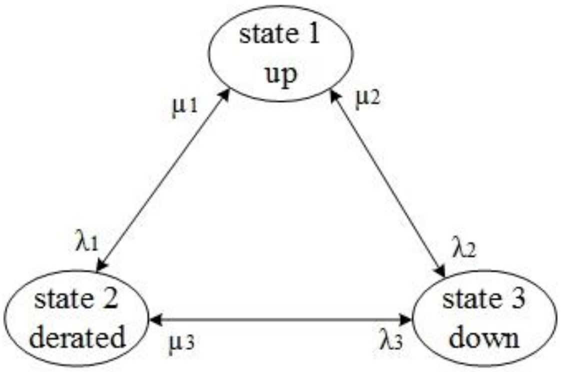

Figure 2-7: State representation of a component with one derated state [119]

The probabilities of components residing in down and derated state are P_{dn} and P_{de}. Similarly, by comparing the generated random number U from uniform distribution (0, 1) with the limiting state probabilities, the state of each component can be obtained as follows:

- if $U \leq P_{dn}$, component state is down;
- if $P_{dn} < U \leq P_{dn} + P_{de}$, component state is derated;
- if $U > P_{dn} + P_{de}$, the component state is up.

2.2.3 Reliability Indices

Reliability indices indicate the system performance from the standpoint of system adequacy. The indices are expected statistical values, and can be used to demonstrate future system performance. There are generally four types of reliability indices for a composite system: probability, duration, frequency and expectation indices. The details are listed in the table below [119].

Table 2-1: Reliability indices and measured objects [119]

Reliability Indices	**Measured Object**
Probability indices	The possibility of an event occurrence
Duration indices	The expected time that an event will last for
Frequency indices	The expected recurrence rate of an event per unit of time

Expected indices	The average of the expected results of an event

Reliability indices are typically calculated for the load points and the entire system. Nodal indices indicate the nodes where the impact from an event is the biggest. If the unreliability of ageing asset is considered, nodal indices may also indicate where asset replacement, refurbishment and maintenance may give the biggest improvement in the system reliability.

The following indices are the most commonly used for the reliability analysis of composite power systems:

Expected Energy Not Supplied (EENS)

EENS is defined as the expected energy not supplied under the circumstance of the load exceeding the available generation (i.e. power outage), or violation of network constraints. EENS is one of the most important transmission system indicators, it models both transmission capacity deficiency and energy limitation due to reduced prime energy [120]. The expression is shown below:

$$EENS = \sum_{i \in S} 8760 \cdot C_i \cdot p_i \quad \text{(MWh/yr)} \tag{2-3}$$

Where S is the set of all system states with load curtailment; C_i and p_i are the curtailed load and the probability of system state i, respectively; 8760 is the total hours of one year. Note that Eq. (2-3) gives the so-called annualized value.

Loss of Load Probability (LOLP)

LOLP is defined as the probability of load exceeding the available generation. Small LOLP value implies good system performance. However, it defines the likelihood of load curtailment but not the severity. For example, for the same LOLP value, the degree of failure can be less than 1 MW or greater than 1000 MW. Therefore, the extent of capacity or energy shortage cannot be identified [121]. The expression is:

$$LOLP = \sum_i p_i \cdot t_i / 8760 \quad \text{(p.u.)} \tag{2-4}$$

where t_i is the time duration of the load loss of the system state *i*; other parameters are defined above.

Loss of Load Expectation (LOLE)

LOLE is defined as the average number of days/hours in a given period of time (usually a year) that the load is expected to exceed the available generation capacity (i.e. a loss of load occurs). Similarly to LOLP, it cannot define the severity of the load loss:

$$LOLE = \sum_i p_i \cdot t_i \quad \text{(days/yr or hours/yr)} \tag{2-5}$$

Specifically, in reliability test network, the indices defined above can be calculated at node level and system level.

I) Node Level

a) EENS

$$EENS_i = \frac{1}{NY}\sum_{k=1}^{NY}\sum_{t=1}^{n} ENS_i \tag{2-6}$$

where $EENS_i$ is the load loss of node *i* in hour *t*, year *k*; *NY* is the number of simulated years; for simplicity, subscripts t and k are dropped. ENS_i can be calculated using the equation below:

$$ENS_i = \begin{cases} P_{i,c} - P_{i,a} & if\ P_{i,c} > P_{i,a} \\ 0 & if\ \ P_{i,c} \le P_{i,a} \end{cases} \tag{2-7}$$

where $P_{i,c}$ is the MW demand at node *i*; $P_{i,a}$ is the delivered MW at node *i*.

b) LOLP

$$LOLP_i = \frac{1}{NY \cdot 8760}\sum_{k=1}^{NY}\sum_{t=1}^{n} \begin{cases} 1 & if\ ENS_i > 0 \\ 0 & if\ ENS_i = 0 \end{cases} \tag{2-8}$$

where $LOLP_i$ is the probability of load loss occurring at node *i*; other parameters are defined above.

c) LOLE

$$LOLE_i = \frac{1}{NY}\sum_{k=1}^{NY}\sum_{t=1}^{n}\begin{cases}1 & if\ ENS_i > 0\\ 0 & if\ ENS_i = 0\end{cases} \tag{2-9}$$

where $LOLE_i$ is the expected number of days (or hours) for which a load loss occurring at node *i*; other parameters are defined above.

II) System Level

a) EENS

$$EENS_{sys} = \sum_{i=1}^{N} EENS_i \tag{2-10}$$

where $EENS_{sys}$ is the power outage of the entire system, which is the sum of the load losses at all nodes; *N* is the number of nodes.

b) LOLP

$$LOLP_{sys} = \frac{1}{NY \cdot 8760}\sum_{k=1}^{NY}\sum_{t=1}^{n}\begin{cases}1 & if\ \sum_{i=1}^{N} ENS_i > 0\\ 0 & if\ \sum_{i=1}^{N} ENS_i = 0\end{cases} \tag{2-11}$$

where $LOLP_{sys}$ is the probability of power outage of the entire system, other parameters are defined above.

c) LOLE

$$LOLE_{sys} = \frac{1}{NY}\sum_{k=1}^{NY}\sum_{t=1}^{n}\begin{cases} 1 & if \ \sum_{i=1}^{N} ENS_i > 0 \\ 0 & if \ \sum_{i=1}^{N} ENS_i = 0 \end{cases} \quad (2\text{-}12)$$

where $LOLE_{sys}$ is the expected duration (in days or hours) of power outage of the entire system, other parameters are defined above.

2.2.4 Reliability Functions

In reliability assessment, the random variable is component in-service time. Assume T ($T \geq 0$) is the continuous random variable, and its distribution is characterized by its probability density function (PDF) $f(t)$ and cumulative distribution function (CDF) $Q(t)$. PDF describes the probability of the random variable located within a specific range of values. CDF, as express in Eq. (2-13), gives the probability that failure has occurred by time duration *t*. The curve of CDF is described in Fig. 2-8, which represents component unavailability that varies from zero to unity as time increase from zero to infinity. At *t=0*, the component or system is in operating state; therefore its probability of failure (or, unavailability) is zero. When *t* is long enough, a failure will occur on the component (or the system) and the unavailability tends to unity [118][119].

$$Q(t) = P\{T \leq t\} \quad (2\text{-}13)$$

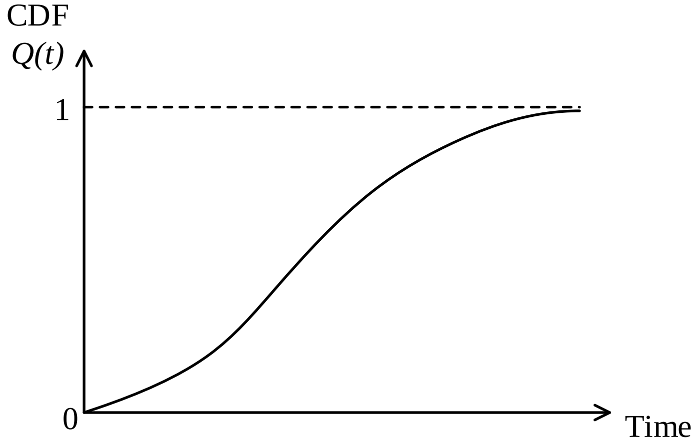

Figure 2-8: Cumulative distribution function [119]

In some practical problems, it is not required to evaluate the probability of failure but the probability of surviving up to the certain moment t (i.e. failure has not occurred by t). This is the complement to the failure function $Q(t)$ [120]. The survivor function, denoted as $R(t)$, has the following relationship with $Q(t)$:

$$R(t) = P\{T > t\} = 1 - Q(t) \tag{2-14}$$

The first derivative of failure function $Q(t)$ is probability density function $f(t)$, as shown in Fig. 2-9, and calculated as:

$$f(t) = \frac{dQ(t)}{dt} = -\frac{dR(t)}{dt} \tag{2-15}$$

which can also be expressed in the integral form:

$$Q(t) = \int_0^t f(t) \tag{2-16}$$

$$R(t) = 1 - \int_0^t f(t) = \int_t^\infty f(t) \tag{2-17}$$

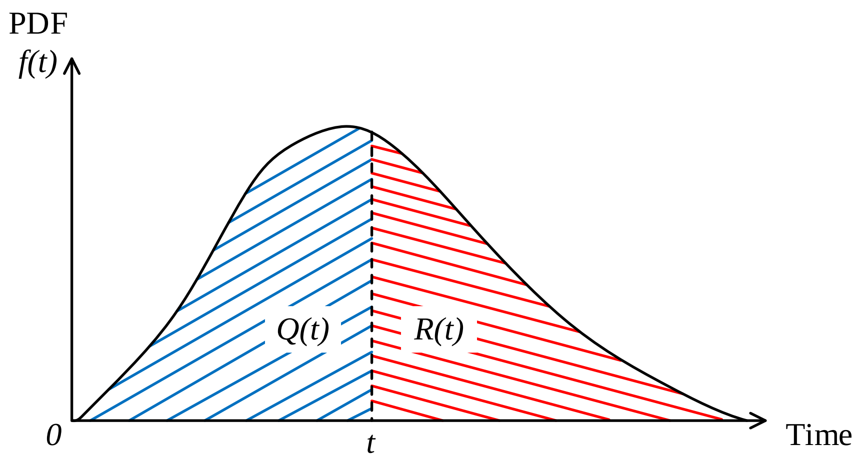

Figure 2-9: Probability density function of in-service time [119]

In reliability analysis, the hazard function $\lambda(t)$ is one of the most broadly used function in assessing asset reliability [120]. The expression is given in Eq. (2-18) [121]. The numerator gives the conditional probability that component fails in interval $(t + \Delta t)$ given that it has not failed before; the denominator is the width of interval.

$$\lambda(t) = \lim_{\Delta t \to 0} \frac{P\{(t < T \leq t + \Delta t)|(T > t)\}}{\Delta t} \tag{2-18}$$

It can be further derived as:

$$\lambda(t) = \lim_{\Delta t \to 0} \frac{P\{(t < T \leq t + \Delta t) \cdot (T > t)\}}{\Delta t \cdot P\{T > t\}} = \lim_{\Delta t \to 0} \frac{P\{t < T \leq t + \Delta t\}}{\Delta t \cdot R(t)} = \frac{f(t)}{R(t)} \tag{2-19}$$

2.3 Reliability Test System

For the purpose of providing a basis for comparing the results obtained from different methods, IEEE has developed a reference or “test” system, which is the IEEE Reliability Test System. In 1979, the IEEE Subcommittee on the Application of Probability Methods (APM) of the Power System Engineering Committee published the first version of the IEEE Reliability Test System (RTS-79) [122]. IEEE RTS-79 aims to test and compare the results obtained by using different reliability assessment methods. It is designed as a reference system with all data and parameters that are necessary for the reliability assessment of composite systems. However, for particular applications, some enhancements to RTS-79 are needed. For example, the additional data can be included by individual researchers or addressed in the future development of the IEEE RTS-79 [123].

In 1986, IEEE RTS-86 was developed and published as the second version of IEEE RTS [124], aiming to make the IEEE RTS more widely used for different reliability modelling and assessment methods. The experience with IEEE RTS-79 helped identify the need for essential additional data and “appropriate” reliability indices that can be calculated on the test system. The extension is made mainly on the data related to the generation system. Specifically, it includes the extension of the generating units in the IEEE RTS-79 database, unit scheduled maintenance, unit derated states, uncertainty in load prediction and the influence of interconnection. These improvements allow IEEE RTS-86 to calculate the reliability indices that are derived through accurate solution techniques, without the need for making approximations. Then the reliability indices are determined in a uniform way and can be used for comparison with results obtained from other techniques [123]. After

1986, in order to bridge the gap between increasing industry demand and current computing tools, other useful network models were proposed and published in [125]. More specifically, the changes in the electrical industry, such as transmission access and emission caps, need to be modelled. These changes and some perceived enhancements to the IEEE RTS-86 motivated the IEEE task group to develop a multi-region RTS with additional data [123].

IEEE test system RTS-96 was developed as an enhanced test system by the former APM-RTS Task Force for large and complex power system reliability assessment studies. The new system can be used for multi-area studies and is expected to allow standard and comparative studies of new and existing reliability assessment techniques [123]. It is important to note that in the development and adoption of the parameters in IEEE RTS-96, it is not intended to develop a test system that represents any particular or typical power system. If this requirement is applied to IEEE RTS-96 as mandatory, it will result in a system with fewer general-purpose features, and testing the influence of different evaluation techniques will be less useful as a reference. Besides, a comparison study of IEEE RTS-79 and IEEE RTS-96 has been done, which verifies that IEEE RTS-96 has more robustness than the old IEEE RTS-79 test system as it produces more representative reliability indices [125].

The topology of one-area IEEE RTS-96 is shown in Fig. 2-10. By merging two one-area systems through interconnections, the two-area system can be obtained. Similarly, the three-area system is formed by adding a third area to the two-area system via interconnections [123].

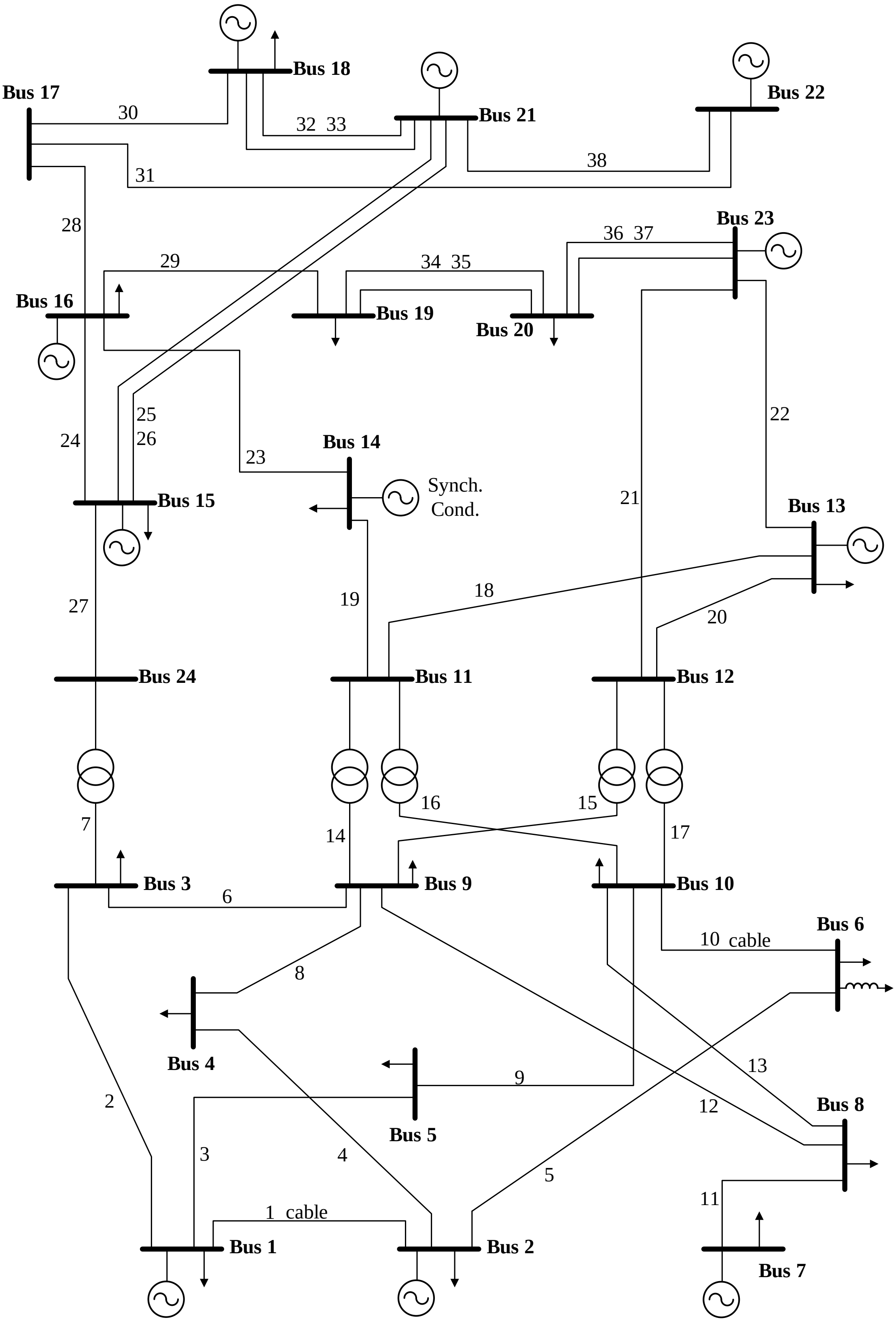

Figure 2-10: The topology of one-area IEEE RTS-96 test system [123]

2.4 Research Gap

In the last price control review, the UK regulator Ofgem has specified a common set of "network output measures"[126], which provide metrics for measuring transmission asset performance; they also bring together reinforcement and asset interventions such as repair, maintenance and replacement. Traditional approach to reinforcement planning does not consider asset conditions, whilst replacement planning sometimes accounts for network operating conditions via so-called "loading factors" [127]. A more realistic modelling of intervention impacts needs to involve reliability analysis, whereby asset hazard models are usually functions of in-service time only [128]. One of early attempts to model exogenous variables was done in the Cox's proportional hazard model (PHM) [129].

The UK utilities have adopted the concept of health indices (HIs) to describe asset health and choose "proper" asset interventions [130]-[131]. Asset HIs are defined as deterministic scores [131] that outline asset conditions via relevant asset and environmental parameters. However, the impact of asset's in-service operation, post-repair result and external factor (such as location) can be combined to model asset hazard more generally. In this research, PHM and Kijima models are utilized to reflect this impact.

Furthermore, a higher level aggregated network planning methodology is proposed, where the concept is inspired by the WASP model (as reviewed in Chapter 2.2.1.2). The details of this methodology are given in Chapter 3.

2.4 Chapter Summary

This chapter first gives an overview of power system planning. Then planning categories are reviewed. Since Reliability is one of the most significant criteria that must be considered at every stage of power system planning, design and operation, this chapter also reviews the basic concepts of power system reliability. The evaluation techniques for assessing the power system reliability are introduced. The related functions in reliability assessment and the quantitative expressions used to indicate system performance are also presented.

In order to provide a basis for comparing the results calculated from different methods of reliability assessment, IEEE has developed a reference or "test" system, which is the IEEE

Reliability Test System. This chapter introduces the development history of the IEEE Reliability Test System, as well as the topology of the one-area IEEE RTS-96.

Research gap is highlighted in this chapter.

CHAPTER 3 AGGREGATED NETWORK PLANNING

This chapter provides an overview of the proposed higher level aggregated network planning that consists of reinforcement and quality-of-supply investment optimization, optimal asset intervention planning and probabilistic simulation methodology for decision verification. The focus of this research is on the development of a probabilistic simulation methodology whose primary goal is to find impact of optimized asset interventions (and reinforcements) on the overall system operation as well as on individual assets.

3.1 Aggregated Planning Methodology

Traditionally, reinforcement (load-driven) and replacement (non-load driven) planning have been done separately. Ofgem has recognized the connection between the two areas, developed aggregated output metrics and encouraged companies to develop probabilistic approaches to the aggregated planning model. The framework for integrated asset intervention and reinforcement planning addresses all major planning blocks in the UK utilities and it is an extension of the work on the integrated reinforcement and quality-of-supply planning [132][133]. The overall problem is set in the form of a decision tree [134], where the nodes denote different network configurations in certain time periods and branch (cost) transitions between two configurations in consecutive time periods. The entire problem is divided into four stages, denoted by I, II, III and IV in Fig. 3-1:

- I Optimal asset intervention planning;
- II Reinforcement planning, both general and connection-driven;
- III Quality-of-supply (QoS) planning;
- IV Probabilistic simulation.

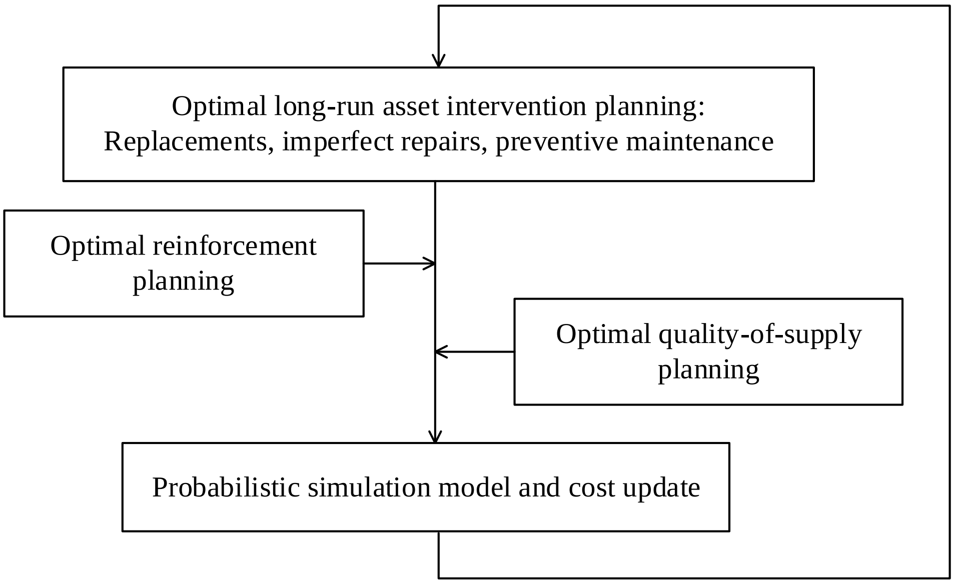

Figure 3-1: Simplified flowchart of the integrated planning methodology

Optimal long-run asset intervention planning is done in the first place. The aim is to find the best imperfect repairs, preventive maintenance and replacements in the considered planning period [134][135]. The optimal replacements are then input into the reinforcement planning which is based on static planning within individual years of the planning period. This leads to the decision tree (in time) concept, where several development alternatives are presented in each year. Decision tree can be of either deterministic or probabilistic nature. An example of the probabilistic tree is shown in Fig. 3-2, where $(R+R)_{x\text{-}y}$ represents discounted replacement and reinforcement (investment) costs; and $Pr_{x\text{-}y}$ denotes the transition probability from state x to state y.

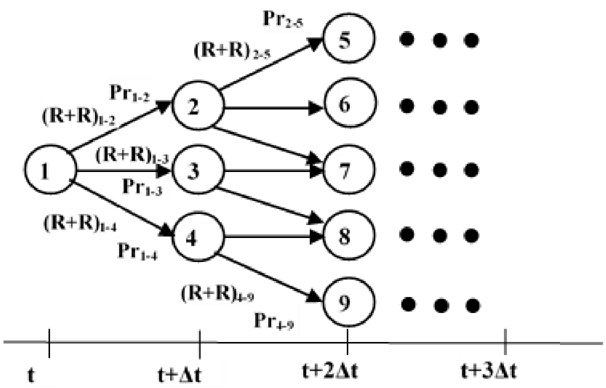

Figure 3-2: Illustrative example of a decision tree

To separate this planning stage from the later stages, the optimum development strategy path is determined at this stage. This path can be obtained based on dynamic programming in the deterministic approach or a set of probability rules in the probabilistic approach.

The optimization of QoS investment cost is done in a similar way as reinforcement planning. Specifically, if the optimal reinforcement & replacement investment strategy is decided in the previous stage, a new set of scenarios (configurations) can then be specified, as well as a new decision tree for the QoS problem; if not, the QoS problem can be solved for each node of the original decision tree (Fig. 3-2). The result of this stage is the optimal and suboptimal development paths characterized with reinforcement, replacement and QoS costs.

Probabilistic simulation of the selected network development strategy is performed in the final stage. It gives system performance in terms of reliability indices, as well as asset performance in terms of asset health indices and/or (virtual) age profiles, required interventions, and costs relating to operation and reliability. If the studied development strategy does not meet reliability constraints, it is discarded and a new set of optimum and suboptimum strategies may need to be determined.

To sum up, the general solution to the aggregated problem consists of three parts:

- Optimization of maintenance, repair and replacement strategies over a longer time period to get corresponding capital costs.
- Integration of reinforcement planning with the optimal replacement, repair and maintenance plans to get an overall optimum development strategy.
- Verification of the optimal and suboptimal development strategy using the probabilistic simulation of the power system operation based on sequential Monte Carlo simulation.

The focus of the thesis is on the probabilistic simulation model.

3.2 Probabilistic Asset Intervention Planning

This thesis completes the last stage shown in the flowchart of Fig. 3-1, which is the probabilistic simulation to quantify asset interventions. This stage is utilized to study the impact of optimized asset interventions on the overall system operation as well as on individual assets. The developed probabilistic simulation methodology contains the following building blocks: a) temporal asset hazard modelling; b) probabilistic asset HI modelling; c) deterministic asset HI modelling; and d) correlation between external inputs.

Here are the details of how this research completes this stage: "Asset health" modelling with the aid of temporal models (or, temporal hazard functions) is initially developed; it incorporates basic blocks of Sequential Monte Carlo simulation including component state modelling, load modelling, LCTs modelling, spatial correlation and optimal power flow model. Two further approaches are developed for modelling asset health indices. The first is the deterministic approach, where asset health scores are modelled as deterministic quantities and integrated into the hazard functions. The second is the probabilistic approach, where the concept of probabilistic asset health indices is proposed to address health index uncertainties and generate results required by the UK regulator on both system and asset level. Asset HIs are described by known pdfs associated with virtual asset age. Degradation of asset towards worse HIs (i.e. asset degradation) is modelled first using the proposed "queueing type" transition model. Improvement of asset towards better HIs is then modelled using a set of rules/processes related to asset repairs. In this way, asset in-service time is sampled from hazard functions based on proportional hazard models (PHMs) in combination with the Kijima KT2 model, whilst out-of-service time is sampled based on the developed repair process. All developed asset HI models are incorporated into a sequential Monte Carlo procedure, where other input blocks are the same as temporal model.

3.3 Chapter Summary

This chapter introduces the higher level aggregated network planning methodology. It includes four main building blocks, that is, reinforcement and quality-of-supply investment optimization, optimal asset intervention planning and probabilistic simulation methodology for decision verification. This thesis addresses the last stage of the aggregated methodology, which can be used to study the impact of optimized asset interventions on both system and individual asset level.

CHAPTER 4 MODELLING OF BLOCKS IN RELIABILITY ANALYSIS

In reliability analysis, all events associated with the calculation of the reliability indices need to be modelled probabilistically. The events, including component operating states, load profiles, and low carbon technology (LCT) production can be treated as input blocks in the power system reliability analysis. This chapter gives the modelling of the input blocks. Sequential Monte Carlo simulation method is used to obtain the chronological operating states of all network components which includes branches, dispatchable generators, transformers and wind turbines.

Spatial correlation between wind generating units and between load points is also studied. This chapter gives a brief introduction into the correlation modelling method. Here Nataf transformation in conjunction with Cholesky decomposition [136] is used to analyse the correlation between wind speeds, and the correlation between nodal loads.

After obtaining the input blocks, system reliability assessment requires an optimization tool which is the Optimal Power Flow (OPF) model to calculate the reliability indices. This chapter introduces the objective function and corresponding constraints of the OPF model and gives an overall simulation algorithm.

4.1 Component State Modelling

The reliability curve is used to describe the change of component failure rate over its lifetime. In the 1950s, a group called AGREE (Electronic Equipment Reliability Advisory Group) pointed out that the classic "bathtub" curve can describe the failure rate of electronic components and systems [137]. This curve is presented in Fig. 4-1.

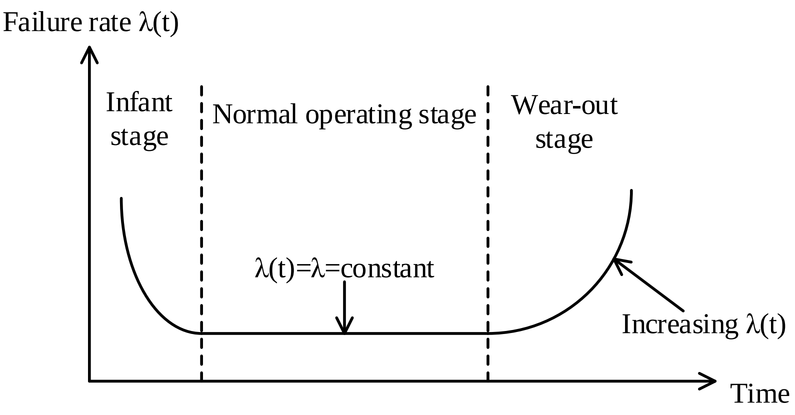

Figure 4-1: Bathtub Curve [137]

Three distinctive stages are presented in the bathtub curve:

- Infant stage
  The failure rate of components in this stage shows a falling trend. Failures in this stage are mainly caused by manufacturing process, inadequate installation, etc.
- Normal operating stage
  Components in this stage have a relatively constant failure rate, which means their in-service time in this period is exponentially distributed. In this stage, failures occur due to unexpected or sudden overstress. Components in this stage are repairable.
- Wear-out stage
  This stage is the ageing stage of the components, featured with a rising failure rate. In-service time of components usually follow Weibull distribution. In this stage, components can either be repaired or replaced.

Generally, the operating states of a reparable component can be divided into up state and down state. The state-space transition between the up and down states is illustrated in Fig. 4-2, whilst Fig. 4-3 shows in-service and out-of-service times.

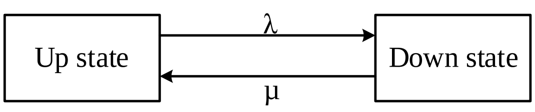

Figure 4-2: Transition between component states

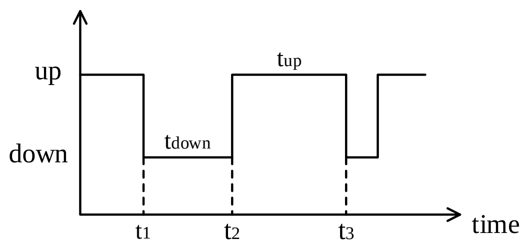

Figure 4-3: In-service and out-of-service times

Here, λ and μ represent the failure rate and the repair rate, respectively; t_{up} is the time duration of components residing in normal operating state, also called time to failure (TTF); t_{down} is time to repair (TTR), representing the time duration of components residing in failed stage.

4.1.1 In-service Time Distributions

As mentioned earlier, stochastic variables in reliability analysis are in-service and out-of-service times. There are three distributions widely used in reliability analysis [138]:

- Normal Distribution
- Exponential Distribution
- Weibull Distribution

4.1.1.1 Normal Distribution

When the asset's in-service time data fit normal distribution, the failure rate (or, hazard function) increases monotonically with time (Fig. 4-4), which fits the wear-out stage in the bathtub curve. Normal distribution is usually applicable to failures influenced by additional factors, such as mechanical failures led by multiple random small mechanical deteriorations. This type of mechanical failure is usually observed as the system wears out in use.

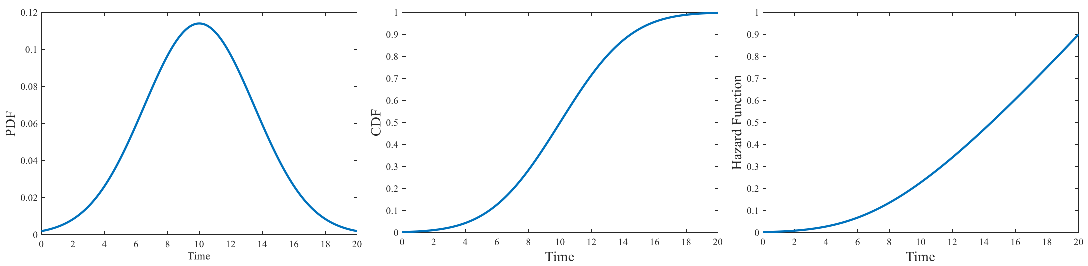

Figure 4-4: Shapes of PDF, CDF, and hazard function of a normal distribution

4.1.1.2 Exponential Distribution

It can be shown that where the failure rate is constant over time, the distribution of the in-service time is exponential (Fig. 4-5). It can be applied to model the asset in normal operating stage of the bathtub curve, during which failures occur randomly.

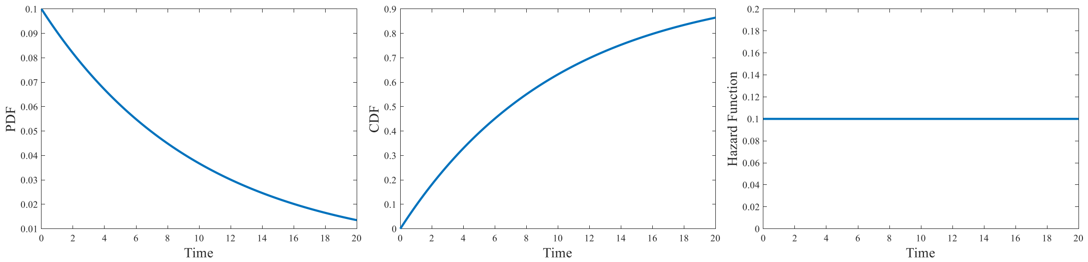

Figure 4-5: Shapes of PDF, CDF, and hazard function of an exponential distribution

4.1.1.3 Weibull Distribution

Weibull Distribution was developed by W. Weibull to analyse failures due to metal fatigue [139]. It is described by the scale parameter α and the shape parameter β. The Weibull PDF can model the characteristics of other distributions as its shape depends on the value of β. All the stages in the bathtub curve, in fact, can be modelled by varying the β value [140]. Details are given below:

- The infant stage, featured by a decreasing failure rate, can be modelled with the aid of Weibull distribution with $0 < \beta < 1$.
- The normal operating stage, where the asset's failure rate is a constant, can be modelled by the Weibull distribution with $\beta = 1$.
- The wear-out stage, featured by an increasing failure rate, can be modelled by the Weibull distribution with $\beta > 1$. The bigger the shape parameter is, the faster the failure rate increases.

A few examples of the Weibull PDF and hazard function are given in Table 4-1 (with varying shape parameter and scale parameter $\alpha = 2$).

Table 4-1: PDF and failure rate function of Weibull distribution with different shape parameter values

Value of β	**PDF**	**Hazard Function**
$\beta = 0.2$	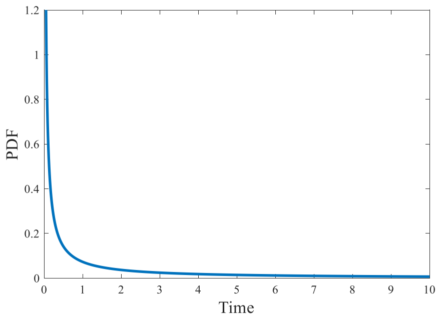	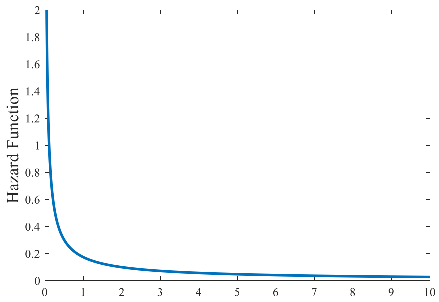
$\beta = 1$	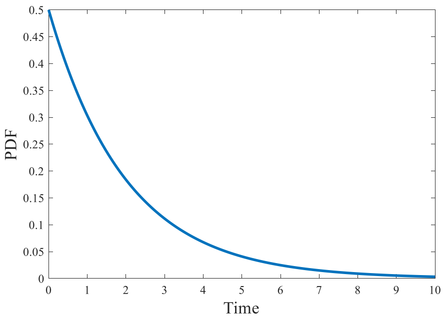	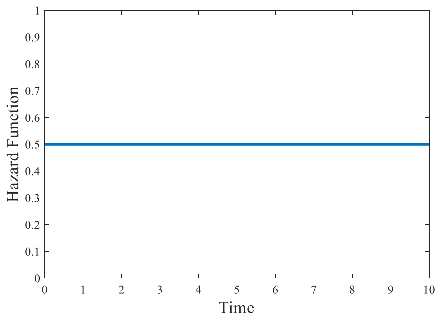
$\beta = 1.5$	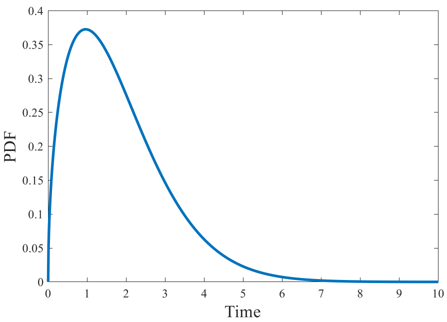	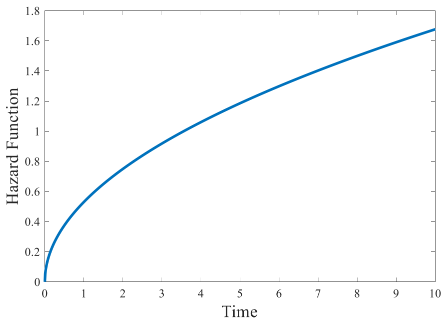

$\beta = 2$	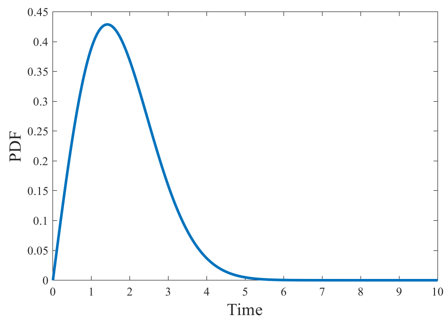	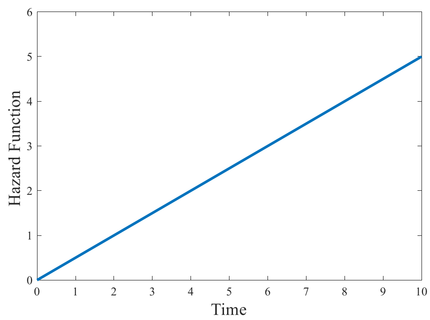
$\beta = 3$	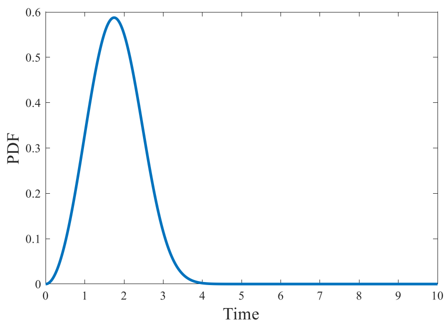	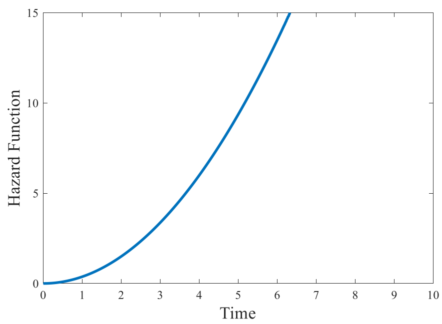

4.1.2 Component in normal operating stage

In normal operating stage, the failure and repair rates of a component are constant. The probability density functions (PDF) of in-service time $f_{up}(t)$ and out-of-service time $f_{down}(t)$ are exponential distribution:

$$f_{up}(t) = \lambda e^{-\lambda t} \tag{4-1}$$

$$f_{down}(t) = \mu e^{-\mu t} \tag{4-2}$$

where λ and μ are the failure rate and repair rate of component, respectively.

The cumulative distribution functions $Q(t)$, representing unreliability, can be calculated by integrating the PDF from time 0 to the required time *t*:

$$Q_{up}(t) = 1 - e^{-\lambda t} \tag{4-3}$$

$$Q_{down}(t) = 1 - e^{-\mu t} \tag{4-4}$$

Assuming that $R(t) = 1 - Q(t) = U$ (which can also be treated as $Q(t) = U$), where U is a random number generated from uniform distribution between 0 and 1, the up-time and down-time of a component in normal operating stage can be obtained by using the inverse transform method as illustrated in Fig. 4-6.

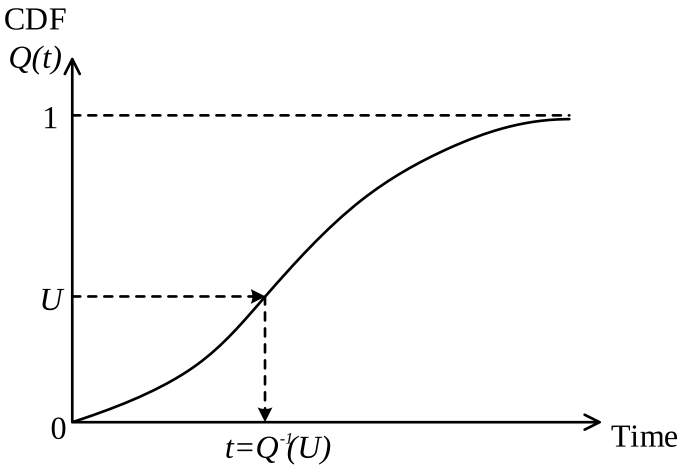

Figure 4-6: Inverse transform method [3]

$$t_{up} = -\frac{1}{\lambda}\ln(U) \tag{4-5}$$

$$t_{down} = -\frac{1}{\mu}\ln(U) \tag{4-6}$$

4.1.3 Component in Ageing Stage

In ageing stage, component has an increasing failure rate. The probability density function (PDF) of in-service time follows Weibull distribution, while PDF of out-of-service time is assumed to remain exponentially distributed. The PDF of in-service time is:

$$f(t) = \frac{\beta \cdot t^{\beta-1}}{\alpha^{\beta}} \cdot exp\,[-(\frac{t}{\alpha})^{\beta}] \tag{4-7}$$

where β is the shape parameter and α is the scale parameter. Note that $t \geq 0, \beta > 0, \alpha > 0$.

The cumulative distribution function is calculated by integrating the PDF from time 0 to the required time *t*:

$$Q(t) = 1 - exp[-(\frac{t}{\alpha})^{\beta}] \tag{4-8}$$

The cumulative reliability function can be then calculated as:

$$R(t) = 1 - Q(t) = exp[-(\frac{t}{\alpha})^{\beta}] \tag{4-9}$$

The failure rate function (or, hazard function) is the ratio of probability density function to cumulative reliability function.

$$\lambda(t) = \frac{f(t)}{R(t)} = \frac{\beta \cdot t^{\beta-1}}{\alpha^{\beta}} \tag{4-10}$$

However, it is a continuous process for the component to turn from normal operating stage into ageing stage. The component failure rate profile adapted from the bathtub curve is shown in Fig. 4-7, featured a time duration *k* when the component stays in normal operating stage before moving to ageing stage. Accordingly, the failure rate of the component in ageing stage is modified as follows:

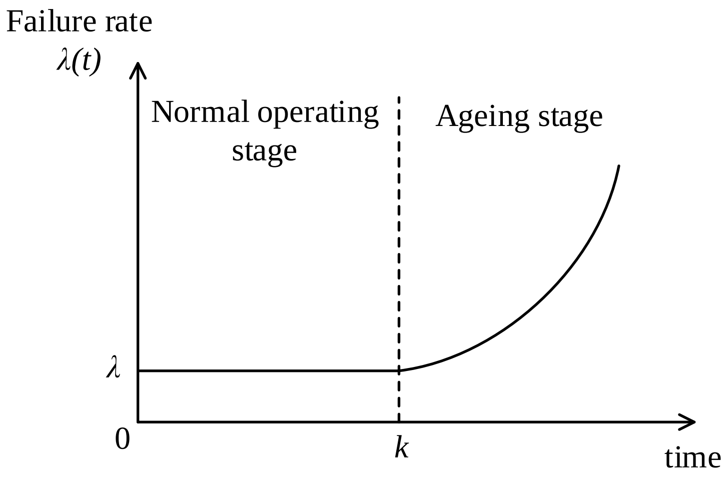

Figure 4-7: Failure rate function of component in ageing stage

$$\lambda(t) = \begin{cases} \lambda, & t \leq k \quad \text{(4-11a)} \\ \lambda + \dfrac{\beta \cdot t^{\beta-1}}{\alpha^{\beta}}, & t > k \quad \text{(4-11b)} \end{cases}$$

The cumulative reliability function can then be obtained.

$$R(t) = \begin{cases} \exp\left[-\int_0^t \lambda\, d\tau\right], & t \leq k \quad \text{(4-12a)} \\ \exp\left[-\int_0^k \lambda\, d\tau - \int_k^t \left(\lambda + \frac{\beta \cdot t^{\beta-1}}{\alpha^\beta}\right) d\tau\right], & t > k \quad \text{(4-12b)} \end{cases}$$

Assuming that $R(t) = 1 - U$, where U is a random number from uniform distribution between 0 and 1, the up-time can be solved only in a numerical way (i.e. there is no explicit solution). In ageing stage, the down-time is always calculated based on the exponential distribution.

4.1.4 Simulation Algorithm for a Component

Within the sequential Monte Carlo simulation, "behaviour" of each component in the studied interval has to be determined first. This is basically a chronological sequence of binary values 1 and 0 denoting up and down states in each hour of the simulation period. To be specific, in this research, the sampling of down-time is actually the modelling of independent failures. Failure modes are not considered. The sampling technique is developed as follows:

1. Select a component which is in up-state.
2. Two uniformly-distributed random numbers U_{up} and U_{down} between 0 and 1 are generated.
3. Time to failure (TTF, i.e. up-time) is sampled from the cumulative distribution function based on the selected lifetime distribution. For normal operating stage, component in-service time is assumed to follow exponential distribution; for ageing stage, it is assumed to follow modified Weibull distribution. Component state is set to be 1 during TTF:

$$TTF = t_{up} = Q_{up}^{-1}(U_{up}) \tag{4-13}$$

4. Time to repair (TTR, i.e. down-time) is sampled from the exponential cumulative distribution function. Component state is set to be 0 during TTR:

$$TTR = t_{town} = Q_{down}^{-1}(U_{down}) \tag{4-14}$$

5. Steps 2 to 4 are repeated over the duration of the simulation period to obtain one row of the matrix that shows status of all components within hours of the simulation period.
6. Steps 1 to 5 are repeated for all network components, including all branches and possibly generators.

The simulation procedure is illustrated in Fig. 4-8.

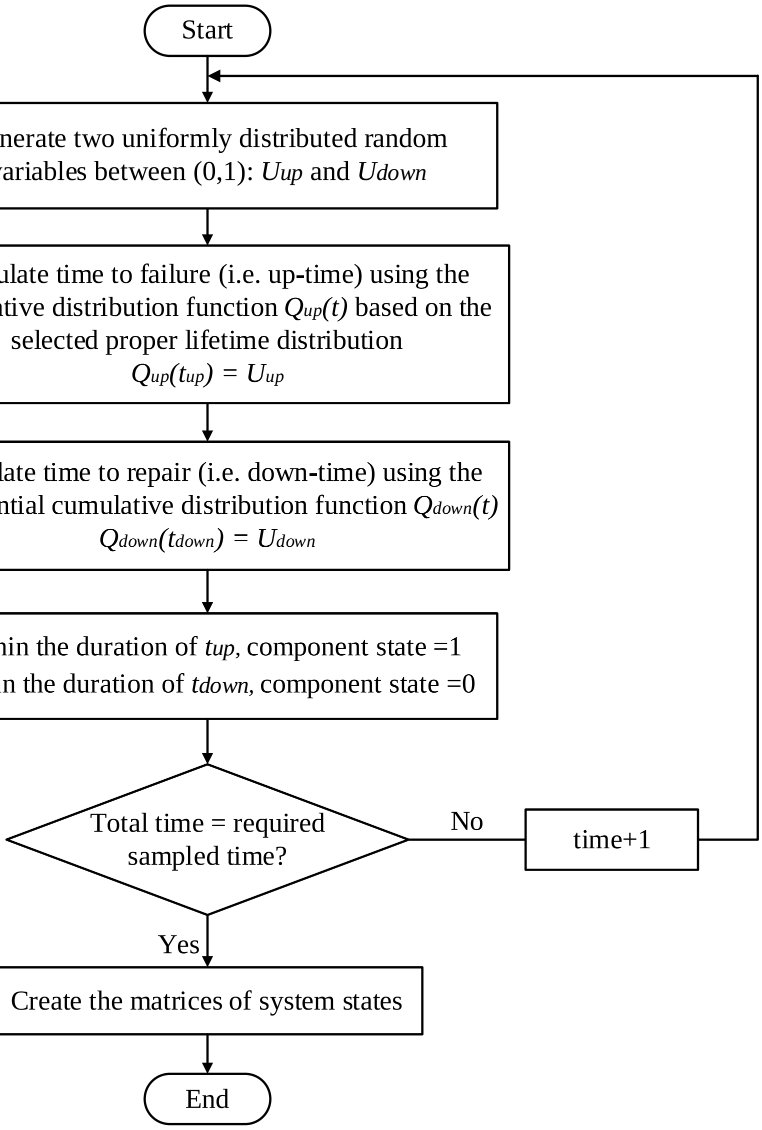

Figure 4-8: Procedure for obtaining component states using Sequential Monte Carlo simulation

4.2 Load Modelling

Load varies with time. Consequently, the load should be modelled as a time-dependent stochastic process. R Billinton and W Li proposed a dynamic hourly load model to access the system reliability [118]. The mean value of hourly loads can be calculated as follows:

$$p_i = p_w \times p_d \times p_h \tag{4-15}$$

$$P_L = P_p \times p_i \tag{4-16}$$

where p_i is the percent hourly load factor; p_w is the weekly peak load, as a percent of annual peak; p_d is the daily peak load, as a percent of weekly peak; p_h is the hourly peak load, as a percent of daily peak; P_p is the annual peak load at each bus; and P_L is the hourly load demand. Fig. 4-9 illustrates the computation procedure for finding the mean values of hourly loads.

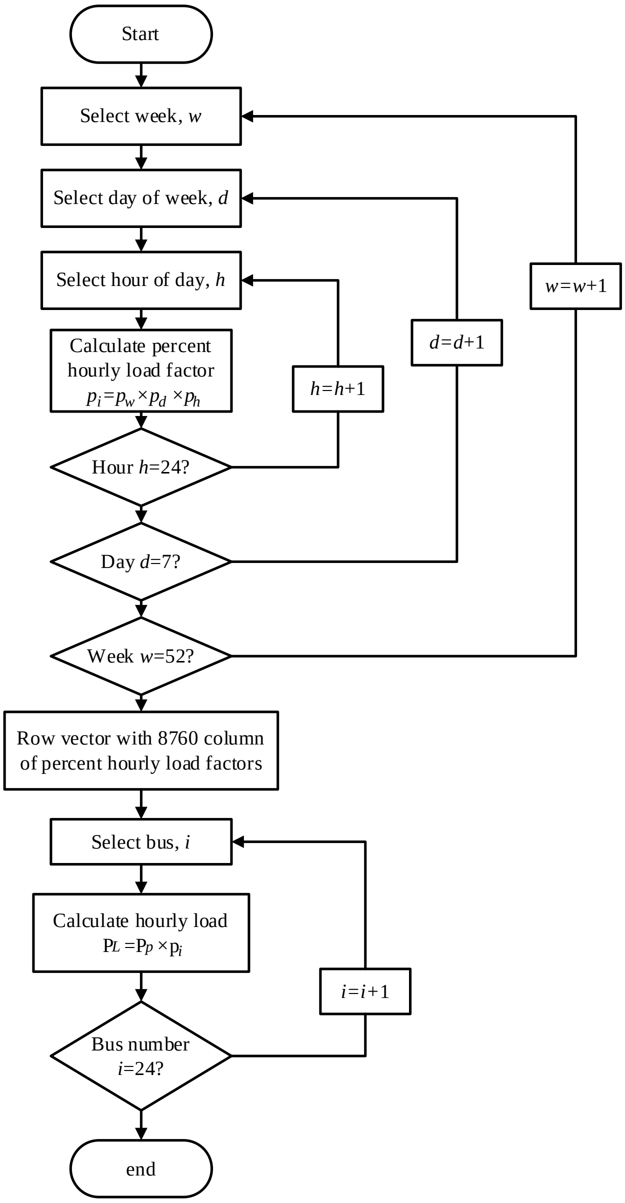

Figure 4-9: Procedure for developing hourly load profiles

It is assumed that each hourly load follows normal distribution, whose mean is defined by Eq. (4-15) and Eq. (4-16), and standard deviation is assumed to be in the range of 20%.

4.3 Models of Low Carbon Technologies -Wind Power

In a long-term perspective, wind power is a clean and reliable energy source. The principle of operation of wind power generation is that airflow through wind turbines provides mechanical power that rotates the electric generator, as described below (Fig. 4-10).

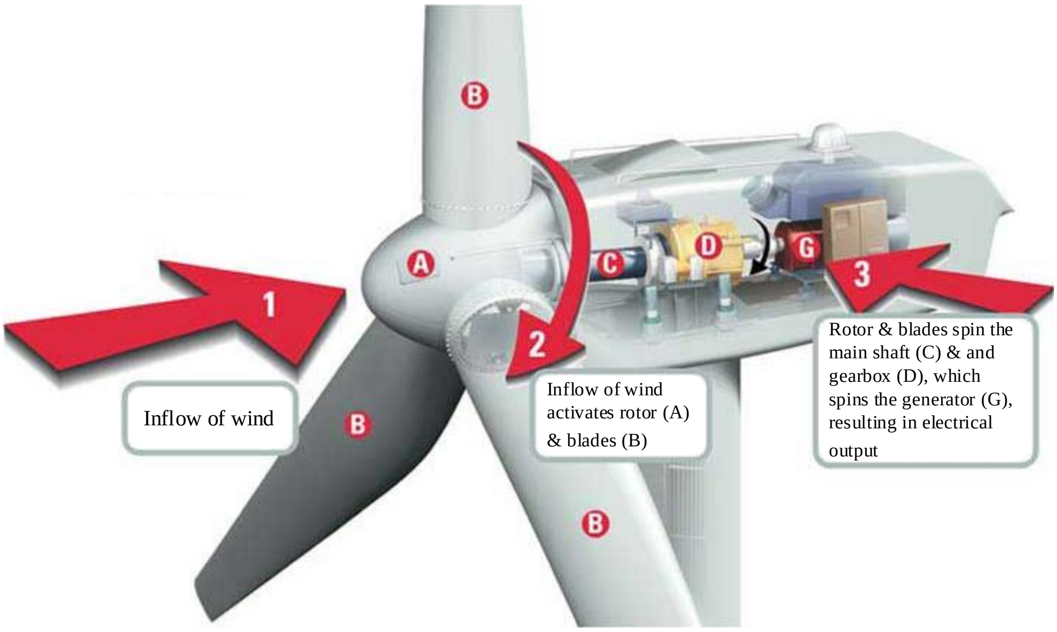

Figure 4-10: The conversion of wind energy into electricity [141]

The modelling of wind generation contains two parts:

- Wind speed modelling
- Wind power calculation

4.3.1 Wind Speed Modelling

The wind generation output is directly dependent on wind speed. Wind speed is an intermittent and non-stationary process. Therefore, an appropriate mathematical model should be developed that reflects these features. Within the probabilistic power system studies, Weibull distribution is widely used to model wind speeds when studying aggregated yearly data. In this research, sequential time intervals are studied and auto-regressive moving average (ARMA) process is adopted to find mean values of wind speeds and forecast future means [142]. In each hour, normal distribution of wind speed is assumed with a mean defined via ARMA process and standard deviation of around 15%.

Time series (ARMA model) is applied for the prediction of wind speed means. It is demonstrated that historical wind speed data can be adequately characterised by ARMA model and then the model can be used for the forecast of future wind speed means. Besides, ARMA model offers a computationally efficient scheme and has a minimum computer storage requirements [143].

ARMA model contains an Auto-Regressive (AR) model and a Moving Average (MA) model. AR model indicates the association between present data and historical data, while MA model describes the error term which is correlated to the previous observations. The general equation of ARMA model is described below:

$$y_t = \varphi_1 y_{t-1} + \varphi_2 y_{t-2} + \cdots + \varphi_n y_{t-n} + \varepsilon_t - \theta_1 \varepsilon_{t-1} - \theta_2 \varepsilon_{t-2} - \cdots - \theta_m \varepsilon_{t-m} \quad (4\text{-}17)$$

where y_t is the time series of the normalised wind speeds; φ_i means the auto-regressive parameter; θ_i means the moving average parameter; ε_t is the white noise which is in normal distribution with zero mean value and variance σ_ε^2.

The hourly wind speed data needs to be collected and then fitted into ARMA model to obtain the forecast data. The first stage is to make the wind stochastic process stationary which is given below.

$$y_t = \frac{v_t - \mu}{\sigma} \quad (4\text{-}18)$$

where μ and σ are the mean value and standard deviation of the all observed wind speed data respectively; v_t is the observed wind speed; y_t is the time series of the normalised wind speeds that are modelled with the ARMA model.

It is essential to select a proper AR order and MA order (i.e. parameters *p, q* respectively) when modelling the hourly wind speed. Decision criteria such as AIC (Akaike Information Criterion), BIC (Bayesian Information Criterion), FPE (Final Prediction Criterion), MSE (Mean Square Error) and RMSE (Root Mean Squared Error) are used to determine the best AR and MA orders [144].

The following table shows the determination of p and q using RMSE method, with the same wind speed data collected as in [145]. This method measures how well the model's response matches the historic data and the results are expressed as a percentage (Fit Percent). Higher Fit Percent implies more accurate model. In this case, the best result is obtained for $p = 4$ and $q = 4$.

Table 4-2: The results of RMSE for each pair of AR order (*p*) and MA order (*q*) in wind speed simulation

p \ q	1	2	3	4	5
1	64.7608	64.7650	64.7922	64.7927	64.7935
2	64.7769	64.7771	64.7930	64.8782	64.7970
3	64.7770	64.7845	64.8206	65.4837	64.7955
4	64.7938	64.7939	65.3476	65.4854	65.3087
5	64.7939	65.3666	64.6155	65.4730	65.4684

With proper values of p and q, wind speed can be sampled by fitting the collected data into ARMA model. An example of sampled results is presented in the Fig. 4-11.

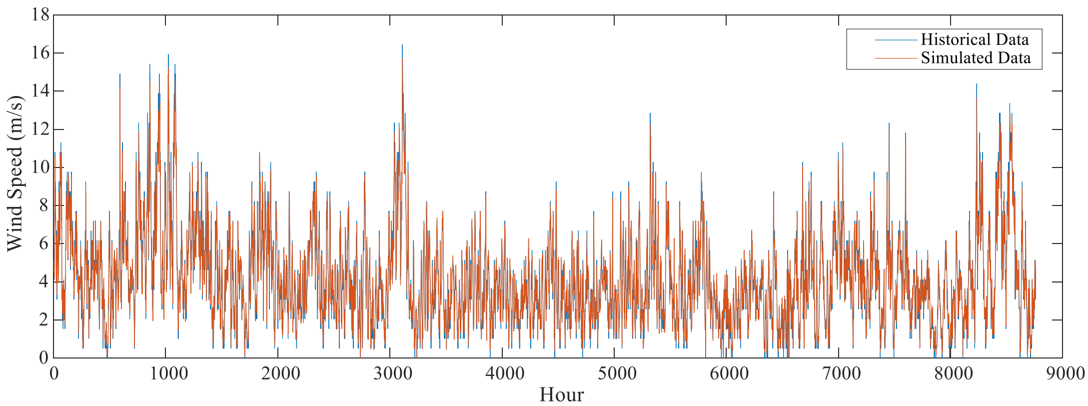

Figure 4-11: Historical and simulated hourly wind speed using ARMA model

4.3.2 Wind Power Calculation

The wind turbine output power is required after obtaining randomly sampled wind speeds. The power curve of a typical wind turbine is shown in Fig. 4-16. Wind output is related to four parameters: cut-in speed (v_{ci}), rated wind speed (v_r), cut-out speed (v_{co}) and maximum output power (P_r). With v_t representing the wind speed at time t, the wind turbine operation can be classified into the following four stages [146]:

- $v_t \leq v_{ci}$

The wind speed is too low to rotate the blades. The wind turbine does not produce any power.

- $v_{ci} < v_t < v_r$

  The wind turbine starts to generate power. The output power goes up steadily until v_t reaches v_r.
- $v_r \leq v_t < v_{ci}$

  The output is limited at the rated power P_r.
- $v_t \geq v_{co}$

  The wind speed is so strong that the turbine may be damaged. Therefore, v_{co} is set to define the safe operating region. When v_t exceeds v_{co}, the turbine is shut down.

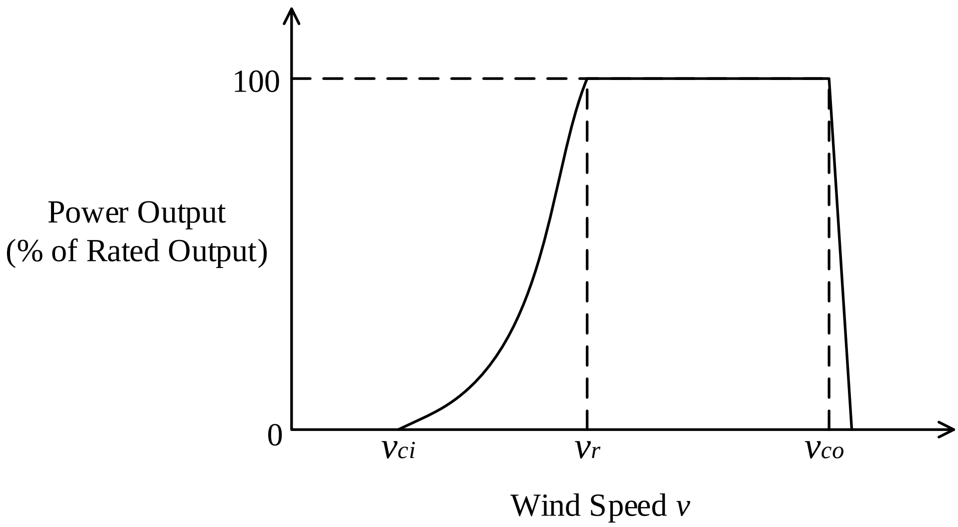

Figure 4-12: Typical wind turbine power curve [146]

The wind turbine power curve is mathematically presented as follows:

$$P = \begin{cases} 0 & v_t \leq v_{ci} \\ (A + Bv_t + Cv_t^2)P_r & v_{ci} < v_t < v_r \\ P_r & v_r \leq v_t < v_{co} \\ 0 & v_t \geq v_{co} \end{cases} \tag{4-19}$$

The coefficients *A*, *B* and *C* can be calculated by using the following equations [146]:

$$A = \frac{1}{(v_{ci} - v_r)^2}[v_{ci}(v_{ci} + v_r) - 4v_{ci}v_r(\frac{v_{ci} + v_r}{2v_r})^3] \tag{4-20}$$

$$B = \frac{1}{(v_{ci} - v_r)^2} [4(v_{ci} + v_r) \left(\frac{v_{ci} + v_r}{2v_r}\right)^3 - (3v_{ci} + v_r)]$$

$$C = \frac{1}{(v_{ci} - v_r)^2} [2 - 4 \left(\frac{v_{ci} + v_r}{2v_r}\right)^3]$$

4.4 Spatial Correlation

Wind speeds and load demands are spatially correlated. The standard probabilistic concept with no correlation is not able to present the real behaviour of the network [147]. Reference [147] also pointed out that there exists an impact from the correlation on system reliability. Therefore, the impact of correlation needs to be analysed.

4.4.1 Overview of Correlation Analysis

Correlation is a mutual relationship between two quantitative variables. The strength of the relationship can be statistically assessed by correlation analysis [148][149]. Fig. 4-17 shows three types of correlation. For the two variables *X* and *Y*, if there is no relation between *X* and *X*, the situation can be defined as no correlation; if there is correlation, it can be either positive or negative [149]. For positive correlation, both variables increase, whilst for negative correlation, *Y* reduces while *X* increases and vice versa.

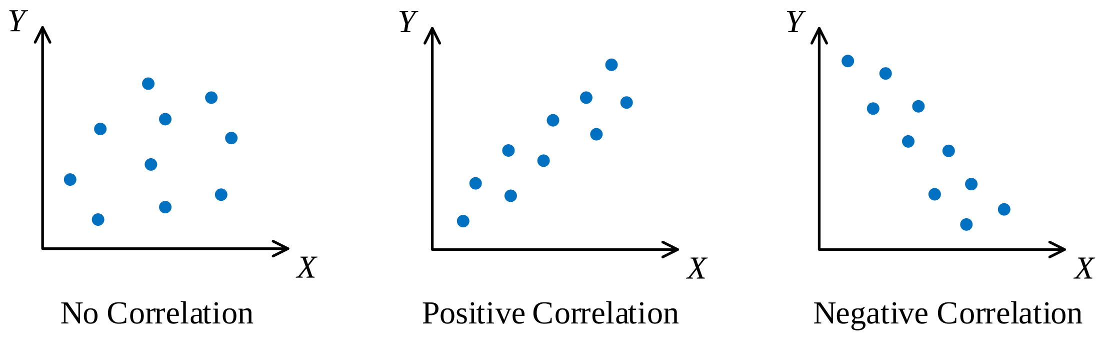

Figure 4-13: Types of correlation [149]

In correlation analysis, correlation coefficient is the measure of correlation degree and ranges from -1 to +1. It can be categorised into three segments [150]:

- Negative value indicates negative correlation. Values between -1 and 0 means a partial correlation, and -1 reflects the strongest ("full") negative correlation.
- 0 means the absence of correlation.

- Positive value indicates positive correlation. Values between 0 and +1 means a partial correlation, and +1 reflects the strongest positive correlation.

The correlation coefficient $\rho_{X,Y}$ between two variables *X* and *Y* is defined as:

$$\rho_{X,Y} = \frac{cov(X,Y)}{\sigma_X \sigma_Y} \tag{4-21}$$

where σ_X and σ_Y refer to standard deviation of variables *X* and *Y* respectively, and $cov(X,Y)$ means covariance which can be calculated using the equation below:

$$cov(X,Y) = E[(X - E(X))(Y - E(Y))] \tag{4-22}$$

where *E* refers to the expected value calculation of the considered variables (for example, *E(X)* is the expected value of *X*, also known as the mean of *X*).

Moreover, for a model consisting of *n* variables, the correlation coefficients can be built as a correlation matrix shown below:

$$\boldsymbol{\rho} = \begin{pmatrix} \rho_{11} & \rho_{12} & \cdots & \rho_{1n} \\ \rho_{21} & \rho_{22} & & \rho_{2n} \\ \vdots & & \ddots & \vdots \\ \rho_{n1} & \rho_{n2} & \cdots & \rho_{nn} \end{pmatrix} \tag{4-23}$$

Further calculations and analyses are based on the correlation coefficient matrix. Details of obtaining correlated results are presented in the following chapter (Chapter 4.4.2).

Three techniques are introduced as the methods of analysing correlation problems: a) Nataf transformation; b) Polynomial normal transformation; and c) Copula theory [136]. These techniques are compared in [151], and the comparisons are performed based on Cholesky decomposition, Nataf transformation in conjunction with Cholesky decomposition and Copula theory, respectively. The results show that Copula theory provides the highest accuracy. However, it also requires the longest computational time because there are complicated functions that need to be determined in each step. The results of Nataf transformation can still be accepted although they are less accurate.

In power system, the effects of correlation have been widely studied mainly by analysing probabilistic power flow. The studies primarily focus on power systems with renewable energy such as wind and solar, and investigate stability, generation adequacy and impact on transmission planning [152]-[154].

4.4.2 Correlation Decoupling Technique

Nataf transformation in conjunction with Cholesky decomposition is widely used to model the correlation. The basic idea is to use correlation matrix from standard normal deviates to generate correlated random vector. For n correlated input parameters, the vectors of the input (correlated) parameters and means are:

$$\boldsymbol{p} = (p_1 \quad \cdots \quad p_n)^T \tag{4-24}$$

$$\boldsymbol{\mu_p} = (\mu_1 \quad \cdots \quad \mu_n)^T \tag{4-25}$$

Then the variance-covariance matrix is:

$$\boldsymbol{C_p} = \begin{pmatrix} \sigma_1^2 & \sigma_{12} & \cdots & \sigma_{1n} \\ \sigma_{21} & \sigma_2^2 & & \sigma_{2n} \\ \vdots & & \ddots & \vdots \\ \sigma_{n1} & \sigma_{n2} & \cdots & \sigma_n^2 \end{pmatrix} \tag{4-26}$$

where σ_i^2 is the variance of the i^{th} input parameter and σ_{ij} means the covariance between the i^{th} and j^{th} inputs.

The correlation matrix can also be written in normalized form giving the correlation coefficient matrix:

$$\boldsymbol{R} = \begin{pmatrix} 1 & r_{12} & \cdots & r_{1n} \\ r_{21} & 1 & & r_{2n} \\ \vdots & & \ddots & \vdots \\ r_{n1} & r_{n2} & \cdots & 1 \end{pmatrix} \tag{4-27}$$

where $r_{ij} = \frac{\sigma_{ij}}{\sigma_i \sigma_j}$, means correlation coefficient, which can be calculated from Eq. (4-21).

Standardization of the correlated input parameters needs to be done based on standard normal distribution:

$$\boldsymbol{p}' = \frac{\boldsymbol{p} - \boldsymbol{\mu_p}}{\sqrt{\boldsymbol{D_p}}} \tag{4-28}$$

where $\boldsymbol{p}'$ is the vector of standardized input parameters; $\boldsymbol{D_p} = diag(\sigma_1^2, \dots, \sigma_n^2)$ are variances of input parameters. Consequently, $\boldsymbol{p}'$ will be a vector with zero mean and unit standard deviation. Based on Eq. (4-21) and Eq. (4-22), the variance-covariance matrix of standardized inputs can be expressed as:

$$\boldsymbol{C_{p'}} = \begin{pmatrix} 1 & \rho_{12} & \dots & \rho_{1n} \\ \rho_{21} & 1 & & \rho_{2n} \\ \vdots & & \ddots & \vdots \\ \rho_{n1} & \rho_{n2} & \cdots & 1 \end{pmatrix} \tag{4-29}$$

The correlation coefficients can be calculated as $r_{ij} = \frac{\sigma_{ij}}{\sigma_i \sigma_j}$, which is denoted as ρ_{ij} in matrix $\boldsymbol{C_{p'}}$. Thus, the matrix $\boldsymbol{C_{p'}}$ is also called correlation coefficient matrix and is renamed $\boldsymbol{R_p}$ (i.e. $\boldsymbol{R_p} = \boldsymbol{C_{p'}}$). Note that the matrix is only possible when all inputs are normally distributed. For other distributions, transformation needs to be done before applying these equations. Transformed correlation coefficient matrix is:

$$\boldsymbol{R_y} = \begin{pmatrix} 1 & \rho'_{12} & \dots & \rho'_{1n} \\ \rho'_{21} & 1 & & \rho'_{2n} \\ \vdots & & \ddots & \vdots \\ \rho'_{n1} & \rho'_{n2} & \cdots & 1 \end{pmatrix} \tag{4-30}$$

$$\rho'_{ij} = G(\rho_{ij}) \cdot \rho_{ij} \tag{4-31}$$

where $G(\rho_{ij})$ is the multiplicative function. Details how to calculate $G(\rho_{ij})$ are given in Table 4-3.

Table 4-3: Multiplicative function of different distributions [155]

Distribution of *i*	Distribution of *j*	Multiplication Factor $G(\rho_{ij})$
Normal	Normal	1

Weibull	Weibull	$1.063 - 0.004\rho_{ij} - 0.200(\gamma_i\gamma_j) - 0.001\rho_{ij}^2 + 0.337(\gamma_i^2 + \gamma_j^2) + 0.007\rho_{ij}(\gamma_i + \gamma_j) - 0.007\gamma_i\gamma_j$

In this table, $\gamma_i = \frac{\sigma_i}{\mu_i}$ and $\gamma_j = \frac{\sigma_j}{\mu_j}$ denote the variance coefficients of variable p_i and p_j respectively.

In most engineering applications, matrix $\boldsymbol{R_y}$ is positive definite. Therefore, Cholesky decomposition can be applied to decompose $\boldsymbol{R_y}$, which is presented below:

$$\boldsymbol{R_y} = \boldsymbol{LL^T} \tag{4-32}$$

where $\boldsymbol{L}$ is a lower triangular matrix.

Then a vector of *mutually independent* standard normal random variables *w* can be used to generate the correlated standard normal variables *y*:

$$\boldsymbol{y} = \boldsymbol{Lw} \tag{4-33}$$

Since the equations above are based on standard normal distribution, the correlated standard normal variables *y*, however, need to be transformed from standard normal distribution to its original distribution. The transformation is applied with the aid of cumulative distribution functions (CDF). The methodology is presented in Fig. 4-18.

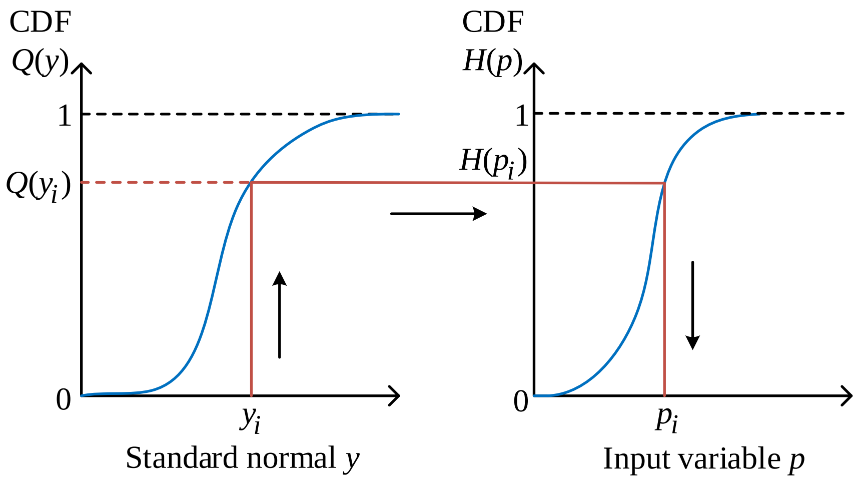

Figure 4-14: Transformation of standard normal variables y

Here, $Q(y)$ is the cumulative distribution function of the correlated results y (standard normal distributed variables) and $H(p)$ is the cumulative distribution function of the input parameters p. The mathematical equation is shown below.

$$p_i = H^{-1}[Q(y_i)] \tag{4-34}$$

4.4.3 Simulation Algorithm

Correlation model is applied to wind speeds at each location and load demands at each bus, for each hour over one year. This means that the wind speeds and load demands are spatially correlated in each time slot, but not in time. The basic idea of correlation modelling is given below:

- Apply Cholesky decomposition to the known correlation coefficient matrix.
- Generate a sample of independent input parameters that follow standard normal distributions.
- Correlate the generated sample of independent standard normal input parameters.
- Perform a transformation of correlated results into the correlated input parameters, which follow the original distribution.

The algorithm is applied to hourly wind speeds and load demands. The procedure is described as follows:

1. For a network with n wind farms/load demands, define the vector of input variables p. The dimension of p is $n \times 1$.

2. Define the correlation coefficient matrix $C_{p'}$, wherein the $n \times 1$ vector p' is standard normal. The assumed values of each correlation factors in $C_{p'}(i, j)$ are presented in the Table 4-4. Note that the dimension of $C_{p'}$ is $n \times n$.

Table 4-4: Correlation factors of different correlation levels

Correlation Level	**Wind Speeds/ Load Demands in The Same Region**	**Wind Speeds/ Load Demands in Different Regions**
Zero	0	0
Partial	0.8	0.5
Full	1	1

3. Build the correlation matrix R_y by using the multiplication factor. Subscript y denotes new correlated parameters which follow the original distributions of input parameters. More specifically:
   - For load demands at nodes i and j, the original distribution is assumed to be normal distribution. Therefore, all the multiplication factors $G(\rho_{ij})$ is 1.
   - For wind speeds, it is firstly forecast by AMAR model the fit into normal distribution. The multiplication factors $G(\rho_{ij})$ is 1.
4. Apply Cholesky decomposition to R_y. Lower triangular matrix L can be obtained consequently.
5. Generate n independent random standard normally distributed variables, and record in the form of $n \times 1$ vector w_s.
6. Calculate the correlated sampled parameters by using relation $y_s = L \cdot w_s$.
7. Transform y_s to the original distribution.

   Assume load demands follow normal distribution. It is only necessary to return to the original domain from the standardized normal domain by using the following equation:

$$x(i) = z(i)\sigma(i) + \mu(i) \qquad i = 1, 2, \dots, n \tag{4-35}$$

   where $x(i)$ is the active load/ wind speed at point i; $z(i)$ is the standardized normally distributed result, which is in fact the correlated value $y(i)$; $\sigma(i)$ is the standard deviation of active load/ wind speed at point i. In this research, it is assumed that $\sigma(i) = 5\% \cdot \mu(i)$; $\mu(i)$ is the average active load/ wind speed at point i. For load, it is calculated by multiplying annual peak load and hourly load factor.

8. Calculate reactive power at each load point by using the following equation.

$$q(i) = x(i) \cdot \frac{Q(i)}{P(i)} \tag{4-36}$$

where $q(i)$ is the reactive power at load point i; $x(i)$ is the active load at load point i; $P(i)$ is the annual peak active demand at load point i; $Q(i)$ is the annual peak reactive demand at load point i. Note that Eq. (4-40) is a simplified assumption as it does not go deep to reactive power load composition and curtailment prioritization at each individual node.

The flowcharts in Fig. 4-19 and Fig. 4-20 illustrate the computation procedures for modelling spatially correlated hourly wind powers and hourly loads considering the correlation of wind speeds and load demands. The procedures are incorporated within the sequential Monte Carlo simulation.

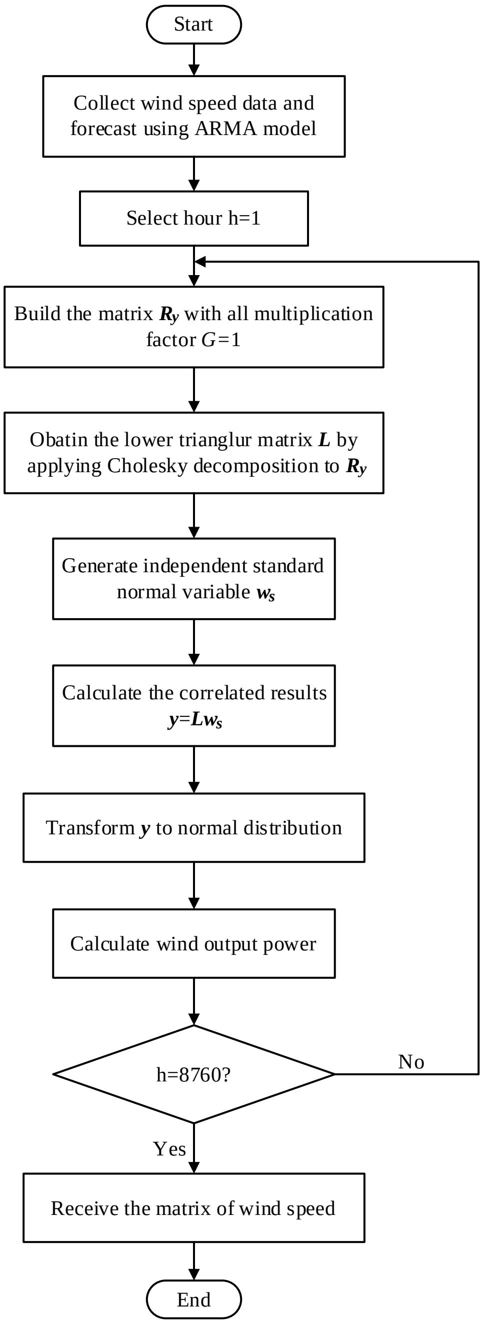

Figure 4-15: Procedure for modelling wind output considering the correlation of wind speeds

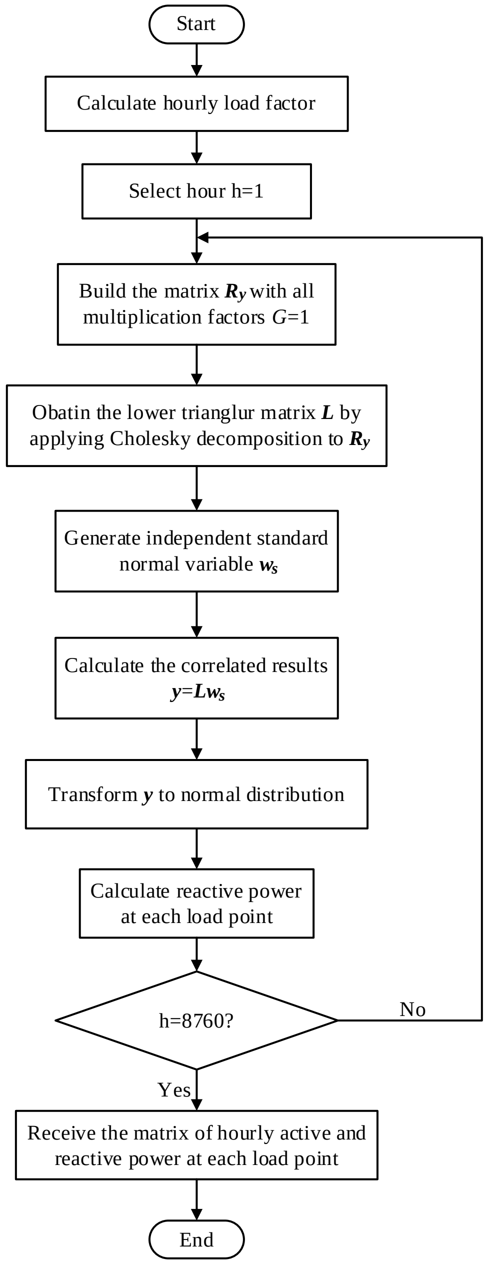

Figure 4-16: Procedure for modelling the correlation of load demands

4.5 Optimal Power Flow Model – MLC Model

Optimal Power Flow (OPF) model is an optimization problem that optimizes the operation of a power system within limits imposed by engineering constraints and electrical laws. The main principle is to minimize the objective function by modifying the controllable variables of the system. Carpentier first proposed OPF model as a further development of the optimal Economic Dispatch (ED) problem (i.e. all generators connected to a single node system), by incorporating the nodal power flow equations in the ED formulation [156]. Today, there are several types of OPF models that are still based on the power flow equations and a set of inequality constraints [157].

The optimization problem is formulated as an objective function with power flow equations and physical inequality constraints (i.e. limitations). The transmission system is modelled as a system with *N* buses connected by *L* branches, and controllable generators are located at *G* buses ($G \subseteq N$). The objective is to minimize the total cost of power generation while maintaining network security. The classic form of the formulation is represented below.

The objective function is:

$$min \sum_{i \in G} C_i(P_i^G) \tag{4-37}$$

The constraints are:

$$\sum_j p_{ij}(V, \delta) = P_i^G - P_i^L \qquad \forall i \in N \tag{4-38}$$

$$\sum_j q_{ij}(V, \delta) = Q_i^G - Q_i^L \qquad \forall i \in N \tag{4-39}$$

$$P_i^{G,min} \leq P_i^G \leq P_i^{G,max} \qquad \forall i \in G \tag{4-40}$$

$$Q_i^{G,min} \leq Q_i^G \leq Q_i^{G,max} \qquad \forall i \in G \tag{4-41}$$

$$V_i^{min} \leq V_i \leq V_i^{max} \qquad \forall i \in N \tag{4-42}$$

$$\sqrt{p_{ij}^2 + q_{ij}^2} \leq S_{lim} \tag{4-43}$$

Where, at bus i, P_i and Q_i are real power and reactive power injection; p_{ij} and q_{ij} are the real and reactive power flow between bus i and j; P_i^G and Q_i^G are real power and reactive power produced by generators; V_i and δ_i are voltage magnitude and angle; P_i^L and Q_i^L are the load; S_{lim} is thermal limit on apparent power at both terminal buses.

In particular, for reliability assessment, the OPF model needs to be modified by including the load curtailments R_i. In such a case, the objective is to minimize the load curtailment at all nodes. The objective function can be written as follows, where ω_i is the load curtailment weighting factor.

$$min \sum_{i \in N} \omega_i R_i \tag{4-44}$$

The constraints can be represented as follows:

$$\sum_j p_{ij}(V,\delta) = P_i^G - P_i^L + R_i \qquad \forall i,j \in N \tag{4-45}$$

$$\sum_j q_{ij}(V,\delta) = Q_i^G - Q_i^L + R_i \frac{Q_i^L}{P_i^L} \qquad \forall i,j \in N \tag{4-46}$$

$$P_i^{G,min} \leq P_i^G \leq P_i^{G,max} \qquad \forall i \in G \tag{4-47}$$

$$Q_i^{G,min} \leq Q_i^G \leq Q_i^{G,max} \qquad \forall i \in G \tag{4-48}$$

$$V_i^{min} \leq V_i \leq V_i^{max} \qquad \forall i \in N \tag{4-49}$$

$$0 \leq R_i \leq P_i^L \qquad \forall i \in N \tag{4-50}$$

$$\sqrt{p_{ij}^2 + q_{ij}^2} \leq S_{lim} \tag{4-51}$$

here $R_i$is the load curtailments at bus i; p_{ij} and q_{ij} are the real and reactive power flow between bus i and j; other variables are introduced above.

4.6 Simulation Algorithm

The simulation algorithm containing the modelling blocks is presented in the Fig. 4-21.

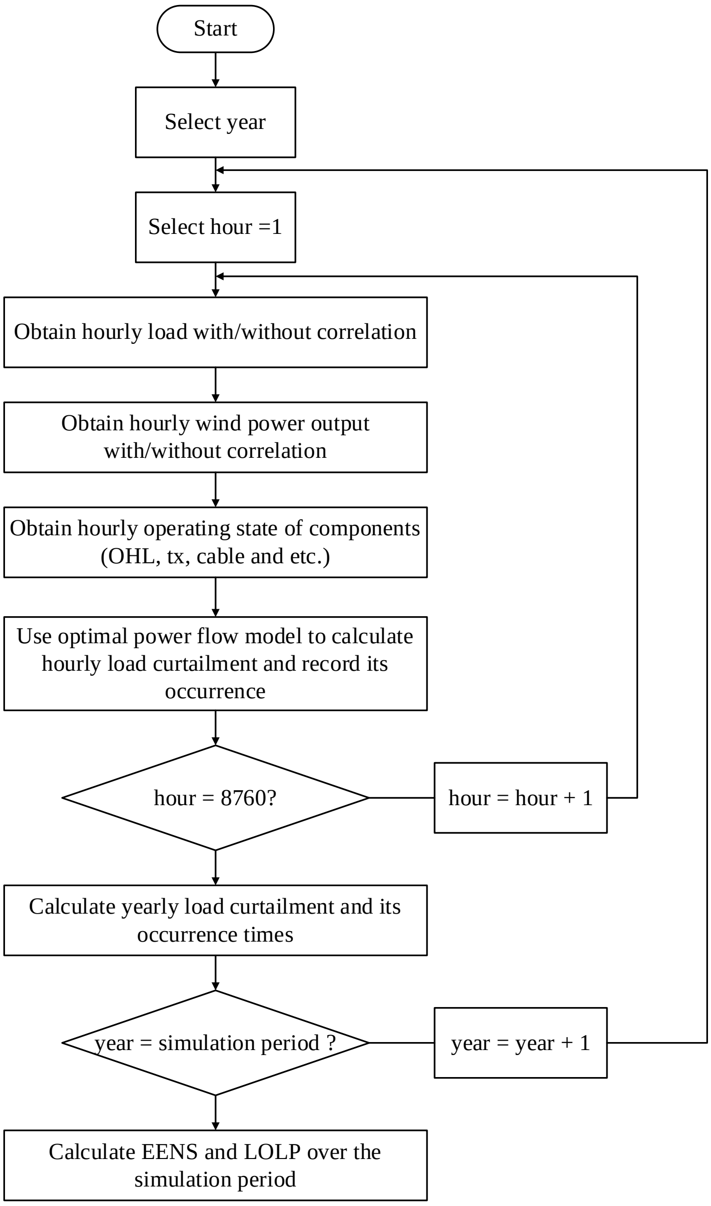

Figure 4-17: Procedure for obtaining system reliability indices over a given simulation period

4.7 Chapter Summary

This chapter gives the modelling of the input blocks in power system reliability study. The input blocks in this project are: component operating states, load demand, LCTs generation and wind/load correlation effect. Sequential Monte Carlo simulation is developed to access the chronological operating states of the network, whose components can be in either normal operating stage, or ageing stage. In normal operating stage, exponential distribution is used to reflect the component failure rate with in-service time; in ageing stage, a modified Weibull distribution is developed to reflect more realistic features of the ageing stage. A dynamic hourly load model is adopted to model the load demand. For LCTs, the models for wind power generation and solar generation are introduced. Some of modelling results are also given in this chapter.

The methodology and models for the correlated inputs, such as wind generation and load demand, are introduced. Nataf transformation in conjunction with Cholesky decomposition is used to analyse the correlation effect.

Optimal power flow model with the reliability objective function is used to minimize the load curtailments at all nodes. This chapter gives a brief introduction of the OPF model and the expressions of the objective function and corresponding constraints. The reliability indices used to express the system reliability are calculated using this model.

CHAPTER 5 ASSET HEALTH CONDITION

The asset health is a result of a series of factors, ranging from the asset's loading condition to its geographical location. The factors can affect the durability or service life of any component, as well as its operational performance and future failure rate [158]. The asset condition is measured by Asset Health Index (AHI), which can be either integer or decimal number; the latter is also called Asset Health Score. The common point between asset health and network analysis is reliability analysis, whereby asset health is incorporated within failure rate functions (or, hazard functions). Asset health can be modelled using either deterministic approach or the proposed probabilistic approach.

5.1 Reliability Analysis Involving Asset Health

Reliability analysis of power system refers to the study of the probability that a system, under the formulated operating conditions, operates satisfactory within a specified period of time without failures. It requires proper selection of probability distributions of in-service and out-of-service times for each asset, which then define temporal hazard functions [159]. The standard approach does not involve asset conditions, just the temporal aspect. However, when replacement/maintenance plans are considered in the analysis, a more realistic model is required, whereby asset failure rate functions need to identify asset ageing conditions and influences of different interventions [160]. One of the early attempts was made in the Cox's proportional hazard model (PHM) [129], which models external (or, exogenous) variables and which has been used in several studies [161][162].

The concept of health indices (HI) has been introduced in the UK utilities to consider asset conditions and utilize it to select appropriate asset interventions, such as replacements and repairs [131][163]. Asset HI is defined as a deterministic score summarizing the asset condition which can reflect the asset characteristics and environment parameters. There are further developments of the approaches for deterministic HI modelling in several studies [164]-[166]. Nevertheless, there is a high level of uncertainty in determining asset health scores due to subjectivity in determining the values of impact factors, for example, environmental parameters. Consequently, fuzzy-based approaches for calculation have been developed in [167] and [168] and probabilistic analysis has been studied in [169], mainly for transformer HIs. However, a general probabilistic HI approach has not been developed so far; that is the main contribution of this research.

5.2 Deterministic Health Index Approach

A deterministic health index approach is developed based on DNO Common Network Asset Indices Methodology [131]. This approach includes a universal methodology for asset health calculation that is applied by all UK DNOs. The calculation is specified by asset types [131].

5.2.1 Asset Classification

According to the DNO Common Network Asset Indices Methodology [69], there are three levels of asset types. Table 5-1 presents an example of asset classification for 132kV towers. The entire table is given in Table 1 in Appendix [131].

Table 5-1: An example of asset classification for 132kV towers [131]

Asset Category	Subcomponent	Observed Condition
132kV Towers	Tower Steelwork	1. Tower Legs 2. Bracings 3. Crossarms 4. Peak
	Tower Paintwork	Paintwork Condition
	Foundations	Foundation Condition

5.2.2 DNO Overall Approach

According to the DNO Common Network Asset Indices Methodology, calculation of asset indices consists of three stages:

- Health Index
  It is determined from Asset Health and Probability of Failure (PoF).
- Criticality Index

It is relevant for Consequences of Failure (CoF).

- Risk Index

  It relates to the combination of the above indices.

The diagram of Fig. 5-1 shows the global calculation process. The risk of condition-based failure, related to individual assets, is the output of PoF and CoF. In the methodology, PoF shows the probability of condition-based failure on a yearly basis and CoF shows the influence of failure, described as a monetised value. The final output Risk Matrix is formed by Health Index Band (column) and Criticality Index Band (row). Each individual asset can be assigned a position within the Risk Matrix.

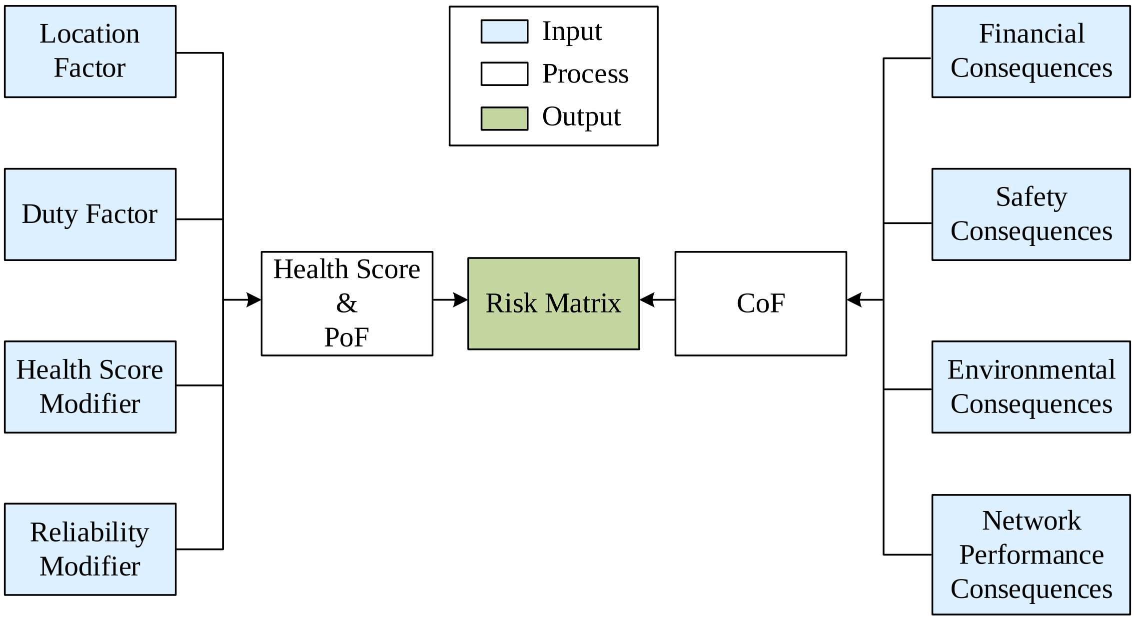

Figure 5-1: Calculation process overview of DNO methodology [131]

Note that this DNO document specifies a general approach to assess the condition-based risk of distribution assets. In this research, this methodology is extended to assets in transmission network. The main task is to obtain failure rate functions (or, hazard functions) from PoF calculation (left-hand side in Fig. 5-1) and then incorporate the failure rate functions into Sequential Monte Carlo Simulation. Failure rate functions are dependent on asset health scores, which are in turn dependent on several factors of influence.

Failure rate function is approximated with the PoF, which is a polynomial function of the Health Score (in fact, third order Taylor expansion of exponential function). Health Score needs to be calculated within three phases consisting of multiple steps: a) Initial Health Score is an exponential function of the asset age using the initial ageing rate; b) Current Health Score is a function of the Initial Health Score and modification factors; and c) Future Health Score is an exponential function of the Current Health Score, current ageing rate and time in future. The diagram of Fig. 5-2 shows the calculation steps.

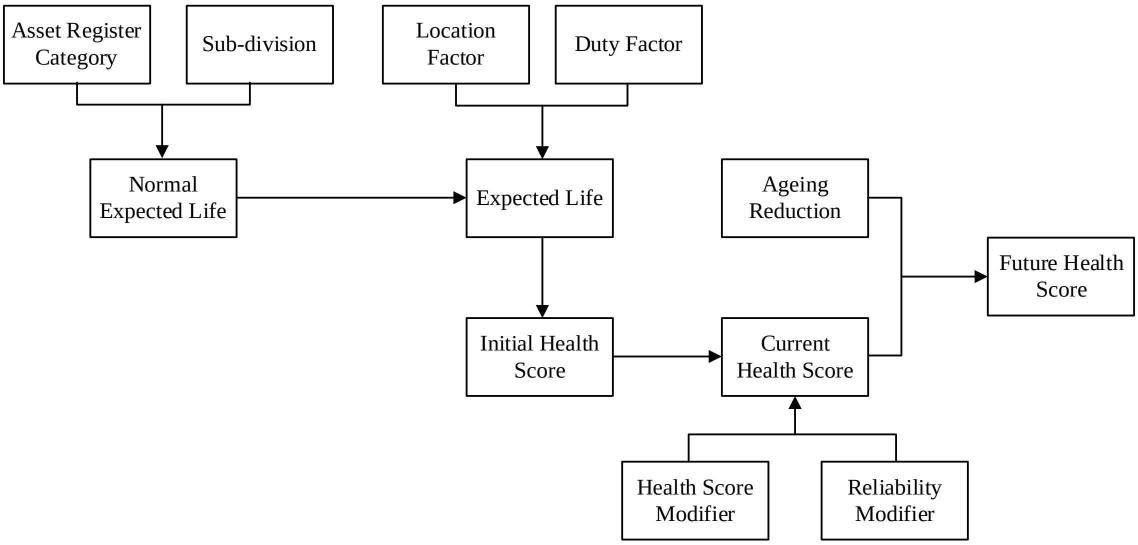

Figure 5-2: Calculation of Health Score [131]

The failure rate (in this case PoF) function is a function of the Health Score. Future Health Score is replaced into the PoF function to get Future PoF. Fig. 5-3 shows the shape of a typical PoF (or, failure rate) curve. The PoF function is defined as:

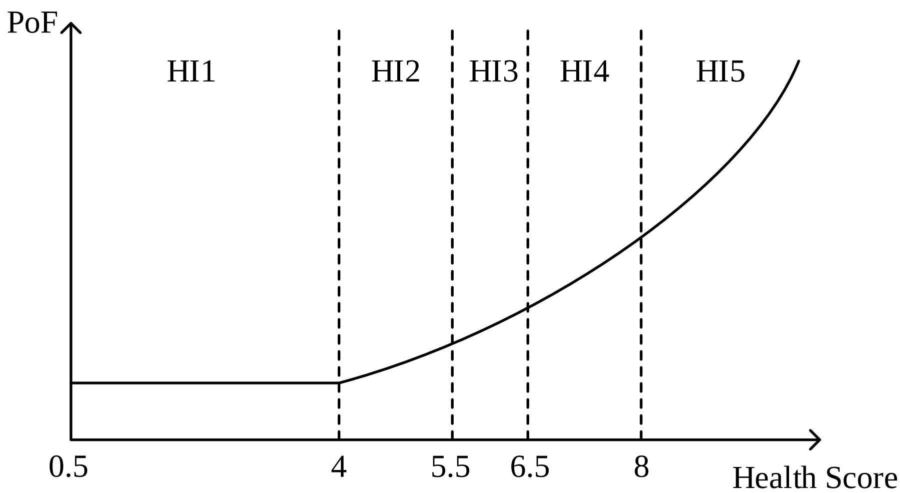

Figure 5-3: PoF curve [131]

$$PoF = K \times [1 + (C \times HS) + \frac{(C \times HS)^2}{2!} + \frac{(C \times HS)^3}{3!}] \tag{5-1}$$

where HS is Health Score (Current or Future); *K* and *C* are constants of the PoF curve. Eq. (5-1) is valid for $HS > 4$, otherwise $HS = 4$ when $HS \leq 4$. Specifically, the shape of the curve is defined by *C*, whilst *K* value scales the value of PoF. The values of *C*, *K* and Health Score limit are presented in Table 2 in Appendix.

The procedure for the PoF calculation is illustrated by the following steps [131]:

1. Normal Expected Life

   It is defined as the age (in years) of an asset when the first critical signs of deterioration occur. It is dependent on the Asset Register Category and sub-category. The specific values are listed in Table 3 in Appendix.

2. Expected Life

   It is determined from Normal Expected Life, while taking two factors into account: Location Factor (LF) and Duty Factor (DF). Location Factor reflects the influences of the surroundings and environment on the asset. Duty Factor refers to any further ageing caused by the way the asset is being applied (e.g. high loading, frequent switching, etc.). Expected Life is obtained using the following equation:

$$Expected\ Life = \frac{Normal\ Expected\ Life}{LF \times DF} \tag{5-2}$$

3. Initial Ageing Rate (β_1)

   It is assumed that the asset deterioration process (e.g. insulation breakdown, corrosion, etc.) is exponential function between the asset installation (new asset) and asset retirement at the Expected life. The Ageing Rate of the asset is then determined as:

$$\beta_1 = \frac{ln\,(\frac{H_{expected\ life}}{H_{new}})}{Expected\ Life} \tag{5-3}$$

where $H_{expcted\ life}$ is the Health Score of the asset when its age is Expected Life, $H_{expcted\ life} = 5.5$; H_{new} is the Health Score of the new asset, $H_{new} = 0.5$.

4. Initial Health Score (IHS)

It is calculated with the aid of the following equation:

$$IHS = H_{new} \times \exp(\beta_1 \times age) \quad (5\text{-}4)$$

where *age* means the current age (in years) of the asset; other parameters are explained above.

5. Current Health Score (CHS)

It is obtained by modifying Initial Health Score using the Health Score Modifier and Reliability Modifier.

$$CHS = IHS \times Health\ Score\ Factor \times Reliability\ Factor \quad (5\text{-}5)$$

where the Health Score Factor is a component of Health Score Modifier and the Reliability Factor is a component of Reliability Modifier **错误!未找到引用源。**.

6. Forecast Ageing Rate (β_2)

In order to predict Future Health Score based on Current Health Score, the Ageing Rate is required to be modified with the consideration of the influences of the Health Score Modifier and Reliability Modifier, which means the forecast is performed using the asset current condition. The modified Ageing Rate is presented below:

$$\beta_2 = \frac{ln\left(\frac{CHS}{H_{new}}\right)}{age} \quad (5\text{-}6)$$

where *age* is the asset's current age (i.e. the age used in IHS calculation).

7. Future Health Score (FHS)

It is calculated in the following way:

$$FHS = CHS \times \exp[(\beta_2/r) \times t] \quad (5\text{-}7)$$

where *t* is future time (in years); *r* is the Ageing Reduction Factor.

Ageing Reduction Factor is applied to adjust the rate of asset deterioration, so that the possible overestimate of the forecast future health score can be overcome. The details are illustrated in Fig. 5-4 **错误!未找到引用源。**.

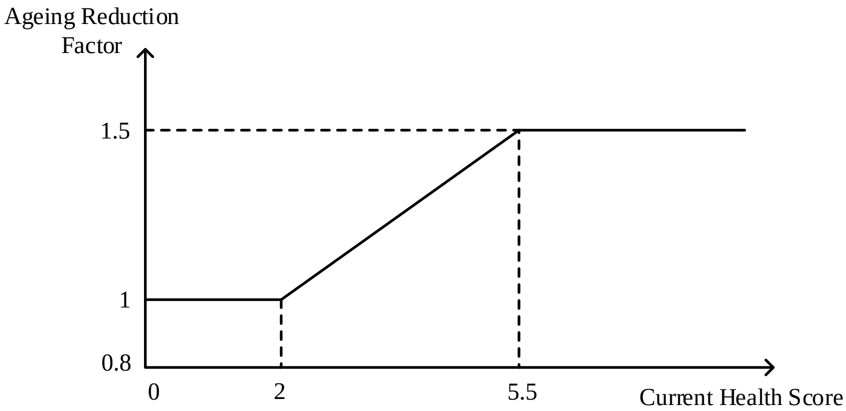

Figure 5- 4: Ageing Reduction Factor [131]

5.2.3 Simulation Algorithm

When the Health Indices are assumed deterministic, the DNO methodology is adopted. According to the PoF calculation introduced in the previous section, the PoF function, which is in fact hazard function, is a function of Health Scores, where Health Scores are a function of time (i.e. the life of the asset). By substituting the expression for Future Health Score (Eq. (5-7)) into Eq. (5-1), the hazard function can be derived as follows:

$$\lambda(t) = PoF = K \cdot [1 + (C \cdot CHS \cdot e^{\beta_2 t}) + \frac{\left(C \cdot CHS \cdot e^{\beta_2 t}\right)^2}{2!} + \frac{(C \cdot CHS \cdot e^{\beta_2 t})^3}{3!}] \tag{5-8}$$

The failure rate function can be simplified as follows:

$$\lambda(t) = K \cdot \gamma + a \cdot e^{\beta_2 t} + b \cdot e^{2\beta_2 t} + c \cdot e^{3\beta_2 t} \tag{5-9}$$

where γ is an additional parameter introduced to control the failure intensity and avoid unrealistically high values of reliability indices. The details for deciding the value of γ is presented in Appendix.

The survival function can be calculated by using the following equation that is based on the definition of hazard function:

$$R(t) = \exp[-\int_{0}^{t} \lambda(x) \cdot dx] \tag{5-10}$$

The sampled up-time can be obtained by solving $R(t) = 1 - U$, where U is a random number sampled from uniform distribution in the 0 to 1 range. This is a non-linear algebraic equation in unknown *t* that can be solved in a numerical way by using MATLAB function, which is based on the Levenberg-Marquardt and trust-region methods [170]. On the other hand, down-time is sampled from the exponential distribution. Fig. 5-5 illustrates the algorithm for random sampling of up- and down-times of a single asset within the Sequential Monte Carlo simulation, when the hazard function is based on the deterministic asset condition.

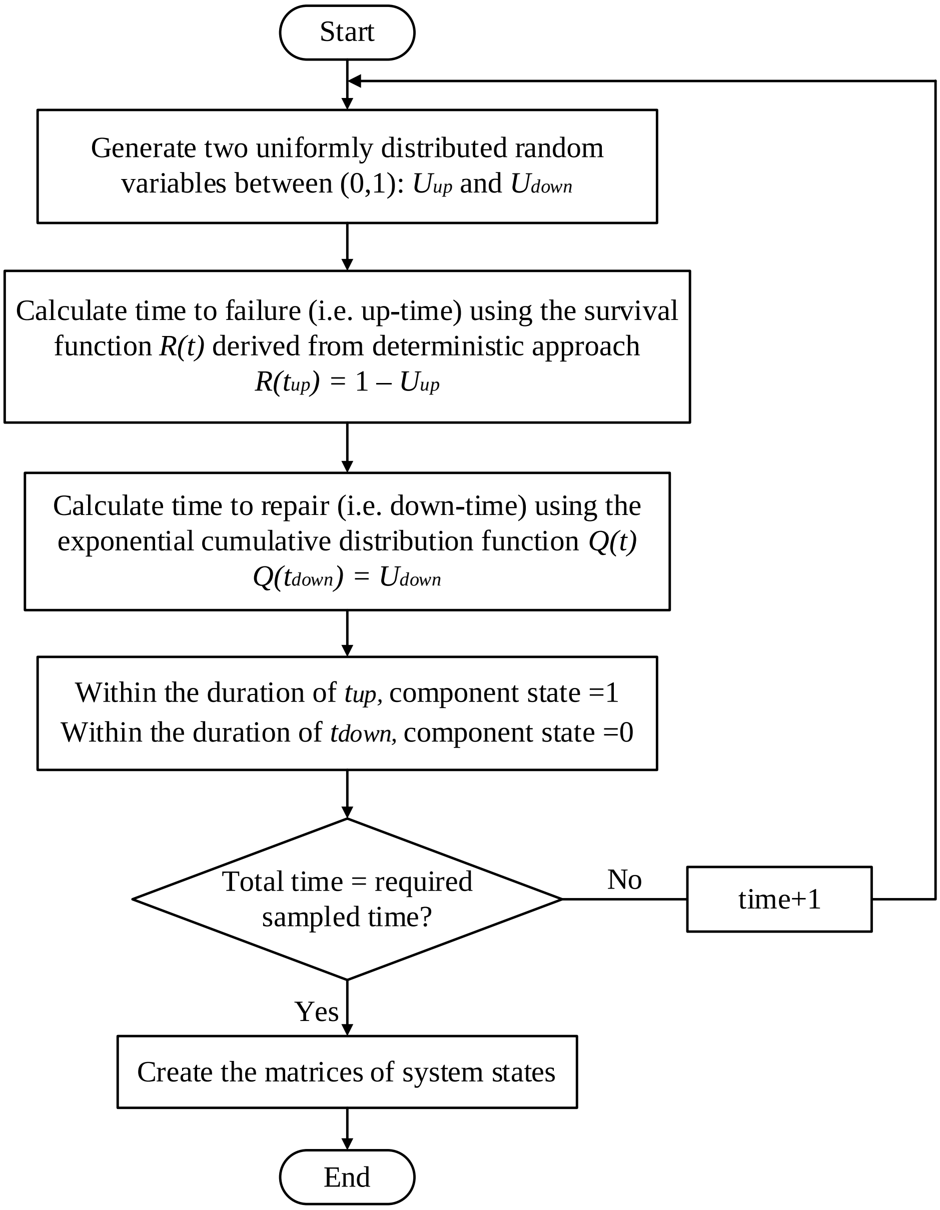

Figure 5-5: Procedure for Sequential Monte Carlo simulation using deterministic asset condition

5.3 Probabilistic Approach

Proposed probabilistic approach is developed based on a National Grid technical note. It aims to estimate the expected asset's age at the end of the simulation period, generate asset transitions among different HIs and eventually determine the asset repair processes and corresponding costs. In the proposed methodology, Asset Health Indices are modelled as probabilistic quantities.

5.3.1 Asset Health Index Categories

The methodology is developed based on the assumptions that Asset Health Indices are divided into 6 categories (Fig. 5-6) in line with the asset's age. Details are shown in Table 5-1; the concept can easily be extended to a higher number of asset health indices.

Table 5-2: Asset Health Indices Categories

HI Category	**Asset Operating Stage**
HI1: New	Infant stage
HI2: Young	Normal operating stage
HI3: Medium	Normal operating stage
HI4: Initial ageing	Ageing stage
HI5: Old	Ageing stage
HI6: Very Old	Ageing stage

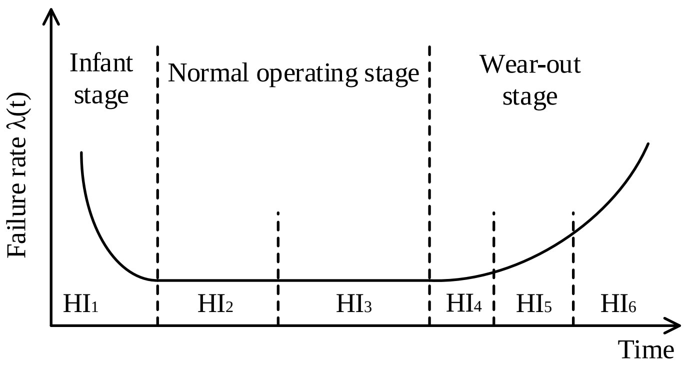

Figure 5-6: Asset health indices for probabilistic approach

Each HI is characterized by an assumed hazard (i.e. failure rate) function. The assumed hazard functions of different types of asset for different HIs are given below.

1. HI1: New

This is infant stage in the asset life. The failure of an asset is caused by “children diseases”, as well as by completely random outages. The failure rate function is:

$$\lambda(t) = \frac{\beta_1 \cdot t^{\beta_1 - 1}}{\alpha^{\beta_1}} + \lambda_1 \tag{5-11}$$

where λ_1 is the constant failure rate associated with random outages; α is the Weibull scale parameter; β_1 is the Weibull shape parameter. In this stage, $\beta_1 < 1$ is used in order to provide monotonically decreasing hazard function. This equation indicates that the in-service time follows modified Weibull distribution.

2. HI2: Young

   Asset is at the beginning of the normal operating stage. The PDF of the in-service time is exponential distribution, so that the hazard function is constant:

$$\lambda(t) = \lambda_1 \tag{5-12}$$

3. HI3: Medium

   Asset is still in the normal operating stage, but the failure rate can be higher.

$$\lambda(t) = \lambda_2, \qquad (\lambda_2 > \lambda_1) \tag{5-13}$$

   where $\lambda_{02} > \lambda_{01}$.

4. HI4: Initial Ageing

   Asset is in the initial ageing stage. The failure rate is assumed to be the failure rate of the last normal operating stage plus the initial ageing failure rate developed from the Weibull Distribution:

$$\lambda(t) = \lambda_2 + \frac{\beta_2 \cdot t^{\beta_2 - 1}}{\alpha^{\beta_2}} \tag{5-14}$$

   where the shape parameter $1 < \beta_2 < 2$. This condition indicates that the increase in failure rate over time is modest, that is, less than the linear increase.

5. HI5: Old

$$\lambda(t) = \lambda_3 + \frac{\beta_3 \cdot t^{\beta_3 - 1}}{\alpha^{\beta_3}} \tag{5-15}$$

   where the shape parameter is assumed to be $\beta_3 = 2$; constant failure rate term λ_3 is determined from the condition that there is no discontinuity between the previous curve and the current hazard curve.

6. HI6:Very Old

   The failure rate of asset in this category is assumed to be polynomial.

$$\lambda(t) = \lambda_4 + a_1 \cdot t^{\beta_4} + a_2 \cdot t^{\beta_5} \tag{5-16}$$

   where $\beta_4 \; or \; \beta_5 > 1$. This equation shows the increment of failure rate is faster than the linear increment. The polynomial form is used to avoid very high values of $\lambda(t)$ if the exponential function were used.

5.3.2 Models of Repair Process

In reliability analysis, the models for the repair process of a maintained system have been intensively studied. The most common models are renewal process (RP) and Non-Homogeneous Poisson Process (NHPP) [58]-[60]. The renewal process assumes that, after repair, the system state is restored to an as-good-as-new state (i.e. original state). Therefore it is also called perfect repair. The NHPP assumes the system is restored to a same-as-old state (i.e. the same state prior to failure). It is also called minimal repair. Fig. 5-7 and Fig. 5-8 show the failure rate functions of RP and NHPP, respectively [60]; time instants t_1, t_2, ..., t_n are moments of component failures.

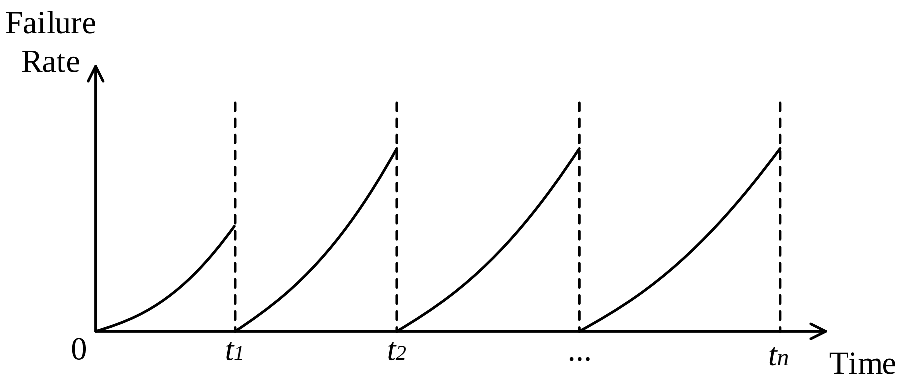

Figure 5-7: Failure rate of the renewal process [60]

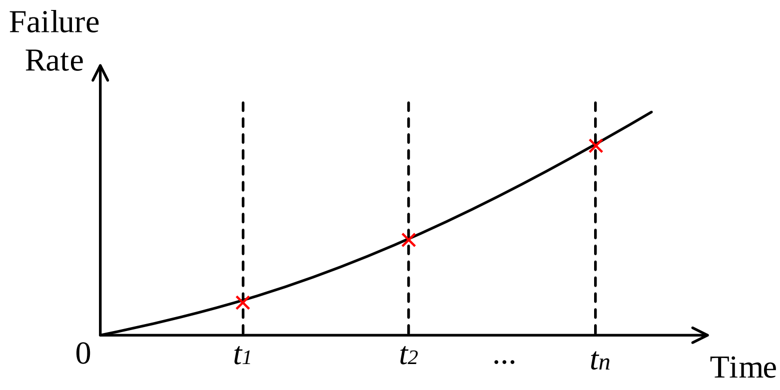

Figure 5-8: Failure rate of the minimal repair [60]

Many repair models have been developed based on RP and NHPP. The (*p*,*q*) rule model assumes the repair can be either perfect with probability p or minimal with probability $q = 1 - p$ [171]. The age-dependent version (*p(t)*, *q(t)*) rule model is then developed, which is more realistic than the constant (*p*,*q*) model [172]. In fact, however, repair process can result in other states than as-good-as new and same-as-old state. To address general repairs, the imperfect repair models have been developed. In this thesis, two imperfect repair models are combined: a) Virtual age model; and b) Proportional Intensity (PI) model [173]-[175].

In this research, again, only multiple independent failures are modelled in repair process. Failure modes are not considered.

I) Virtual Age Model

The virtual age model is the most commonly used imperfect repair model [60]. In general, virtual age model assumes the system is restored to a state younger than the state prior to failure, i.e. it rejuvenates the system. The virtual age model does not change the shape of the system failure intensity curve, but shifts the curve horizontally along the time axis [176].

Two general repair models have been developed by Kijima to introduce the concept of virtual age [63][177]. For a repairable system installed at time $t = 0$, denote the successive failure times by $t_1, t_2, \ldots$, and the inter-arrival times between failures by $x_1, x_2, \ldots$. Then inter-arrival times can be expressed as:

$$x_i = t_i - t_{i-1}, \qquad i = 1, 2, \ldots \tag{5-17}$$

Consider the system under the n_{th} repair. Introduce the repair factor q $(0 \leq q \leq 1)$, and the system virtual age v_n ($v_n = 0$ when the system is new).

Kijima I model assumes the repair only removes the damage generated in the last inter-arrival time. Accordingly, the system virtual age after the n_{th} repair is:

$$v_n = v_{n-1} + q x_n \tag{5-18}$$

Thus giving:

$$v_n = q(x_1 + x_2 + \cdots + x_n) \tag{5-19}$$

Kijima II model assumes the repair removes all damages accumulated up to the considered time point. Thus the system virtual age after the n_{th} repair is:

$$v_n = q(v_{n-1} + x_n) \tag{5-20}$$

giving

$$v_n = q(q^{n-1} x_1 + q^{n-1} x_2 + \cdots + x_n) \tag{5-21}$$

In case different types of repairs are considered, different repair factors q_m need to be applied (m denotes the repair type). Eq. (5-20) then becomes:

$$v_n = q_{n,m}(v_{n-1} + x_n) \tag{5-22}$$

where $q_{n,m}$ is repair factor of m_{th} type at n_{th} stage. Eq. (5-21) needs also to be modified accordingly.

II) Proportional Intensity Model

The proportional intensity (PI) model assumes that the system failure can be increased or decreased in proportion to pre-specified internal and external factors. This model does not change the shape of failure intensity curve, but shifts the curve vertically along the intensity axis, which is illustrated in Fig. 5-9.

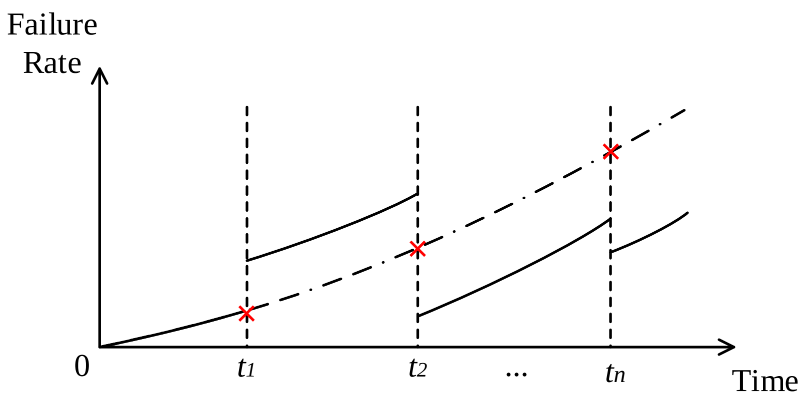

Figure 5-9: Proportional intensity model [60]

The general PI model function can be defined as:

$$\lambda(t) = \lambda_0(t) \cdot \exp\,(\boldsymbol{\theta} \cdot \boldsymbol{z}(t)) \tag{5-23}$$

where $\lambda_0(t)$ is the baseline failure rate function; $\boldsymbol{\theta}$ is the row-vector of parameters; and $\boldsymbol{z}(t)$ is the column-vector of temporal functions that represent internal (e.g. loading) and external (e.g. environment) factors of influence.

5.3.3 Asset Degradation Processes Modelling

In the National Grid (NG) guide document [126], it is assumed that asset conditions always deteriorate over time and accordingly the HI transition is always from HI_i to the next HI_{i+1}. If it is assumed, for simplicity, that there are 4 HIs only, the procedure can be summarized as follows [126]:

- Assume the asset has the best HI_1.
- Age at which the asset becomes HI_2 = minimum (Age asset becomes HI_2;
  Age asset becomes HI_3;
  Age asset becomes HI_4)
- Age at which the asset becomes HI_3 = minimum (Age asset becomes HI_3;
  Age asset becomes HI_4)

Using the basic idea of the NG methodology, a new degradation transition process between HIs is developed and performed before the main sequential Monte Carlo (SMC) procedure. Results from this stage are used for in-service time sampling in the main SMC. In this new methodology, asset HIs are extended to 6 HIs. And it assumes asset condition can deteriorate to any further HI, and also can be the same as the current one.

The analysis starts with classification of assets of certain type by age and health. The total number of one type of assets is assumed to be N_T. It is assumed there are 6 age bins (each bin represents 10 years), and all assets are classified by bins *j=1,2,…,6* (table rows) and by health indices *i=1,2,…,6* (table columns), which gives numbers of assets in individual cells $N(j,i)$, so that $N_T = \sum_j \sum_i N(j,i)$. Normalization of the asset numbers needs to be done and this can be performed in two ways:

I) By rows and columns (i.e. dividing by $\sum_i N(j,i)$ for each bin *j=1,2,…,6*) giving discrete conditional probabilities $P(HI_i|x_j)$, where x_j is virtual age bin;
II) By columns (i.e. dividing by $\sum_j N(j,i)$ for each HI *i=1,2,…,6*) giving discrete conditional probabilities $P(x_j|HI_i)$.

These two normalizations are used in asset deterioration algorithms.

I) Algorithm Based on Normalization by Rows and Columns

Conditional probabilities $P(x_j|HI_i)$ and $P(HI_i|x_j)$ are calculated from asset number table using, respectively, normalization by rows. Probabilities $P(x_j|HI_i)$ are illustrated in Fig. 5-10 as dashed areas under pdfs. They are used to find the age bin x_j when the asset health is HI_i. On the other hand, probabilities $P(HI_i|x_j)$ are required to determine transition to a new (worse) HI; this is illustrated in Fig. 5-11, where blue arrows denote transitions to the next HI and violet arrows transitions to any HI.

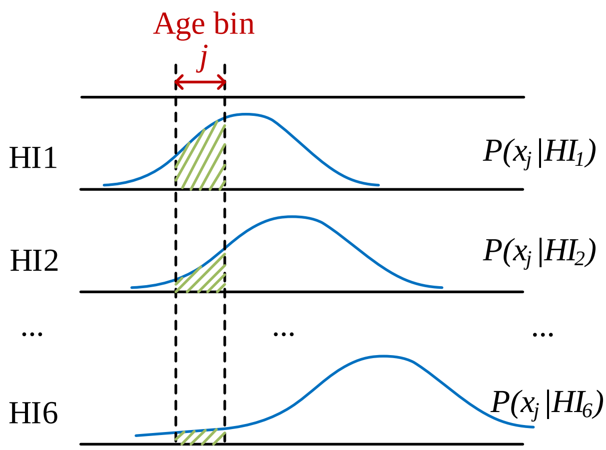

Figure 5-10: Probability of HI_i for the age bin j

The HI deterioration transition process can now be obtained by performing an independent Monte Carlo Simulation before the main SMC procedure. The algorithmic steps are as follows:

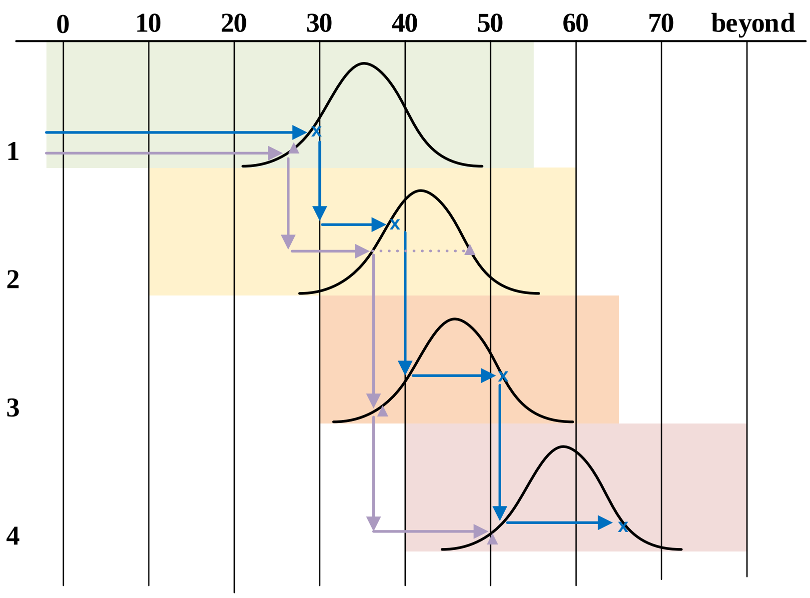

Figure 5-11: Movement through asset health indices: a) To next HI (blue); b) To any HI (violet)

1. Assume the asset condition is new, so the asset HI is HI_1. The age x_{j1} can be sampled from the corresponding conditional CDF $P(x|HI_1)$, obtained by "normalization by columns".
2. The sample bin j is known from x_{j1}. Calculate the conditional probabilities $P\left(HI_i|x_j\right)$, $i = 1,2, \dots ,6$, by using "normalization by rows".

3. Randomly sample a uniformly-distributed number U between 0 and 1 to determine the next HI_k that the asset moves to (Fig. 5-12). Here, HI_k must be worse than the previous HI.

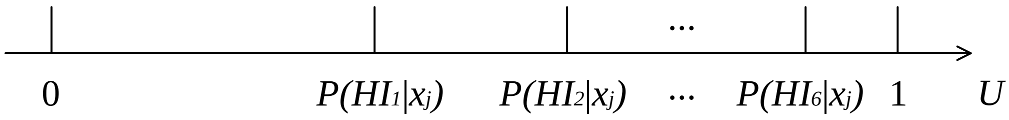

Figure 5-12: Conditional probabilities for each HI when the bin is *j*

4. Randomly sample x_{j2} from the CDF $P(x|HI_k)$. Note that $x_{j2} > x_{j1}$.
5. Return to step 2 and repeat the following steps to obtain the next transition. The process stops when the transition reaches the worst HI_6.
6. Generate matrices A_r and B_r for the current simulation r (see below).

II) Algorithms Based on Normalization by Columns

Assumed conditional probabilities $P(x_j|HI_i)$, an example of which is shown in Table 5-3, are interpolated to get yearly values $P(x|HI_i)$. Interpolation is done in such a way to follow the Weibull pdf shapes (Fig. 5-13), whose hazard functions are specified in section 5.2.1. More specifically, the following methods are used:

- Monotonically decreasing geometric series for HI1,
- Monotonically decreasing arithmetic series for HI2 and HI3,
- Increasing geometric series and decreasing arithmetic series for HI4,
- Increasing and decreasing geometric series for HI5, and
- Monotonically increasing geometric series for HI6.

"Smooth" transitions between bins are always maintained. So calculated 60 x 6 input matrix for each asset category is used to calculate transitions between health indices.

Table 5-3: Bin probabilities for each HI

	HI1	**HI2**	**HI3**	**HI4**	**HI5**	**HI6**
Bin 1	0.9	0.1				
Bin 2	0.1	0.5				

Bin 3		0.4	0.3	0.3	0.2	
Bin 4			0.4	0.4	0.3	0.1
Bin 5			0.1	0.25	0.4	0.3
Bin 6				0.05	0.1	0.6

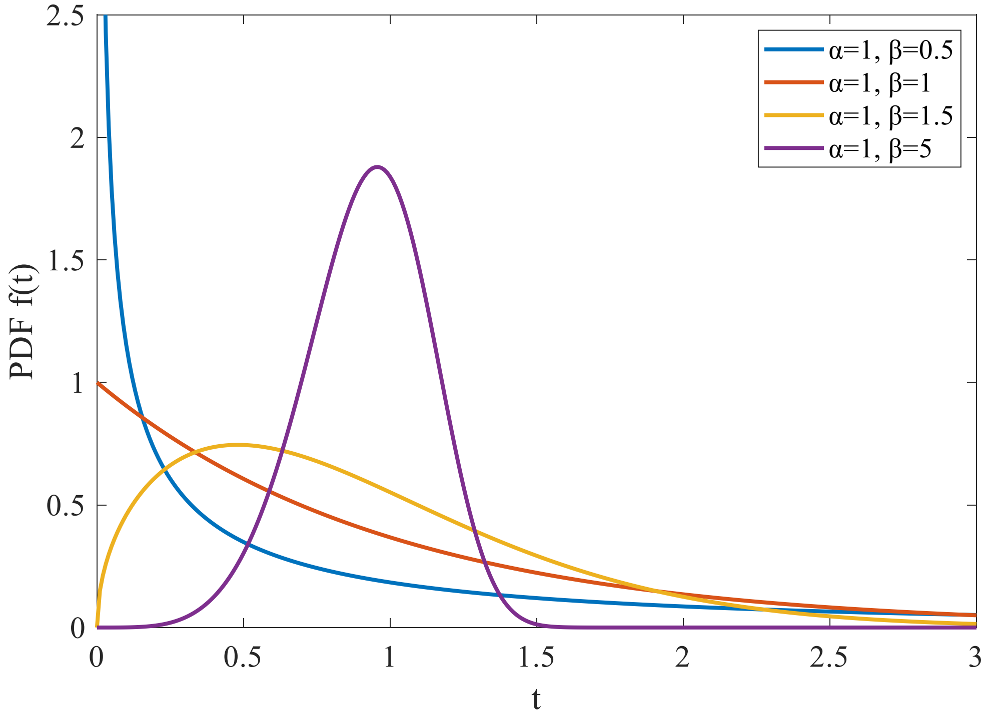

Figure 5-13: PDF shapes for different Weibull parameters β

An example of the calculation of annual probabilities from the bin totals, when a geometric series is used, is as follows. The sum of annual probabilities over 10 years is:

$$S_n = \frac{a(r^n - 1)}{r - 1} \tag{5-24}$$

where S_n is bin probability; a is the initial value (i.e. probability of the first/last year in the age bin); n is 10 years; $r < 1$ is common ratio. Eq. (5-25) can be solved for the unknown common ratio r. In case of a monotonically increasing series, this is done in the reverse order from the last to the first year giving $ar^9, ar^8, \ldots, ar^0$.

Input probabilities $P(x|HI_i)$ are used to find transition probabilities stored in a matrix $\boldsymbol{M}$ whose elements are $M(x, i, j)$, where *x* is the age, *i* is the current HI and *j* is the "arriving" HI. Two algorithms are developed: a) Asset health always moves to the next deteriorated state, which is called "To next HI" algorithm; and b) Asset health moves to any deteriorated state, which is called "To any HI" algorithm. These two transition approaches are summarized below.

a) Transition to Any HI

1. Set the asset HI $i = 1$. Determine virtual age x_i in years from the generated pseudo-random number.
2. Generate pseudo-random numbers U_m for each HI index $m = i + 1,\ i + 2, \dots 6$, and determine the corresponding virtual ages x_m $(m = i + 1,\ i + 2, \dots 6)$.
3. Find the new HI index *j* based on:

$$j = arg\ \{min[(x_m)\ ;\ \ m = i + 1, i + 2, \dots 6]\} \tag{5-25}$$

   where the corresponding virtual age must be greater than the virtual age determined in the previous step.
4. If HI index $j < 6$, set $i = j$ and return to step 2. Otherwise, go to the next step.
5. Generate matrices $\boldsymbol{A_r}$ and $\boldsymbol{B_r}$ for the current simulation *r* (see below).

b) Transition to Next HI

1. Set the asset HI $i = 1$. Determine virtual age x_i from the generated pseudo-random number.
2. Generate pseudo-random numbers *U* for next HI index $j = i + 1$, and determine the corresponding virtual age x_j $(j = i + 1)$, where x_j must be greater than the virtual age determined in the previous step.
3. If HI index $j < 6$, set $i = j$ and return to step 2. Otherwise, go to the next step.
4. Generate matrices $\boldsymbol{A_r}$ and $\boldsymbol{B_r}$ for the current simulation *r*.

Matrix $\boldsymbol{A_r}$ contains binary values representing asset virtual age (rows) for each HI (columns). An example matrix $\boldsymbol{A_r}$ is shown below. It means asset has HI=1 at age 0; HI=2 at age 3; HI=3 at age 5; HI=4 at age 7; HI=5 at age 10; and HI=6 at age 12.

$$
\boldsymbol{A_r} = \begin{pmatrix} 1 & 0 & 0 & 0 & 0 & 0 \\ 1 & 0 & 0 & 0 & 0 & 0 \\ 1 & 0 & 0 & 0 & 0 & 0 \\ 0 & 1 & 0 & 0 & 0 & 0 \\ 0 & 1 & 0 & 0 & 0 & 0 \\ 0 & 0 & 1 & 0 & 0 & 0 \\ 0 & 0 & 1 & 0 & 0 & 0 \\ 0 & 0 & 0 & 1 & 0 & 0 \\ 0 & 0 & 0 & 1 & 0 & 0 \\ 0 & 0 & 0 & 1 & 0 & 0 \\ 0 & 0 & 0 & 0 & 1 & 0 \\ 0 & 0 & 0 & 0 & 1 & 0 \\ 0 & 0 & 0 & 0 & 0 & 1 \\ 0 & 0 & 0 & 0 & 0 & 1 \end{pmatrix} \tag{5-26}
$$

Based on matrix $\boldsymbol{A_r}$, matrix $\boldsymbol{B_r}$ that describes the age at which the asset moves from one HI to another HI can be obtained. In matrix $\boldsymbol{B_r}$, there are fifteen columns which represents transitions from HI1 to HI2, HI1 to HI3, HI1 to HI4, HI1 to HI5, HI1 to HI6, HI2 to HI3, HI2 to HI4, HI2 to HI5, HI2 to HI6, HI3 to HI4, HI3 to HI5, HI 3 to HI6, HI4 to HI5, HI4 to HI6 and HI5 to HI6. Based on the above example, matrix $\boldsymbol{B_r}$ is:

$$
\boldsymbol{B_r} = \begin{pmatrix} 0 & 0 & 0 & 0 & 0 & 0 & & 0 \\ 0 & 0 & 0 & 0 & 0 & 0 & & 0 \\ 0 & 0 & 0 & 0 & 0 & 0 & \cdots & 0 \\ 1 & 0 & 0 & 0 & 0 & 0 & & 0 \\ 0 & 0 & 0 & 0 & 0 & 0 & & 0 \\ 0 & 0 & 0 & 0 & 0 & 1 & & 0 \\ & & & \vdots & & & \ddots & \vdots \\ 0 & 0 & 0 & 0 & 0 & 0 & \cdots & 1 \\ 0 & 0 & 0 & 0 & 0 & 0 & & 0 \end{pmatrix} \tag{5-27}
$$

Following the completion of the independent MC procedure, averaged matrices $\boldsymbol{A}$ and $\boldsymbol{B}$ are calculated:

$$
\boldsymbol{A} = \frac{\sum_r \boldsymbol{A_r}}{n} \tag{5-28}
$$

$$
\boldsymbol{B} = \frac{\sum_r \boldsymbol{B_r}}{n} \tag{5-29}
$$

where n is the number of Monte-Carlo simulations. Matrices $\boldsymbol{A}$ and $\boldsymbol{B}$ are used for the calculation of transition matrix $\boldsymbol{M}$, whose element $M(x, i, j)$ is conditional probability based on known asset health index at $(x - 1)$:

$$M(x,i,j) = \frac{B(x,i,j)}{A(x-1,i)} \tag{5-30}$$

Tables 4, 5 and 6 in Appendix give an example of transition matrix ***M*** obtained using normalization by rows (Table 4), normalization by columns for transitions to any HI (Table 5) and next HI (Table 6). Algorithms based on the normalization by columns are utilized in this research.

5.3.4 Asset Condition Improvement Processes

Asset conditions can be improved through interventions. To develop the repair process, repair policies have to be assumed. The "full" set of repairs is given below:

- Absolutely Minimal Repair
  Following a failure, asset stays on the "arrived" HI at the arrived age (i.e. repair factor is 1.0). Both post-failure asset HI and virtual age are defined.
- Marginally Improved Repair (Minor Repair)
  Following a failure, asset stays on the "arrived" HI, however virtual age is reduced.
- Significantly Improved Repair (Major Repair 1)
  Following a fault, the asset is brought to the previous HI (better than the "arrived" HI) and the virtual age is reduced.
- Significantly Improved Ageing Repair (Major Repair 2)
  Following a fault, the asset is brought down by two HIs and the virtual age is reduced.
- Replacement
  After replacement, asset has the best HI and the virtual age is set to zero.

The possible repair types for each HI category are given in Table 5-4.

Table 5-4: Possible repair types for each HI category

Post-Failure HI	**Possible Repair Types**	**Post-Repair HI**
HI1 (New)	Minimal repair	HI1

HI2 (Young)	Minimal repair	HI2
	Minor repair	HI1
HI3 (Medium)	Minimal repair	HI3
	Minor repair	HI2
	Major 1 repair	HI1
HI4 (Initial Ageing)	Minimal repair	HI4
	Minor repair	HI3
	Major 1 repair	HI2
	Major 2 repair	HI1
HI5 (Old)	Minimal repair	HI5
	Minor repair	HI4
	Major 1 repair	HI3
	Major 2 repair	HI2, HI1
HI6 (Very Old)	Replacement	HI1

It is assumed that data on %-ages of repair types for each asset health index are available. Asset post-failure (deteriorated) HI is known and shown in the first column of Table 5-4. Assuming uniform distribution of repair types for each HI, random sampling determines the repair type (second column in Table 5-4), which in turn defines the improved post-repair HI, where an asset has "landed" to (third column).

Following the repair, the virtual age can be reduced or reset. Kijima II model is applied:

$$va_m = q_m \cdot va'_m = q_m \cdot (va_{m-1} + \varphi_m \cdot t_{sampled}^{up}) \qquad (5\text{-}31)$$

Where q_m is repair factor at the m_{th} repair stage. The following repair factors for each repair type are assumed:

- $q_m = 1.0$ for absolutely minimal repair;
- $q_m = 0.8$ for minor repair;
- $q_m = 0.6$ for major 1 repair;
- $q_m = 0.4$ for major 2 repair;
- $q_m = 0$ for replacement.

5.3.5 Simulation Algorithms

5.3.5.1 In-service Time Sampling

In the simulation using probabilistic asset health approach, there are two timelines: one is asset virtual age and the other is simulation time, which is shown in Fig. 5-14. It is recognized the asset virtual age can be "accelerated" or "decelerated" during in-service operation. The following equation describes this process:

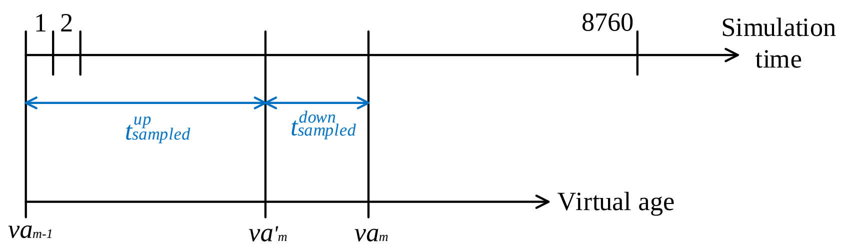

Figure 5-14: Illustration of the two timelines in probabilistic approach

$$va'_m = va_{m-1} + \varphi_m \cdot t_{sampled}^{up} \qquad (5\text{-}32)$$

where va'_m is the asset virtual age at the beginning of repair stage m; factor φ gives the information of the impact during in-service time. For example, when the asset suffers ageing during in-service operation, $\varphi_m > 1$, asset virtual age is accelerated; when the loading is less than nominal or the ambient temperature is lower than design ambient temperature, $0 < \varphi_m < 1$, asset virtual age is decelerated.

Besides, during the in-service operation, there exists impact from loading condition, environment, etc. on the asset virtual age and hazard function 错误!未找到引用源。. Therefore baseline hazard functions need to be modified to reflect the impact of these exogenous factors on failure intensity, which gives a Proportional Hazard Model (PHM) [129]:

$$\lambda(va) = \lambda_0(va) \cdot \exp[\boldsymbol{\theta}^T \cdot \boldsymbol{z}(t)] \tag{5-33}$$

where $\lambda_0(va)$ is the baseline hazard function previously specified by HI levels; $\exp[\boldsymbol{\theta}^T \cdot \boldsymbol{z}(t)]$ is proportional intensity (PI) function; $\boldsymbol{\theta}$ is vector of parameters and $\boldsymbol{z}(t)$ is vector of time functions that describe the exogenous phenomena. Several exogenous factors are introduced in the DNO document: location factor, duty factor, observed condition modifier, measured condition modifier, oil test modifier and reliability modifier; details are shown in Table 5-5. If the location factor z_1 and duty factor z_2 is considered, the PI function is:

$$PI = \exp(\theta_1 \cdot z_1 + \theta_2 \cdot z_2) / e^{\theta_1 + \theta_2} \tag{5-34}$$

$$\theta_1 + \theta_2 = 1 \tag{5-35}$$

where nominal conditions are described by $z_1 = z_2 = 1$ and factor $e^{\theta_1 + \theta_2}$ is introduced to make PI function equal to 1 for nominal conditions. For light conditions, $z_1 < 1,\ z_2 < 1$; for heavy conditions $z_1 > 1, z_2 > 1$. Note that the PI function needs to be defined by asset types and that location constant θ_1 can be 0. For simplicity, the following values are assumed:

- For OHL, environment is very important. Let $\theta_1 = 0.7, \theta_2 = 0.3$.
- For transformer, environment is indoor or outdoor, but loading is much more important. Let $\theta_1 = 0.2, \theta_2 = 0.8$.
- For cable, environment can be neglected. So, $\theta_1 = 0, \theta_2 = 1.0$.

Table 5-5: Exogenous factors affecting asset HI [131]错误!未找到引用源。

Exogenous Factor	**Description**
Asset Location	Influenced by: a) Indoor/outdoor; b) Distance from coast; c) Altitude; d) Corrosion
Asset Duty	Influenced by: a) Loading; b) Number of operations; c) Operating/design voltage
Asset Reliability	Additional reliability modifier that is a result of generic issues that affect asset health
Asset Condition	Observed condition, measured condition, oil test modifiers (deterministic HI approach)

The assumed asset hazard functions consists of a constant and Weibull terms:

$$\lambda(va) = \begin{cases} PI \cdot \lambda = \lambda', & va \leq va^{thr} \\ PI \cdot \lambda + PI \cdot \dfrac{\beta \cdot va^{\beta-1}}{\alpha^{\beta}} = \lambda' + \dfrac{\beta' \cdot va^{\beta-1}}{\alpha^{\beta}}, & va > va^{thr} \end{cases} \tag{5-36}$$

where PI is a constant given by Eq. (5-35) ; va^{thr} is threshold value of the virtual age when ageing is initiated, and α and β are Weibull shape and scale parameters. To determine in-service time, $R(t_{m+1}^{up}) = 1 - U$ is solved via the following equations:

$$R(t_{m+1}^{up}) = exp\left[-\int_{va_m}^{va_m+\varphi_{m+1}\cdot t_{m+1}^{up}} \lambda' \cdot d\tau\right] = exp[-\lambda' \cdot \varphi_{m+1} \cdot t_{m+1}^{up}], \quad va \leq va^{thr} \tag{5-37a}$$

$$R\left(t_{m+1}^{up}\right) = exp\left[-\int_{va_m}^{va_m+\varphi_{m+1}\cdot t_{m+1}^{up}} (\lambda' + \frac{\beta' \cdot (\tau)^{\beta-1}}{\alpha^{\beta}}) d\tau\right]$$

$$= exp\left[-\lambda' \cdot \varphi_{m+1} \cdot t_{m+1}^{up} - \frac{\beta' \cdot \left(va_m + \varphi_{m+1} \cdot t_{m+1}^{up}\right)^{\beta-1}}{\alpha^{\beta}} + \frac{\beta' \cdot (va_m)^{\beta-1}}{\alpha^{\beta}}\right], \qquad va \leq va^{thr} \tag{5-37b}$$

5.3.5.2 Out-of-service Time Sampling

It is assumed that repair durations are not dependent on asset health indices but only on repair types. Boundary values in the ±(40-50)% range of the base repair time as given in [123] are specified for each repair type (Table 5-6), uniform distribution is assumed in all cases, and repair duration is determined by random sampling from the uniform distribution.

Table 5-6: Percentages of base repair duration for each repair type

Repair Type	Percentage of Base Repair Duration
Minimal Repair	60%
Minor Repair	80%
Major 1 Repair	100%
Major 2 Repair	120%
Replacement	150%

5.3.5.3 Simulation Algorithm within Sequential Monte Carlo Procedure

The algorithm for obtaining asset operating states on a yearly basis is shown in Fig. 5-15. Its individual steps are as follows:

1. Select asset type and calculate transition matrix *M*.

2. Input the asset's initial virtual age and HI.
3. Find the corresponding row of transition matrix *M* and calculate the cumulative transition probability. Generate a uniformly distributed number U to decide the next HI the asset moves to.
4. Calculate the up-time based on the input virtual age and HI.
5. Based on the next HI, the repair type can be determined and down-time is obtained consequently. Asset virtual age and HI are also updated.
6. Use the new virtual age and HI in step 4 as input data. Return to step 3 and repeat the following steps until the required sampled time is met.
7. Generate the asset state matrix in chronological order.

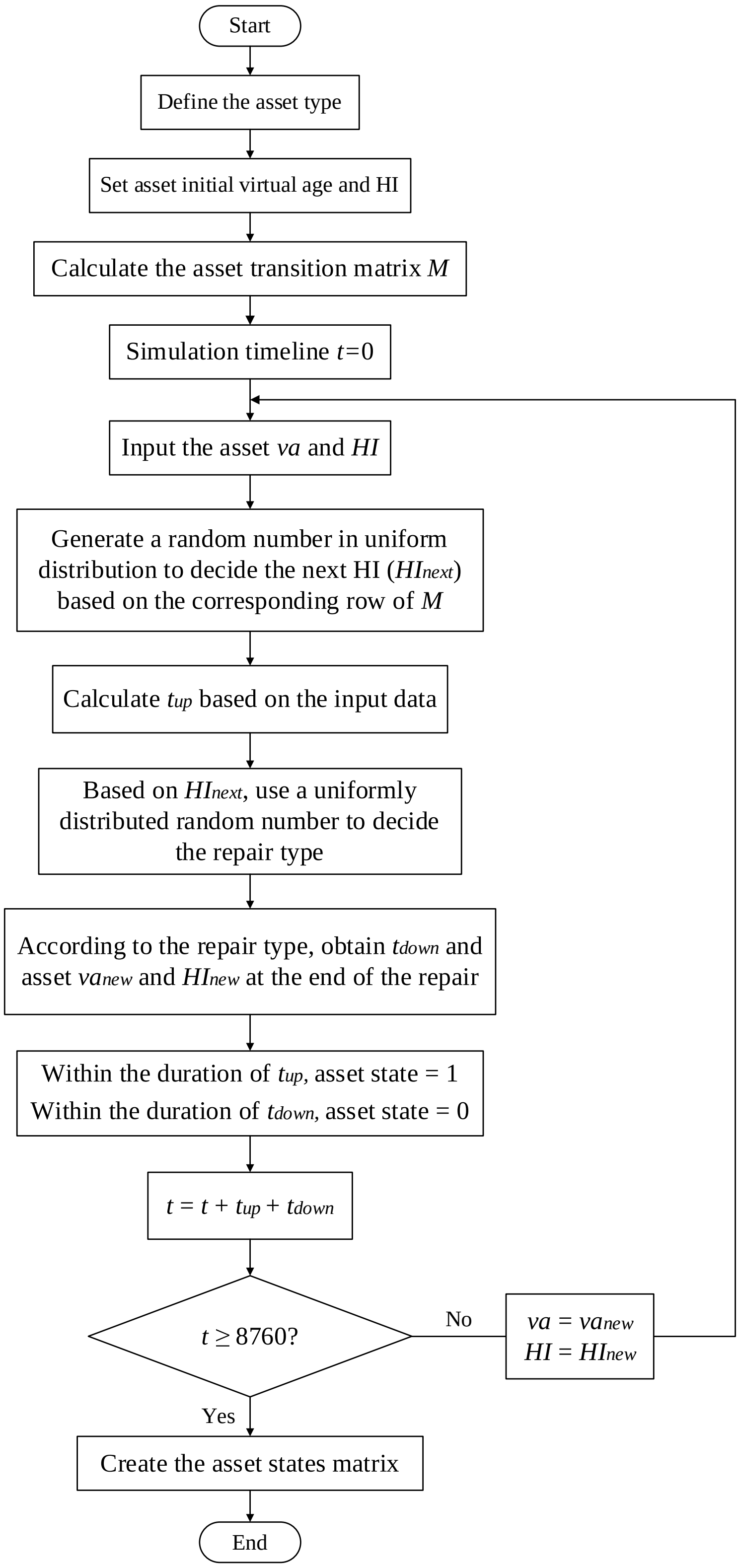

Figure 5-15: Procedure for obtaining yearly asset operating states

5.3.6 Simulation Results Classification

The simulation output can be classified as system- and asset-oriented.

System and nodal EENS and LOLP are essential system indicators, whilst on asset level, average up- and down times, numbers and types of asset interventions, asset health indices (or scores) at the end of the simulation period and transitions between indices are produced.

Asset-orientated results are fed back into the optimal long-run asset intervention planning (first block in Fig. 3-1) in case further asset improvements are required. Similarly, system-orientated indices can be used to tighten network planning standards if the results are outside satisfactory limits.

5.4 Chapter Summary

This chapter introduces the basic concept of asset health modelling. Two approaches are applied, based on deterministic and probabilistic modelling. For deterministic approach, the methodology involves asset classification and PoF calculation process which is developed in line with the UK DNO approach. The proposed probabilistic approach distinguishes between asset deterioration (transition to worse HIs) and improvement of asset conditions (transitions to better HIs). Asset degradation is modelled based on a "queueing type" transition model, and two algorithms for asset health transitions are developed. The improvement process is based on Kijima II virtual age model, several repair types and semi-probabilistic approach for finding the post-repair states. To assess the network reliability, the developed approach is then incorporated into the sequential Monte Carlo simulation. The simulation model gives reliability indices on system level (e.g. EENS, LOLP), asset profiles in terms of health indices and virtual ages, as well as repair numbers by types and their costs.

CHAPTER 6 PROBABILISTIC ASSET INTERVENTION PLANNING – RESULTS

This chapter gives the modifications made to the IEEE RTS-96 due to the addition of wind generation. Network reliability is studied based on the three models developed in the previous chapters: temporal model, deterministic approach and probabilistic approach.

6.1 Modified Reliability Test System

IEEE RTS-96 is utilized in the entire research for system reliability studies. The following characteristics of one-area IEEE RTS-96 (Fig.2-10) are identified:

- 2 voltage levels: 230kV in the "north" and 138kV in the "south"
- 24 buses: first 10 in the "south" and last 14 in the "north"
- 17 demand points
- 5 230/138 kV transformers
- 38 branches including 5 transformers and 2 underground cables
- 32 generating units connected at 10 buses
- A synchronous compensator connected at bus 14

In this research, wind generation is added to IEEE RTS-96. The following modifications are done:

- Addition of wind generation

  Four wind farms with 700MW capacity in total are connected to four buses of the test network, 400MW in the southern region and 300MW in the northern region. The total wind generation capacity is about 20% of the conventional generation. The assumed parameters are listed in Table 6-1. Note it is assumed that wind generation is limited to active power (in reality, a lot of wind generation can generate reactive power, which has an impact on the grid voltage stability. The effect from wind reactive power is not considered in order to reduce the number of study cases. It can be added in future work).

Table 6-1: Wind farm data

Wind Farm	Bus	Unit Size (MW)	MTTF (hour)	MTTR (hour)
1	1	150	780	20
2	7	150	780	20
3	21	200	550	20
4	23	200	550	20

- Modification of load demand

  Four additional windfarms (Table 6-1) are connected to the network, giving an increase of generation capacity of 20% so that the nodal peak loads are multiplied by 1.2.

6.2 Additional Specifications

6.2.1 Cost of Repairs

Costs of each repair type for different assets are collected in [178]-[183] and modified:

Table 6-2: Repair cost of each repair type for different asset types

Repair Cost (M£)	Minimal	Minor	Major 1	Major 2	Replacement
OHL (/km)	0.0105	0.0174	0.0348	0.0452	0.522
Cable (/km)	0.0261	0.0305	0.0435	0.174	3.045
Transformer	0.0022	0.022	0.25	0.55	0.66

6.2.2 Base Case Specifications

Asset's age is not an actual input in temporal model. To be consistent with deterministic approach and probabilistic approach where asset's age is an input data, asset's initial age of 1, 21 and 31 years are assumed as three base cases in temporal model and corresponding failure rates are assigned to each case.

In all the three models, the simulation period for each case is set for 10 years. On one hand, this simulation period can help analyse the impact of ageing asset (or asset's age) in all the models; one the other hand, it can save the extreme long computational time since a number of cases are studied in this research. However, in asset condition modelling, six age bins are assumed, meaning assets' expected lifetime is 60 years. It is not possible to receive global results by using the 10-year simulation.

6.3 Temporal Asset Health Modelling

In temporal model, three base cases are specified and illustrated as follows:

- Asset initial age = 1, asset in-service time follows exponential distribution with failure rate λ_0;
- Asset initial age = 21, asset in-service time follows exponential distribution with failure rate λ_1 ($\lambda_1 = 1.1\lambda_0$);
- Asset initial age = 31, asset in-service time follows modified Weibull distribution with failure rate λ_2 ($\lambda_2 = \lambda_1 + \frac{\beta \cdot t^{\beta-1}}{\alpha^{\beta}}$, where $\alpha = \frac{1}{\lambda_1}, \beta = 2$).

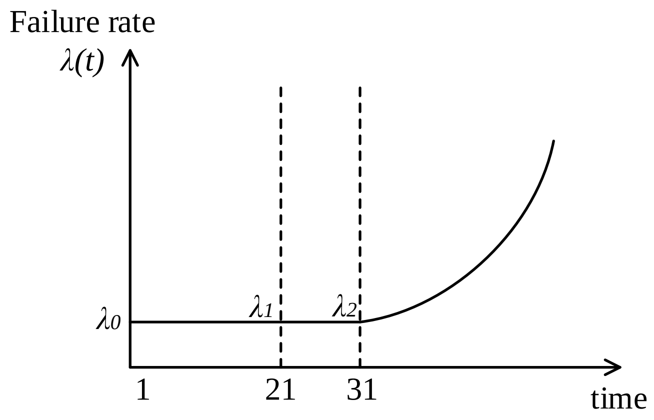

Figure 6-1: Illustration of failure rate for temporal model

Asset out-of-service time is modelled via exponential distribution. Since repair types are not modelled in the temporal model, total asset repair costs are calculated for the five types of repairs listed in Table 6-2.

6.3.1 Impact of Asset Ageing

6.3.1.1 Base Case Study

The reliability results for three base cases are presented in Table 6-3, Fig. 6-2 and Fig. 6-3. The reliability results show decrease of reliability with the increase of asset age. From the nodal level results, it can be found that the worst performance occurs at bus 6, followed by bus 3 and 8. All of these buses are located in southern area and have no generating units, which contributes to higher load curtailment. The same reason also applies to bus 4, 5, 9 and 10.

Bus 6 is connected to two transmission lines; either of them becoming unavailable leads to load curtailment in order to satisfy the power flow constraints. Bus 3 also has large load curtailment but is slightly better than 6 due to one more transmission link connected. Bus 3 and bus 8 have similar values of LOLP, but EENS at bus 3 is nearly twice of bus 8. The reason is bus 3 and bus 8 are both connected to three transmission lines; however, power flow results show that bus 3 is only supplied by the transformer link (branch 7), and the other two links consume power; whilst the links connected to bus 8 all supply the load. This causes higher load curtailment at bus 3.

The significant outage time of transformers connected to bus 9 and 10 also contributes to higher load curtailment at these buses. However, the reliability at bus 9 is worse than bus 10. Bus 9 are linked to bus 3, 4, 8, 11 and 12; while bus 10 are linked to bus 5, 6, 8, 11 and 12. The difference is that the loads at bus 5 and 6 are smaller than bus 3 and 4. Therefore, more load curtailment at bus 9 is needed to supply the further load.

In the north, the relatively worse performance occurs at bus 14 and 18. The reason is that bus 14 has no generators and limited transmission capacity due to two transmission links. Bus 18 is connected to a nuclear generator with large capacity (400MW). The load, however, at bus 18 is the biggest. The reason for load curtailment at bus 18 is mainly due to the large consumption of power by the link between bus 17 and 18 (branch 30) and outages of branch 32 and 33.

Table 6-3: System reliability results for different initial ages (temporal model)

Initial Age (yr)	EENS (MWh/yr)	LOLP (p.u.)
1	24003.54	0.017717
21	27519.17	0.019566
31	31491.83	0.020205

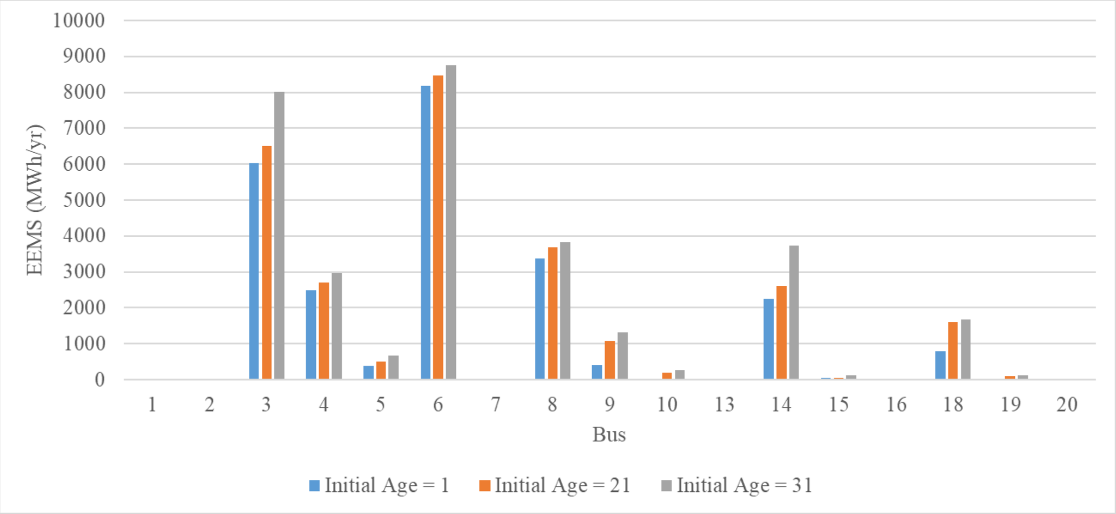

Figure 6-2: Nodal EENS for different initial ages (temporal model)

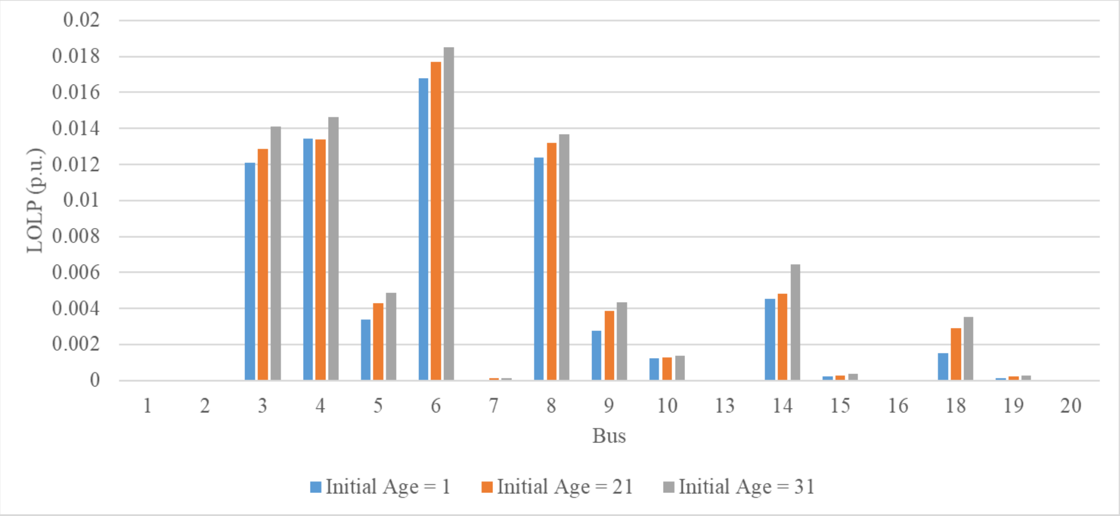

Figure 6-3: Nodal LOLP for different initial ages (temporal model)

Transformer branches 14 and 17 have the highest average down-time, while the other transformer branches (15 and 16) experienced no outages. The highest number of repairs occurs on overhead lines. The total numbers of repairs for these cases are 92 (initial age = 1), 149 (initial age = 21) and 202 (initial age = 31), which indicates more repairs and subsequently higher repair costs are required when assets become old.

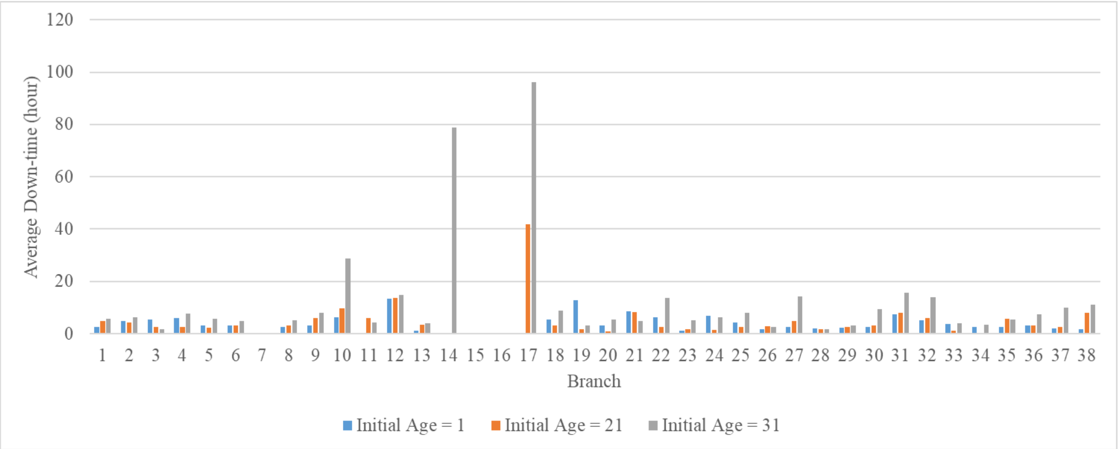

Figure 6-4: Average down-time of each branch for different initial ages (temporal model)

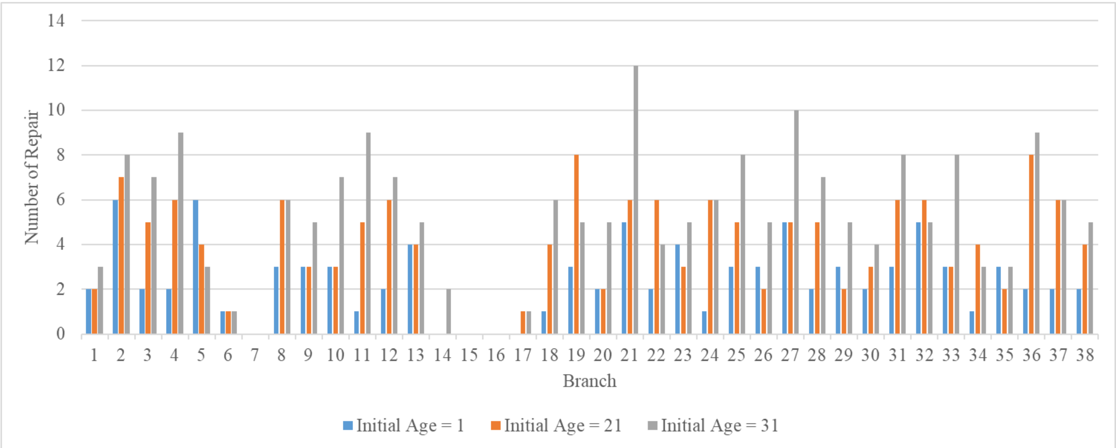

Figure 6- 5: Number of repair in each branch for different initial ages (temporal model)

Table 6-4: Total repair costs for different initial ages (temporal model)

Initial Age (yr)	Total Repair Costs for Different Repair Types (M£)				
	Minimal Repair	Minor Repair	Major 1 Repair	Major 2 Repair	Replacement
1	33.634	55.048	109.150	148.115	1766.448
21	51.150	84.093	167.447	224.058	2637.804
31	68.811	112.541	223.583	305.294	3633.969

6.3.1.2 Partial Ageing Case Study

Partial ageing means that some of the network assets are in ageing state while others are in normal operating state. Specifically, branches 2, 5, 8, 12, 16, 18, 22, 26, 32 and 36 are ageing. This case is compared to networks whose initial age is 1 and 31.

The results presented in Table 6-5 show that EENS and LOLP of partial ageing network is higher than network with initial age of 1 and lower when initial age is 31. This indicates that part of the assets becoming ageing also exacerbates system reliability. Compared to the case of initial age = 21, the values of partial ageing network are slightly higher.

As for nodal results (Fig. 6-6 and Fig. 6-7), EENS at bus 3 is reduced. Bus 3 is supplied through transformer, whilst power flows in branches 2 and 6, connected to bus 3, are from bus 3 (they "consume" power). When branch 2 is in ageing stage, frequent outages happen, which leads to decreased loading of the transformer branch and less curtailment is needed at bus 3. On the other side, EENS at bus 6 is increased when compared to initial age = 31. This is because bus 6 is fed from branches 5 and 10. When only branch 5 is in ageing stage, frequent outage leads to decreased supply and consequently increased load curtailment. Next, EENS at bus 18 is also reduced. The supply side of bus 18 is a nuclear generator connected at bus 21, via branches 32 and 33, whilst load at bus 18 and branch 30 are "consumers". Bus 21, where is a nuclear generator is connected, is also supplied by branch 38, but branches 25, 26, 32 and 33 are all fed from bus 21. Branches 25 and 26 transfer much more power than branches 32 and 33. In the partial ageing network, branch

26 and 32 are in the ageing stage. When branch 26 is on outage, its power flow is transferred by branch 33. Therefore, the supply at bus 18 is increased, and load curtailment is reduced consequently.

Table 6-5: System reliability results for different ageing conditions (temporal model)

Ageing Condition	EENS (MWh/yr)	LOLP (p.u.)
Initial Age = 1	24003.54	0.017717
Partial Ageing	26322.97	0.019132
Initial Age = 31	31491.83	0.020205

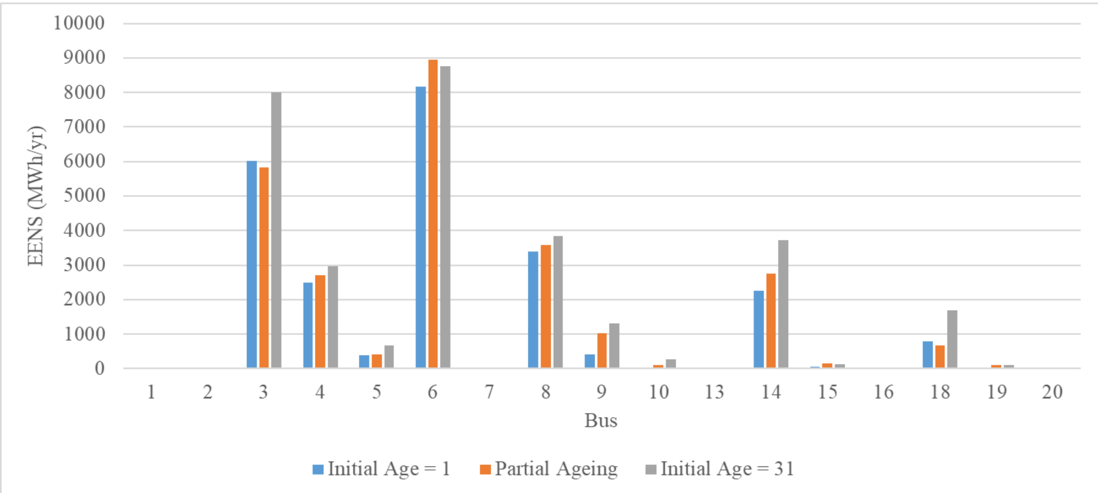

Figure 6-6: Nodal EENS for different ageing conditions (temporal model)

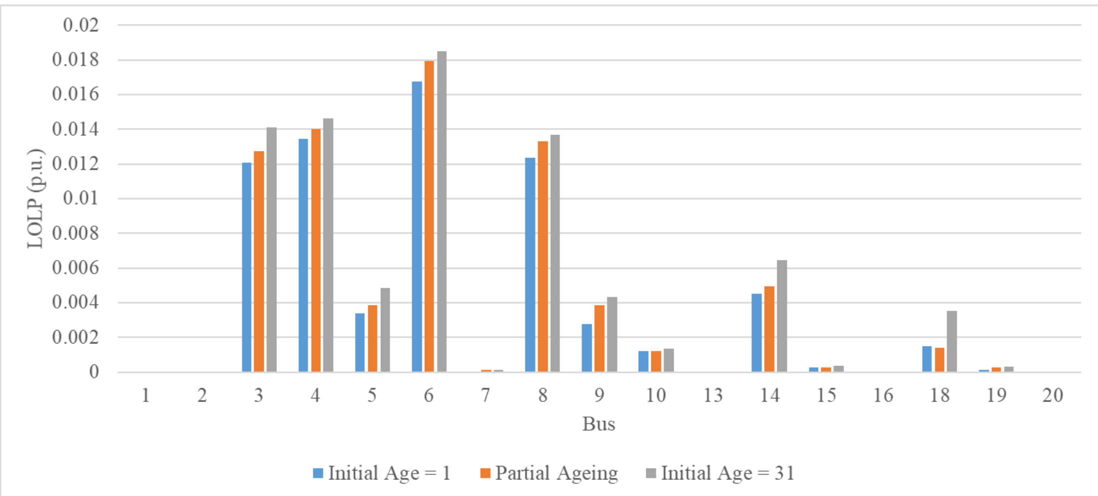

Figure 6-7: Nodal LOLP for different ageing conditions (temporal model)

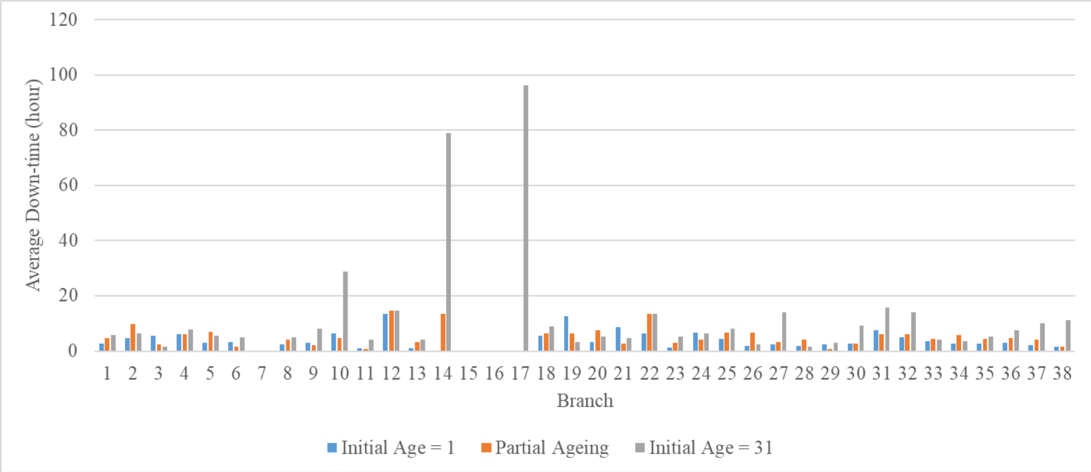

Figure 6-8: Average down-time of each branch for different ageing conditions (temporal model)

Average down-time by branches is shown in Fig. 6-8, whilst average number of repairs in Fig. 6-9. The total number of repairs for the partial ageing network is 153. The total number and total repair costs (Table 6-6) show the same phenomenon as system reliability results.

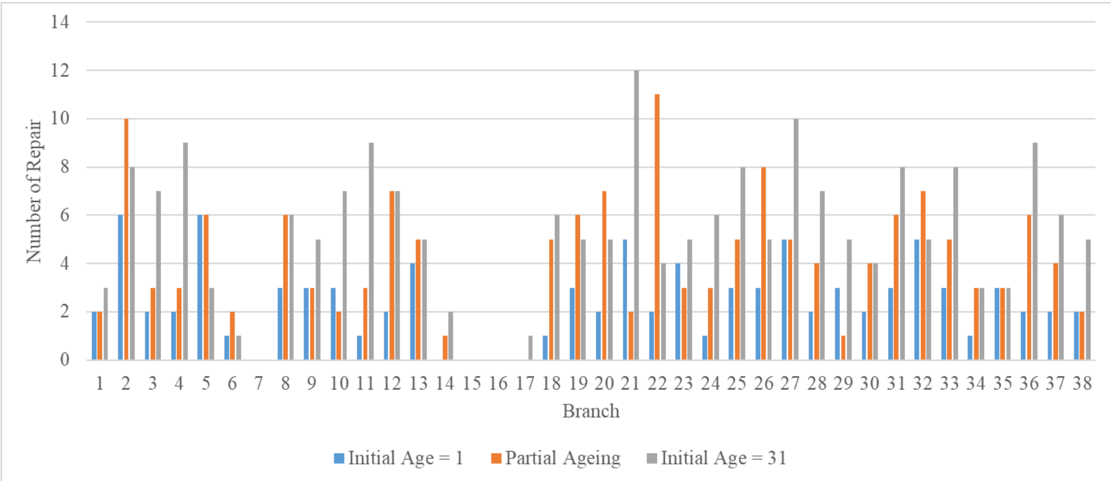

Figure 6-9: Number of repair in each branch for different ageing conditions (temporal model)

Table 6-6: Total repair costs for different ageing conditions (temporal model)

Ageing Condition	Total Repair Costs for Different Repair Types (M£)				
	Minimal Repair	Minor Repair	Major 1 Repair	Major 2 Repair	Replacement
Initial Age = 1	33.634	55.048	109.150	148.115	1766.448
Partial Ageing	55.164	90.948	181.436	240.349	2809.368
Initial Age = 31	68.811	112.541	223.583	305.294	3633.969

6.3.2 Impact of Spatial Correlation

To study the impact of correlation, the following studies cases are done with the given correlation factors:

- No Correlation: the correlation factor is 0.
- Partial correlation: the correlation factor is 0.8 for variables in the same region (north/south) and 0.5 in different regions.
- Full correlation: the correlation factor is 1.

6.3.2.1 Wind Correlation

Initial Age = 1

The reliability indices of the system at initial age of 1 with different wind correlation levels are presented in Table 6-7, Fig. 6-10 and Fig. 6-11. The results indicate that a higher correlation level leads to worse reliability performance. Wind generation is non-dispatchable (i.e. there is no wind curtailment) and causes branch congestions that can only be rectified via load shedding, particularly in the south region. This effect is pronounced when the wind farms are fully correlated. Nodal indices usually follow the same pattern.

Table 6-7: System reliability results with different wind correlation levels – initial age = 1 (temporal model)

Correlation Level	**EENS (MWh/yr)**	**LOLP (p.u.)**
No Correlation	24003.54	0.017717
Partial Correlation	26777.57	0.019418
Full Correlation	32425.65	0.021324

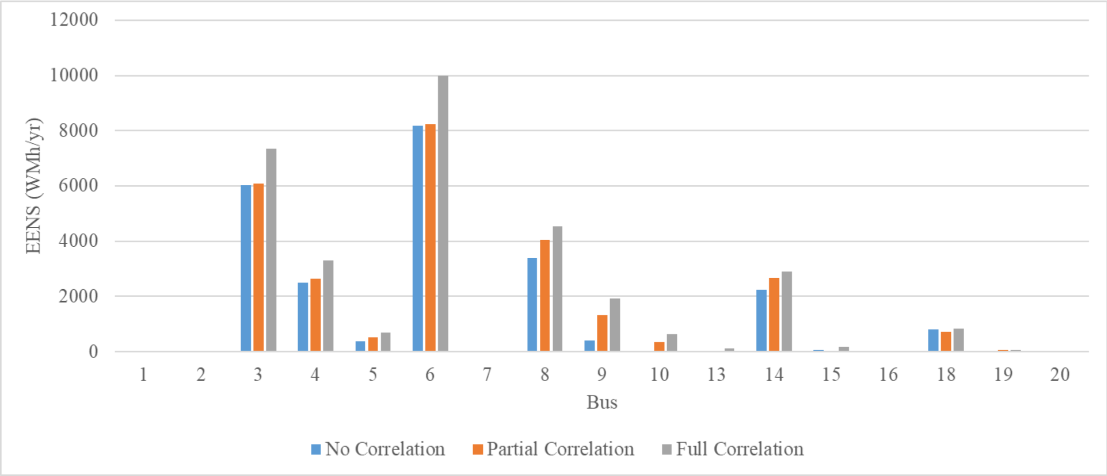

Figure 6-10: Nodal EENS for different wind correlation levels – initial age = 1 (temporal model)

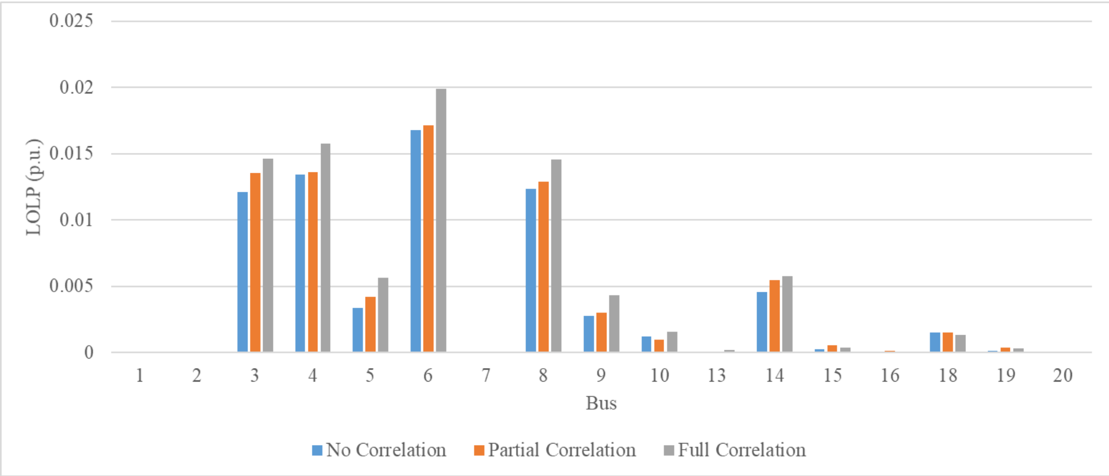

Figure 6-11: Nodal LOLP for different wind correlation levels – initial age = 1 (temporal model)

Average down-times and number of repairs in each branch are shown in Fig. 6-12. The number of repairs in some branches is higher for partial correlation than full correlation, for example, branches 10, 11, 12 and 27. In the cases of no correlation and partial correlation, there are no repairs for transformer branches 7, 14, 15, 16 and 17, whilst branch 14 has the highest average down-time when wind speeds are fully correlated.

The total numbers of repair for the three cases are 92, 129 and 145, and the total repair costs for each repair type are given in Fig. 6-13. It can be found that when correlation level rises, system reliability reduces and total repair costs increase.

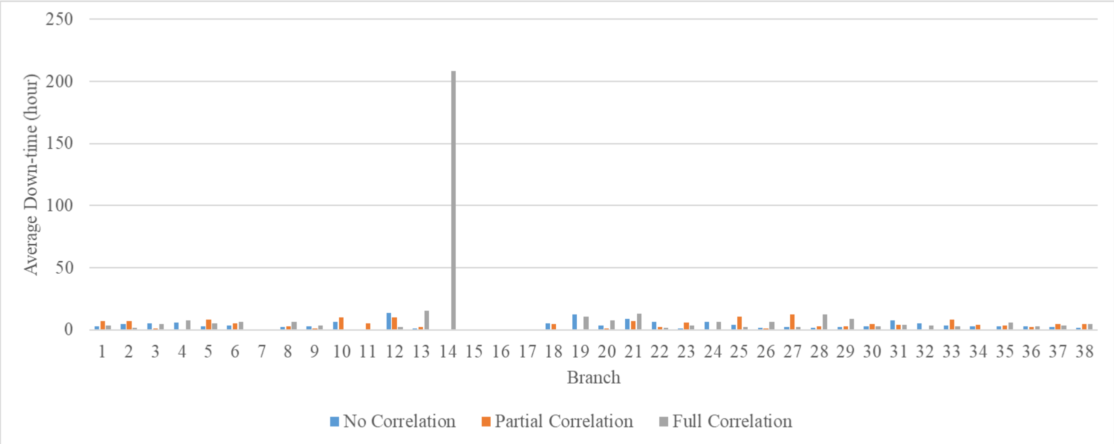

Figure 6-12: Average down-time of each branch for different wind correlation levels – initial age = 1 (temporal model)

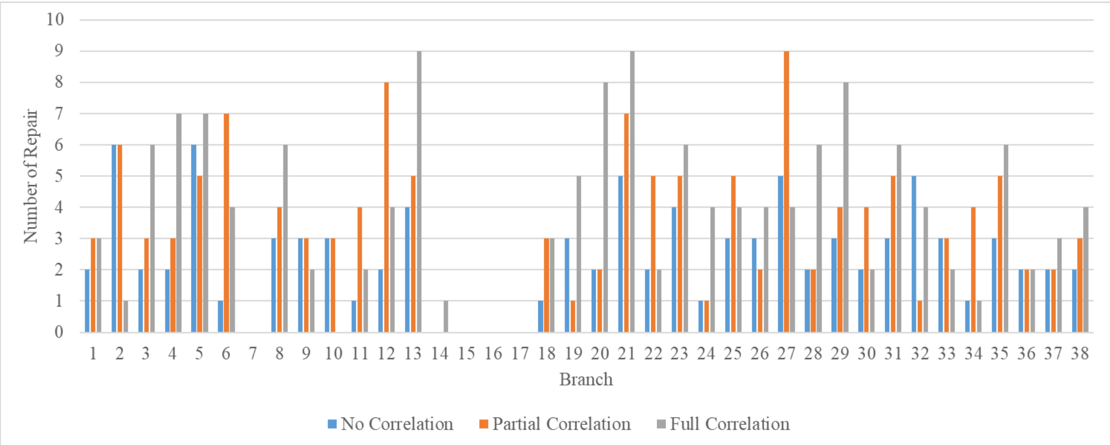

Figure 6-13: Number of repair in each branch for different wind correlation levels – initial age = 1 (temporal model)

Table 6-8: Total repair costs for different repair types of system with different wind correlation levels – initial age = 1 (temporal model)

Correlation Level	**Total Repair Costs for Different Repair Types (M£)**				
	Minimal Repair	**Minor Repair**	**Major 1 Repair**	**Major 2 Repair**	**Replacement**
Zero	33.634	55.048	109.150	148.115	1766.448
Partial	48.228	79.195	157.392	211.126	2497.248
Full	50.653	83.843	167.734	219.144	2534.448

Initial Age = 21

The values of reliability indices with different wind correlation levels are higher than the previous case (initial age = 1). The same phenomenon applied to this study case: an increment in correlation level causes weakening in network reliability.

Table 6-9: System reliability results with different wind correlation levels – initial age = 21 (temporal model)

Correlation Level	**EENS (MWh/yr)**	**LOLP (p.u.)**
No Correlation	27519.17	0.019566
Partial Correlation	28490.75	0.021418
Full Correlation	32670.31	0.023482

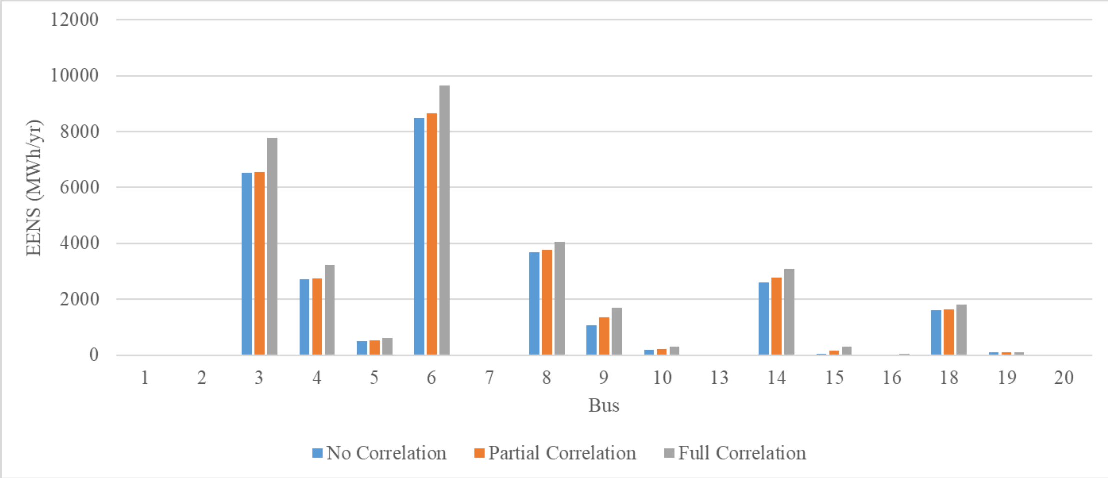

Figure 6-14: Nodal EENS for different wind correlation levels – initial age = 21 (temporal model)

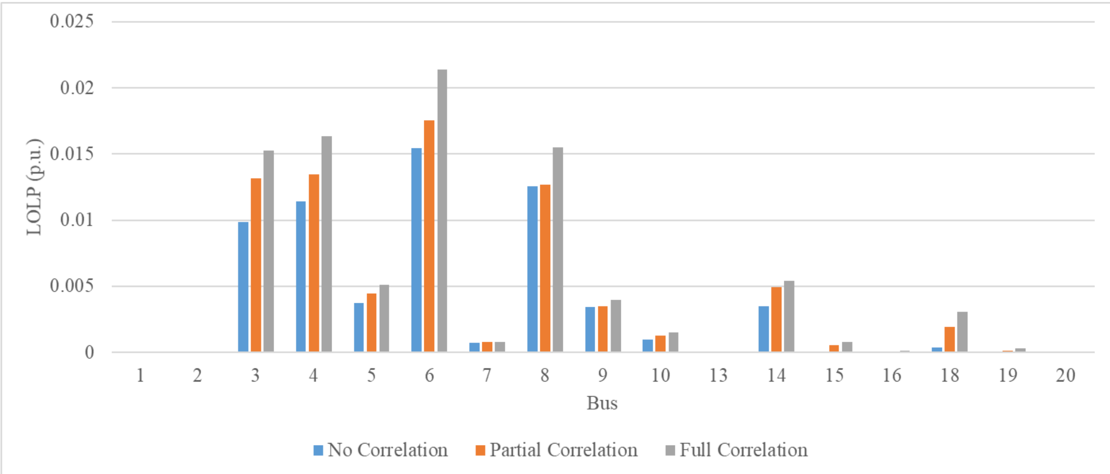

Figure 6-15: Nodal LOLP for different wind correlation levels – initial age = 21 (temporal model)

In this study case, transformer branch 17 has the highest average down-time. The total numbers of repair for the three cases are 149, 156 and 181, which are higher than the previous case (initial age = 1), and the total repair costs for each repair type are in Table 6-10. It can be found that when correlation level rises, system reliability reduces and total repair costs increase.

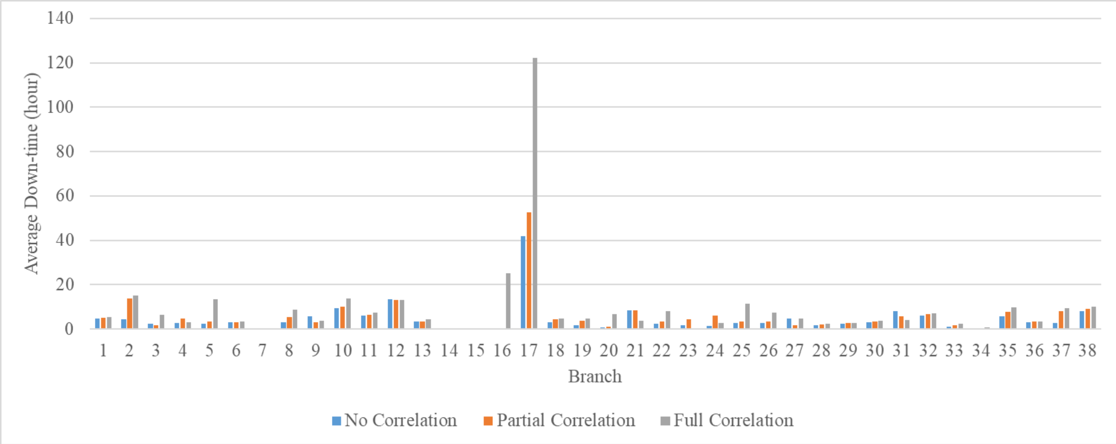

Figure 6-16: Average down-time of each branch for different wind correlation levels – initial age = 21 (temporal model)

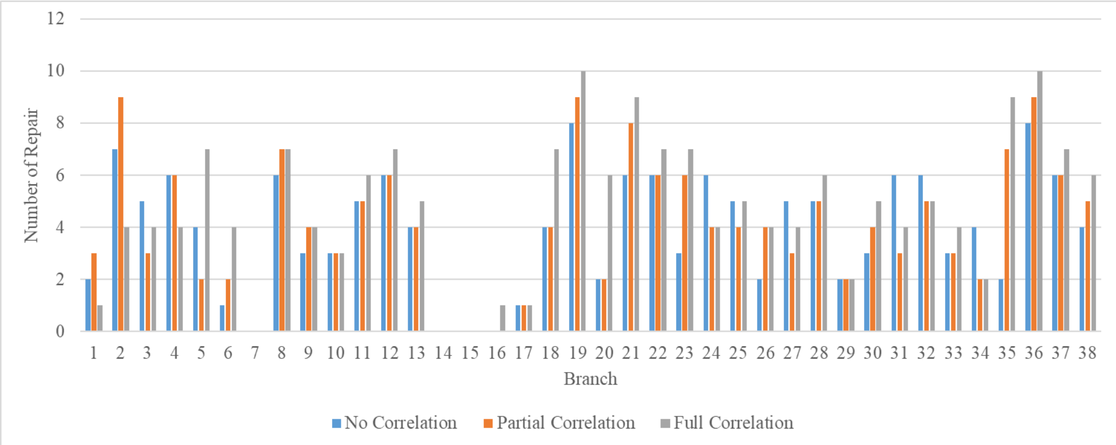

Figure 6-17: Number of repair in each branch for different wind correlation levels – initial age = 21 (temporal model)

Table 6-10: Total repair costs for different repair types of system with different wind correlation levels – initial age = 21 (temporal model)

Correlation Level	**Total Repair Costs for Different Repair Types (M£)**				
	Minimal Repair	**Minor Repair**	**Major 1 Repair**	**Major 2 Repair**	**Replacement**
Zero	51.150	84.093	167.447	224.058	2637.804
Partial	52.767	86.733	172.675	231.202	3138.540
Full	61.317	100.997	201.514	268.179	3138.540

Initial Age = 31

In this case, the reliability results are higher than the previous cases (initial age = 1&21). And the same conclusion applies to this study case: the higher correlation level leads to worse system performance.

Table 6-11: System reliability results with different wind correlation levels – initial age = 31 (temporal model)

Correlation Level	EENS (MWh/yr)	LOLP (p.u.)
No Correlation	31491.83	0.020205
Partial Correlation	32722.14	0.021685
Full Correlation	34046.96	0.023084

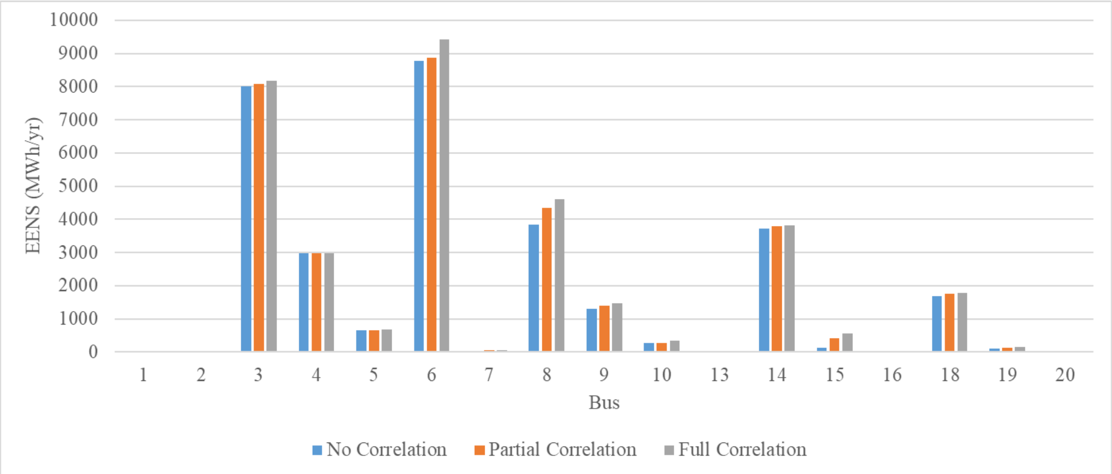

Figure 6-18: Nodal EENS for different wind correlation levels – initial age = 31 (temporal model)

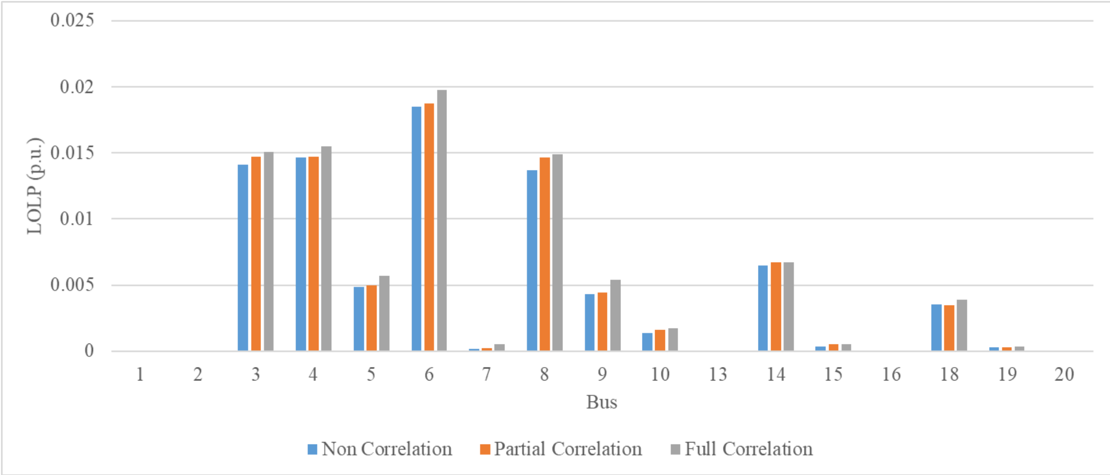

Figure 6-19: Nodal LOLP for different wind correlation levels – initial age = 31 (temporal model)

In this case, higher average down-time occurs at bus 14 and 17, which shows an exacerbation compared to the previous cases. The total numbers of repair for the three cases are 202, 229 and 256, which are higher than the previous cases, and the total repair costs for each repair type are given in Table 6-12. It can be found that when correlation level rises, system reliability reduces and total repair costs increase.

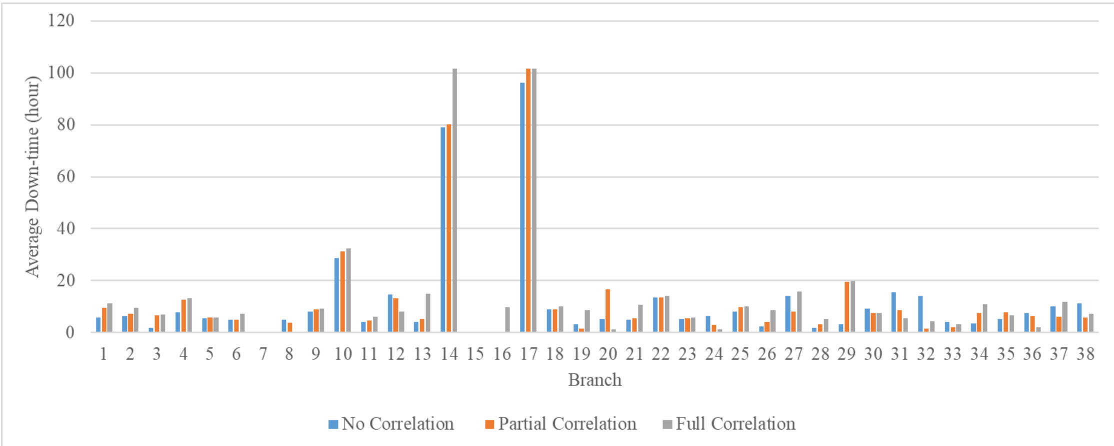

Figure 6-20: Average down-time of each branch for different wind correlation levels – initial age = 31 (temporal model)

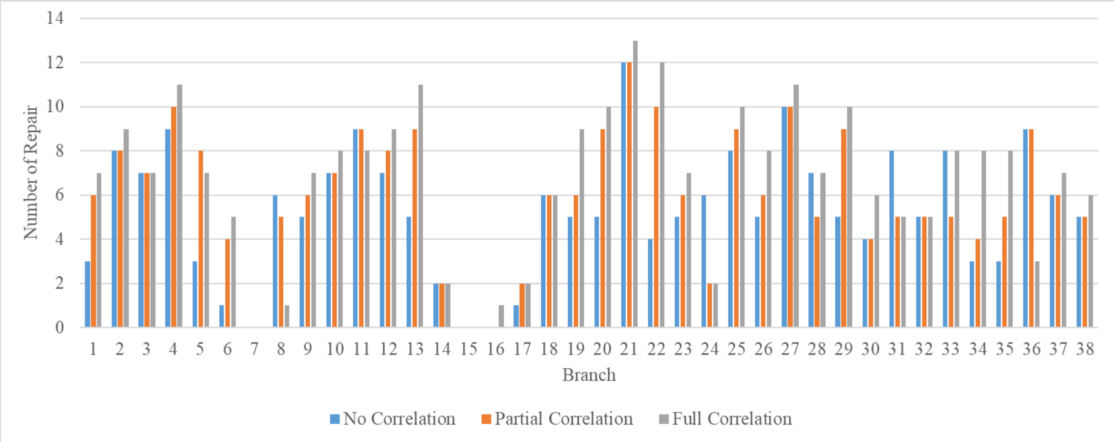

Figure 6-21: Number of repair in each branch for different wind correlation levels – initial age = 31 (temporal model)

Table 6-12: Total repair costs for different repair types of system with different wind correlation levels – initial age = 31 (temporal model)

Correlation Level	**Total Repair Costs for Different Repair Types (M£)**				
	Minimal Repair	**Minor Repair**	**Major 1 Repair**	**Major 2 Repair**	**Replacement**
Zero	68.811	112.541	223.583	305.294	3633.969
Partial	79.459	130.090	258.729	352.226	4179.597
Full	88.971	145.629	289.681	394.886	4686.249

6.3.2.2 Wind and Load Correlation

Initial Age = 1

The reliability results of the three wind correlation and load correlation levels are given in Table 6-13, Fig. 6-22 and Fig. 6-23. Compared to the study of wind correlation, the increment of reliability indices between each correlation level is bigger, which indicates the combination of different correlations has a high impact on the network performance.

Table 6-13: System reliability results with different wind and load correlation levels – initial age = 1 (temporal model)

Correlation Level	EENS (MWh/yr)	LOLP (p.u.)
No Correlation	24003.54	0.017717
Partial Correlation	29889.17	0.020845
Full Correlation	34172.02	0.022500

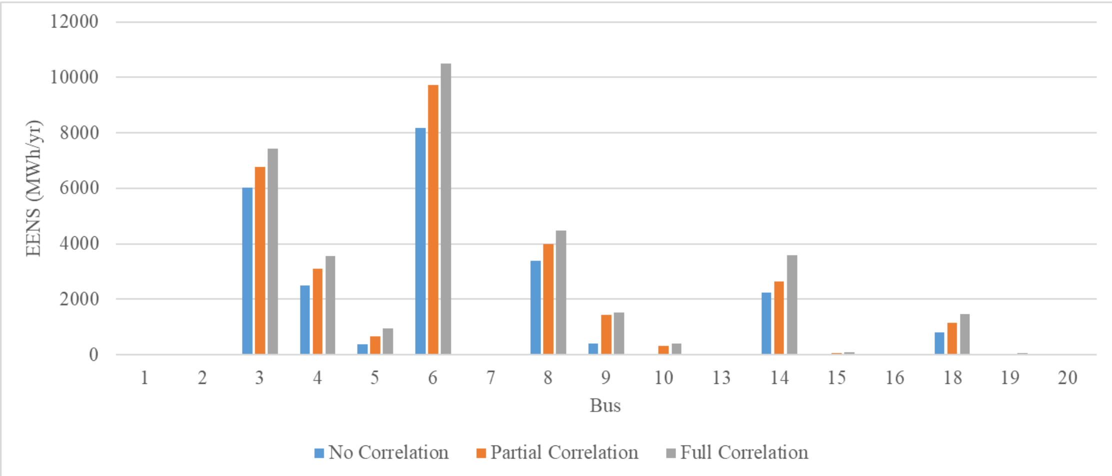

Figure 6-22: Nodal EENS for different wind and load correlation levels – initial age = 1 (temporal model)

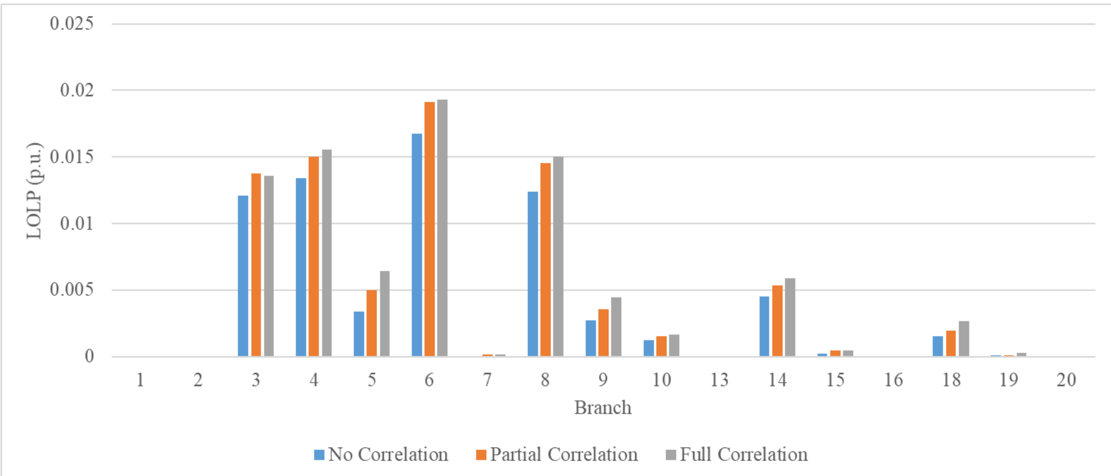

Figure 6-23: Nodal LOLP for different wind and load correlation levels – initial age = 1 (temporal model)

Average down-times and number of repairs in each branch are shown in Fig. 6-24 and Fig. 6-25 respectively. The number of repairs of transformer branches 7, 14 and 17 is highest for the full correlations. The total numbers of repair of the three study cases are 92, 138 and 172, which are higher than the study of wind correlation only. And the repair costs show the same trend: the repair costs of network with combined correlation are higher than wind correlation only.

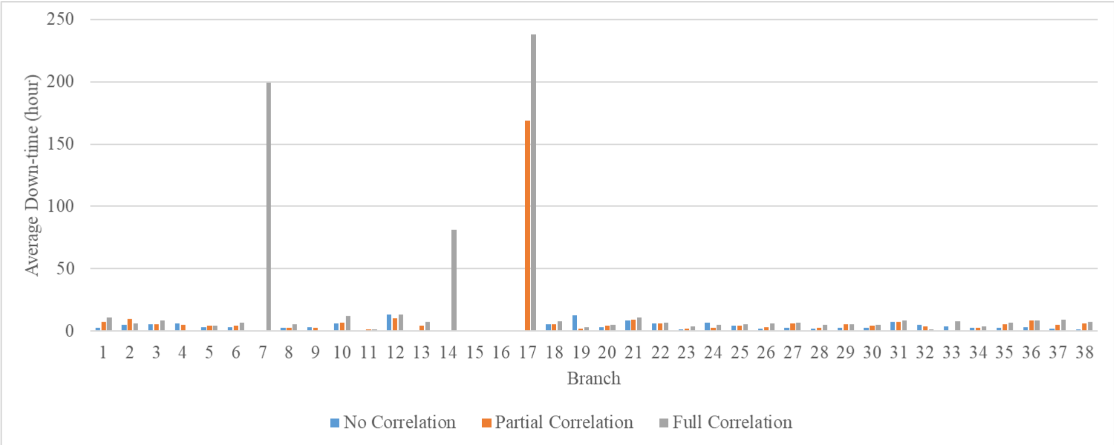

Figure 6-24: Average down-time of each branch for different wind and load correlation levels – initial age = 1 (temporal model)

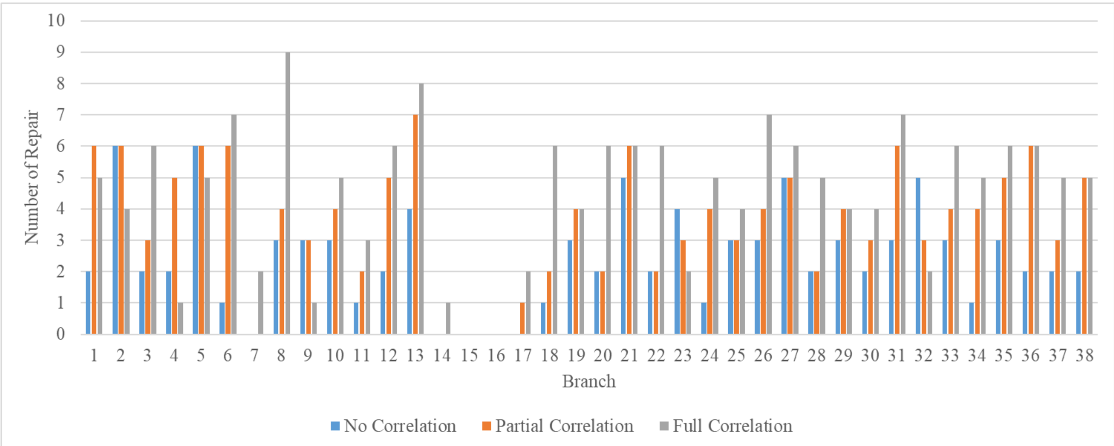

Figure 6-25: Number of repair in each branch for different wind and load correlation levels – initial age = 1 (temporal model)

Table 6-14: Total repair costs for different repair types of system with different wind and load correlation levels – initial age = 1 (temporal model)

Correlation Level	Total Repair Costs for Different Repair Types (M£)				
	Minimal Repair	Minor Repair	Major 1 Repair	Major 2 Repair	Replacement
Zero	33.634	55.048	109.150	148.115	1766.448
Partial	48.295	79.005	156.780	213.495	2544.801
Full	58.051	95.080	189.527	258.456	3054.738

Initial Age = 21

Compared to the study of wind correlation, the same conclusion applies to this study case. Compared to the previous case (initial age = 1), it can be found that ageing assets have a negative impact on the network reliability.

Table 6-15: System reliability results with different wind and load correlation levels – initial age = 21 (temporal model)

Correlation Level	EENS (MWh/yr)	LOLP (p.u.)
No Correlation	27519.17	0.019566
Partial Correlation	33032.40	0.022043
Full Correlation	36685.33	0.025171

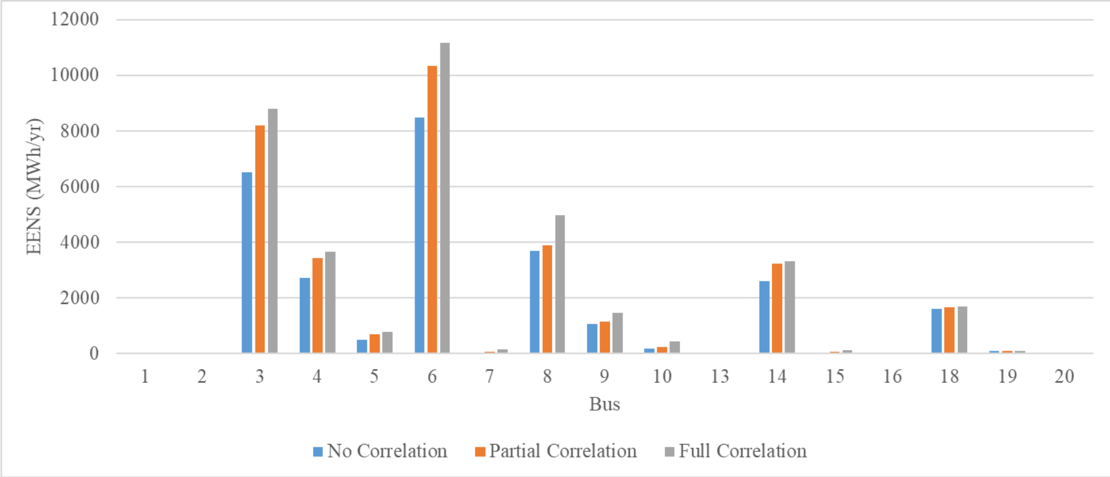

Figure 6-26: Nodal EENS for different wind and load correlation levels – initial age = 21 (temporal model)

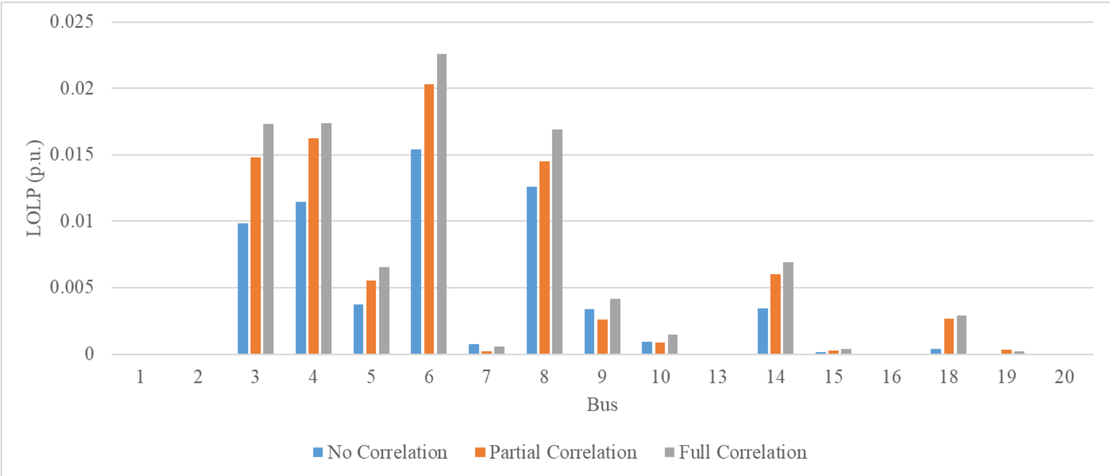

Figure 6- 27: Nodal LOLP for different wind and load correlation levels – initial age = 21 (temporal model)

Average down-times and number of repairs in each branch are shown in Fig. 6-28 and Fig. 6-29 respectively. The highest average down-time occurs at transformer branch 16 and 17 for fully correlated case. The total numbers of repair for the three cases are 149, 173 and 202, which is higher than the case of initial age =1, as well as the case of initial age =21 with wind correlation only. And the repair costs are higher than these cases as well.

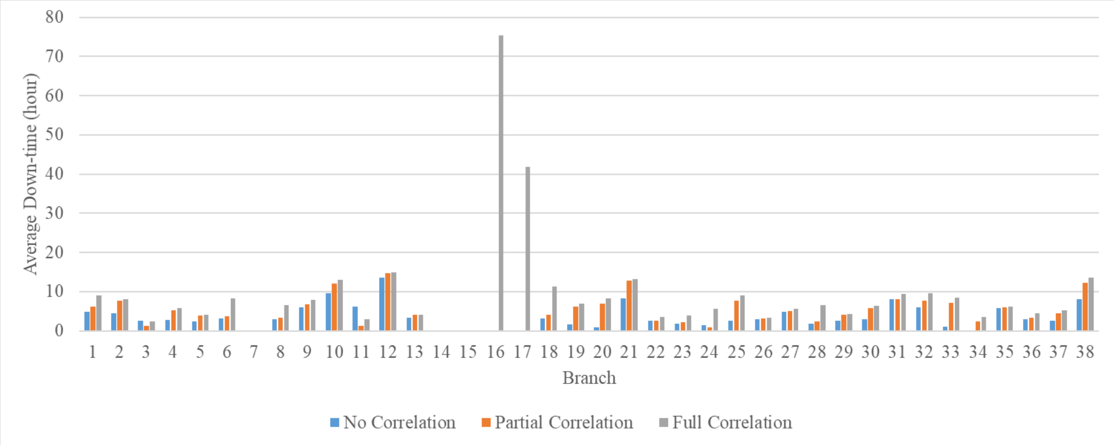

Figure 6-28: Average down-time of each branch for different wind and load correlation levels – initial age = 21 (temporal model)

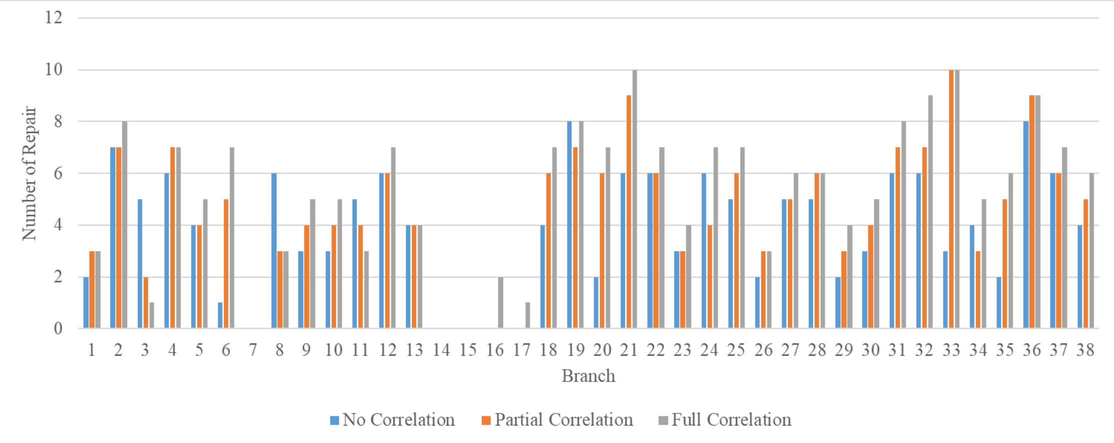

Figure 6-29: Number of repair in each branch for different wind and load correlation levels – initial age = 21 (temporal model)

Table 6-16: Total repair costs for different repair types of system with different wind and load correlation levels – initial age = 21 (temporal model)

Correlation Level	Total Repair Costs for Different Repair Types (M£)				
	Minimal Repair	**Minor Repair**	**Major 1 Repair**	**Major 2 Repair**	**Replacement**
Zero	51.148	84.071	167.197	223.508	2637.144
Partial	60.138	98.727	196.176	263.381	3117.297
Full	69.262	113.697	226.454	305.263	3600.474

Initial Age = 31

In this study, the same conclusion applies to this study case: ageing assets have a negative impact on the network reliability.

Table 6-17: System reliability results with different wind and load correlation levels – initial age = 31 (temporal model)

Correlation Level	EENS (MWh/yr)	LOLP (p.u.)
No Correlation	31491.83	0.020205
Partial Correlation	35086.59	0.023180
Full Correlation	38811.49	0.025651

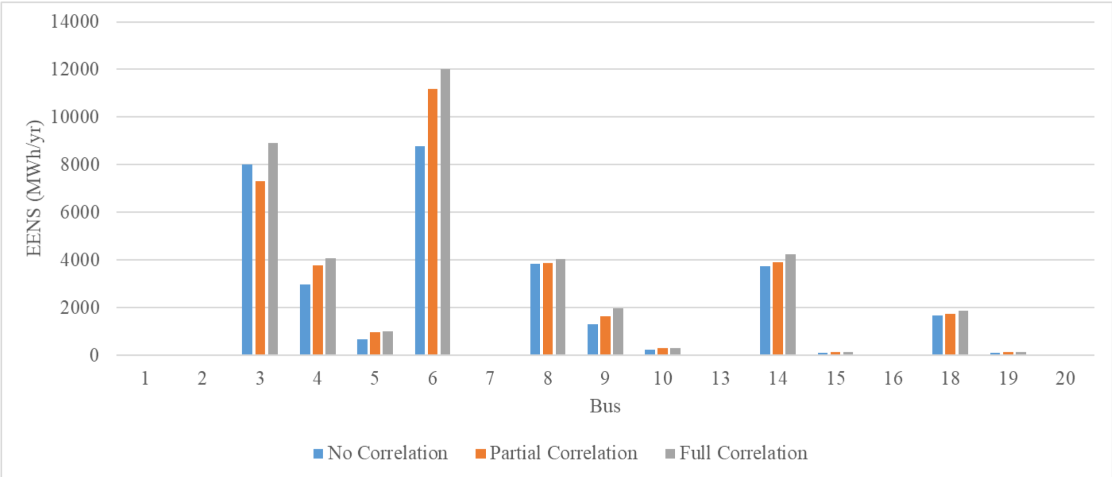

Figure 6-30: Nodal EENS for different wind and load correlation levels – initial age = 31 (temporal model)

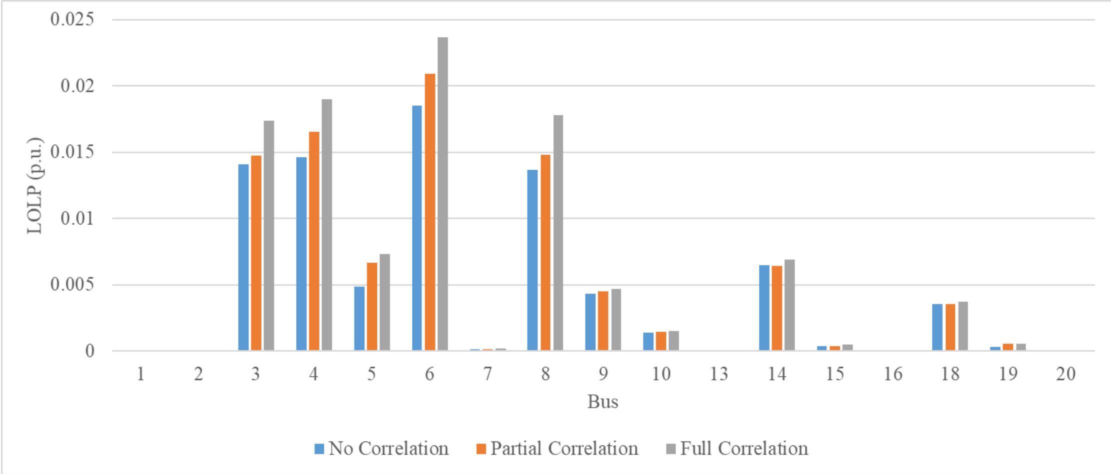

Figure 6-31: Nodal LOLP for different wind and load correlation levels – initial age = 31 (temporal model)

Average down-times and number of repairs in each branch are shown in the Fig. 6-32 and Fig. 6-33 respectively. The highest average down-time occurs at transformer branches 14, 16 and 17, followed by cable branch 10. The total numbers of repair for the three cases are 196, 220 and 258, which is higher than all the previous cases. It can be concluded that ageing assets and the combination of different correlations can cause frequent repairs and consequently high repair costs.

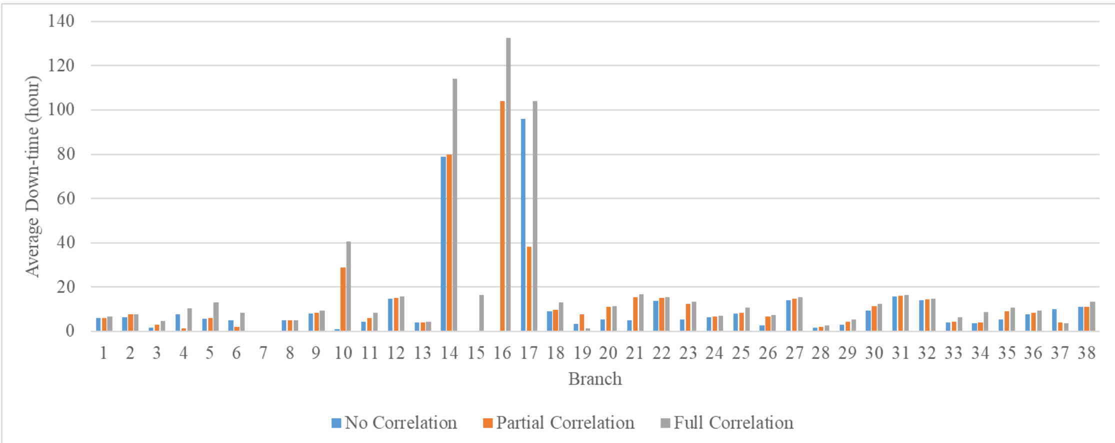

Figure 6-32: Average down-time of each branch for different wind and load correlation levels – initial age = 31 (temporal model)

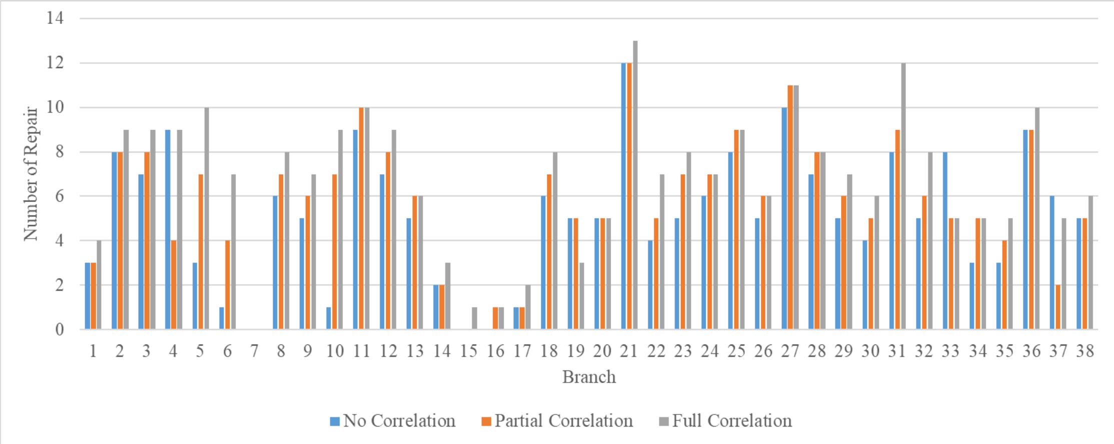

Figure 6-33: Number of repair in each branch for different wind and load correlation levels – initial age = 31 (temporal model)

Table 6-18: Total repair costs for different repair types of system with different wind and load correlation levels – initial age = 31 (temporal model)

Correlation Level	Total Repair Costs for Different Repair Types (M£)				
	Minimal Repair	Minor Repair	Major 1 Repair	Major 2 Repair	Replacement
Zero	66.305	109.613	219.407	288.590	3341.649
Partial	75.822	124.178	247.062	336.015	3983.064
Full	89.148	145.869	290.451	397.159	4708.362

6.3.3 Impact of Generation Reliability

Generation reliability is studied in the base case without correlation. In-service time of ageing generator is assumed to be modified Weibull distribution with shape parameter $\beta = 2$, and out-of-service time is modelled via exponential distribution. Other involved parameters are given in [56]. The reliability results are drastically larger than base case, which shows that ageing generation has a significant, negative impact on system reliability. EENS and LOLP differences between different initial ages are relatively small because the overall reliability is driven by ageing generation.

Table 6-19: System reliability results with generation reliability (temporal model)

Initial Age (yr)	Generator Reliability	EENS (MWh/yr)	LOLP (p.u.)
1	Without	24003.54	0.017717
	With	750725.35	0.060776
21	Without	27519.17	0.019566
	With	768675.84	0.061130
31	Without	31491.83	0.020205
	With	781233.02	0.062272

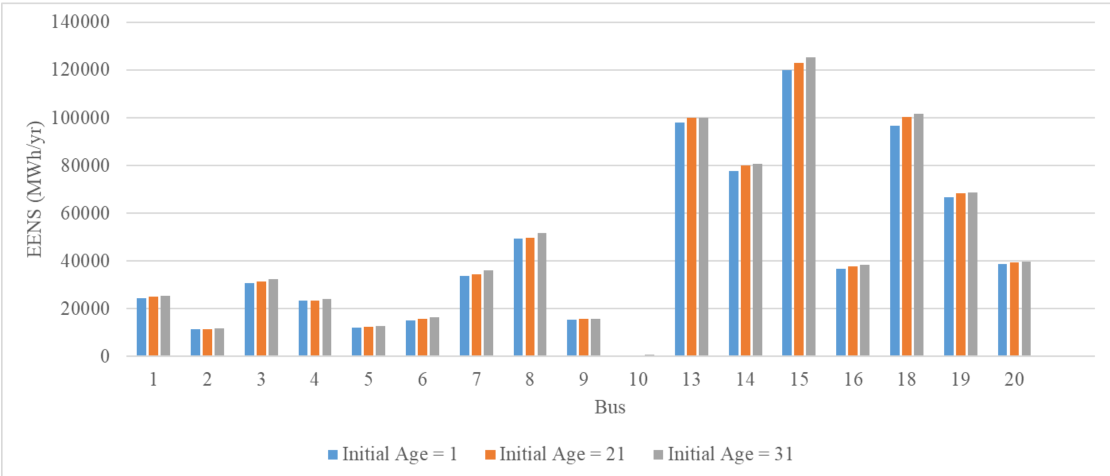

Figure 6-34: Nodal EENS with generation reliability (temporal model)

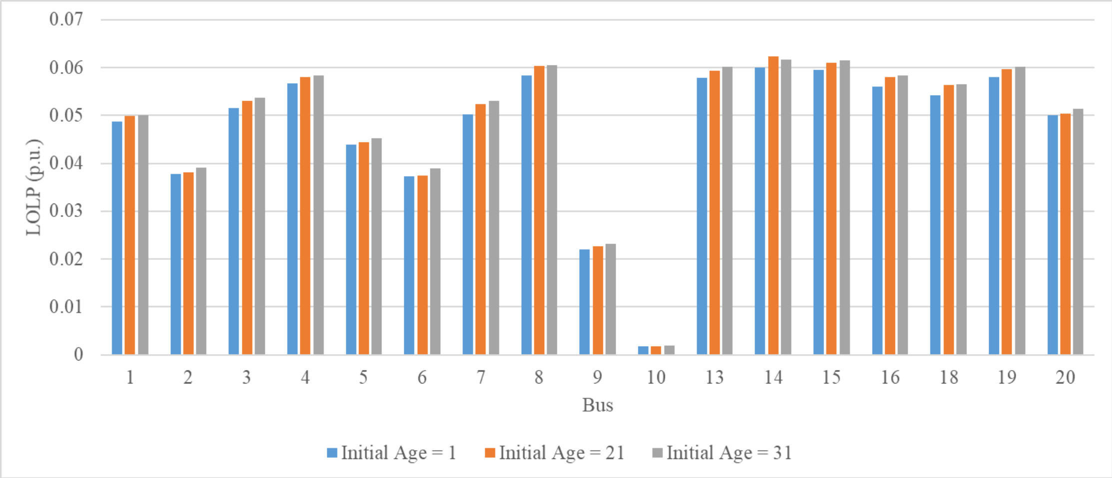

Figure 6-35: Nodal LOLP with generation reliability (temporal model)

6.4 Deterministic Asset Health Modelling

6.4.1 Addition Input Data

Parameters used in hazard functions (Eq.(5-9)) are specified in the following tables:

Table 6-20: Parameters for deterministic asset health modelling [131]

Asset Type	Normal Expected Life (yr)	K-value	C-value	γ-value
Cable	100	0.0658%	1.087	0.08
Transformer	60	0.0454%	1.087	0.1
Overhead Line	50	0.0080%	1.087	0.3

Table 6-21: Default values of factors for deterministic asset health modelling

Factor	Default Value
Location Factor	1
Duty Factor	1
Health Score Factor	1
Reliability Factor	1

Table 6-22: Functions of ageing reduction factor [131]

Current Health Score (CHS)	Ageing Reduction Factor
< 2	1
2 to 5.5	$[CHS - 2] / 7 + 1$
> 5.5	1.5

6.4.2 Base Case Study

Three base-case studies are done; the initial asset age is 1 yr, 21 yr and 31 yr. System reliability indices substantially increase with the increase in asset age. Fig. 6-36 and Fig. 6-37 present nodal reliability results of the three study cases. The results at node level follow the same trend as system level. It can be seen that, in deterministic approach, bus 3 and 6 have the worst performance. Both of these buses have no generating units, which contributes to the higher load curtailment. The same reason applies to bus 4, 5, 8, 9 and 10. All these buses are located in southern area. In addition, the significant outage time of transformers connected to bus 3, 9 and 10 also contributes to higher load curtailment at these buses. In the north, the relatively worse performance occurs at bus 14. The reason is that bus 14 has no generators and limited transmission capacity due to two transmission links.

Table 6-23: System reliability results with three initial ages (deterministic approach)

Initial Age (yr)	EENS (MWh/yr)	LOLP (p.u.)
1	25026.99	0.022158
21	31488.89	0.029703
31	54997.05	0.060845

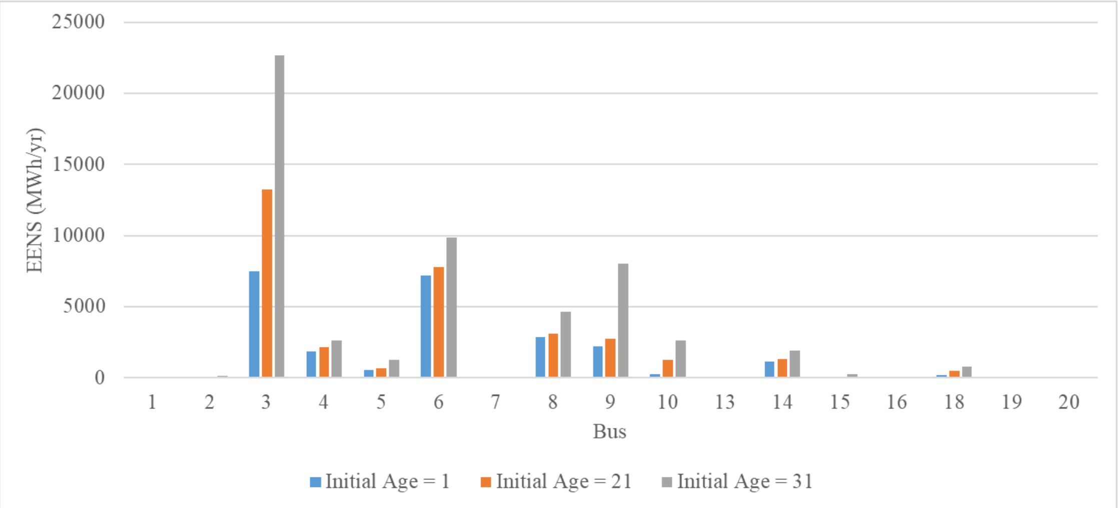

Figure 6-36: Nodal EENS for different initial ages (deterministic approach)

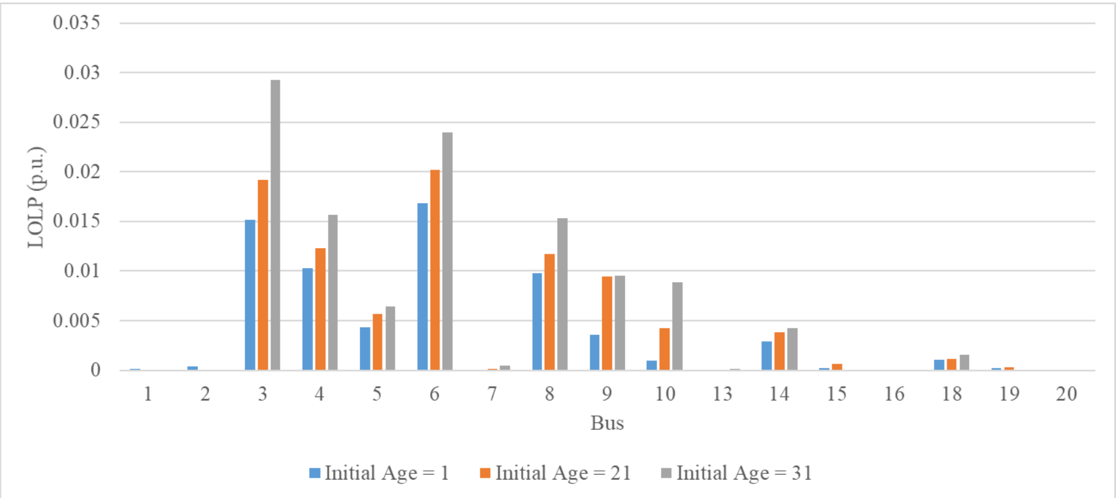

Figure 6-37: Nodal LOLP for different initial ages (deterministic approach)

HI score results show that different asset categories exhibit different paths as assets become older. When assets are new and young, their HIs all stay at 1. When assets are in service for a certain time (initial age = 21), overhead lines transition from HI1 to HI3, whilst transformers and cables remain at HI1. When assets become older (initial age = 31), overhead lines go to HI5; transformers transition from HI1 to HI3; and cables remain at HI1. The HI score results of deterministic approach indicate the deterioration of cable is the slowest, followed by transformer.

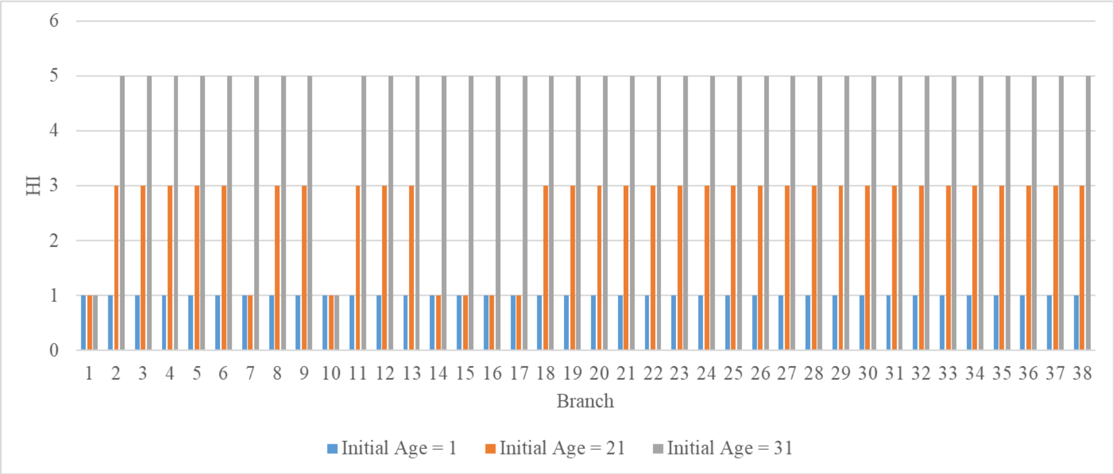

Figure 6-38: Asset rounded-off HI at the end of simulation period for different initial ages (deterministic approach)

Fig. 6-39 and Fig. 6-40 present average down-time and number of repairs in each branch. Total repair numbers of all assets are 207 (initial age =1), 548 (initial age =21) and 1162 (initial age =31). The numbers are much higher than in the cases of temporal model.

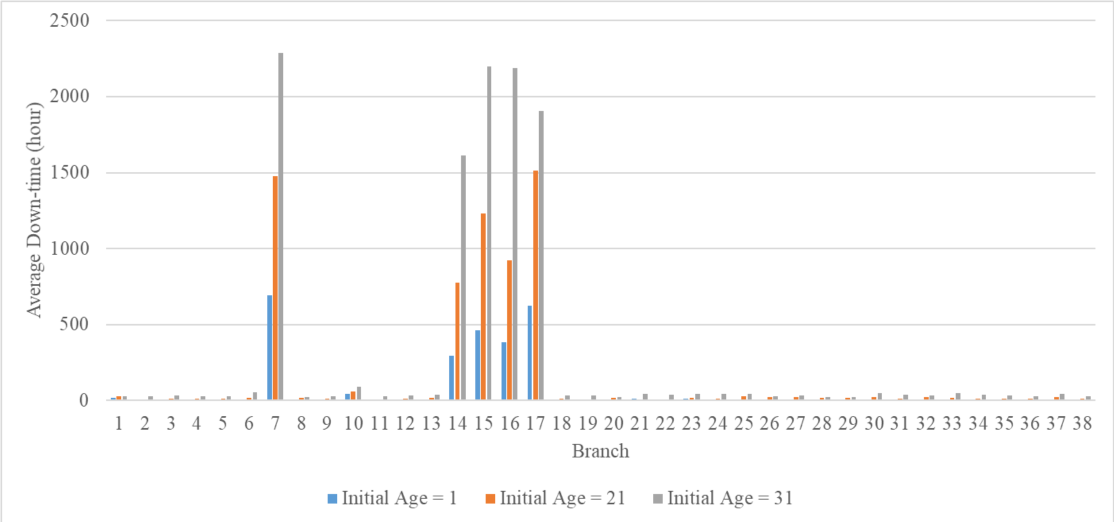

Figure 6-39: Average down-time of each branch for different initial ages (deterministic approach)

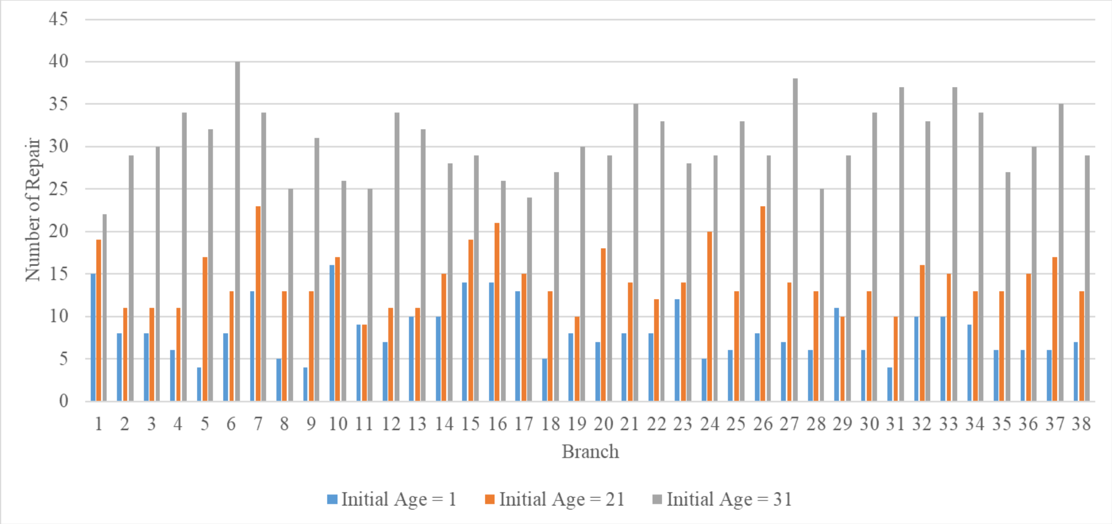

Figure 6-40: Number of repair in each branch for different initial ages (deterministic approach)

Similar to temporal model, repair types are not modelled in the deterministic HI model; total asset repair costs are calculated for the five types of repairs given in Table 6-2. Variation of costs by repair types is huge.

Table 6-24: Asset repair costs for different repair types (deterministic approach)

Initial Age (yr)	Asset	Repair Costs for Different Repair Types (M£)				
		Minimal Repair	Minor Repair	Major 1 Repair	Major 2 Repair	Replacement
1	Cable	7.308	8.540	12.180	48.720	852.600
	Tx	0.086	0.858	9.750	21.450	25.740
	OHL	49.092	81.354	162.707	211.333	2440.611
	Total	56.487	90.752	184.637	281.503	3318.951
21	Cable	8.579	10.035	14.312	57.246	1001.805
	Tx	0.205	2.046	23.250	51.150	61.380

	OHL	137.834	228.410	456.820	593.340	6852.294
	Total	146.625	240.490	494.381	701.736	7915.479
31	Cable	12.580	14.701	20.967	83.868	1467.690
	Tx	0.3102	3.102	35.250	77.550	93.060
	OHL	332.456	550.928	1101.855	1431.145	16527.825
	Total	345.347	568.731	1158.072	1592.563	18088.575

6.4.3 Impact of Location and Duty Factor

Assumed location- (LF) and duty-factors (DF) are shown in Table 6-25.

Table 6-25: Assumed location and duty factors

Branch	"From" Bus	"To" Bus	Asset Type	Influenced Location	Location Factor	Duty Factor
1	1	2	Cable	/	1	1.1
7	3	24	Transformer	Distance from Coast	1.1	1.05
17	11	13	Transformer	Distance from Coast	1.05	1.05
20	12	13	Overhead Line	Distance from Coast	1.2	1
27	15	24	Overhead Line	Distance from Coast	1.5	1

30	17	18	Overhead Line	Altitude	1.15	1
31	17	22	Overhead Line	Altitude	1.05	1
32	18	21	Overhead Line	Altitude	1.05	1
33	18	21	Overhead Line	Altitude	1.05	1
38	21	22	Overhead Line	Altitude	1.05	1

When assets are young, system reliability is relatively similar; the difference increases when assets are older. However, there is no exponential increase in unreliability. Similar conclusions can be drawn for total repair costs.

Table 6-26: System reliability results for modified duty and location factor (deterministic approach)

Initial Age (yr)	**Factor Value**	**EENS (MWh/yr)**	**LOLP (p.u.)**
1	Default	25026.99	0.022158
	Modified	25759.15	0.023721
21	Default	31488.89	0.029703
	Modified	33612.14	0.034759

31	Default	54997.05	0.060845
	Modified	58904.43	0.065881

Table 6-27: Total repair costs for modified location and duty factors (deterministic approach)

Initial Age (yr)	**Total Repair Costs for Different Repair Types (M£)**				
	Minimal Repair	**Minor Repair**	**Major 1 Repair**	**Major 2 Repair**	**Replacement**
1	59.817	96.919	197.755	305.353	4628.706
21	156.803	266.557	520.692	746.903	8518.881
31	368.761	606.773	1204.480	1654.580	19040.384

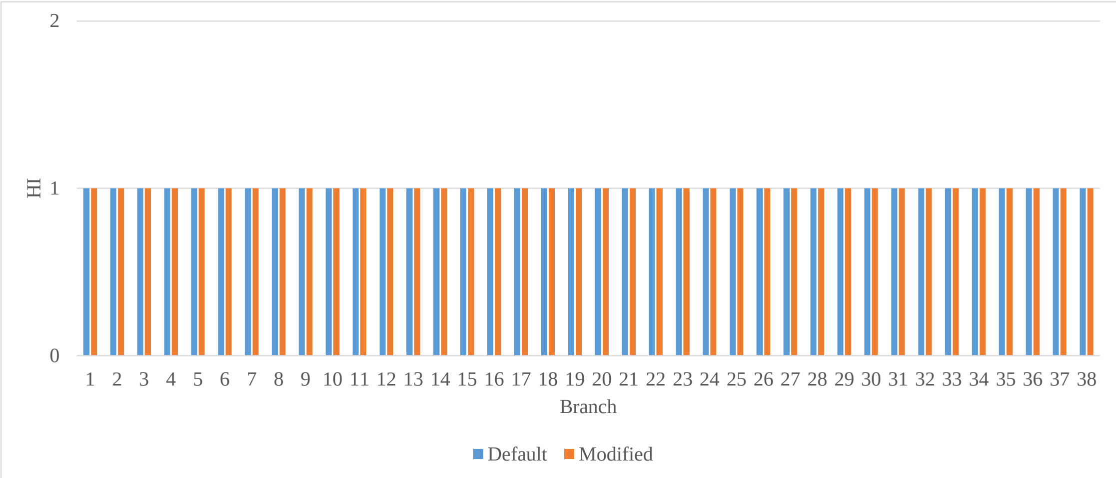

a). Initial Age = 1

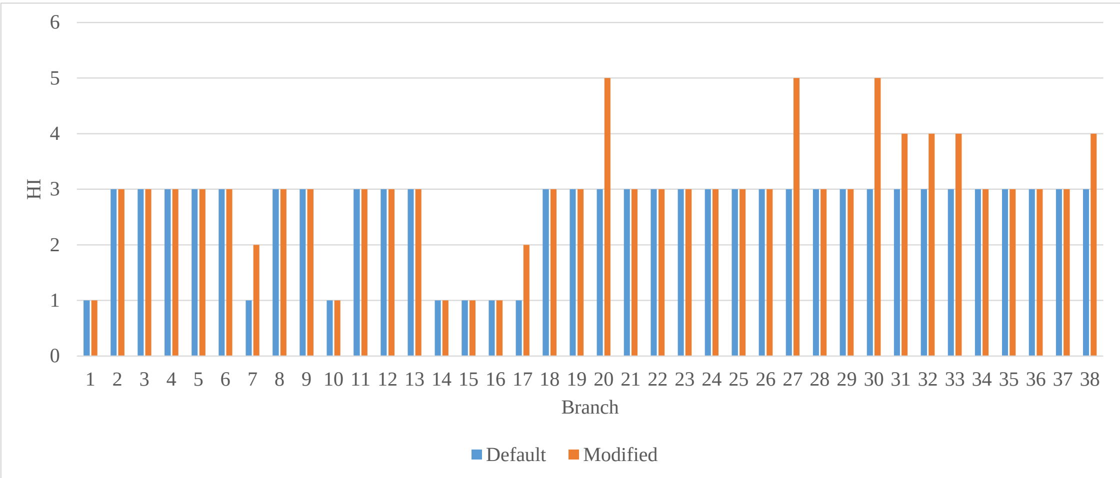

b). Initial Age = 21

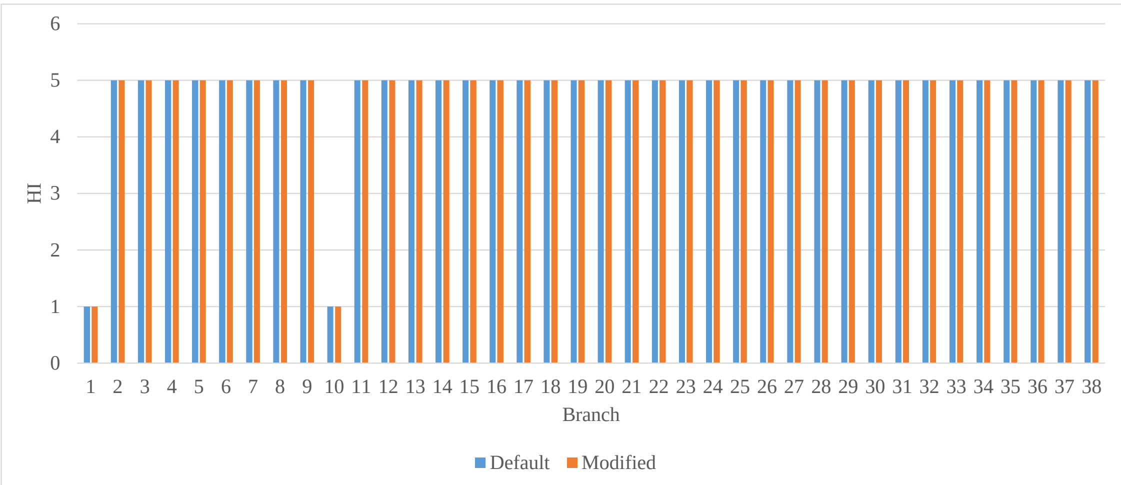

c). Initial Age = 31

Figure 6-41: Asset HI at the end of simulation period with different duty and location factors (deterministic approach)

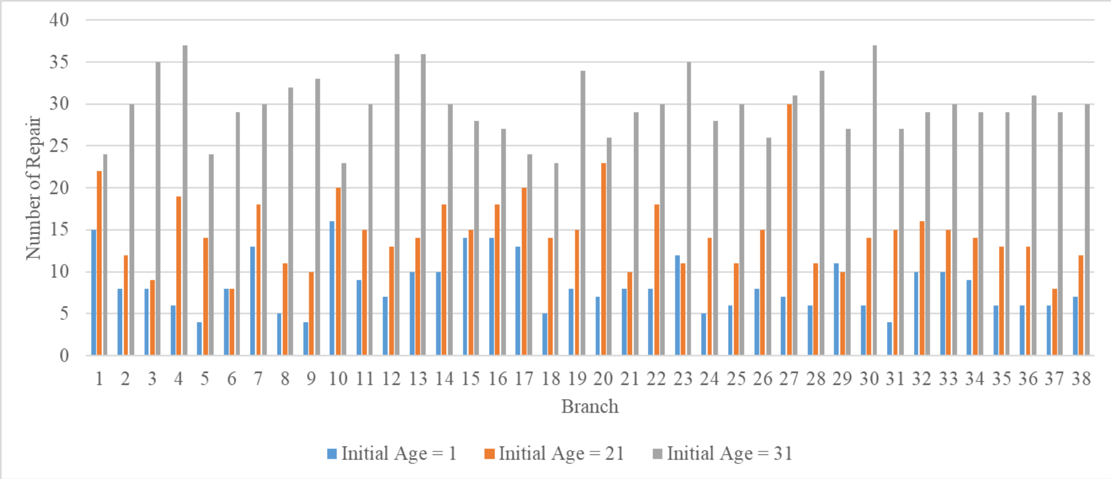

Figure 6-42: Number of repair with modified duty and location factor for different initial ages (deterministic approach)

6.4.4 Impact of Health Score Factor

Health score factor is determined from observed condition factor and measured condition factor. The calculation is presented in Table 6-28:

- a is the maximum value of observed condition factor and measured condition factor;
- b is the minimum value of observed condition factor and measured condition factor.

Table 6-28: Calculation of health score factor [131]

a	**b**	**Health Score Factor**
> 1	> 1	a + [(b – 1) / 1.5]
> 1	≤ 1	a
≤ 1	≤ 1	b + [(a – 1) / 1.5]

The other related data are introduced in [131]. In this study, ten branches (the same as partial ageing case in temporal model) are considered to have normal wear. For these branches, observed condition input is set to be 1.1 (normal wear), and measured condition input is set to be 1.1 (medium/normal wear).

System reliability indices and intervention costs are shown in Table 6-29 and Table 6-30. HSF>1 gives worse reliability performance and higher repair costs; the differences grow with the asset age. This can also be seen on the asset health score profile when initial age is 21 yr.

Table 6-29: System reliability results for modified Health Score Factor (deterministic approach)

Initial Age (yr)	Factor Value	EENS (MWh/yr)	LOLP (p.u.)
1	Default	25026.99	0.022158
	Modified	25409.17	0.023288
21	Default	31488.89	0.029703
	Modified	32079.82	0.033744
31	Default	54997.05	0.060845
	Modified	56740.34	0.064795

Table 6-30: Total repair costs for modified Health Score Factor (deterministic approach)

Initial Age (yr)	Total Repair Costs for Different Repair Types (M£)				
	Minimal Repair	Minor Repair	Major 1 Repair	Major 2 Repair	Replacement
1	57.854	92.827	191.284	290.629	3823.450
21	159.908	262.280	537.475	759.363	8603.250
31	378.208	621.794	1263.011	1743.277	19925.436

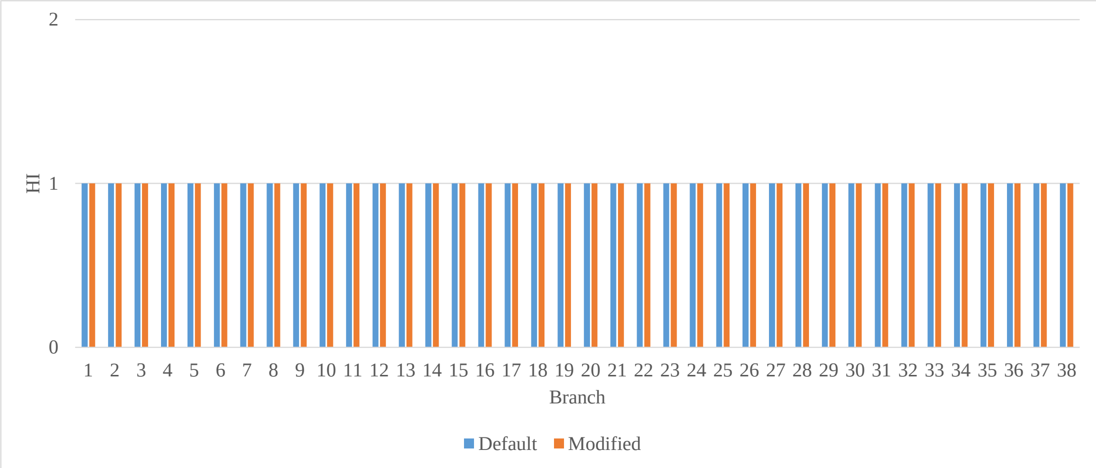

a). Initial Age = 1

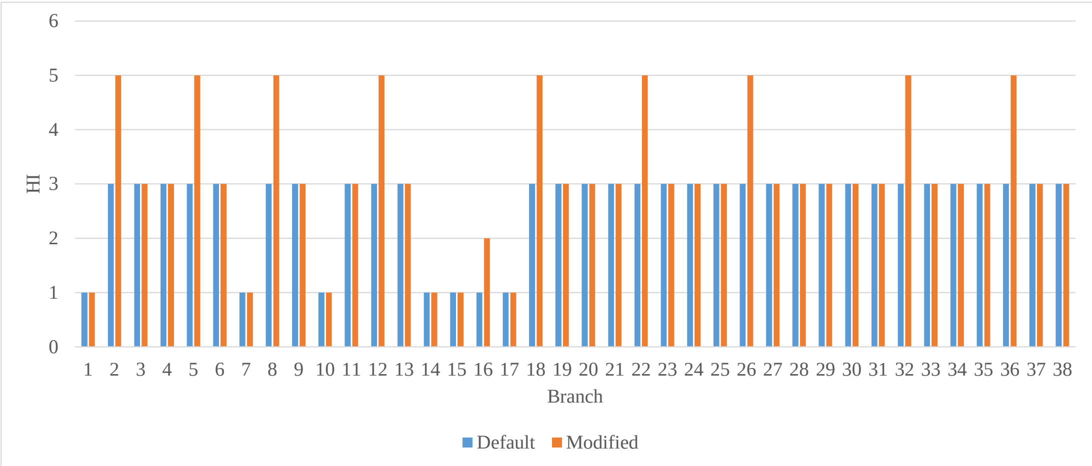

b). Initial Age = 21

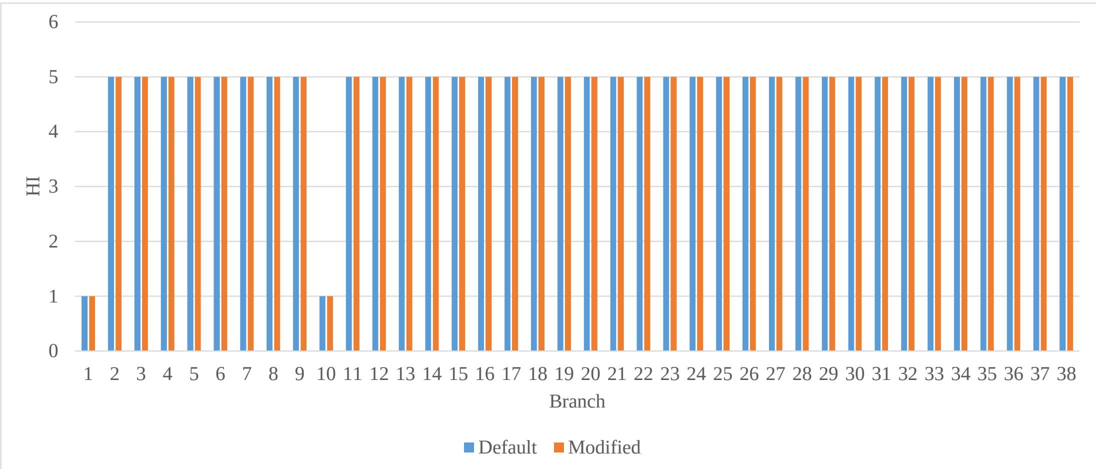

c). Initial Age = 31

Figure 6-43: Asset HI at the end of simulation period with different health score factors (deterministic approach)

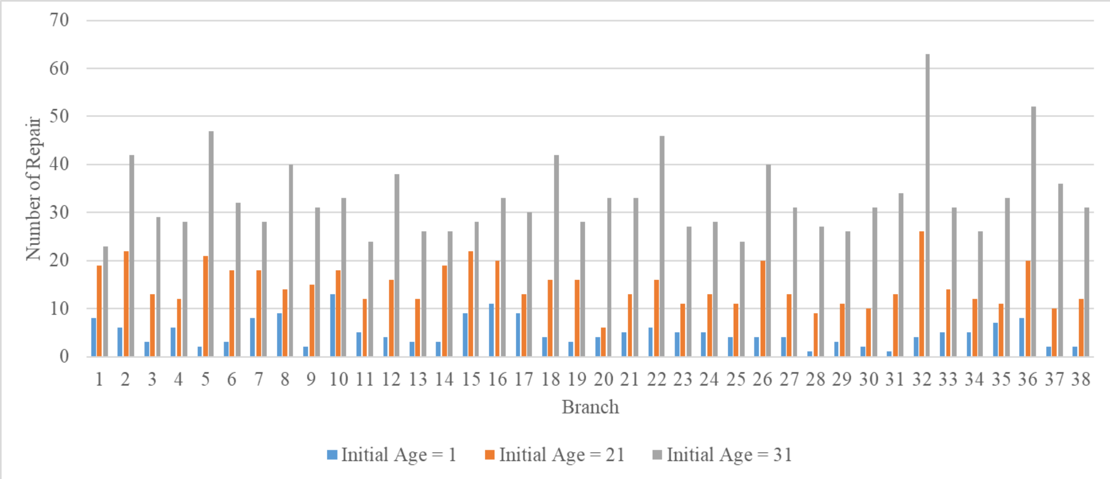

Figure 6-44: Number of repair with modified health score factor for different initial ages (deterministic approach)

6.4.5 Impact of Ageing Reduction Factor

Ageing reduction factor is initially introduced to decelerate the asset ageing rate in order to avoid assets at low Health Score/HI deteriorating faster than high Health Score/HI. In this study, the default value is calculated from the Ageing Reduction Factor calibration table (Table 6-22). The modified values are:

- when initial age = 1, ARF = 1;
- when initial age = 21, ARF = 1.15;
- when initial age = 31, ARF = 1.4.

The reliability results show that at early age (initial age = 1), the differences of both reliability indices are quite small which can be treated as the same; when assets are in service for a certain time (initial age = 21&31), the results show that the ARF$\neq$1 leads to better system performance. The results for asset HI at the end of simulation period also show that the ageing reduction factor has no influence on young assets; whilst it can decelerate asset deterioration process when assets get old. The repair costs are also lower than default case.

Table 6-31: System reliability results for modified Ageing Reduction Factor (deterministic approach)

Initial Age (yr)	Factor Value	EENS (MWh/yr)	LOLP (p.u.)
1	Default	25026.99	0.022158
	Modified	25507.03	0.022163
21	Default	31488.89	0.029703
	Modified	30197.88	0.028516
31	Default	54997.05	0.060845
	Modified	52887.38	0.058525

Table 6-32: Total repair costs for modified Ageing Reduction Factor (deterministic approach)

Initial Age (yr)	Total Repair Costs for Different Repair Types (M£)				
	Minimal Repair	Minor Repair	Major 1 Repair	Major 2 Repair	Replacement
1	54.709	89.784	180.322	267.428	2974.686
21	144.126	235.804	484.804	695.496	7375.003
31	338.836	557.865	1136.235	1564.905	17775.375

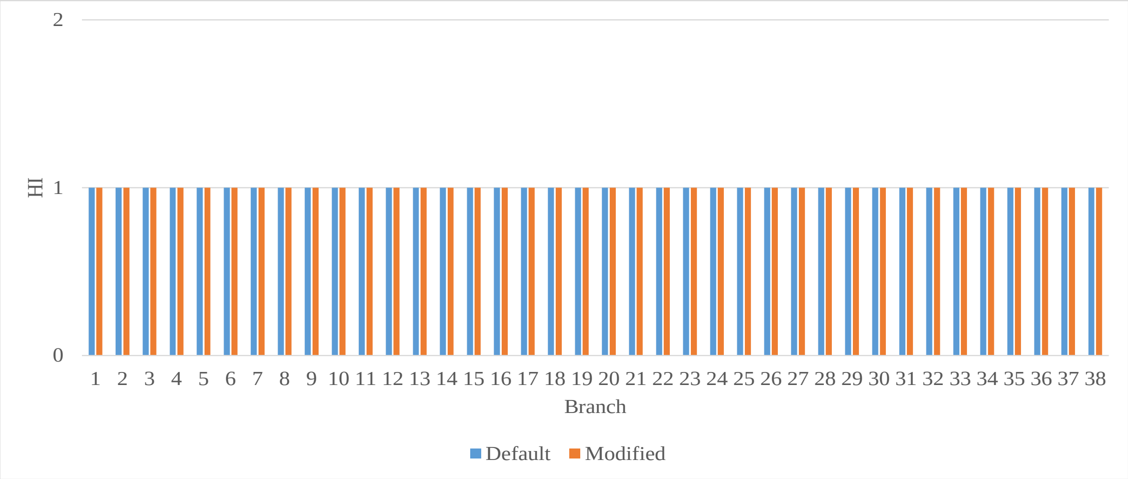

a). Initial Age = 1

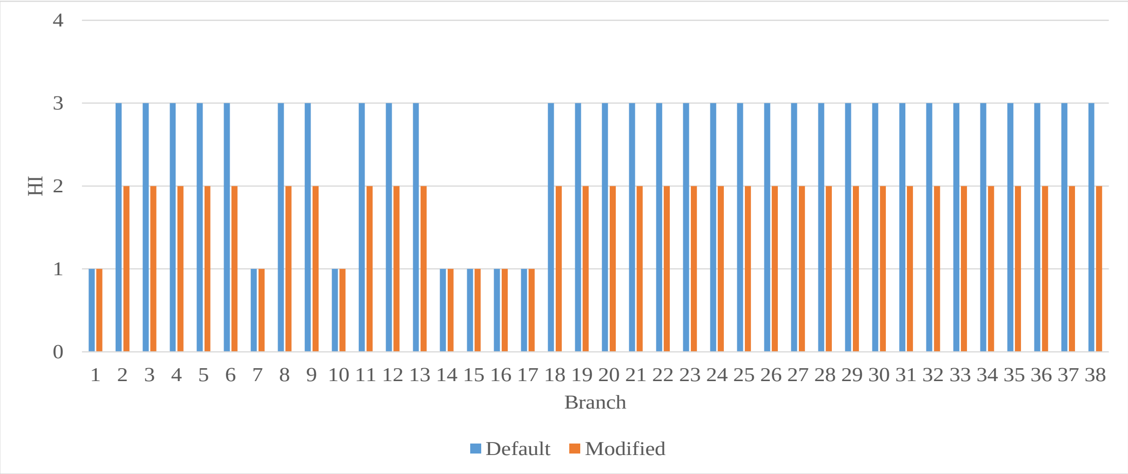

b). Initial Age = 21

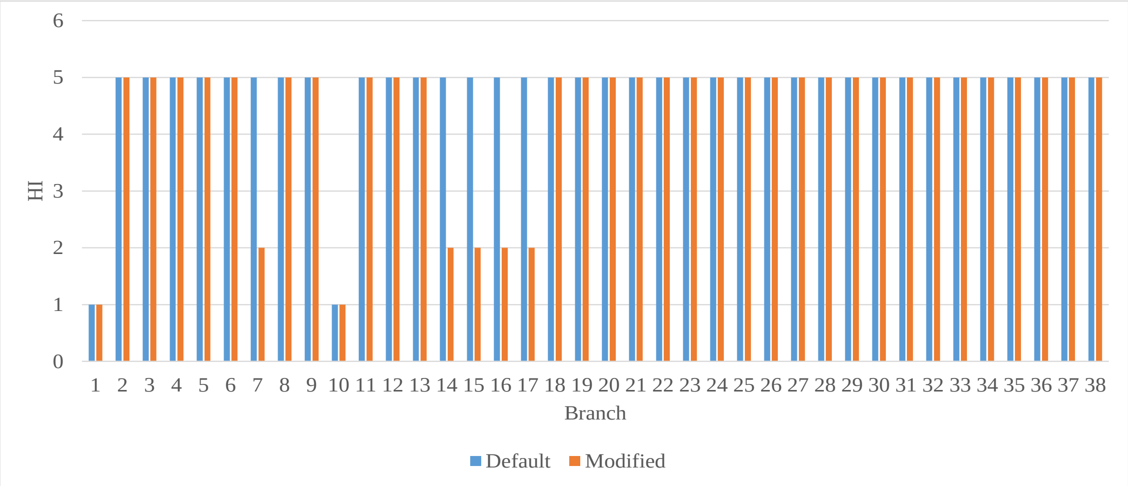

c). Initial Age = 31

Figure 6-45: Asset HI at the end of simulation period with different ageing reduction factors (deterministic approach)

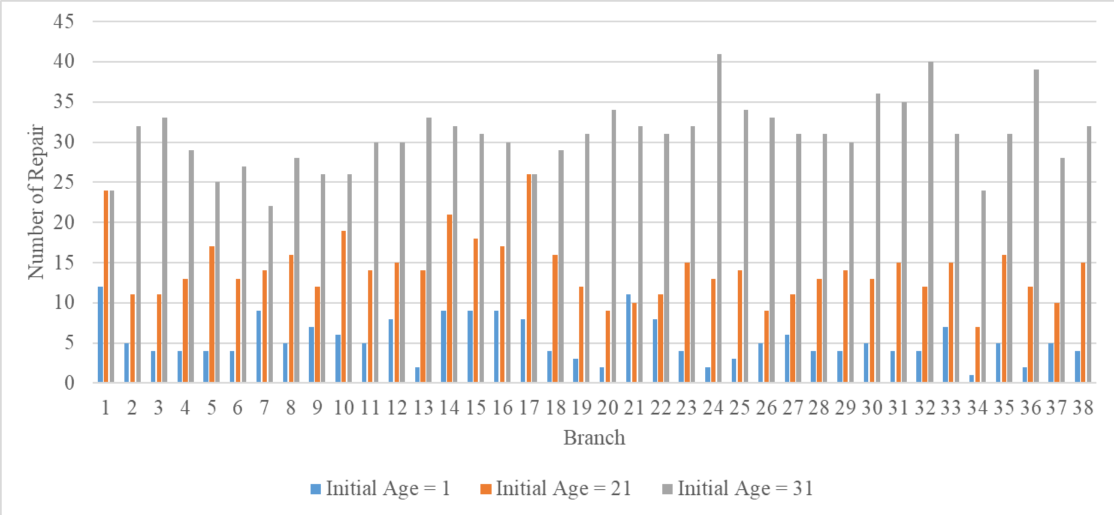

Figure 6-46: Number of repair with modified ageing reduction factor for different initial ages (deterministic approach)

6.4.6 Impact of Generation Reliability

The base-case deterministic HI studies are repeated with ageing generating units, where the parameters are the same as generation reliability study in temporal model. Compared to the case of temporal model (Table 6-19), reliability results are worse. They again show that ageing generation has a significant, negative impact on system and nodal reliability; EENS and LOLP indices are drastically larger than in the base cases. EENS indices show that load curtailments in the north are higher than the south due to higher generation capacity. However, LOLP results are not that different at buses with connected generation.

In this case, bus 10 becomes the most reliable bus. The reason is no generators are connected to bus 10, therefore the outages of generators have no impact on bus 10. And bus 10 is supplied by two transformer links, one cable and two overhead lines which reduces the probability of interrupted power supply. Although bus 9 is also connected to five links, its reliability is much lower. This is because the power transferred on link between bus 9 and bus 3 (branch 6) highly relies on the transformer link (branch 7) connected to bus 3. Once an outage of the transformer occurs, branch 6 has to supply bus 3 to satisfy its load. Hence, the load curtailment at bus 9, as well as its probability, is higher than bus 10.

Table 6-33: System reliability results with generation reliability (deterministic approach)

Initial Age (yr)	Generator Reliability	EENS (MWh/yr)	LOLP (p.u.)
1	Without	25026.99	0.022158
	With	781626.97	0.063002
21	Without	31488.89	0.029703
	With	900208.39	0.071164
31	Without	54997.05	0.060845
	With	1032267.41	0.082021

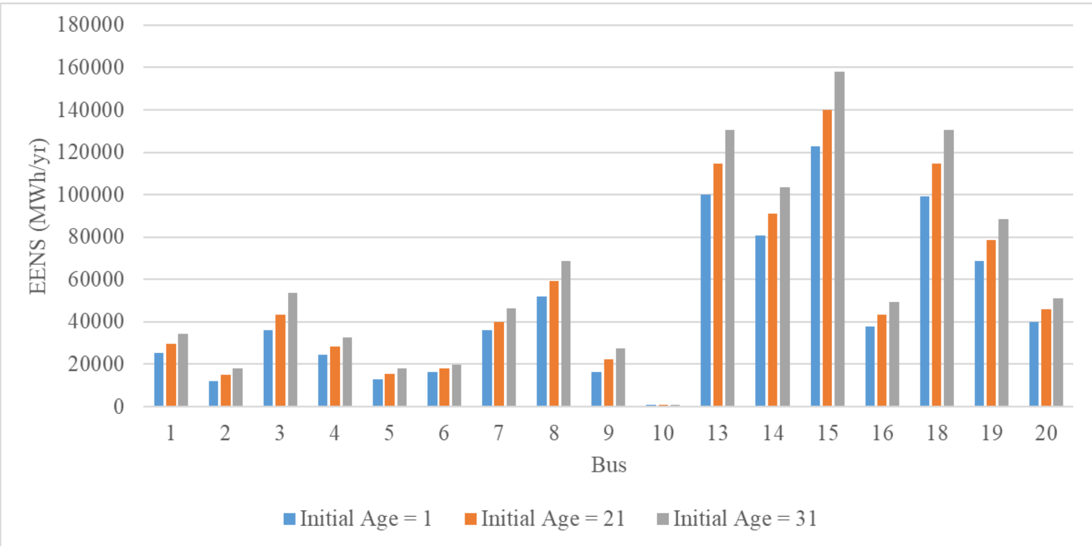

Figure 6-47: Nodal EENS with generation reliability (deterministic approach)

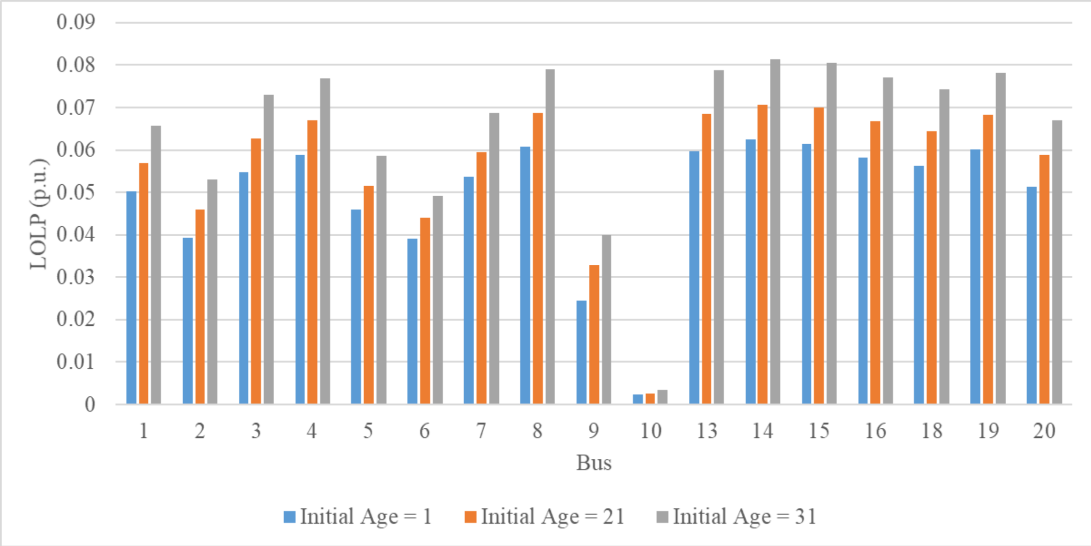

Figure 6-48: Nodal LOLP with generation reliability (deterministic approach)

6.5 Probabilistic Asset Health Modelling

6.5.1 Pre-Processor for Asset Health Deterioration

In this research, the number of MC simulations *n* in Eq. (5-28) and Eq. (5-29) is 1000. The transition matrix M for the same asset with different values of *n* are provided in Table 7, Table 8 and Table 9 in Appendix, as well as the corresponding computational time. It can be seen that $n = 1000$ can save the computational time while ensuring the transition accuracy. Two transition approaches are applied to access asset HI transition matrix *M*. Examples of the entire matrix *M* of one single asset has been given in Appendix. Table 6-34 and Table 6-35 provide the elements in the matrix *M* of one asset from each group (OHL, Tx; Cable) at three virtual ages (1, 21, 31).

Transition to Any HI

As the initial asset age increases, the probabilities of asset transitions towards higher HIs increase; there are very few transitions when assets are young. Cables have higher transition probabilities than OHLs and transformers, whilst transformers are close to OHL.

Table 6-34: Elements M(x,i-j) when asset moves to any HI

Asset/yr	**Elements M(x, i-j)**							
	1-2	**1-3**	**1-4**	**1-5**	**1-6**	**2-3**	**2-4**	**2-5**
OHL/1	0.025	0.002						
OHL/21	0.088	0.036	0.016			0.044	0.030	0.014
OHL/31						0.06	0.032	0.046
Tx/1	0.002							
Tx/21	0.098	0.052	0.014	0.005		0.061	0.02	0.008
Tx/31						0.091	0.012	0.009
Cable/1	0.024	0.003						
Cable/21	0.111	0.069	0.021	0.014		0.069	0.026	0.017
Cable/31						0.039	0.034	0.03
Asset/yr	**2-6**	**3-4**	**3-5**	**3-6**	**4-5**	**4-6**	**5-6**	
OHL/1								
OHL/21		0.022	0.044					
OHL/31	0.018	0.033	0.029	0.008	0.02	0.013	0.023	
Tx/1								
Tx/21		0.03						

Tx/31		0.019	0.004		0.01	0.004	0.006	
Cable/1								
Cable/21		0.044	0.026		0.04			
Cable/31	0.023	0.056	0.026	0.013	0.02	0.013	0.014	

Transition to Next HI

In this case, there are five transitions only. Similar conclusions as in the previous case can be drawn. This approach is simpler and faster to apply in the SMC procedure; however, it offers less diversity in asset degradation and consequent repairs.

Table 6-35: Elements M(x,i-j) when asset moves to next HI

Asset/Yr	**Elements *M(x, i-j)***				
	1-2	**2-3**	**3-4**	**4-5**	**5-6**
OHL/1	0.02				
OHL/21	0.104	0.056	0.063		
OHL/31		0.098	0.094	0.089	0.019
Tx/1	0.001				
Tx/21	0.115	0.083	0.071		
Tx/31		0.168	0.121	0.161	
Cable/1	0.04				
Cable/21	0.134	0.057	0.085		
Cable/31		0.128	0.076	0.093	0.005

6.5.2 Base Case Studies

The following cases are studied for two transition approaches:

- all assets with initial ages of 1 year and initial HI=1;
- all assets with initial age of 21 years and initial HI=2;
- all assets with initial age of 31 years and initial HI=3.

6.5.2.1 Transition to Any HI

The results at system and node level show that the network reliability decreases as asset initial age increases. In this approach, the worst performance occurs at bus 6, followed by bus 3, 8 and 4. All of these buses have no generating units, which contributes to the load curtailment. Bus 6 is connected to two transmission lines; either of them becoming unavailable leads to load curtailment. Bus 3 also has considerable load curtailment but slightly better than 6 due to one more transmission link connected. The difference of load curtailment between bus 4 and 8 is small. The difference of the probabilities, however, is significant. The reason is that the demand at bus 4 is much smaller than bus 8. But bus 4 is connected to only two transmission line (similar to bus 6). In the southern area, load curtailment also occurs at bus 5, 9 and 10 due to the lack of generators and/or relatively higher load demand. In the north, the relatively worse performance occurs at bus 14 and 18. The reason for bus 14 are lack of generators and limited transmission capacity due to two transmission links. Bus 18 is connected to a nuclear generator with a large capacity (400MW). The load, however, at bus 18 is the biggest. The reason for load curtailment at bus 18 is mainly due to the large consumption of power by the link between bus 17 and 18 (branch 30).

Table 6-36: System reliability results for transition to any HI (probabilistic approach)

Initial Age (yr)	**EENS (MWh/yr)**	**LOLP (p.u.)**	**Total Repair Cost (M£)**
1	20146.92	0.019224	78.58
21	24155.77	0.019966	208.92
31	33813.35	0.021610	321.02

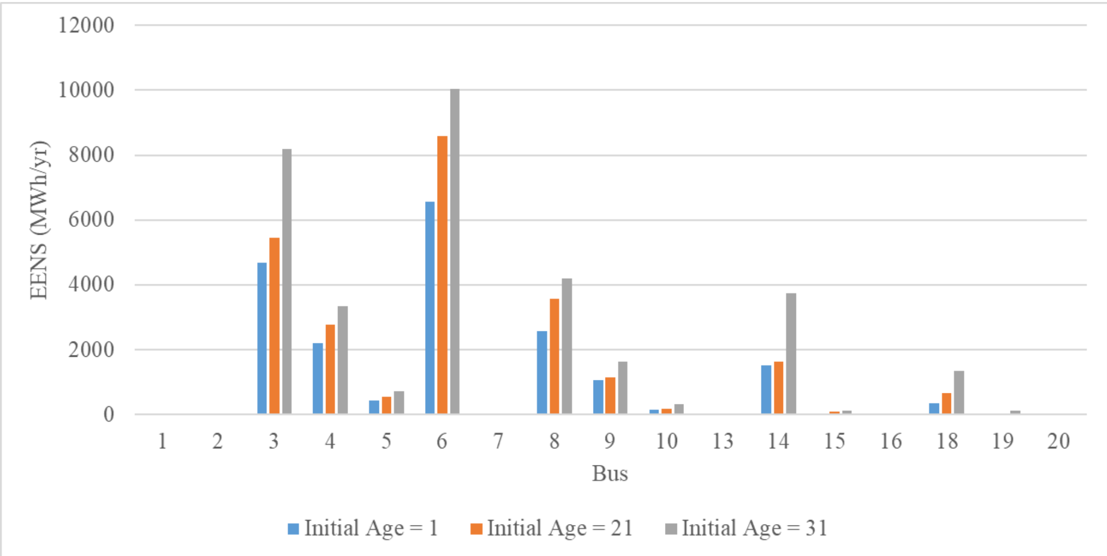

Figure 6-49: Nodal EENS for different initial ages for transition to any HI (probabilistic model)

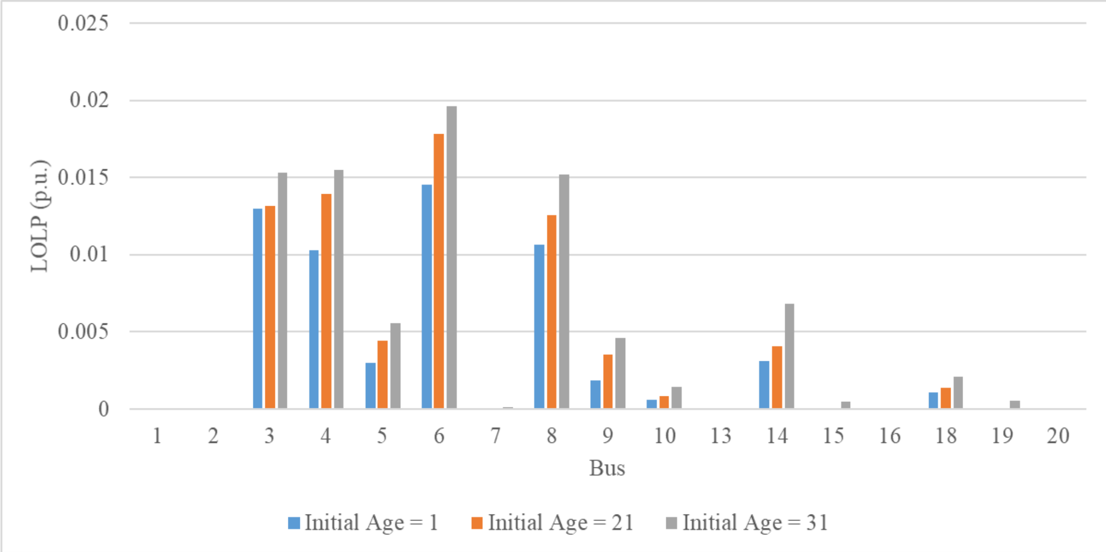

Figure 6-50: Nodal LOLP for different initial ages for transition to any HI (probabilistic model)

Average asset HIs at the end of the simulation period, rounded to the nearest integer, are shown by deterioration methods, initial virtual ages and asset groups in the following table. For OHL and transformers, initial asset ages contribute significantly to worsening of HIs, whilst HI results are similar for "older" cables (initial age is 21 and 31).

Table 6-37: Asset profiles at the end of simulation period for transition to any HI

Initial Age (yr)	**Asset**	**Numbers of Assets in Each HI Category**					
		HI1	**HI2**	**HI3**	**HI4**	**HI5**	**HI6**
1	OHL	23	8				
	Tx	5					
	Cbl	1	1				
21	OHL	9	16	3	3		
	Tx	1	1	3			

	Cbl	1	1				
31	OHL	10	10	8	2		1
	Tx	1		1	2	1	
	Cbl			1	1		

Average virtual ages of branch assets at the end of simulation period for "to any HI" deterioration are shown in Fig. 6-51. For young assets, the majority of assets' virtual age is 10 years, because there were either minimal ($q_m = 1.0$) or no repairs, and default aggregated in-service factor $\varphi_m = 1$ is used. On the other hand, for older assets whose initial age is 31 yr, only a few assets have virtual age of 40 years, because higher levels of repair types are applied.

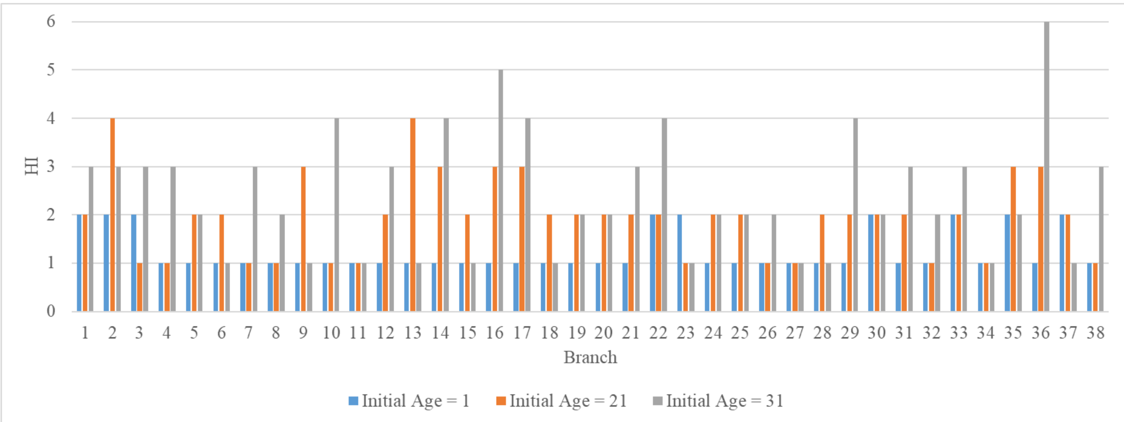

Figure 6-51: Asset HI at the end of simulation period for transition to any HI (probabilistic model)

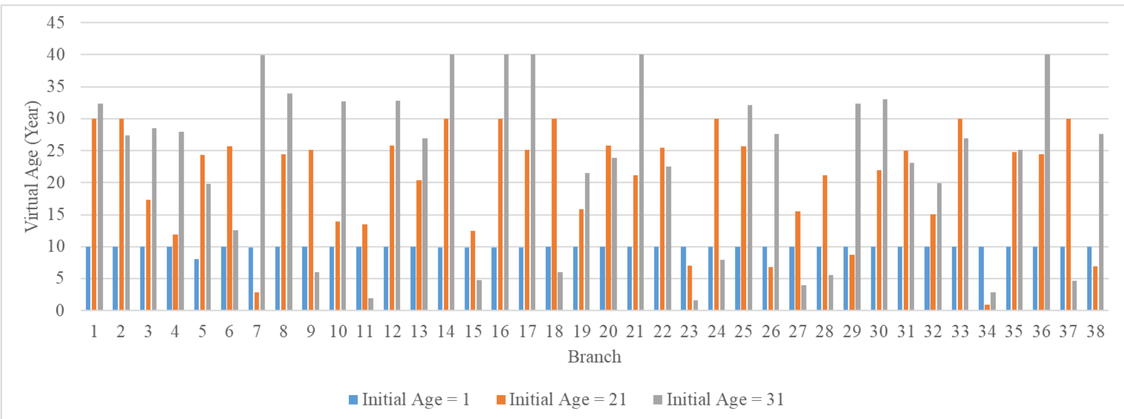

Figure 6-52: Asset virtual age at the end of simulation period for transition to any HI (probabilistic model)

6.5.2.2 Transition to Next HI

There is no significant difference in system reliability results between the two deterioration approaches ("to any HI" and "to next HI"). In a similar manner, total asset intervention costs are higher when the assets are older; however, there is a big difference in costs between two deterioration approaches for older assets. This is caused by transitions to worse HIs and more demanding repair requirements in the "to any HI" approach. This approach is deemed better suited to real-life systems based on comparison with real data on repair types and numbers of "older" assets.

The results at system and node level show that the network reliability decreases as asset initial age increases. In the south, the most unreliable bus is bus 6, followed by 3, 8, 4, 9 and 10. In the south, the load curtailment occurs at bus 14 and 18. The reasons are similar to the transition to any HI.

Table 6-38: System reliability results for transition to next HI (probabilistic approach)

Initial Age (yr)	**EENS (MWh/yr)**	**LOLP (p.u.)**	**Total Repair Cost (M£)**
1	21825.47	0.018573	78.64
21	25436.92	0.019726	89.29
31	34484.55	0.022363	113.85

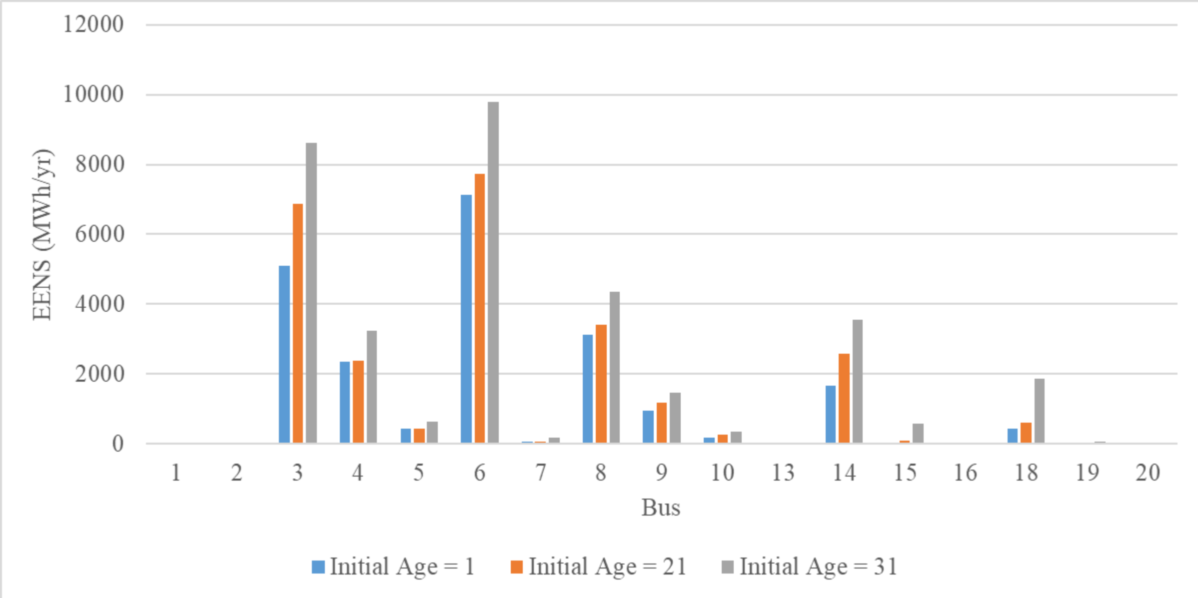

Figure 6-53: Nodal EENS for different initial ages for transition to next HI (probabilistic model)

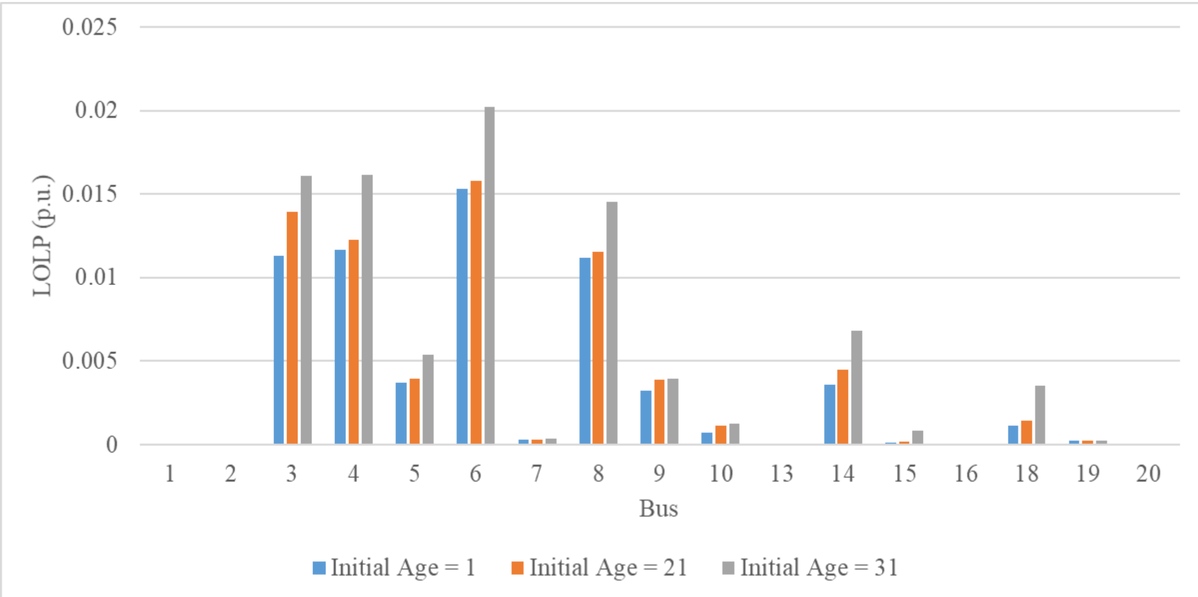

Figure 6-54: Nodal LOLP for different initial ages for transition to next HI (probabilistic model)

This transition approach gives similar HI profiles to the previous one, and the results are slightly better. The results also show the same phenomenon: for OHL and transformers, initial asset ages contribute significantly to worsening of HIs, whilst HI results are similar for "older" cables.

Table 6-39: Asset profiles at the end of simulation period for transition to next HI

Initial Age (yr)	Asset	Numbers of Assets in Each HI Category					
		HI1	HI2	HI3	HI4	HI5	HI6
1	OHL	25	6				
	Tx	5					
	Cbl	2					
21	OHL	5	17	7	2		
	Tx		3	2			
	Cbl		1		1		
31	OHL	6	14	8	3		
	Tx	1			4		
	Cbl		1	1			

In the case of "to next HI" deterioration, virtual age profile of young assets is very similar to the profile in the previous approach with possibly different values for individual branches. However, age profiles for "older" assets (initial ages are 21 and 31) are higher because less demanding repairs are done.

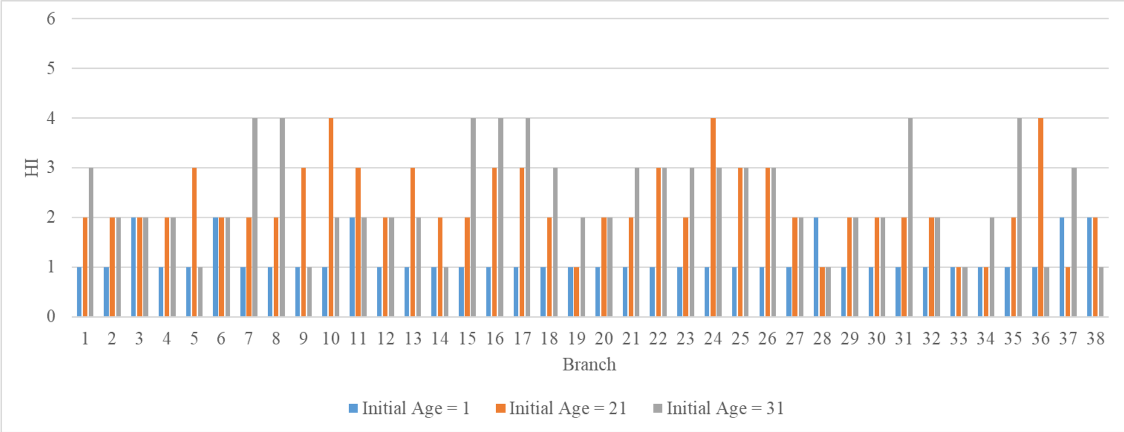

Figure 6-55: Asset HI at the end of simulation period for transition to next HI (probabilistic model)

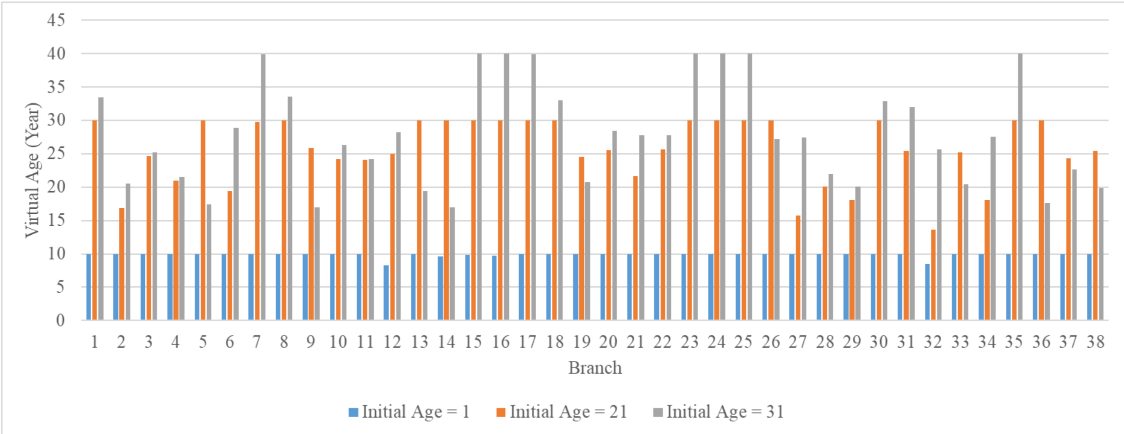

Figure 6-56: Asset virtual age at the end of simulation period for transition to next HI (probabilistic model)

6.5.3 Asset Repairs in Base Case Studies

Table 6-40 and Table 6-41 present the number of repairs, classified by initial ages 1, 21 and 31, for each asset group using both transition approaches. The total numbers of asset interventions are 139, 147 and 158 for transition to any HI, and 130, 138 and 164 for transition to next HI, which are relatively similar. When assets are young, there is almost no difference in repair types between two deterioration approaches and the total costs are similar as well. For older assets, transition to any HI approach produces transitions to worse HIs, which require higher level of interventions, including replacements, and more funding. Hence, there exists a significant difference between the two approaches.

Table 6-40: Total number of repairs in the simulation period for transition to any HI

Initial Age (yr)	Asset	Minimal	Minor	Major 1	Major 2	Replacement
1	OHL	132	1			
	Tx	3				
	Cbl	3				
21	OHL	103	22	4	3	5
	Tx	2	1		1	1
	Cbl	4			1	
31	OHL	94	24	9	2	9
	Tx	6	3		2	1
	Cbl	5	3			1

Table 6-41: Total number of repairs in the simulation period for transition to next HI

Initial Age (yr)	Asset	Minimal	Minor	Major 1	Major 2	Replacement
1	OHL	127	1			
	Tx					
	Cbl	2				

21	OHL	106	19	3	1	
	Tx	4	1			
	Cbl	4				
31	OHL	108	28	7	1	
	Tx	11	1	1		
	Cbl	4	2	1		

Fig. 6-55 and Fig. 6-56 show the results of the average down-time and number of repairs of each branch for both transition approaches, respectively. The longest out-of-service times are obtained for transformer branches 7, 15, 17, 14 and 16; the increased initial age significantly contributes to the down-time increase; they are much smaller for OHLs. On the other hand, OHLs fail most frequently but there is no regular pattern related to individual branch ages.

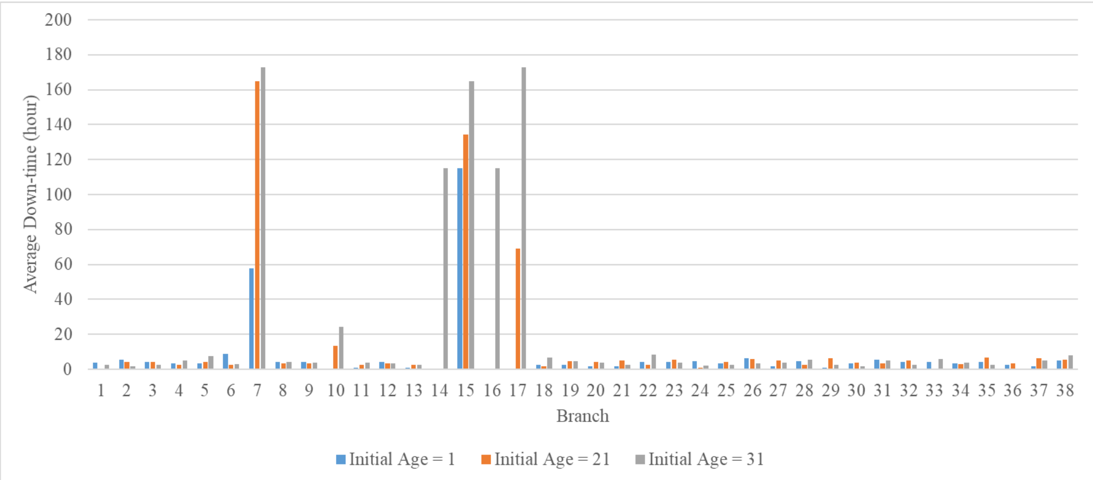

Figure 6-57: Average down-time of each branch for different initial ages for transition to any HI (probabilistic approach)

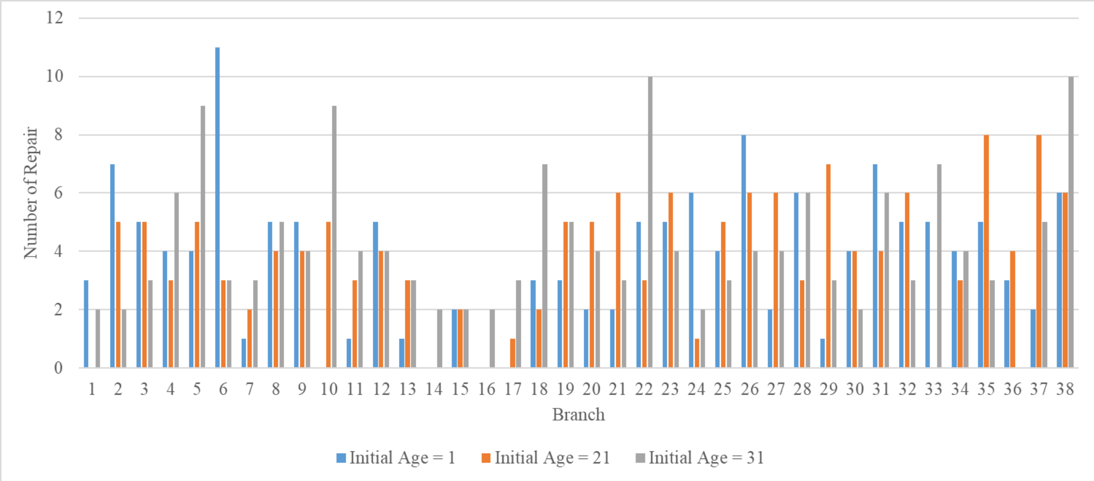

Figure 6-58: Number of repair in each branch for different initial ages for transition to any HI (probabilistic approach)

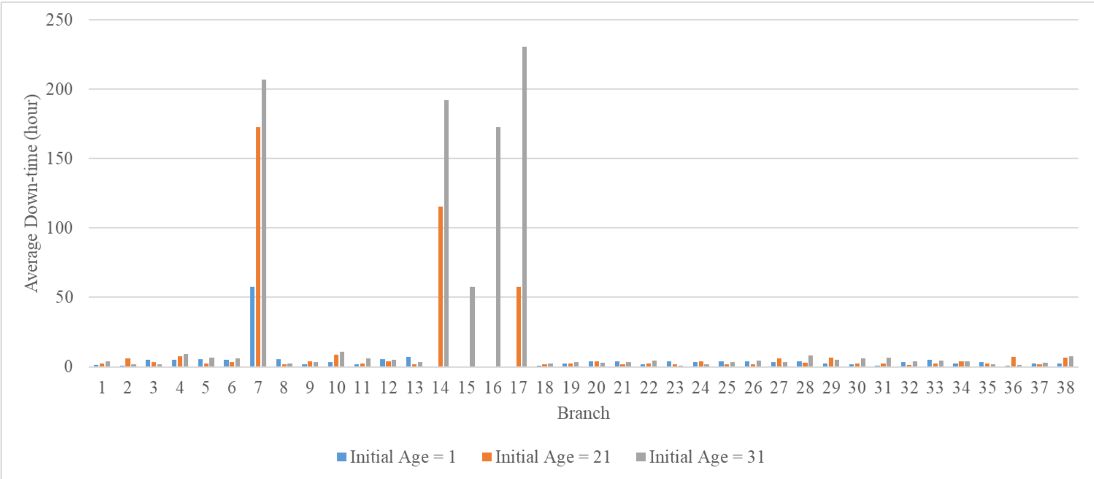

Figure 6-59: Average down-time of each branch for different initial ages for transition to next HI (probabilistic approach)

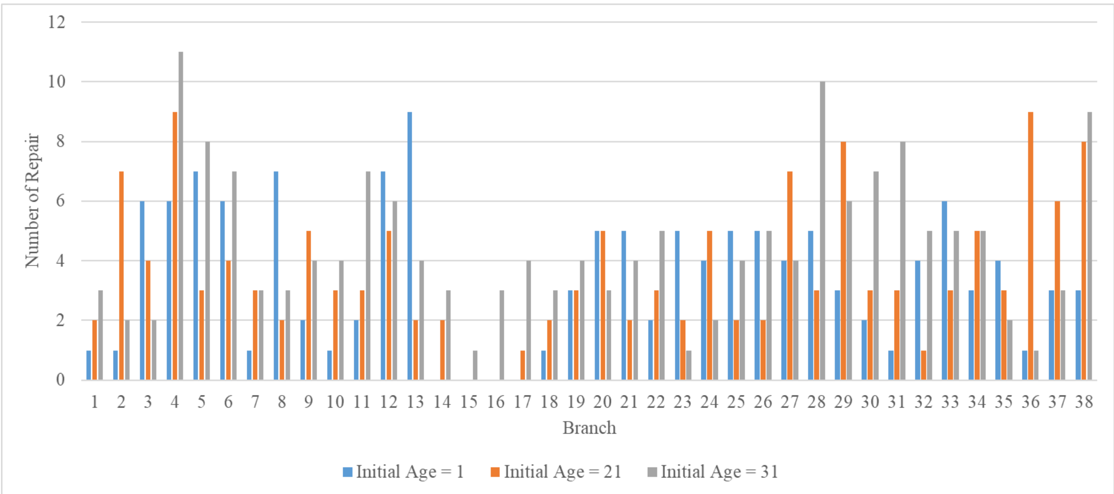

Figure 6-60: Number of repair in each branch for different initial ages for transition to next HI (probabilistic approach)

6.5.4 Asset Trajectories in Base Case Studies

Fig. 6-59, Fig. 6-60 and Fig. 6-61 show an asset in each group (i.e. overhead line, transformer and cable) movements between HIs and virtual age changes within one simulation year.

Overhead Line

An OHL in the 1st year had one minimal repair with no change of HI1. Its virtual age at the end of the first year is equal to 8760h minus repair times ($q_m = 1$ in Table 5-6). An OHL had HI2 at the beginning of the 21st year and experienced a failure in the 7284th hour. Then a minor repair improved health to HI1 and brought down the virtual age to 16 years and 5828h ($q_m = 0.8$). In the 31st year, an OHL had a transition from HI3 to HI4 and no virtual age change due to minimal repair.

Transformer

In these three study years, all the transformers experienced no repairs and there are no changes on HIs. Their virtual ages are equal to their in-service times which are 8760h.

Cable

A cable at young age had two failures in the first simulation year with no change of HI1. Its virtual age at the end of the first year is equal to 8760h minus repair. The same process applies to a cable in the 21st year as well. In the 31st year, a cable experienced two failures. Minimum repair does not change HI3, however major 1 ($q_m = 0.6$) repair starting in the 5182nd hour improved health to HI1 and brought virtual age back to 18yr and 3110h.

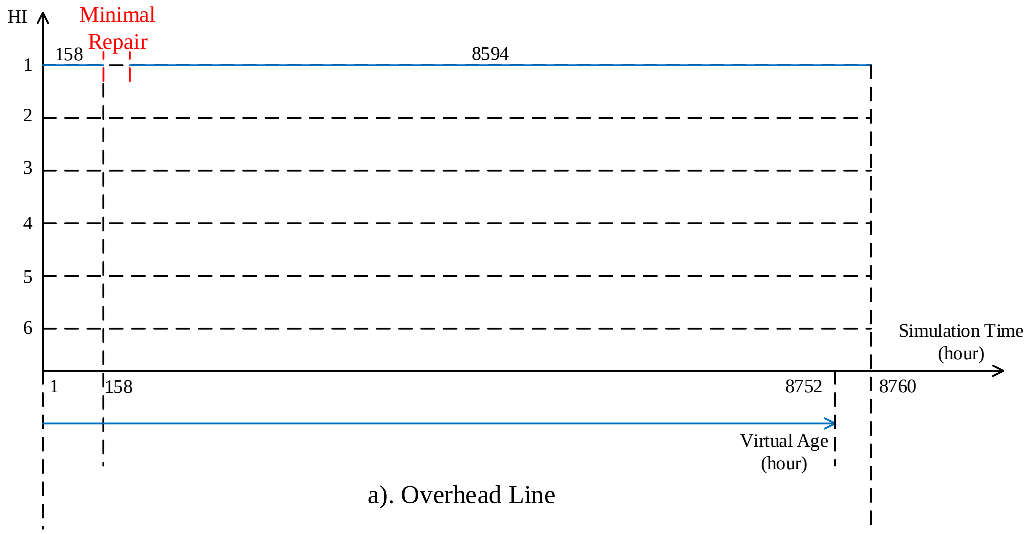

a). Overhead Line

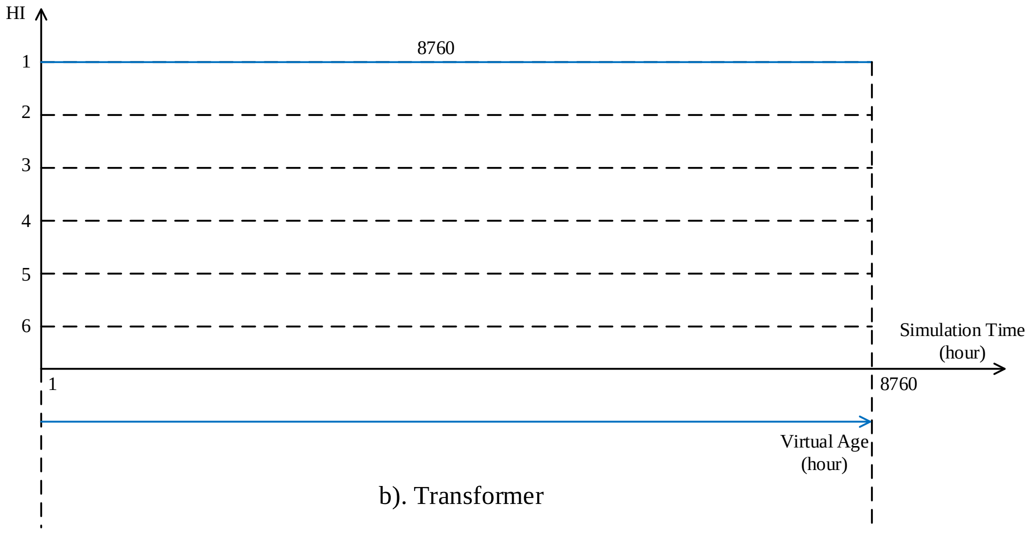

b). Transformer

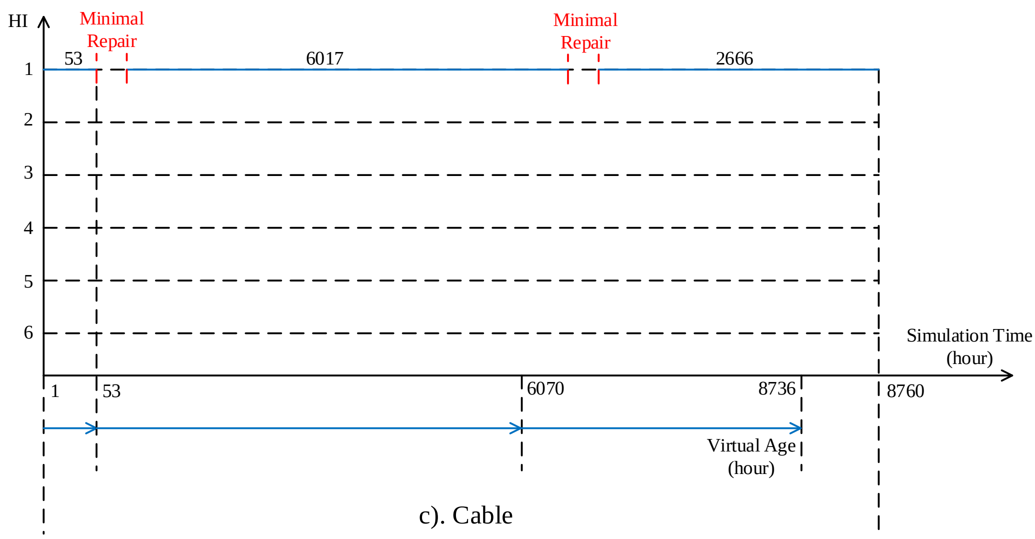

c). Cable

Figure 6-61: Transitions and repairs of an asset in each type in Year 1

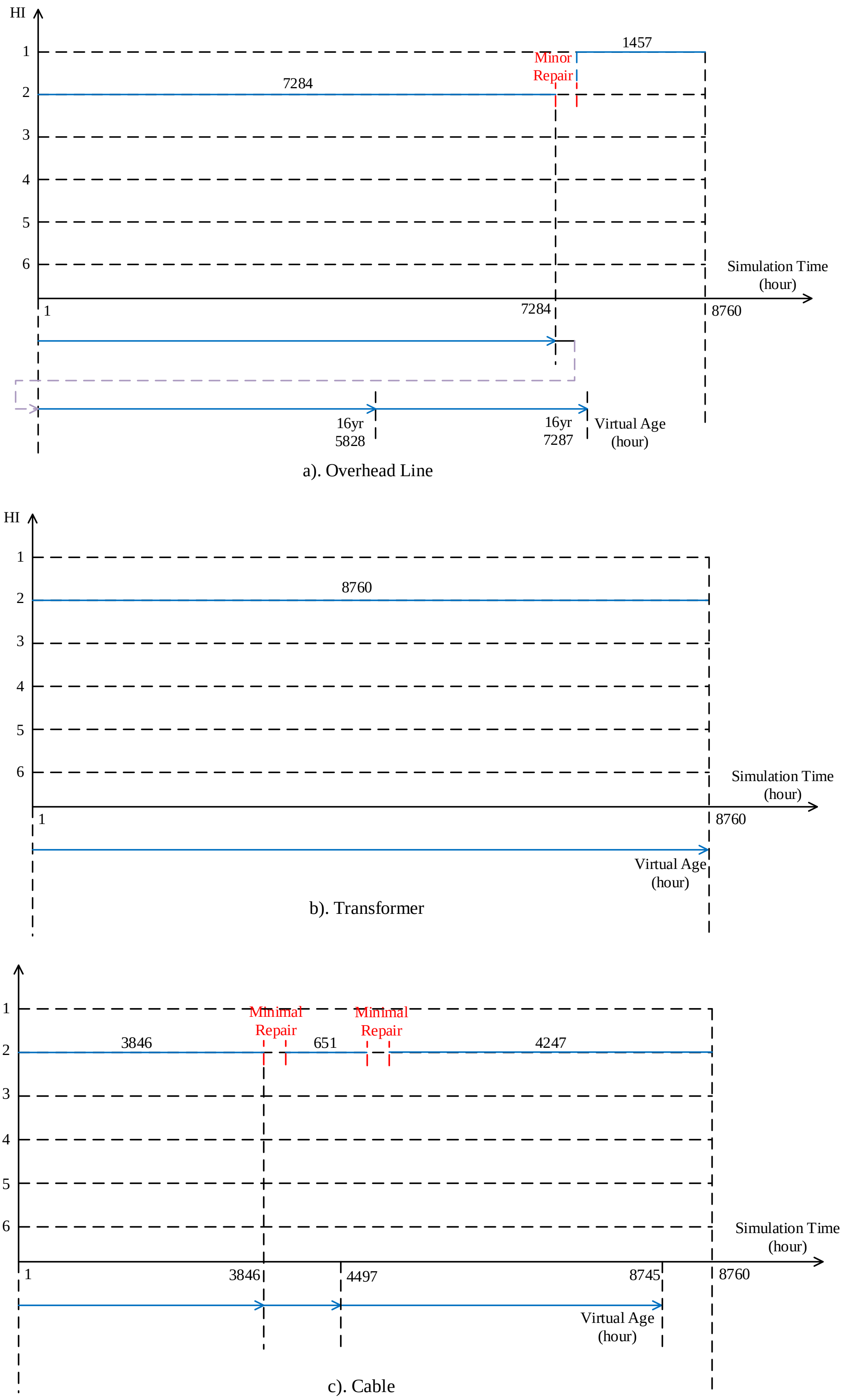

Figure 6-62: Transitions and repairs of an asset in each type in Year 21

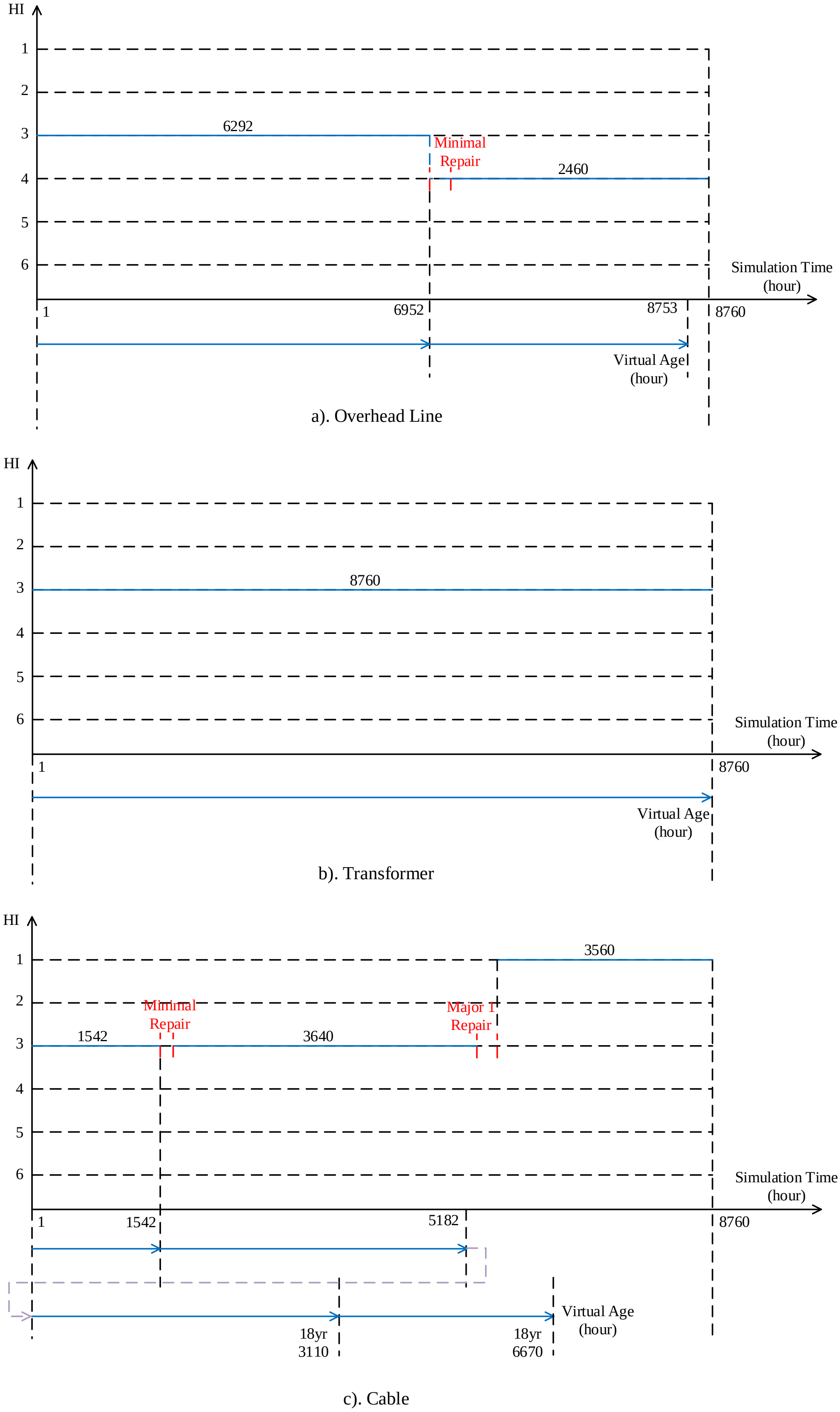

Figure 6-63: Transitions and repairs of an asset in each type in Year 31

6.5.5 Sensitivity Studies

The following sensitivity studies are presented based on the transition approach to any HI:

- Impact of in-service factor φ_m;
- Impact of a reduced set of repairs;
- Impact of external variables.

6.5.5.1 Impact of In-service Factor

In the base case, in-service factor $\varphi_m = 1$. In this study, cases with $\varphi_m = 1.1$ and $\varphi_m = 0.9$ are studied.

System-wide results are shown in Table 6-42. They show in-service factor and system reliability, as well as repair costs, are positively correlated. The total intervention costs vary in ranges [-11.5% - 4.6%], [-13.9% - 7.0%] and [-24.5% - 11.7%] for initial ages 1, 21 and 31, respectively. This shows high sensitivity of total intervention costs to input parameters

Table 6-42: System-based results for different in-service factors (probabilistic approach)

Initial Age (yr)	Study Case	EENS (MWh/yr)	LOLP (p.u.)	Total Repair Cost (M£)
1	Base Case	20146.92	0.019224	78.58
	$\varphi = 0.9$	19685.09	0.017192	69.51
	$\varphi = 1.1$	22854.30	0.021370	82.20
21	Base Case	24155.77	0.019966	208.92
	$\varphi = 0.9$	21405.68	0.018493	179.79
	$\varphi = 1.1$	26143.12	0.020235	223.60

31	Base Case	33813.35	0.021610	321.02
	$\varphi = 0.9$	31122.63	0.021062	242.36
	$\varphi = 1.1$	36777.84	0.023128	358.68

6.5.5.2 Impact of A Reduced Set of Repairs

The simplified set of repairs are given in Table 6-43:

Table 6-43: Simplified set of repairs

Repair Type	**Repair Factor q_m**
Minimal Repair	1
Minor Repair	0.7
Major Repair	0.5
Replacement	0

The reduced set of repairs presents similar reliability indices to the base cases and always gives smaller total costs because “Major 2” category is not used.

Table 6-44: System-based results for different sets of repairs (probabilistic approach)

Initial Age (yr)	**Study Case**	**EENS (MWh/yr)**	**LOLP (p.u.)**	**Total Repair Cost (M£)**
1	Base Case	20146.92	0.019224	78.58
	Reduced Repair Set	19693.59	0.019235	71.49

21	Base Case	24155.77	0.019966	208.92
	Reduced Repair Set	23531.66	0.019977	166.50
31	Base Case	33813.35	0.021610	321.02
	Reduced Repair Set	31754.74	0.020845	284.13

6.5.5.3 Impact of External Variables

Assumed location and duty variables are shown in Table 6-45:

Table 6-45: Location and duty variables

Factor	**OHL**	**Outdoor Transformer**	**Cable**
Location (z_1)	1.3	1.2	1
Duty (z_2)	1.0	1.2	1.5

The results show that $z_1 > 1.0$ and $z_2 > 1.0$ have a negative impact on the system reliability. Compared to the other sensitivity studies, exogenous variables give the most significant difference to base case. The results indicate that low-mild external factors can provide better reliability indices and lower intervention costs.

Table 6-46: System-based results for different external variables (probabilistic approach)

Initial Age (yr)	**Study Case**	**EENS (MWh/yr)**	**LOLP (p.u.)**	**Total Repair Cost (M£)**
1	Base Case	20146.92	0.019224	78.58
	External Variables	24241.25	0.019973	103.77
21	Base Case	24155.77	0.019966	208.92
	External Variables	28295.87	0.020000	239.13
31	Base Case	33813.35	0.021610	321.02
	External Variables	36320.05	0.022489	392.55

The number of asset repairs in the simulation period for this study is presented in Fig. 6-62. The higher number of repairs compared to the base case occurred in the majority of branches, indicating a negative effect of factors $z_1 > 1.0; z_2 > 1.0$.

Asset HI profiles and virtual ages are shown in Fig. 6-63 and Fig. 6-64 for the same study and parameters. It can be found that asset HIs and virtual ages are often higher in the base case because fewer interventions and lower levels of interventions are carried out.

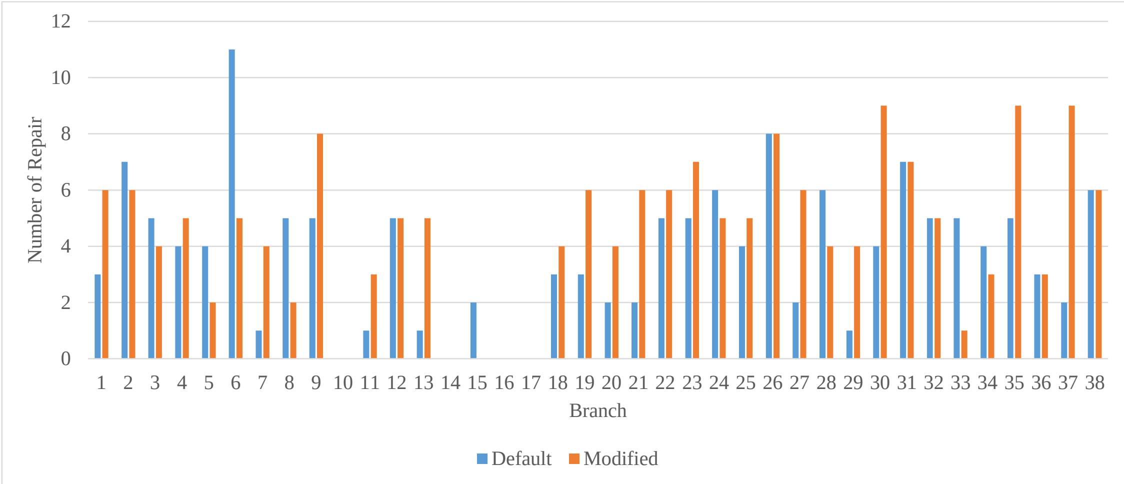

a). Initial Age = 1

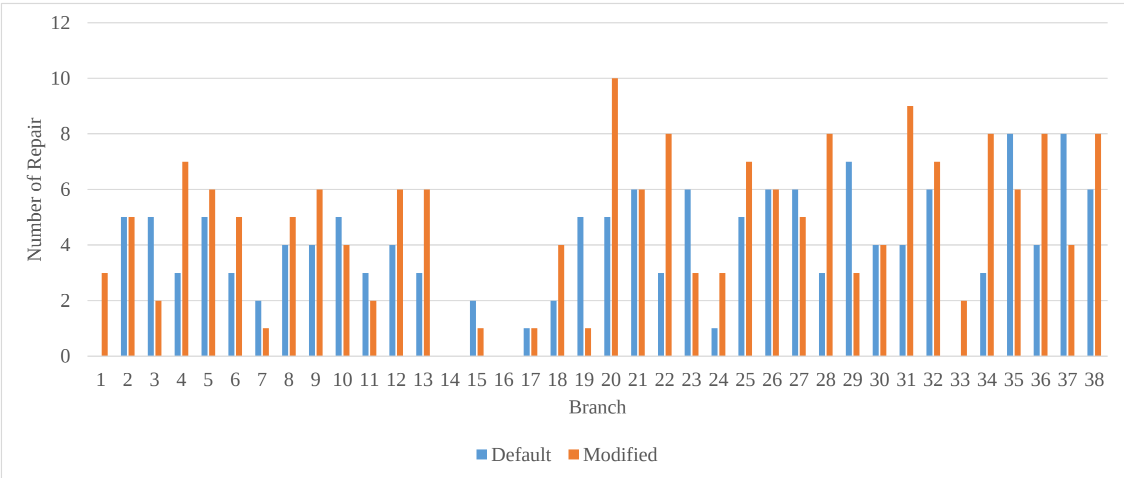

b). Initial Age = 21

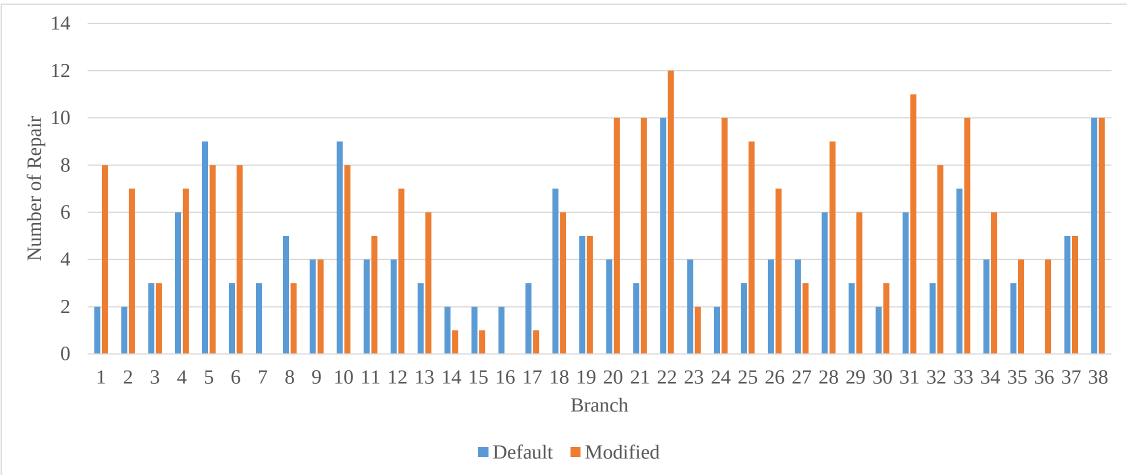

c). Initial Age = 31

Figure 6-64: Number of repair in each branch with different external variables (probabilistic approach)

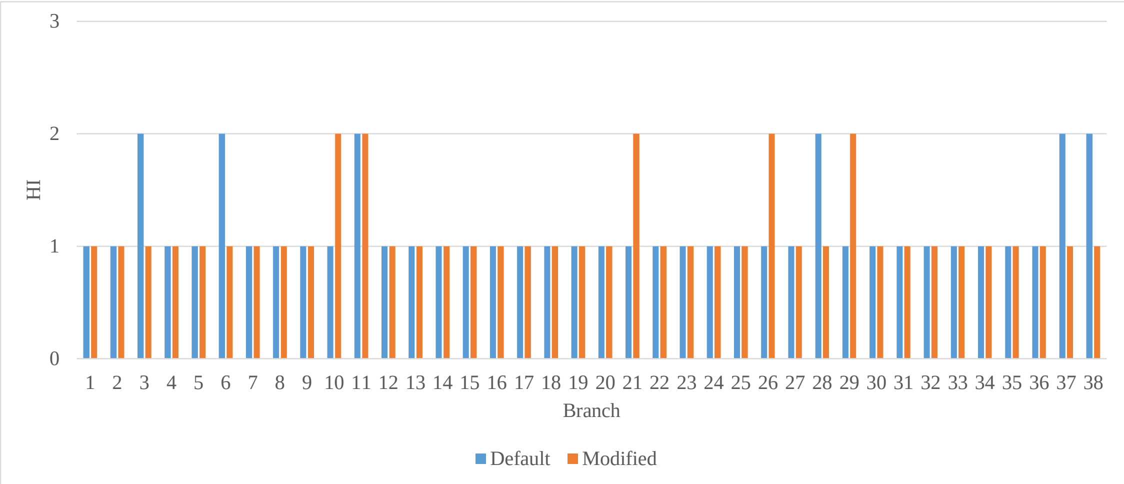

a). Initial Age = 1

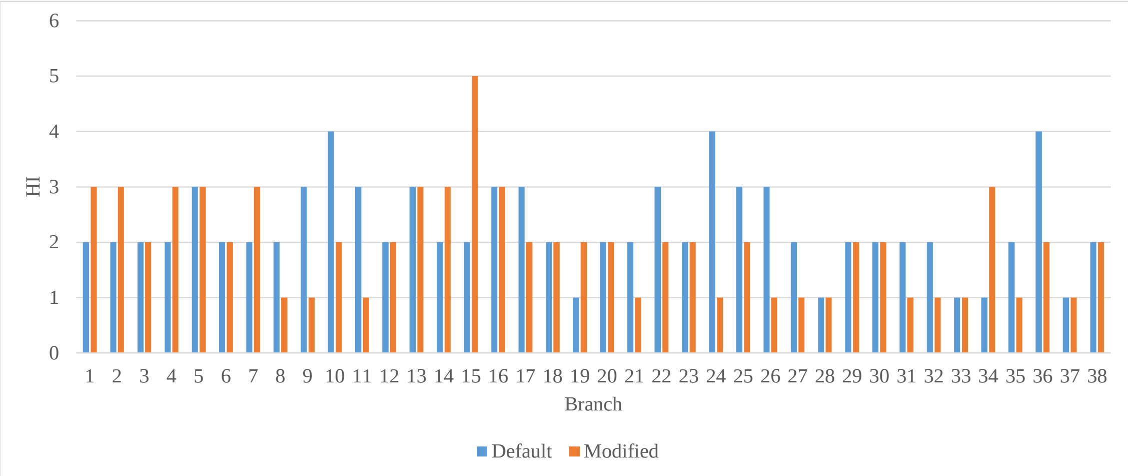

b). Initial Age = 21

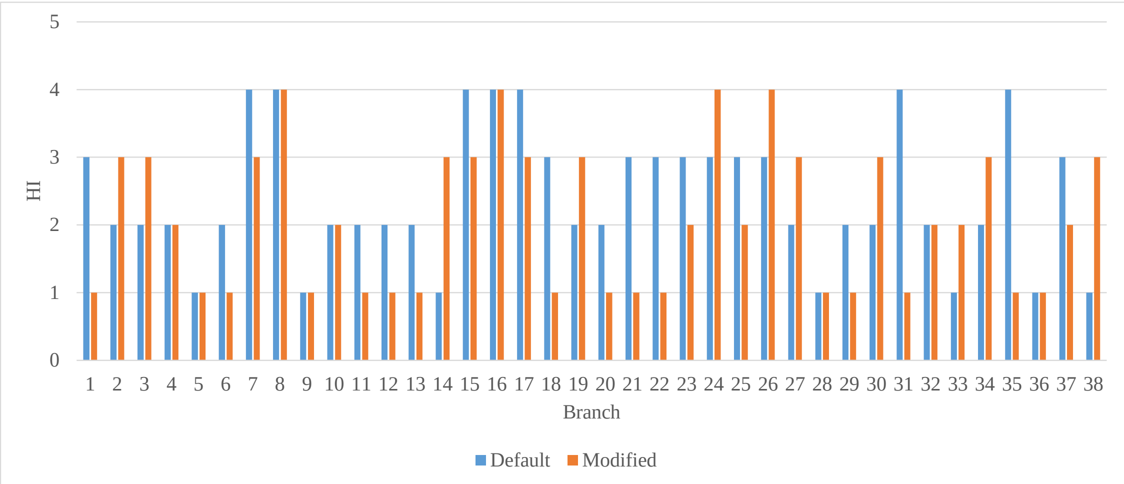

c). Initial Age = 31

Figure 6-65: Asset HI at the end of simulation period with different external variables (probabilistic approach)

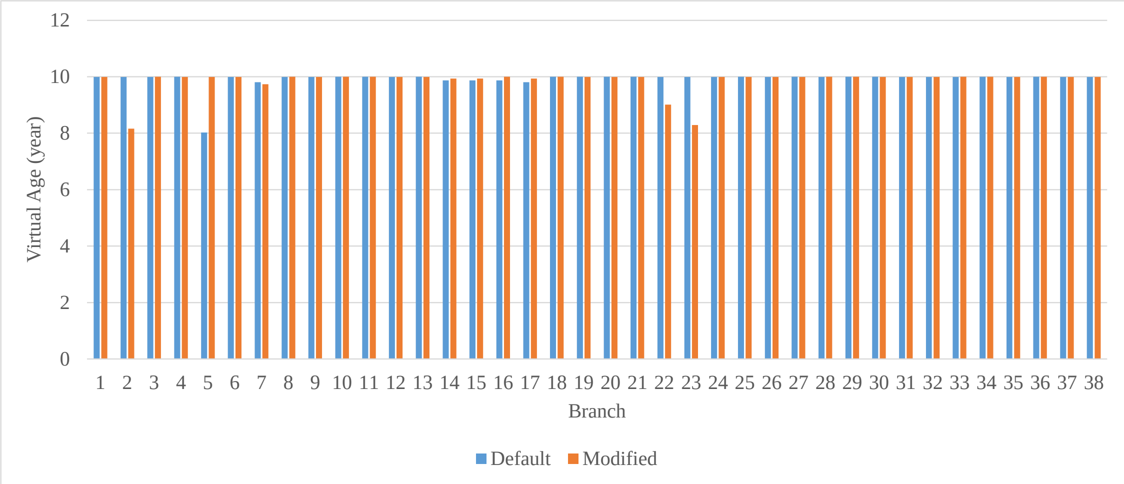

a). Initial Age = 1

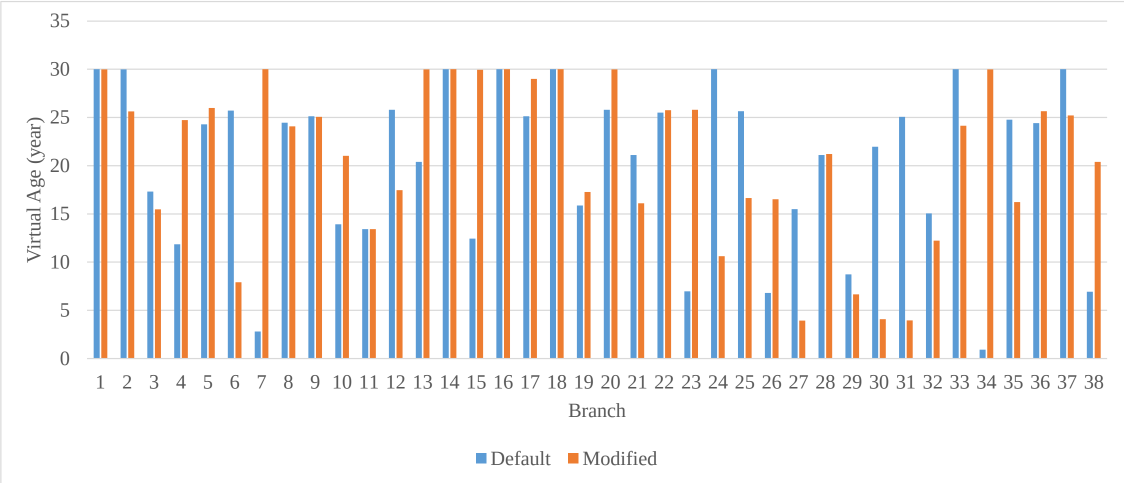

b). Initial Age = 21

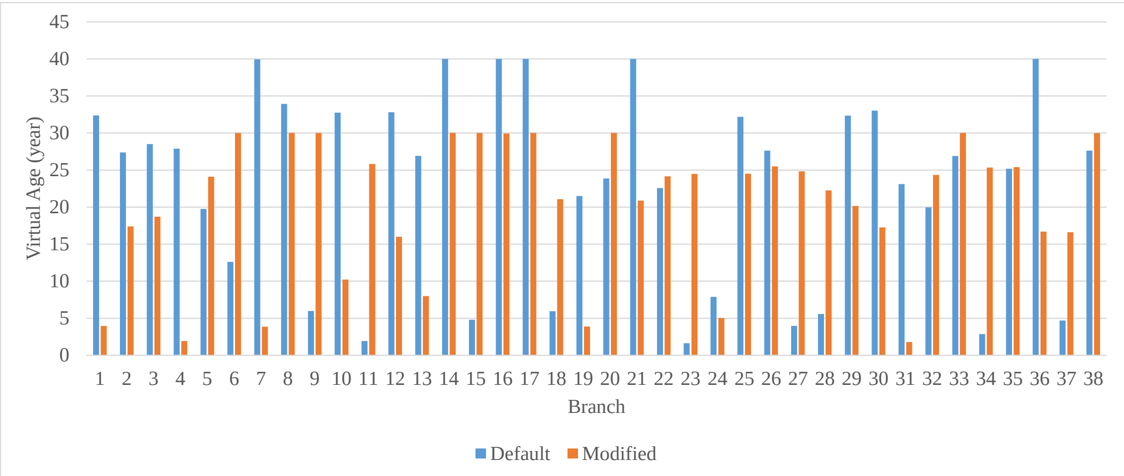

c). Initial Age = 31

Figure 6-66: Asset virtual age at the end of simulation period with different external variables (probabilistic approach)

6.6 Comparison

Table 6-47 presents the system level reliability indices for the three models. Since temporal does not include asset age as an input or asset HI as an output, the results of temporal model, to some extent, provide a “reference” value to deterministic and probabilistic approach.

By comparing probabilistic approach to deterministic approach, UK deterministic HI approach gives higher unreliability results, particularly when the initial asset age grows older. Comparison is also made between the total costs for the probabilistic approach (Table 6-36 for “to any HI” approach and Table 6-38 for “to next HI” approach) and for the deterministic HI approach (Table 6-24). It shows that deterministic approach gives much higher costs in all cases but one (initial age = 1, minimal repair). If the average repair costs are used in the deterministic approach instead, the totals of £153.34M, £395.81M and 916.18M for initial ages of, respectively, 1, 21 and 31 years, are still much higher than in the probabilistic case. This indicates that the use of exponential functions can be challenged.

Table 6-47: Comparisons of base cases in three models

Initial Age (yr)	**Model**	**EENS (MWh/yr)**	**LOLP (p.u.)**
1	Temporal	24003.54	0.017717
	Deterministic	25026.99	0.022158
	Probabilistic (to any HI)	20146.92	0.019224
	Probabilistic (to next HI)	21825.47	0.018573
21	Temporal	27519.17	0.019566
	Deterministic	31488.89	0.029703

	Probabilistic (to any HI)	24155.77	0.019966
	Probabilistic (to next HI)	25436.92	0.019726
31	Temporal	31491.83	0.020205
	Deterministic	54997.05	0.060845
	Probabilistic (to any HI)	33813.35	0.021610
	Probabilistic (to next HI)	34484.55	0.022363

Furthermore, transition to any HI approach produces more diverse intervention and asset health profiles, as well as higher repair costs. This approach is general and deemed better because the level of repair costs is more realistic when compared to UK real-life figures.

6.7 Chapter Summary

Network reliability analyses are performed on three models: temporal model, deterministic approach and probabilistic approach.

In temporal model, impact of ageing asset is studied. The results show that ageing assets have a negative impact on system reliability. Then impact of correlation is analysed, which is based on the correct operation of the temporal model. Results illustrate the detrimental effect of the increasing correlation level, as well as the combination of different correlations. Besides, impact of generation reliability is also studied, where results show a significant and negative impact on system reliability.

In deterministic approach, base cases are classified by asset initial age: 1 year, 21 years and 31 years. Results show a decreasing trend of system reliability as asset initial age increases. Impacts of several factors in the deterministic functions are studied: location and duty factor, health score factor and ageing reduction factor. Only ageing reduction factor study gives a better system performance, whilst the others lead to worse reliability. Generation reliability is also analysed within deterministic approach which has again a significant and negative impact on system reliability.

In probabilistic approach, base cases are also classified by asset initial age: 1 year, 21 years and 31 years; and two transition approaches are applied: “to any HI” and “to next HI”. Results indicate system reliability reduces as asset initial age rises. Transition to any HI approach is deemed better suited to real-life systems. Asset repairs and trajectories are also provided in the base case study. Three sensitivity studies are carried out within this approach: in-service factor, reduced set of repair and external variables.

A comparison among the developed models is made, which draws a conclusion that probabilistic approach is more realistic in terms of reliability results, along with repair costs.

CHAPTER 7 CONCLUSIONS AND FUTURE WORKS

7.1 Conclusions

In this research, a higher level aggregated network planning methodology is proposed to address asset interventions, reinforcements and quality-of-supply investments. The focus of this research is put on the developed probabilistic simulation methodology whose primary goal is to find impact of optimized asset interventions and reinforcements on the overall system performance, as well as on individual assets.

The first version of the probabilistic simulation methodology Temporal Asset Health Modelling. The modelling blocks in this model include nodal loads on an hourly basis, component operating states, uncertain renewable generations, spatial correlation and optimal power flow model. All of these blocks are built within sequential Monte Carlo simulation. In temporal model, asset in-service time is sampled from exponential distribution for assets in normal operating stage, and modified Weibull distribution for ageing assets; out-of-service time is sampled from exponential distribution. The impacts of ageing assets as well as correlation between wind speeds and nodal load are studied.

The second version of the probabilistic simulation methodology is Deterministic Asset Health Models. Within the sequential Monte Carlo simulation, asset in-service time is sampled from hazard functions based on deterministic functions of asset health scores for different asset types; out-of-service times are sampled from exponential distributions. This approach is able to incorporate asset age and asset health score and address the impact of several external influence factors on different asset types.

The most important contribution is the third version of the probabilistic simulation methodology that is Probabilistic Asset Health Modelling. In this approach, asset virtual age is introduced to describe asset condition, along with asset heath indices. Two processes are modelled: asset degradation process and asset condition improvement process. Asset in-service time is sampled using a proportional hazard model (PHM) in combination with the Kijima II virtual age model, which makes this approach is able to reflect the impact from some external (or environmental) factors, as well as the impact from the last in-service and out-of-service cycle; out-of-service time is determined by random sampling from the uniform distribution, which depends on repair types. In this approach, the impacts of asset initial age, exogenous factors and reduced set of repairs are studied. Overall, this approach is able to incorporate asset virtual age and HI, and generate an asset intervention plan which includes the total repair cost.

Moreover, a comparison is made mainly between deterministic approach and probability approach. It presents that the probabilistic model gives more realistic results when compared to the deterministic approach as deterministic approach gives very high reliability indices and repair costs. Besides, the probabilistic asset health approach makes it possible to obtain averages of individual asset health indices and virtual ages, as well as pdfs. These are exactly the information required by the UK national regulator.

7.2 Future Works

The following studies can be done to improve the current model:

- The impact of reactive power can be included in the current model. For example, the calculation of reactive power at each load point needs to be reconsidered and improved, and reactive power generated from wind farms can be involved.
- A comparison of test cases with wind/load correlation when the hazard function is modelled via time and asset HIs can to be done.
- The simulation period can be extended to 60 years to receive global results in probabilistic approach.

Then, following this research, optimization of different types of interventions, such as maintenance, repair and replacement needs to be considered. This completes the link between the last and the first stage in Fig. 3-1. The optimization can be done by developing a higher level optimization model that considers the entire planning period. The optimization model also needs to account for:

- The consideration of different uncertainties: wind, future demand, component unavailability, etc.;
- The establishment of optimization objective and criteria for intervention;
- A trade-off between costs of interventions and system reliability (or outage costs).

REFERENCES

[1] R. Moreno, A. Street, J.M. Arroyo and P. Mancarella, "Planning low-carbon electricity systems under uncertainty considering operational flexibility and smart grid technologies", *Philosophical Transactions of the Royal Society A: Mathematical, Physical and Engineering Sciences* 375, no. 2100, 2017.

[2] M. Ebeed and S.H.A. Aleem, "Overview of uncertainties in modern power systems: Uncertainty models and methods", *Uncertainties in Modern Power Systems*, pp. 1-34. Academic Press, 2021.

[3] R. Billinton and W. Li, *Reliability Assessment of Electric Power Systems Using Monte Carlo Methods*. New York: Plenum Press, 1994.

[4] "Low-Carbon Power: Monitor the Transition to Low Carbon Energy", *lowcarbonpower.org*. [Online]. Available: https://lowcarbonpower.org/

[5] N. Stern, *The Economics of Climate Change: The Stern Review*. Cambridge, U.K.: Cambridge University Press, 2007.

[6] H. Ritchie and M. Roser, "CO2 and Greenhouse Gas Emissions", *Our World Data*, 2020. [Online]. Available: https://ourworldindata.org/ emissions-by-sector

[7] J. Tollefson, "COVID curbed carbon emissions in 2020 — but not by much", *Nature*, vol. 589, no. 7842, pp. 343–343, 2021.

[8] European Commission, "Europe 2020 Targets", 2007. [Online]. Available: http://ec.europa.eu/europe2020/europe-2020-in-a-nutshell/targets/index_en.htm

[9] HM Government, “The UK Renewable Energy Strategy,” 2009. [Online]. Available: https://www.gov.uk/government/publications/the-uk-renewable-energy-strategy

[10] "UK enshrines new target in law to slash emissions by 78% by 2035", *gov.uk*, 2021. [Online]. Available: https://www.gov.uk/government/news/uk-enshrines-new-target-in-law-to-slash-emissions-by-78-by-2035

[11] "COP26 Goals - UN Climate Change Conference (COP26) at the SEC – Glasgow 2021", *UN Climate Change Conference (COP26) at the SEC – Glasgow 2021*, 2022. [Online]. Available: https://ukcop26.org/cop26-goals/

[12] W. Shen, J. Qiu, K. Meng, X. Chen and Z. Y. Dong, "Low-Carbon Electricity Network Transition Considering Retirement of Aging Coal Generators", *IEEE Transactions on Power Systems*, vol. 35, no. 6, pp. 4193-4205, 2020.

[13] A. Navarro-Espinosa and L. F. Ochoa, "Probabilistic Impact Assessment of Low Carbon Technologies in LV Distribution Systems", *IEEE Transactions on Power Systems*, vol. 31, no. 3, pp. 2192-2203, 2016.

[14] B. Zeng, J. Zhang, X. Yang, J. Wang, J. Dong and Y. Zhang, "Integrated Planning for Transition to Low-Carbon Distribution System With Renewable Energy Generation and Demand Response", *IEEE Transactions on Power Systems*, vol. 29, no. 3, pp. 1153-1165, 2014.

[15] Y. Tao, J. Qiu, S. Lai, J. Zhao and Y. Xue, "Carbon-Oriented Electricity Network Planning and Transformation", *IEEE Transactions on Power Systems*, vol. 36, no. 2, pp. 1034-1048, 2021.

[16] R. Moreno, A. Street, J. Arroyo and P. Mancarella, "Planning low-carbon electricity systems under uncertainty considering operational flexibility and smart grid technologies", *Philosophical Transactions of the Royal Society A: Mathematical, Physical and Engineering Sciences*, vol. 375, no. 2100, p. 20160305, 2017.

[17] H. Willis, R. Schrieber and G. Welch, *Aging Power Delivery Infrastructures*. New York: M. Dekker, 2001.

[18] M. S. Hussin, M. S. Al-Mehairi and H. Al-Madhani, "DEWA distribution power asset management system in view of ISO 55000 Standard", *Asset Management Conference (AM 2016)*, pp. 1-5, 2016.

[19] J. Scott, "Keynote Address: The Implications of an Aging Asset Base", *The IEE Seminar on Managing the Complexity of an Aging Asset Base*, pp. 1-10, 2006.

[20] A. Laird, "How can asset management techniques help resolve the, issue of an aging asset base?", *The IEE Seminar on Managing the Complexity of an Aging Asset Base*, pp. 11-18, 2006.

[21] D. M. Allan, "Asset management challenges in ageing power systems", *Proceedings of 2005 International Symposium on Electrical Insulating Materials (ISEIM 2005)*, vol. 1, pp. 265-268, 2005.

[22] R. P. Y. Mehairjan, D. Djairam, Q. Zhuang, J. J. Smit and A. M. van Voorden, "Statistical life data analysis for electricity distribution cable assets — An Asset

Management approach", *IET and IAM Asset Management Conference 2011*, pp. 1-6, 2011.

[23] Y. Wang, C. Peng, R. Liao, H. Zhou, Y. Zhang and T. Ke, "Aging Risk Assessment based on Fuzzy logic for overhead transmission line", *IECON 2020 The 46th Annual Conference of the IEEE Industrial Electronics Society*, pp. 2606-2611, 2020

[24] A. Minaud, J. Pezard and J. -. Priam, "Ageing of medium voltage overhead lines," *CIRED 2009 - The 20th International Conference and Exhibition on Electricity Distribution - Part 2*, pp. 1-18, 2009.

[25] A. Ellam, "Refurbishment on overhead lines", *IEE Seminar on Managing the Complexity of an Aging Asset Base*, pp. 61-69, 2006.

[26] "Plans unveiled to decarbonise UK power system by 2035", *gov.uk*. [Online]. Available: https://www.gov.uk/government/news/plans-unveiled-to-decarbonise-uk-power-system-by-2035

[27] "What is Integrated Transmission Planning and Regulation (ITPR)", *ofgem*, 2013. [Online]. Available: https://www.ofgem.gov.uk/publications/what-integrated-transmission-planning-and-regulation-itpr

[28] "Regulatory regimes in GB - a high level summary", *ofgem.gov.uk*, 2014. [Online]. Available: https://www.ofgem.gov.uk/sites/default/files/docs/2014/10/regulatory_regimes_in_gb_0.pdf

[29] "RIIO: A new way to regulate energy networks", *ukpowernetworks.co.uk*, 2010. [Online]. Available: https://www.ukpowernetworks.co.uk/internet/en/have-your-say/documents/RIIO%20guide.pdf.

[30] "Our RIIO-T1 performance | National Grid ET", *Nationalgrid.com*. [Online]. Available: https://www.nationalgrid.com/electricity-transmission/about-us/planning-together/our-riio-t1-performance#:~:text=providing%20a%20safe%20energy%20network,of%20stakeholder%20and%20customer%20satisfaction.

[31] A. Al-Shaalan, "Essential aspects of power system planning in developing countries", *Journal of King Saud University - Engineering Sciences*, vol. 23, no. 1, pp. 27-32, 2011.

[32] K. Bell, "Planning to manage power interruption events", *Electra*, no. 252, 2010.

[33] "Electricity networks - handling a shock to the system (technical statement)", *theiet.org*. [Online]. Available: https://www.theiet.org/impact-society/factfiles/energy-factfiles/energy-generation-and-policy/electricity-networks-technical-statement/

[34] V. Neimane, "On Development Planning of Electricity Distribution Networks", Ph.D. dissertation, Kungliga Tekniska Högskolan, 2001.

[35] R. Bacher, "Power system models, objectives and constraints in optimal power flow calculations", *Optimization in planning and operation of electric power systems*, pp. 217-263, Physica, Heidelberg, 1993.

[36] "Planning and operating standards under BETTA: Volume 1 - An Ofgem/DTI consultation document", *ofgem*. [Online]. Available: https://www.ofgem.gov.uk/publications-and-updates/planning-and-operating-standards-under-betta-volume-1-ofgemdti-consultation-document

[37] K. Bell, "Methods and Tools for Planning the Future Power System: Issues and Priorities", *strathprints.strath.ac.uk*. [Online]. Available: https://strathprints.strath.ac.uk/54341/1/Bell_IET_2015_Methods_and_tools_for_planning_the_future_power_system.pdf

[38] C. Li, A. Conejo, P. Liu, B. Omell, J. Siirola and I. Grossmann, "Mixed-integer linear programming models and algorithms for generation and transmission expansion planning of power systems", *European Journal of Operational Research*, vol. 297, no. 3, pp. 1071-1082, 2022.

[39] F. Ugranli and E. Karatepe, "Transmission Expansion Planning for Wind Turbine Integrated Power Systems Considering Contingency", *IEEE Transactions on Power Systems*, vol. 31, no. 2, pp. 1476-1485, 2016.

[40] G. Mokryani, Y. Hu, P. Pillai and H. Rajamani, "Active distribution networks planning with high penetration of wind power", *Renewable Energy*, vol. 104, pp. 40-49, 2017.

[41] A. Keane *et al.*, "State-of-the-Art Techniques and Challenges Ahead for Distributed Generation Planning and Optimization", *IEEE Transactions on Power Systems*, vol. 28, no. 2, pp. 1493-1502, 2013.

[42] W. Yaolei, L. Rong, W. Kuihua, Z. Ren and L. Zhao, "Construction and Application of Distribution Network Grid Planning System", *Journal of Physics: Conference Series*, vol. 1659, no. 1, p. 012026, 2020.

[43] R. Fiorotti, J. Fardin, L. Encarnacao and C. Donadel, "A Novel Strategy for Distribution Network Reinforcement Planning considering the Firm Capacity of Distributed Generation Units", *IEEE Latin America Transactions*, vol. 17, no. 04, pp. 530-539, 2019.

[44] S. Favuzza, G. Graditi, M. G. Ippolito and E. R. Sanseverino, "Optimal Electrical Distribution Systems Reinforcement Planning Using Gas Micro Turbines by Dynamic Ant Colony Search Algorithm", *IEEE Transactions on Power Systems*, vol. 22, no. 2, pp. 580-587, 2007.

[45] I. Ziari, G. Ledwich and A. Ghosh, "Optimal distribution network reinforcement considering load growth, line loss and reliability", *2013 IEEE Power & Energy Society General Meeting*, p. 1, 2013.

[46] P. Samal, S. Ganguly, and S. Mohanty, "Planning of unbalanced radial distribution systems using differential evolution algorithm", *Energy Systems*, pp. 1-22, 2016.

[47] S. Heidari, M. Fotuhi-Firuzabad, and S. Kazemi, "Power Distribution Network Expansion Planning Considering Distribution Automation", *IEEE Transactions on Power Systems*, vol. 30, no. 3, pp. 1261-1269, 2015.

[48] S. N. Ravadanegh and R. G. Roshanagh, "On optimal multistage electric power distribution networks expansion planning", *International Journal of Electrical Power & Energy Systems*, vol. 54, pp. 487-497, 2014.

[49] M. Esmaeeli, A. Kazemi, H. Shayanfar, G. Chicco, and P. Siano, "Riskbased planning of the distribution network structure considering uncertainties in demand and cost of energy", *Energy,* vol. 119, pp. 578- 587, 2017.

[50] "National Electricity Transmission System Security and Quality of Supply Standard", *nationalgrid.com*. [Online]. Available: https://www.nationalgrid.com/sites/default/files/documents/NETS%20SQSS%20V2.3.pdf

[51] "Engineering Recommendation P2 Issue 7", *dcode.org.uk,* 2019. [Online]. Available: http://www.dcode.org.uk/assets/files/Working%20Groups/P2/ENA_ER_P2_Issue_6_(2006).pdf

[52] "Electricity Engineering Standards Review Technical Analysis of Topic Areas", *assets.publishing.service.gov.uk*, 2022. [Online]. Available: https://assets.publishing.service.gov.uk/government/uploads/system/uploads/atta

chment_data/file/943700/electricity-engineering-standards-review-technical-analysis-topic-areas.pdf

[53] J. Douglas, “Replacement of the ageing asset base – the challenge to regulators”, *CIRED 19th International Conference on Electricity Distribution*, no. 160, pp. 1-4, 2007.

[54] Wenyuan Li, P. Choudhury, D. Gillespie and J. Jue, "A risk evaluation based approach to replacement strategy of aged HVDC components and its application at BCTC", *2008 IEEE Power and Energy Society General Meeting - Conversion and Delivery of Electrical Energy in the 21st Century*, p.1, 2008.

[55] "RIIO-T1: Final Proposals for National Grid Electricity Transmission and National Grid Gas", *ofgem.gov.uk*, 2012. [Online]. Available: https://www.ofgem.gov.uk/sites/default/files/docs/2012/12/1_riiot1_fp_overview_dec12_0.pdf

[56] "Electricity Distribution Price Control Review - Final Proposals", *ofgem.gov.uk*, 2009. [Online]. Available: https://www.ofgem.gov.uk/sites/default/files/docs/2009/12/fp_1_core-document-ss-final_0.pdf

[57] A. Veevers, "Repairable Systems Reliability: Modeling, Inference, Misconceptions and Their Causes", *Journal of The Royal Statistical Society Series C-applied Statistics*, vol. 35, no. 1, p. 76, 1986.

[58] R. Barlow and F. Proschan, *Mathematical theory of reliability*. New York: Wiley, 1965.

[59] Y. Fuqing and U. Kumar, "A General Imperfect Repair Model Considering Time-Dependent Repair Effectiveness", *IEEE Transactions on Reliability*, vol. 61, no. 1, pp. 95-100, 2012.

[60] F. Q. Yuan and J. M. Lu, "Imperfect repair model for complex repairable system - a literature survey with discussion", *2015 IEEE International Conference on Industrial Engineering and Engineering Management (IEEM)*, pp. 807-811, 2015.

[61] A. Syamsundar and V. N. A. Naikan, "Imperfect Repair Proportional Intensity Models for Maintained Systems", *IEEE Transactions on Reliability*, vol. 60, no. 4, pp. 782-787, 2011.

[62] M. Kijima, H. Morimura, and Y. Suzuki, "Periodical replacement-problem without assuming minimal repair", *European Journal of Operational Research*, vol. 37, pp. 194–203, 1988.

[63] M. Kijima, "Some results for repairable systems with general repair", *Journal of Applied Probability*, vol. 26, pp. 89–102, 1989.

[64] "Modeling Maintenance-induced Failures During the Scheduled Maintenance of a Component Using Reliability Block Diagrams (RBDs)", *Weibull.com*. [Online]. Available: https://www.weibull.com/hotwire/issue174/hottopics174.htm.

[65] C. Jackson and B. Mailler, "Post-servicing failure rates: Optimizing preventive maintenance interval and quantifying maintenance induced failure in repairable systems", *2013 Proceedings Annual Reliability and Maintainability Symposium (RAMS)*, 2013.

[66] J. Selvik and H. Lohne, "Modelling the Effect of Maintenance-Induced Failures from Periodic Testing of Safety-Critical Equipment as Part of RCM Analysis in the Oil and Gas Industry", *Lecture Notes in Mechanical Engineering*, pp. 208-218, 2022.

[67] A. Chowdhury and D. Koval, "Outline of the Book", in *Power Distribution System Reliability: Practical Methods and Applications*, Wiley-IEEE Press, 2009, pp.1-11.

[68] C. D'Annunzio, S. -H. Huang and S. Santoso, "Generation adequacy assessment of power systems with wind generation: A system operations perspective", *2009 IEEE Power & Energy Society General Meeting*, pp. 1-7, 2009.

[69] Y. Zhang, A. Chowdhury and D. Koval, "Probabilistic wind energy modeling in electric generation system reliability assessment", *2010 IEEE Industrial and Commercial Power Systems Technical Conference - Conference Record*, pp. 1-8, 2010.

[70] V. Tremyasov, A. Bobrov and T. Krivenko, "Reliability Theoretical Frequency Assessment of Generation Systems with Photovoltaic Solar Panels", *2018 International Ural Conference on Green Energy (UralCon)*, pp. 20-25, 2018.

[71] S. Das, S. R. Pani and P. K. Modi, "A probabilistic approach to assess the adequacy of wind and solar energy", *2016 National Power Systems Conference (NPSC)*, pp. 1-6, 2016.

[72] M. Schwan, C. Schwaegerl, W. H. WellBow and T. Connor, "Generation System Reliability in a Market Environment", *2006 International Conference on Probabilistic Methods Applied to Power Systems*, pp. 1-6, 2006.

[73] H. Haroonabadi and M. -. R. Haghifam, "Generation Reliability Assessment in Power Market Using Fuzzy Logic and Monte Carlo Simulation", *2007*

International Conference on Intelligent Systems Applications to Power Systems, pp. 1-6, 2007.

[74] V. Levi, "Fundamentals of Engineering Economy Generation Expansion Planning".

[75] S. Ekisheva and H. Gugel, "North American transformer outage rates and durations in assessment of transmission system reliability and availability", *2015 IEEE Power & Energy Society General Meeting*, pp. 1-5, 2015.

[76] R. Billinton, R. Ghajar, F. Filippelli and R. Del Bianco, "Transmission equipment reliability using the Canadian Electrical Association information system", *Second International Conference on the Reliability of Transmission and Distribution Equipment*, pp. 13-18, 1995.

[77] B. Hu, K. Xie and H. Tai, "Optimal Reliability Allocation of ±800 kV Ultra HVDC Transmission Systems", *IEEE Transactions on Power Delivery*, vol. 33, no. 3, pp. 1174-1184, 2018.

[78] B. Hu, K. Xie and H. Tai, "Reliability Evaluation and Weak Component Identification of ±500-kV HVDC Transmission Systems With Double-Circuit Lines on the Same Tower", *IEEE Transactions on Power Delivery*, vol. 33, no. 4, pp. 1716-1726, 2018.

[79] R. Billinton and G. D. Singh, "Reliability assessment of transmission and distribution systems considering repair in adverse weather conditions", *IEEE Canadian Conference on Electrical and Computer Engineering Conference Proceedings (Cat. No.02CH37373)*, vol.1, pp. 88-93, 2002.

[80] R. Billinton and J. Acharya, "Consideration of multi-state weather models in reliability evaluation of transmission and distribution systems", *Canadian Conference on Electrical and Computer Engineering*, pp. 916-922, 2005.

[81] R. Billinton and Chenjian Wu, "Predictive reliability assessment of distribution systems including extreme adverse weather", *Canadian Conference on Electrical and Computer Engineering 2001 Conference Proceedings (Cat. No.01TH8555)*, vol.2, pp. 719-724, 2001.

[82] J. Wu, X. Song, S. Hu, Z. Wang and K. Wang, "Operational reliability analysis considering multi-factors in large-scale freezing weather", *International Conference on Sustainable Power Generation and Supply (SUPERGEN 2012)*, pp. 1-6, 2012.

[83] Y. Hu, Y. Ding and S. Zhang, "Reliability Assessment of Transmission Lines Considering Extreme Weather Conditions and Human Factors", *2019 IEEE Power & Energy Society General Meeting (PESGM)*, pp. 1-5, 2019.

[84] A. Abul'Wafa, A. El'Garably, and S. Nasser, "Power system security assessment under n-1 and n-1-1 contingency conditions", *International Journal of Engineering Research and Technology*, vol.12, no. 11, pp. 1854-1863, 2019.

[85] J. Choi, "A Method for Transmission System Expansion Planning Considering Probabilistic Reliability Criteria", *2005/2006 IEEE/PES Transmission and Distribution Conference and Exhibition*, pp. 1240-1240, 2006.

[86] A. Bagheri and C. Zhao, "Distributionally Robust Reliability Assessment for Transmission System Hardening Plan Under N-k Security Criterion", *IEEE Transactions on Reliability*, vol. 68, no. 2, pp. 653-662, 2019.

[87] V. Kekatos, "Lecture 1: Power Distribution Systems Overview", *faculty.ece.vt.edu*, 2022. [Online]. Available: https://www.faculty.ece.vt.edu/kekatos/pdsa/Lecture1.pdf

[88] T. Goenen, *Electric Power Distribution System Engineering*. New York: McGraw Hill, 1986.

[89] J. Burke, *Power distribution engineering*. New York: Marcel Dekker, 1994.

[90] R. Brown, *Electric power distribution reliability*. Abingdon: CRC Press, 2002.

[91] "IEEE Guide for Electric Power Distribution Reliability Indices," *IEEE Std 1366-1998*, vol., no., pp.1-21, 1999.

[92] X. Zhang and H. Liao, "Reliability Assessment of Power Converters with Partial Redundancy and Variable Power Distribution", *2018 Asian Conference on Energy, Power and Transportation Electrification (ACEPT)*, pp. 1-5, 2018.

[93] M. Youhannaei, M. Youhannaei, M. R. Haghifam, M. E. Honarmand and A. Sharifi, "Calculation and analysis of customer dissatisfaction index for reliability studies in gilan electric distribution network", *22nd International Conference and Exhibition on Electricity Distribution (CIRED 2013)*, pp. 1-3, 2013.

[94] D. Liang, C. Qin, S. Wang and H. Guo, "Reliability Evaluation of DC Distribution Power Network", *2018 China International Conference on Electricity Distribution (CICED)*, pp. 654-658, 2018.

[95] J. Ouyang, S. Liang, S. Chen, S. Li, Y. Zhou and L. Qin, "Identification and Analysis of Key Equipment for Power Supply Reliability of Distribution Network

based on ETAP", *2021 China International Conference on Electricity Distribution (CICED)*, pp. 81-85, 2021.

[96] S. M. Elmi and M. Rafiei, "Effects of reclosing devices and distributed generation (DG) to improve reliability indices in radial distribution lines", *2012 Proceedings of 17th Conference on Electrical Power Distribution*, pp. 1-5, 2012.

[97] W. Tao *et al.*, "A Data Restoration Strategy in terms of Distribution Network Reliability", *2021 IEEE International Conference on Power Electronics, Computer Applications (ICPECA)*, pp. 525-527, 2021.

[98] L. Yuanhong *et al.*, "Big Data Based Analysis Between Power Distribution Network Reliability Parameters and Economic and Social External Environment", *2021 IEEE International Conference on Power Electronics, Computer Applications (ICPECA)*, pp. 528-531, 2021.

[99] J. Crisp, "Asset Management in Electricity Transmission Utilities: Investigation into Factors Affecting and their Impact on the Network", Ph.D. dissertation, Queensland University of Technology, 2003.

[100] A. Kapetanaki, "Probabilistic Analysis for Optimal Power System Operation Using Flexible Smart Solutions", Ph.D. dissertation, The University of Manchester, 2017.

[101] A. M. L. da Silva, A. Violin, C. Ferreira and Z. S. Machado, "Probabilistic Evaluation of Substation Criticality Based on Static and Dynamic System Performances," *IEEE Transactions on Power Systems*, vol. 29, no. 3, pp. 1410-1418, 2014.

[102] H. Abunima, J. Teh, C. Lai and H. Jabir, "A Systematic Review of Reliability Studies on Composite Power Systems: A Coherent Taxonomy Motivations, Open Challenges, Recommendations, and New Research Directions", *Energies*, vol. 11, no. 9, p. 2417, 2018.

[103] W. Oliveira, J. Vieira, U. Bezerra, D. Martins and B. Rodrigues, "Power system security assessment for multiple contingencies using multiway decision tree", *Electric Power Systems Research*, vol. 148, pp. 264-272, 2017.

[104] R. Billinton, R. Karki, Y. Gao, D. Huang, P. Hu and W. Wangdee, "Adequacy Assessment Considerations in Wind Integrated Power Systems", *IEEE Transactions on Power Systems*, vol. 27, no. 4, pp. 2297-2305, 2012.

[105] Z. Liu *et al.*, "A Lagrange Multiplier Based State Enumeration Reliability Assessment for Power Systems With Multiple Types of Loads and Renewable

Generations", *IEEE Transactions on Power Systems*, vol. 36, no. 4, pp. 3260-3270, 2021.

[106] L. Zhao, J. Ma and Z. Lei, "Power system operation risk assessment based on possibility prioritization search strategy of cascading outage", *5th International Conference on Critical Infrastructure (CRIS)*, pp. 1-10, 2010.

[107] K. Hou, H. Jia, X. Yu, Y. Li, C. Xie and J. Yan, "Composite generation and transmission system reliability assessment using impact increment-based state enumeration method", *2016 International Conference on Probabilistic Methods Applied to Power Systems (PMAPS)*, pp. 1-6, 2016.

[108] Y. Zhang, B. Wei, Z. Liu, T. Xu, X. Liu and K. Hou, "Component Importance Indices of Transmission Systems Based on The Impact-increment Based State Enumeration Method", *2019 IEEE Innovative Smart Grid Technologies - Asia (ISGT Asia)*, pp. 976-979, 2019.

[109] R. Tanabe, H. Amano and A. Yokoyama, "An analytical method for assessing flexible resource adequacy of power systems with a high share of renewables", *2017 IEEE Manchester PowerTech*, pp. 1-6, 2017.

[110] C. Singh, X. Luo and H. Kim, "Power System Adequacy and Security Calculations Using Monte Carlo Simulation incorporating Intelligent System Methodology", *2006 International Conference on Probabilistic Methods Applied to Power Systems*, pp. 1-9, 2006.

[111] G. -h. Yang, Y. Li, Q. Yao and R. Yong, "Study of reliability of grid connected photovoltaic power based on Monte Carlo method", *2011 IEEE Power Engineering and Automation Conference*, pp. 92-95, 2011.

[112] J. Tucker, R. Dhakal, G. Thiel and V. Jadhav, "A Monte Carlo Approach to Predicting Failure Across Multiple Temperature and Humidity Field Environments", *2018 IEEE 68th Electronic Components and Technology Conference (ECTC)*, pp. 144-149, 2018.

[113] Z. Hao, D. Li and S. Zhou, "Preliminary research of reactor protection system reliability based on Monte Carlo methods", *2017 2nd International Conference on System Reliability and Safety (ICSRS)*, pp. 186-189, 2017.

[114] M. Pereira, M. Maceira, G. Oliveira and L. Pinto, "Combining analytical models and Monte-Carlo techniques in probabilistic power system analysis", *IEEE Transactions on Power Systems*, vol. 7, no. 1, pp. 265-272, 1992.

[115] C. Singh and J. Mitra, "Composite System Reliability Evaluation Using State Space Pruning", *IEEE Transactions on Power Systems*, vol. 12, no. 1, pp. 471-479, Feb. 1997.

[116] R. Billinton and S. Adzanu, "Composite generation and transmission system adequacy assessment with time varying loads using a contingency enumeration approach", *IEEE WESCANEX 97 Communications, Power and Computing. Conference Proceedings*, pp. 41-46, 1997.

[117] J. Hammersley and D. Handscomb, *Monte Carlo methods*. London: Methuen, 1979.

[118] R. Billinton and Li Wenyuan, "Composite system reliability assessment using a Monte Carlo approach," *1991 Third International Conference on Probabilistic Methods Applied to Electric Power Systems*, pp. 53-57, 1991.

[119] R. Billinton and R. Allan, *Reliability evaluation of power systems*. New York: Plenum Press, 1984.

[120] L. Goel, "Power System Reliability Assessment", *sites.ieee.org*, 2006. [Online]. Available: http://sites.ieee.org/madras/files/2016/05/powersystems.ppt

[121] V. Levi, "Reliability Analysis of Power Systems", Lecture Notes in Electrical and Electronic Engineering.

[122] Probability Methods Subcommittee, "IEEE Reliability Test System", *IEEE Transactions on Power Apparatus and Systems*, vol. 98, no. 6, pp. 2047-2054, 1979.

[123] IEEE Committee, "The IEEE reliability test system – 1996." *IEEE Trans on Power Systems*, vol. 14, no. 3, pp. 1010-1020, 1999.

[124] R. N. Allan, R. Billinton and N. M. K. Abdel-Gawad, "The IEEE Reliability Test System - Extensions to and Evaluation of the Generating System", *IEEE Transactions on Power Systems*, vol. 1, no. 4, pp. 1-7, Nov. 1986.

[125] J. M. S. Pinheiro, C. R. R. Dornellas, M. T. Schilling, A. C. G. Melo and J. C. O. Mello, "Probing the new IEEE Reliability Test System (RTS-96): HL-II assessment", *IEEE Transactions on Power Systems*, vol. 13, no. 1, pp. 171-176, Feb. 1998.

[126] "Network Output Measures Methodology", *ofgem.gov.uk*, 2015. [Online]. Available: https://www.ofgem.gov.uk/sites/default/files/docs/2017/05/a.1_common_methodology_issue_16_0.pdf

[127] "Condition Based Risk Management (CBRM)", *eatechnology.com*. [Online]. Available: https://eatechnology.com/media/wbspw1nk/cbrm-brochure.pdf

[128] K. Hagkwen and C. Singh, "Reliability Modelling and Simulation in Power Systems with Aging Characteristics," *IEEE Transactions on Power Systems*, vol. 25, pp. 21-28, 2010.

[129] D. Cox, "Regression Models and Life-Tables", *Journal of the Royal Statistical Society: Series B (Methodological)*, vol. 34, no. 2, pp. 187-202, 1972.

[130] National Grid Plc, "*Modelling Asset Lives, Rates of Deterioration and Asset Replacement Volumes*", National Grid, Nov. 2009.

[131] Network Asset Indices Methodology Working Group, "*DNO Common Network Asset Indices Methodology – Health & Criticality (Version 1.1)*", London, 2017.

[132] N. Mansor, V. Levi, "Operational planning of distribution networks based on utility planning concepts", *IEEE Transactions on Power Systems*, vol. 34, no. 3, pp.2114–27, 2019.

[133] N. Mansor, V. Levi, "Integrated planning of distribution networks considering utility planning concepts", *IEEE Transaction on Power Systems*, vol. 32, no. 6, pp.4656–72, 2017.

[134] V. Levi, M. Calovic, "A new decomposition based method for optimal expansion planning of large transmission networks," *IEEE Trans. on Power Systems*, vol. 6, no. 3, pp. 937–943, 1991.

[135] I. Gertsbakh, *Reliability Theory: With Applications to Preventive Maintenance*. Berlin, Heidelberg: Springer Berlin / Heidelberg, 2013.

[136] D. Cai, X. Li, K. Zhou, J. Xin, and K. Cao, "Probabilistic load flow algorithms considering correlation between input random variables: A review", *2015 IEEE 10th Conference on Industrial Electronics and Applications (ICIEA)*, pp. 1139-1144, 2015.

[137] M. Waldron, "Introduction to Reliability Historical Perspective Current Devices Trends", *slideplayer.com*. [Online]. Available: https://slideplayer.com/slide/3878022/

[138] "Life Distributions", *eesemi.com*. [Online]. Available: https://eesemi.com/lifedist.htm

[139] W. Weibull, *Fatigue Testing and Analysis of Results*. Kent: Elsevier Science, 2014.

[140] "Weibull distribution in reliability analysis - Minitab", *support.minitab.com*. [Online]. Available: https://support.minitab.com/en-us/minitab/18/help-and-how-to/modeling-statistics/reliability/supporting-topics/distribution-models/weibull-distribution/

[141] "Wind energy | EcoPlanet Energy", *ecoplanetenergy.com*. [Online]. Available: http://www.ecoplanetenergy.com/all-about-eco-energy/overview/wind/

[142] K. Philippopoulos and D. Deligiorgi, "Statistical simulation of wind speed in Athens, Greece based on Weibull and ARMA models." *International Journal of energy and environment*, vol. 3, no. 4, pp. 151-158, 2009.

[143] Y. Li and A. Kareem, "ARMA systems in wind engineering", *Probabilistic Engineering Mechanics*, vol. 5, no. 2, pp. 49-59, 1990.

[144] J. Torres, A. García, M. De Blas and A. De Francisco, "Forecast of hourly average wind speed with ARMA models in Navarre (Spain)", Solar Energy, vol. 79, no. 1, pp. 65-77, 2005.

[145] Met Office, "Dataset Record: MIDAS: UK Mean Wind Data", *catalogue.ceda.ac.uk*. [Online]. Available: https://catalogue.ceda.ac.uk/uuid/a1f65a362c26c9fa667d98c431a1ad38

[146] V. Sohoni, S.C. Gupta and R.K. Nema, "A critical review on wind turbine power curve modelling techniques and their applications in wind based energy systems", *Journal of Energy*, 2016.

[147] B. Martin and J. Carlin, "Wind-Load Correlation and Estimates of the Capacity Credit of Wind Power: An Empirical Investigation", *Wind Engineering*, vol. 7, no. 2, pp. 79-84, 1983.

[148] M. Franzese and A. Iuliano, "Correlation Analysis", *Encyclopedia of Bioinformatics and Computational Biology*, pp. 706-721, 2019.

[149] I. Stockwell, "Introduction to Correlation and Regression Analysis", *support.sas.com*, 2008. [Online]. Available: https://support.sas.com/resources/papers/proceedings/pdfs/sgf2008/364-2008.pdf

[150] B. Ratner, "The correlation coefficient: Its values range between +1/−1, or do they?", *Journal of Targeting, Measurement and Analysis for Marketing*, vol. 17, no. 2, pp. 139-142, 2009.

[151] F. Chen, H. Liu, J. Li, and X. Zhang, "Comparison of simulation methods of spatially correlated wind speeds", *2015 5th International Conference on Electric*

Utility Deregulation and Restructuring and Power Technologies (DRPT), pp. 255-261, 2015.

[152] H. Wang, X. Xu, Z. Yan, Z. Yang, N. Feng, and Y. Cui, "Probabilistic static voltage stability analysis considering the correlation of wind power", *2016 International Conference on Probabilistic Methods Applied to Power Systems (PMAPS)*, pp. 1-6. IEEE, 2016.

[153] E. Tomasson and L. Soder, "Generation Adequacy Analysis of Multi-Area Power Systems With a High Share of Wind Power", *IEEE Transactions on Power Systems*, vol. 33, no. 4, pp. 3854-3862, 2018.

[154] M. Mehdizadeh, R. Ghazi and M. Ghayeni, "Power system security assessment with high wind penetration using the farms models based on their correlation", *IET Renewable Power Generation*, vol. 12, no. 8, pp. 893-900, 2018.

[155] J. Morales, L. Baringo, A. Conejo and R. Mínguez, "Probabilistic power flow with correlated wind sources", *IET Generation, Transmission & Distribution*, vol. 4, no. 5, p. 641, 2010.

[156] J. Carpentier, "Optimal power flows", *International Journal of Electrical Power & Energy Systems*, vol. 1, no. 1, pp. 3-15, 1979.

[157] S. Frank and S. Rebennack. "An introduction to optimal power flow: Theory, formulation, and examples." *IIE Transactions* 48, no. 12, pp.1172-1197, 2016.

[158] O. Durán, F. Orellana, P. Perez and T. Hidalgo, "Incorporating an Asset Health Index into a Life Cycle Costing: A Proposition and Study Case", *Mathematics*, vol. 8, no. 10, p. 1787, 2020.

[159] R. Mohammad, "New Methods for Reliability Evaluation and Enhancement of Power Systems", *Vuir.vu.edu.au*, 2013. [Online]. Available: https://vuir.vu.edu.au/25838/1/Rahamathualla%20Mohammad.pdf

[160] "Condition Based Risk Management (CBRM)", *eatechnology.com*. [Online]. Available: https://eatechnology.com/media/mq3l3kpd/cbrm-brochure.pdf

[161] C. Dale, "Application of the proportional hazards model in the reliability field", *Reliability Engineering*, vol. 10, no. 1, pp. 1-14, 1985.

[162] A. Bendell, "Proportional hazards modelling in reliability assessment", *Reliability Engineering*, vol. 11, no. 3, pp. 175-183, 1985.

[163] National Grid, "Modelling Asset Lives, Rates of Deterioration and Asset Replacement Volumes", 2009.

[164] A. Jahromi, R. Piercy, S. Cress, J. Service, W. Fan, "An approach to power transformer asset management using health index", *IEEE Electrical Insulation Magazine*, vol. 25, issue 2, 2009.

[165] F. Ortiz, I. Fernandez, A. Ortiz, C.J. Renedo, F. Delgado, C. Fernandez, "Health Indices for Power Transformers: a Case Study", *IEEE Electrical Insulation Magazine*, vol. 32, issue 5, 2016.

[166] F.O. Fernández, A. Ortiz, F. Delgado, I. Fernández, A. Santisteban, A. Cavallini, "Transformer Health Indices Calculation Considering Hot-spot Temperature and load index", *IEEE Electrical Insulation Magazine*, vol. 33, issue 2, 2017.

[167] M. Dong, W. Li, A.B. Nassif, "Long-term Health Index Prediction for Power Asset Classes Based on Sequence Learning", *IEEE Transactions on Power Delivery*, 2021.

[168] A. Chantola, M. Sharma and A. Saini, "Integrated Fuzzy Logic Approach for Calculation of Health Index of Power Transformer", *2018 Second International Conference on Inventive Communication and Computational Technologies (ICICCT)*, 2018.

[169] S. Li, G. Wu, H. Dong, L. Yang and X. Zhen, "Probabilistic Health Index-Based Apparent Age Estimation for Power Transformers", *IEEE Access*, vol. 8, pp. 9692-9701, 2020.

[170] A. Edelman, and H. Murakami. "Polynomial roots from companion matrix eigenvalues", *Mathematics of Computation 64*, no. 210, pp. 763-776, 1995.

[171] M. Brown and F. Proschan, "Imperfect Repair," *Journal of Applied Probability*, vol. 20, pp. 851- 859, 1983.

[172] H. Pham and H. Z. Wang, "Imperfect maintenance," *European Journal of Operational Research*, vol. 94, pp. 425-438, Nov 8, 1996.

[173] T. Nguyen, Y. Dijoux and M. Fouladirad, "On application of an imperfect repair model in maintenance scheduling," *2015 Annual Reliability and Maintainability Symposium (RAMS)*, Palm Harbor, FL, pp. 1-5, 2015.

[174] Z. Wu, B. Liu, Z. Wang, S. Ma and G. Ni, "Research on condition-based maintenance approach of power system considering equipment imperfect maintenance model", *2017 Chinese Automation Congress (CAC)*, Jinan, pp. 3695-3700, 2017.

[175] H. R. Guo, H. Liao, W. Zhao and A. Mettas, "A New Stochastic Model for Systems Under General Repairs," *IEEE Transactions on Reliability*, vol. 56, no. 1, pp. 40-49, 2007.

[176] S. Gasmi, C. E. Love and W. Kahle, "A general repair, proportional-hazards, framework to model complex repairable systems," *IEEE Transactions on Reliability*, vol. 52, no. 1, pp. 26-32, 2003.

[177] M. Kijima and N. Sumita, "A useful generalization of renewal theory: Counting process governed by non-negative Markovian increments", *Journal of Applied Probability*, vol. 23, pp. 71–88, 1986.

[178] R. Benato and D. Napolitano, "Overall Cost Comparison Between Cable and Overhead Lines Including the Costs for Repair After Random Failures", *IEEE Transactions on Power Delivery*, vol. 27, no. 3, pp. 1213-1222, 2012.

[179] T. S. Kishore and S. K. Singal, "Development of generic life cycle costing model for analysis of power transmission lines," *2014 International Conference on Science Engineering and Management Research (ICSEMR)*, pp. 1-5, 2014.

[180] L. Souto and S. Santoso, "Overhead versus Underground: Designing Power Lines for Resilient, Cost-Effective Distribution Networks under Windstorms", *2020 Resilience Week (RWS)*, pp. 113-118, 2020.

[181] M. Mahdavi, H. Monsef and R. Romero, "Reliability Effects of Maintenance on TNEP Considering Preventive and Corrective Repairs," *IEEE Transactions on Power Systems*, vol. 32, no. 5, pp. 3768-3781, 2017.

[182] J. C. Carneiro, "Substation power transformer risk management: Predictive methodology based on reliability centered maintenance data," *4th International Conference on Power Engineering, Energy and Electrical Drives*, pp. 1431-1436, 2013.

[183] M. Dong *et al.*, "A Novel Maintenance Decision Making Model of Power Transformers Based on Reliability and Economy Assessment," *IEEE Access*, vol. 7, pp. 28778-28790, 2019.

APPENDIX

1. Asset Classification

Table 1: Classification of Assets [131]

Asset Category	Subcomponent	Observed Condition
132kV Transformer	Main Transformer	1. Main tank condition 2. Coolers/Radiator condition 3. Bushings condition 4. Kiosk condition 5. Cable boxes condition
	Tapchanger	1. Tapchanger external condition 2. Internal Condition 3. Drive Mechanism Condition 4. Condition of Selector & Divertor Contacts 5. Condition of Selector & Divertor Braids
132kV Cable (Non Pressurised)	N/A	None
132kV Cable (Oil)	N/A	None
132kV Cable (Gas)	N/A	None
132kV Towers	Tower Steelwork	1. Tower Legs 2. Bracings 3. Crossarms 4. Peak
	Tower Paintwork	Paintwork Condition
	Foundations	Foundation Condition
132kV Fittings	N/A	1. Tower fittings 2. Conductor fittings

		3. Insulators - Electrical 4. Insulators - Mechanical
132kV Tower Line Conductor	N/A	1. Visual Condition 2. Midspan joints

2. PoF Curve Parameters

Table 2: PoF curve parameters [131]

Functional Failure Category	**K-Value**	**C-Value**	**Health Score Limit**
HV Switchgear (GM) - Primary	0.0052%	1.087	4
HV Switchgear (GM) - Distribution (GM)	0.0067%	1.087	4
EHV Switchgear (GM) (33kV & 22kV assets only)	0.0223%	1.087	4
EHV Switchgear (GM) (66kV assets only)	0.0512%	1.087	4
HV Transformer (GM)	0.0078%	1.087	4
EHV Transformer/ 132kV Transformer	0.0454%	1.087	4
Towers	0.0545%	1.087	4
Fittings	0.0096%	1.087	4
OHL Conductor	0.0080%	1.087	4
Pressurised Cable (EHV UG Cable (Oil) and 132kV UG Cable (Oil))	2.0944%	1.087	4
Pressurised Cable (EHV UG Cable (Gas) and 132kV UG Cable (Gas))	4.5036%	1.087	4
Submarine Cables	0.0202%	1.087	4
Non Pressurised Cable	0.0658%	1.087	4

3. PoF Calculation

Table 3: Normal Expected Life [131]

Asset Register Category	**Sub-division**	**Normal Expected Life (yr)**
132kV Transformer (GM)	Transformer – Pre 1980	60
	Transformer – Post 1980	50
	Tapchanger	60
132kV OHL (Tower Line) Conductor	ACSR - greased	55
	ACSR - non-greased	50
	AAAC	60
	Cad Cu	50
	Cu	70
	Other	50
132kV Tower	Steelwork	80
	Foundation – Fully Encased Concrete	95
	Foundation – Earth Grillage	60
	Paint System – Galvanising	30
	Paint System – Paint	20
132kV Fittings		40
132kV UG Cable (Oil)	Aluminium sheath – Aluminium conductor	75
	Aluminium sheath – Copper conductor	75
	Lead sheath – Aluminium conductor	80
	Lead sheath –	80

	Copper conductor	
132kV UG Cable (Gas)	Aluminium sheath – Aluminium conductor	65
	Aluminium sheath – Copper conductor	70
	Lead sheath – Aluminium conductor	75
	Lead sheath – Copper conductor	75
132kV Sub Cable		60

4. Deterministic Hazard Function

Deterministic hazard function:

$$\lambda(t) = K \cdot \gamma + a \cdot e^{\beta_2 t} + b \cdot e^{2\beta_2 t} + c \cdot e^{3\beta_2 t}$$

Here, γ is introduced to control the failure intensity and avoid unrealistically high values of reliability indices. The steps for finding the proper value of γ are given as follows:

1. For each asset type, it starts from no control, meaning $\gamma = 1$. Use average up-time as an indicator to decide if the indicator fits the reality. For example, the average up-time over a simulation year for a cable whose age is 1 year is about 400-500 hours. In this case, the average up-time is considered short for a young cable.
2. Reduce to $\gamma = 0.1$. The average up-time for the cable with the same condition is 4340-8745 hours. This value is better compared to the previous step.
3. The approximated range of the γ value is between 0.1 and 1. The lower boundary value can be increased or decreased to receive a more realistic value. In the case of the cable, the lower boundary is reduced to 0.08, which makes its average up-time locate between 8746 and 8760 hours.

5. Transition Matrix M

5.1 Entire Transition Matrix M with Different Approaches

Table 4: Matrix M using normalization by rows

Year	1→2	1→3	1→4	1→5	1→6	2→3	2→4	2→5	2→6	3→4	3→5	3→6	4→5	4→6	5→6
1	0	0	0	0	0	0	0	0	0	0	0	0	0	0	0
2	0	0.05	0.087	0.104	0.14	0	0	0	0	0	0	0	0	0	0
3	0.0194	0.02469	0.04409	0.02469	0.0388	0	0.01923	0.01923	0.01923	0.02	0	0.04	0.02299	0.02299	0.01923
4	0.01455	0.01871	0.03119	0.02287	0.03326	0	0.01667	0.03333	0.01667	0	0	0	0.01818	0.00909	0.01681
5	0.01182	0.00946	0.01418	0.01655	0.04255	0	0.01587	0.01587	0.01587	0.01429	0	0.01429	0	0.02439	0.05303
6	0.00522	0.01044	0.01567	0.02089	0.02611	0	0.01538	0	0.06154	0.01389	0.05556	0	0.00781	0.03125	0.05263
7	0.00567	0.01416	0.01416	0.017	0.01983	0	0	0	0.04839	0	0.01408	0.02817	0.0229	0.01527	0.08633
8	0.00915	0.00915	0.00915	0.01524	0.03963	0	0.01639	0.01639	0.01639	0	0.0137	0.0137	0.00763	0.0229	0.07299
9	0.00332	0.00997	0.00332	0.00664	0.0299	0	0.01639	0.01639	0.03279	0	0	0.02703	0.01527	0.0458	0.05926
10	0.01053	0	0.01404	0.01404	0.02807	0	0	0	0.01724	0	0.01333	0	0.024	0.056	0.02273
11	0.00376	0	0.01128	0.02256	0.02256	0	0	0	0.01667	0	0.01351	0	0.01681	0.02521	0.0438
12	0.012	0.004	0.004	0.008	0	0.01667	0	0	0	0	0.0274	0	0.01709	0	0
13	0.01646	0.02058	0.01646	0.00823	0	0.01613	0.01613	0.03226	0	0.05479	0	0	0.00862	0	0
14	0.01316	0.01754	0.02193	0.01316	0	0.03226	0	0.03226	0	0.01333	0	0	0.00806	0	0
15	0.00939	0.02347	0.01408	0.01878	0	0	0	0	0	0	0	0	0.00775	0.00775	0
16	0.0201	0.01005	0.00503	0.00503	0	0	0	0	0	0.01176	0	0	0.03077	0	0
17	0.04712	0.01047	0.02094	0	0	0	0	0.01493	0	0.01163	0.01163	0	0.00781	0	0
18	0.01705	0.02841	0.01705	0.00568	0	0	0.02667	0.01333	0	0.02326	0	0	0.00758	0	0
19	0.0061	0.0122	0.01829	0.02439	0	0	0	0	0	0.01124	0	0	0.01449	0	0
20	0.01299	0	0.02597	0.01299	0	0	0	0	0	0.02222	0.01111	0	0.01429	0	0
21	0.02055	0.0137	0	0.00685	0	0.01282	0.01282	0.01282	0	0.02299	0	0	0.01389	0	0
22	0.00714	0.02857	0.00714	0.00714	0	0	0.01282	0	0	0.01136	0	0	0	0	0
23	0.01504	0.00752	0.01504	0.00752	0	0.01282	0	0	0	0.02198	0	0	0.00676	0	0
24	0.00787	0.02362	0	0.00787	0	0	0.01266	0	0	0	0	0	0	0	0
25	0.01639	0	0.01639	0	0	0.02532	0.01266	0	0	0.01064	0	0	0	0	0
26	0.02542	0	0.01695	0	0	0	0	0	0	0.01053	0	0	0	0	0
27	0.0177	0.02655	0	0	0	0.02469	0.01235	0	0	0.01064	0	0	0	0	0
28	0	0.00926	0	0.00926	0	0.025	0	0	0	0.02041	0	0	0.00621	0	0
29	0.01887	0.00943	0.01887	0	0	0.01282	0	0	0	0.0101	0	0	0	0	0
30	0.0099	0.0099	0.0099	0.0099	0	0.02532	0.02532	0	0	0	0	0	0.01212	0	0
31	0.01031	0.01031	0.02062	0	0	0.01316	0.02632	0	0	0	0	0	0.01205	0	0
32	0.01075	0.04301	0	0	0	0	0	0	0	0	0	0	0	0	0
33	0.02273	0.01136	0	0	0	0	0.01333	0	0	0.00917	0	0	0	0	0
34	0.01176	0.01176	0	0	0	0.02632	0	0	0	0	0	0	0	0	0
35	0.01205	0	0	0	0	0.01333	0.01333	0	0	0.01786	0	0	0	0	0
36	0.03659	0.02439	0.02439	0	0	0.01351	0	0	0	0.01802	0	0	0	0	0
37	0.01333	0.02667	0.02667	0	0	0.01316	0.01316	0	0	0.00893	0	0	0.00565	0	0
38	0.01429	0.02857	0	0	0	0	0	0	0	0.00877	0	0	0	0	0
39	0.04478	0.04478	0.01493	0	0	0.01316	0	0	0	0	0	0	0	0	0
40	0	0	0.01667	0	0	0	0.01282	0	0	0	0	0	0	0	0
41	0	0	0	0	0	0.03896	0.01299	0	0	0	0	0	0	0	0
42	0	0.0339	0.01695	0	0	0	0.0137	0	0	0.0082	0	0	0	0	0
43	0.01786	0.01786	0	0	0	0	0	0	0	0	0	0	0	0	0
44	0	0.03704	0	0	0	0.0411	0	0	0	0	0	0	0	0	0
45	0.01923	0.03846	0.01923	0	0	0.01429	0	0	0	0	0	0	0	0	0
46	0.02083	0.02083	0	0	0	0.02857	0	0	0	0	0	0	0	0	0
47	0.04348	0.02174	0	0	0	0.01449	0.01449	0	0	0.00741	0	0	0	0	0
48	0.02326	0.02326	0	0	0	0.02899	0	0	0	0.01471	0	0	0	0	0
49	0	0	0	0	0	0.04412	0	0	0	0.0073	0	0	0	0	0
50	0.02439	0	0	0	0	0.01538	0	0	0	0	0	0	0	0	0
51	0	0	0	0	0	0	0	0	0	0	0	0	0	0	0
52	0.025	0.025	0	0	0	0.01538	0	0	0	0	0	0	0	0	0
53	0	0.02632	0	0	0	0.03077	0	0	0	0	0	0	0	0	0
54	0.08108	0	0	0	0	0	0	0	0	0.0069	0	0	0	0	0
55	0.02941	0.02941	0	0	0	0.01515	0.01515	0	0	0.01389	0	0	0	0	0
56	0	0.03125	0	0	0	0.03077	0	0	0	0	0	0	0	0	0
57	0	0.03226	0	0	0	0	0	0	0	0	0	0	0	0	0
58	0.06667	0	0	0	0	0.01587	0	0	0	0	0	0	0	0	0
59	0	0.03571	0	0	0	0	0	0	0	0.00671	0	0	0	0	0
60	0	0	0	0	0	0	0	0	0	0	0	0	0	0	0

Table 5: Matrix M using normalization by columns – transition to any HI

Year	1→2	1→3	1→4	1→5	1→6	2→3	2→4	2→5	2→6	3→4	3→5	3→6	4→5	4→6	5→6
1	0	0	0	0	0	0	0	0	0	0	0	0	0	0	0
2	0.018	0	0	0	0	0	0	0	0	0	0	0	0	0	0
3	0.01969	0	0	0	0	0	0	0	0	0	0	0	0	0	0
4	0.02748	0	0	0	0	0	0	0	0	0	0	0	0	0	0
5	0.02065	0	0	0	0	0	0	0	0	0	0	0	0	0	0
6	0.01887	0	0	0	0	0	0	0	0	0	0	0	0	0	0
7	0.02149	0	0	0	0	0	0	0	0	0	0	0	0	0	0
8	0.03699	0	0	0	0	0	0	0	0	0	0	0	0	0	0
9	0.03001	0	0	0	0	0	0	0	0	0	0	0	0	0	0
10	0.0297	0	0	0	0	0	0	0	0	0	0	0	0	0	0
11	0.06505	0	0	0	0	0	0	0	0	0	0	0	0	0	0
12	0.06139	0	0	0	0	0	0	0	0	0	0	0	0	0	0
13	0.08721	0	0	0	0	0	0	0	0	0	0	0	0	0	0
14	0.07962	0	0	0	0	0	0	0	0	0	0	0	0	0	0
15	0.08304	0	0	0	0	0	0	0	0	0	0	0	0	0	0
16	0.10189	0	0	0	0	0	0	0	0	0	0	0	0	0	0
17	0.08613	0	0	0	0	0	0	0	0	0	0	0	0	0	0
18	0.11034	0	0	0	0	0	0	0	0	0	0	0	0	0	0
19	0.1447	0	0	0	0	0	0	0	0	0	0	0	0	0	0
20	0.15408	0	0	0	0	0	0	0	0	0	0	0	0	0	0
21	0.07857	0.05714	0.03214	0.025	0	0.05139	0.02222	0.02083	0	0	0	0	0	0	0
22	0.08036	0.04911	0.01786	0.02232	0	0.06667	0.02074	0.02074	0	0.01887	0	0	0.03846	0	0
23	0.12903	0.06452	0.01075	0.01613	0	0.06947	0.02908	0.021	0	0.02778	0	0	0.04444	0	0
24	0.11111	0.04167	0.02083	0.02083	0	0.06151	0.02812	0.01406	0	0.01863	0.01863	0	0.01515	0	0
25	0.13793	0.06897	0.0431	0	0	0.07605	0.02662	0.03042	0	0.05612	0.0051	0	0.03448	0	0
26	0.25	0.04545	0.03409	0.03409	0	0.07676	0.04264	0.02345	0	0.03846	0.02564	0	0.01754	0	0
27	0.17544	0.10526	0.03509	0.03509	0	0.10142	0.04717	0.01179	0	0.04247	0.03861	0	0.02098	0	0
28	0.26316	0.13158	0.05263	0.02632	0	0.0989	0.02473	0.02473	0	0.02076	0.0346	0	0.03488	0	0
29	0.26316	0.15789	0	0.15789	0	0.08723	0.04984	0.03427	0	0.03822	0.03503	0	0.01093	0	0
30	1	0	0	0	0	0.11397	0.05147	0.02206	0	0.04063	0.02813	0	0.02392	0	0
31	0	0	0	0	0	0.03896	0.0303	0.02597	0.00433	0.05775	0.03647	0.01216	0.03043	0.01304	0.00476
32	0	0	0	0	0	0.04306	0.02392	0.00478	0.01435	0.06601	0.0297	0.0066	0.02033	0.0122	0.00858
33	0	0	0	0	0	0.03684	0.03158	0.06316	0.01053	0.04965	0.0461	0.00709	0.03422	0.01141	0.0122
34	0	0	0	0	0	0.01829	0.07927	0.04268	0.0122	0.05769	0.04231	0.00769	0.02583	0.01845	0.00725
35	0	0	0	0	0	0.02878	0.09353	0.06475	0.01439	0.05085	0.02119	0	0.03846	0.0035	0.00334
36	0	0	0	0	0	0.05455	0.04545	0.04545	0	0.03125	0.04464	0.00446	0.02007	0.00669	0.0031
37	0	0	0	0	0	0.05263	0.08421	0.05263	0.01053	0.07547	0.0283	0	0.03642	0.00331	0.01166
38	0	0	0	0	0	0.03947	0.14474	0.02632	0	0.05641	0.04103	0.01538	0.03175	0.00952	0.02222
39	0	0	0	0	0	0.03333	0.13333	0.03333	0	0.04545	0.03977	0.01136	0.0463	0.00926	0.00806
40	0	0	0	0	0	0.0625	0.08333	0.0625	0	0.1118	0.04348	0.00621	0.03106	0.00932	0.00763
41	0	0	0	0	0	0.13158	0.02632	0	0.02632	0.04348	0.08696	0.00725	0.05136	0.02417	0.01707
42	0	0	0	0	0	0.03333	0.06667	0.06667	0.03333	0.06504	0.04065	0.01626	0.06667	0.02857	0.01389
43	0	0	0	0	0	0.08333	0.04167	0.04167	0	0.06422	0.00917	0.01835	0.05085	0.02373	0.02423
44	0	0	0	0	0	0.1	0.25	0.05	0	0.07619	0.04762	0.01905	0.04676	0.00719	0.02832
45	0	0	0	0	0	0.07692	0	0	0	0.07609	0.07609	0.05435	0.06182	0.02545	0.02151
46	0	0	0	0	0	0.16667	0	0.08333	0.08333	0.05405	0.05405	0.02703	0.06615	0.05058	0.03542
47	0	0	0	0	0	0	0.125	0.25	0.125	0.09091	0.06061	0	0.09914	0.0431	0.05372
48	0	0	0	0	0	0	0	0.25	0	0.05455	0.07273	0.05455	0.0625	0.05288	0.02881
49	0	0	0	0	0	0	0.33333	0	0	0.06667	0.06667	0.06667	0.09043	0.03723	0.03067
50	0	0	0	0	0	0.5	0	0	0	0.05714	0.02857	0.02857	0.09524	0.04762	0.04242
51	0	0	0	0	0	0	0	0.5	0	0.03226	0	0.06452	0.02703	0.07432	0.07362
52	0	0	0	0	0	0	0	0	0	0	0.03571	0.07143	0.02985	0.09701	0.08734
53	0	0	0	0	0	0	0	0	0	0	0	0.12	0.03419	0.17094	0.08747
54	0	0	0	0	0	0	0	0	0	0	0	0	0.03261	0.08696	0.12788
55	0	0	0	0	0	0	0	0	0	0.1	0.05	0.05	0.03614	0.14458	0.10465
56	0	0	0	0	0	0	0	0	0	0	0	0.05882	0.01389	0.08333	0.19417
57	0	0	0	0	0	0	0	0	0	0	0.06667	0.13333	0.03125	0.17188	0.19048
58	0	0	0	0	0	0	0	0	0	0.2	0	0.3	0.01923	0.23077	0.23077
59	0	0	0	0	0	0	0	0	0	0	0	0.2	0.025	0.3	0.2716
60	0	0	0	0	0	0	0	0	0	0	0	0	0	0.48148	0.30252

Table 6: Matrix M using normalization by columns – transition to next HI

Year	1→2	1→3	1→4	1→5	1→6	2→3	2→4	2→5	2→6	3→4	3→5	3→6	4→5	4→6	5→6
1	0	0	0	0	0	0	0	0	0	0	0	0	0	0	0
2	0	0	0	0	0	0	0	0	0	0	0	0	0	0	0
3	0.0228	0	0	0	0	0	0	0	0	0	0	0	0	0	0
4	0.03075	0	0	0	0	0	0	0	0	0	0	0	0	0	0
5	0.02626	0	0	0	0	0	0	0	0	0	0	0	0	0	0
6	0.02022	0	0	0	0	0	0	0	0	0	0	0	0	0	0
7	0.02982	0	0	0	0	0	0	0	0	0	0	0	0	0	0
8	0.03901	0	0	0	0	0	0	0	0	0	0	0	0	0	0
9	0.01845	0	0	0	0	0	0	0	0	0	0	0	0	0	0
10	0.02256	0	0	0	0	0	0	0	0	0	0	0	0	0	0
11	0.0641	0	0	0	0	0	0	0	0	0	0	0	0	0	0
12	0.06301	0	0	0	0	0	0	0	0	0	0	0	0	0	0
13	0.08626	0	0	0	0	0	0	0	0	0	0	0	0	0	0
14	0.0848	0	0	0	0	0	0	0	0	0	0	0	0	0	0
15	0.10839	0	0	0	0	0	0	0	0	0	0	0	0	0	0
16	0.10784	0	0	0	0	0	0	0	0	0	0	0	0	0	0
17	0.10549	0	0	0	0	0	0	0	0	0	0	0	0	0	0
18	0.14005	0	0	0	0	0	0	0	0	0	0	0	0	0	0
19	0.15714	0	0	0	0	0	0	0	0	0	0	0	0	0	0
20	0.14915	0	0	0	0	0	0	0	0	0	0	0	0	0	0
21	0.11952	0	0	0	0	0.05607	0	0	0	0	0	0	0	0	0
22	0.0905	0	0	0	0	0.07327	0	0	0	0.04762	0	0	0	0	0
23	0.0995	0	0	0	0	0.07966	0	0	0	0.07447	0	0	0	0	0
24	0.1326	0	0	0	0	0.10495	0	0	0	0.04196	0	0	0.11111	0	0
25	0.17834	0	0	0	0	0.08696	0	0	0	0.0628	0	0	0.07143	0	0
26	0.20155	0	0	0	0	0.11092	0	0	0	0.10081	0	0	0	0	0
27	0.27184	0	0	0	0	0.1009	0	0	0	0.0692	0	0	0.11765	0	0
28	0.34667	0	0	0	0	0.12524	0	0	0	0.06462	0	0	0.07692	0	0
29	0.55102	0	0	0	0	0.15195	0	0	0	0.1	0	0	0.08642	0	0
30	1	0	0	0	0	0.175	0	0	0	0.09582	0	0	0.04505	0	0
31	0	0	0	0	0	0.08052	0	0	0	0.1236	0	0	0.06897	0	0
32	0	0	0	0	0	0.05932	0	0	0	0.06888	0	0	0.08947	0	0
33	0	0	0	0	0	0.04204	0	0	0	0.08475	0	0	0.07921	0	0
34	0	0	0	0	0	0.04075	0	0	0	0.04592	0	0	0.07692	0	0
35	0	0	0	0	0	0.06209	0	0	0	0.06977	0	0	0.04955	0	0.02353
36	0	0	0	0	0	0.04181	0	0	0	0.12401	0	0	0.07563	0	0.02128
37	0	0	0	0	0	0.06909	0	0	0	0.10174	0	0	0.12734	0	0.01818
38	0	0	0	0	0	0.05078	0	0	0	0.1189	0	0	0.11567	0	0.04225
39	0	0	0	0	0	0.04115	0	0	0	0.12914	0	0	0.09058	0	0.02994
40	0	0	0	0	0	0.06867	0	0	0	0.17216	0	0	0.13793	0	0.03209
41	0	0	0	0	0	0.10599	0	0	0	0.11157	0	0	0.15152	0	0.02262
42	0	0	0	0	0	0.10825	0	0	0	0.15966	0	0	0.14695	0	0.03831
43	0	0	0	0	0	0.16763	0	0	0	0.19005	0	0	0.15217	0	0.0411
44	0	0	0	0	0	0.11111	0	0	0	0.20673	0	0	0.19928	0	0.04658
45	0	0	0	0	0	0.17188	0	0	0	0.14917	0	0	0.22348	0	0.08011
46	0	0	0	0	0	0.23585	0	0	0	0.20455	0	0	0.20259	0	0.07398
47	0	0	0	0	0	0.20988	0	0	0	0.30909	0	0	0.27602	0	0.07561
48	0	0	0	0	0	0.29688	0	0	0	0.29008	0	0	0.33175	0	0.1
49	0	0	0	0	0	0.57778	0	0	0	0.35714	0	0	0.36872	0	0.10086
50	0	0	0	0	0	1	0	0	0	0.52041	0	0	0.48366	0	0.10103
51	0	0	0	0	0	0	0	0	0	0.36364	0	0	0.43846	0	0.1549
52	0	0	0	0	0	0	0	0	0	0.11905	0	0	0.3299	0	0.16393
53	0	0	0	0	0	0	0	0	0	0	0	0	0.18571	0	0.11818
54	0	0	0	0	0	0	0	0	0	0.18919	0	0	0.19298	0	0.1596
55	0	0	0	0	0	0	0	0	0	0.16667	0	0	0.32075	0	0.21264
56	0	0	0	0	0	0	0	0	0	0.04	0	0	0.34146	0	0.27491
57	0	0	0	0	0	0	0	0	0	0.125	0	0	0.32143	0	0.32444
58	0	0	0	0	0	0	0	0	0	0.38095	0	0	0.5	0	0.36025
59	0	0	0	0	0	0	0	0	0	0.53846	0	0	0.73684	0	0.57018
60	0	0	0	0	0	0	0	0	0	1	0	0	1	0	1

5.2 Determination of *n* Value

Three values of *n* are investigated; the computational time is for one single asset.

- $n = 100$: computational time = 2.923s;
- $n = 1000$: computational time = 23.025s;
- $n = 2000$: computational time = 46.831s;

Table 7: Matrix M with $n = 100$

Year	1→2	1→3	1→4	1→5	1→6	2→3	2→4	2→5	2→6	3→4	3→5	3→6	4→5	4→6	5→6
1	0	0	0	0	0	0	0	0	0	0	0	0	0	0	0
2	0.01	0	0	0	0	0	0	0	0	0	0	0	0	0	0
3	0.020833	0	0	0	0	0	0	0	0	0	0	0	0	0	0
4	0.021277	0	0	0	0	0	0	0	0	0	0	0	0	0	0
5	0.021739	0	0	0	0	0	0	0	0	0	0	0	0	0	0
6	0.022222	0	0	0	0	0	0	0	0	0	0	0	0	0	0
7	0.045455	0	0	0	0	0	0	0	0	0	0	0	0	0	0
8	0.047619	0	0	0	0	0	0	0	0	0	0	0	0	0	0
9	0.0625	0	0	0	0	0	0	0	0	0	0	0	0	0	0
10	0.04	0	0	0	0	0	0	0	0	0	0	0	0	0	0
11	0.055556	0	0	0	0	0	0	0	0	0	0	0	0	0	0
12	0.073529	0	0	0	0	0	0	0	0	0	0	0	0	0	0
13	0.063492	0	0	0	0	0	0	0	0	0	0	0	0	0	0
14	0.050847	0	0	0	0	0	0	0	0	0	0	0	0	0	0
15	0.107143	0	0	0	0	0	0	0	0	0	0	0	0	0	0
16	0.12	0	0	0	0	0	0	0	0	0	0	0	0	0	0
17	0.090909	0	0	0	0	0	0	0	0	0	0	0	0	0	0
18	0.15	0	0	0	0	0	0	0	0	0	0	0	0	0	0
19	0.117647	0	0	0	0	0	0	0	0	0	0	0	0	0	0
20	0.1	0	0	0	0	0	0	0	0	0	0	0	0	0	0
21	0	0	0.074074	0	0	0.054795	0.041096	0.013699	0	0	0	0	0	0	0
22	0.08	0.08	0	0	0	0.015385	0.030769	0.015385	0	0	0	0	0	0	0
23	0.285714	0	0	0.047619	0	0.126984	0.047619	0.015873	0	0	0.142857	0	0	0	0
24	0	0.071429	0.071429	0	0	0.087719	0.017544	0.017544	0	0	0.071429	0	0	0	0
25	0.083333	0.083333	0	0	0	0.08	0	0	0	0.052632	0	0	0	0	0
26	0.1	0	0	0.1	0	0.042553	0.06383	0.042553	0	0.043478	0.043478	0	0	0	0
27	0.375	0	0	0	0	0.146341	0.02439	0	0	0.043478	0.043478	0	0	0	0
28	0.2	0.2	0	0	0	0.083333	0.027778	0.055556	0	0.035714	0	0	0	0	0
29	0	0.666667	0	0	0	0.032258	0.032258	0.032258	0	0.032258	0.032258	0	0.095238	0	0
30	1	0	0	0	0	0.107143	0.107143	0.071429	0	0.03125	0.0625	0	0	0	0
31	0	0	0	0	0	0.047619	0.095238	0	0	0.125	0	0.03125	0	0	0
32	0	0	0	0	0	0.111111	0	0	0	0.035714	0	0	0	0.032258	0
33	0	0	0	0	0	0	0.0625	0.125	0	0.034483	0.034483	0	0.032258	0	0.045455
34	0	0	0	0	0	0	0.076923	0	0	0.148148	0.037037	0	0.03125	0	0
35	0	0	0	0	0	0.083333	0	0	0	0	0.090909	0	0.027778	0.027778	0
36	0	0	0	0	0	0.181818	0.090909	0.181818	0	0.190476	0	0	0.029412	0	0
37	0	0	0	0	0	0	0.166667	0	0	0.052632	0	0	0.078947	0.026316	0.030303
38	0	0	0	0	0	0	0	0	0	0	0	0	0.027778	0	0.028571
39	0	0	0	0	0	0	0	0	0	0.166667	0.055556	0	0	0	0
40	0	0	0	0	0	0	0	0	0	0.214286	0.071429	0	0.026316	0	0
41	0	0	0	0	0	0	0	0.2	0	0	0.1	0.1	0.05	0	0.052632
42	0	0	0	0	0	0.25	0	0	0	0	0.125	0	0	0.052632	0
43	0	0	0	0	0	0	0.25	0	0	0.125	0.125	0	0.028571	0.028571	0.04878
44	0	0	0	0	0	0	0	0	0	0	0	0	0.028571	0	0.02439
45	0	0	0	0	0	0	0.333333	0.333333	0	0	0	0	0.090909	0.060606	0.04878
46	0	0	0	0	0	0	0	0	0	0	0	0	0	0.034483	0
47	0	0	0	0	0	0	0	0	0	0.142857	0.142857	0	0.107143	0.035714	0.046512
48	0	0	0	0	0	0	1	0	0	0	0	0	0.076923	0.038462	0.066667
49	0	0	0	0	0	0	0	0	0	0	0	0.25	0.208333	0.083333	0.022727
50	0	0	0	0	0	0	0	0	0	0.333333	0	0	0.176471	0.117647	0.020833
51	0	0	0	0	0	0	0	0	0	0	0	0	0	0	0.142857
52	0	0	0	0	0	0	0	0	0	0	0	0.5	0.142857	0	0.02381
53	0	0	0	0	0	0	0	0	0	0	0	0	0	0.083333	0.186047
54	0	0	0	0	0	0	0	0	0	0	0	0	0	0	0.057143
55	0	0	0	0	0	0	0	0	0	0	0	0	0	0	0.151515
56	0	0	0	0	0	0	0	0	0	0	0	0	0	0.090909	0.142857
57	0	0	0	0	0	0	0	0	0	0	0	0	0	0.181818	0.166667
58	0	0	0	0	0	0	0	0	0	0	0	0	0	0.125	0.190476
59	0	0	0	0	0	0	0	0	0	0	0	0	0.142857	0.142857	0.235294
60	0	0	0	0	0	0	0	0	0	0	0	0	0	0.6	0.285714

Table 8: Matrix M with $n = 1000$

Year	1→2	1→3	1→4	1→5	1→6	2→3	2→4	2→5	2→6	3→4	3→5	3→6	4→5	4→6	5→6
1	0	0	0	0	0	0	0	0	0	0	0	0	0	0	0
2	0.009	0	0	0	0	0	0	0	0	0	0	0	0	0	0
3	0.020492	0	0	0	0	0	0	0	0	0	0	0	0	0	0
4	0.025105	0	0	0	0	0	0	0	0	0	0	0	0	0	0
5	0.022532	0	0	0	0	0	0	0	0	0	0	0	0	0	0
6	0.021954	0	0	0	0	0	0	0	0	0	0	0	0	0	0
7	0.032548	0	0	0	0	0	0	0	0	0	0	0	0	0	0
8	0.020882	0	0	0	0	0	0	0	0	0	0	0	0	0	0
9	0.027251	0	0	0	0	0	0	0	0	0	0	0	0	0	0
10	0.029233	0	0	0	0	0	0	0	0	0	0	0	0	0	0
11	0.053952	0	0	0	0	0	0	0	0	0	0	0	0	0	0
12	0.06366	0	0	0	0	0	0	0	0	0	0	0	0	0	0
13	0.09915	0	0	0	0	0	0	0	0	0	0	0	0	0	0
14	0.056604	0	0	0	0	0	0	0	0	0	0	0	0	0	0
15	0.075	0	0	0	0	0	0	0	0	0	0	0	0	0	0
16	0.117117	0	0	0	0	0	0	0	0	0	0	0	0	0	0
17	0.089796	0	0	0	0	0	0	0	0	0	0	0	0	0	0
18	0.100897	0	0	0	0	0	0	0	0	0	0	0	0	0	0
19	0.134663	0	0	0	0	0	0	0	0	0	0	0	0	0	0
20	0.152738	0	0	0	0	0	0	0	0	0	0	0	0	0	0
21	0.105442	0	0.017007	0	0	0	0	0	0	0	0	0	0	0	0
22	0.097458	0.050847	0.050847	0.008475	0	0.056972	0.022489	0.016492	0	0	0.015152	0	0.086957	0	0
23	0.13369	0.069519	0.026738	0.005348	0	0.054313	0.023962	0.022364	0	0.034783	0.043478	0	0	0	0
24	0.06993	0.076923	0.041958	0.048951	0	0.064516	0.022071	0.027165	0	0.026316	0.019737	0	0.027778	0	0
25	0.192661	0.06422	0.036697	0.009174	0	0.088512	0.054614	0.009416	0	0.015464	0.010309	0	0.010638	0	0
26	0.197368	0.078947	0.039474	0.039474	0	0.067797	0.03178	0.021186	0	0.033058	0.024793	0	0.03876	0	0
27	0.244898	0.081633	0.020408	0.020408	0	0.069767	0.025581	0.027907	0	0.033835	0.018797	0	0.02	0	0
28	0.483871	0.032258	0	0.064516	0	0.102828	0.046272	0.015424	0	0.031469	0.017483	0	0.005952	0	0
29	0.538462	0.153846	0	0	0	0.108187	0.032164	0.026316	0	0.041667	0.016026	0	0.010363	0	0
30	1	0	0	0	0	0.078767	0.037671	0.034247	0	0.048048	0.024024	0	0.027907	0	0
31	0	0	0	0	0	0	0	0	0	0	0.018072	0.009036	0.017021	0.008511	0.011111
32	0	0	0	0	0	0	0	0	0	0	0.031949	0.00639	0.034351	0.01145	0.010309
33	0	0	0	0	0	0	0	0	0	0	0.023891	0.006826	0.025362	0.003623	0.004464
34	0	0	0	0	0	0	0	0	0	0	0.039146	0.010676	0.016892	0.006757	0.012245
35	0	0	0	0	0	0	0	0	0	0	0.030303	0.015152	0.045455	0.00974	0.007692
36	0	0	0	0	0	0	0	0	0	0	0.058091	0.008299	0.019231	0.003205	0.003521
37	0	0	0	0	0	0	0	0	0	0	0.050228	0.022831	0.058642	0.009259	0.01634
38	0	0	0	0	0	0	0	0	0	0	0.010471	0.010471	0.024615	0.012308	0.002967
39	0	0	0	0	0	0	0	0	0	0	0.038889	0.022222	0.050898	0.005988	0.014327
40	0	0	0	0	0	0	0	0	0	0	0.031646	0	0.035608	0.014837	0.01626
41	0	0	0	0	0	0	0	0	0	0	0.036765	0.058824	0.049275	0.02029	0.023499
42	0	0	0	0	0	0.088235	0.029412	0.029412	0	0.067227	0.016807	0.016807	0.05136	0.02719	0.022556
43	0	0	0	0	0	0	0.103448	0.137931	0.103448	0.036036	0.072072	0.027027	0.047923	0.01278	0.026829
44	0	0	0	0	0	0.105263	0	0	0.052632	0.03125	0.0625	0.041667	0.093023	0.023256	0.044601
45	0	0	0	0	0	0.176471	0.176471	0	0	0.094118	0.164706	0.023529	0.063433	0.029851	0.024943
46	0	0	0	0	0	0.166667	0	0.25	0.083333	0.046875	0.0625	0.0625	0.063241	0.035573	0.034707
47	0	0	0	0	0	0.2	0.4	0	0	0.035714	0.107143	0.035714	0.060606	0.034632	0.042735
48	0	0	0	0	0	0	0.333333	0	0	0.041667	0.125	0.0625	0.07109	0.028436	0.042735
49	0	0	0	0	0	0	0	0	0	0.052632	0.105263	0.026316	0.083333	0.0625	0.044872
50	0	0	0	0	0	0	0	0	0	0	0.206897	0.034483	0.08284	0.04142	0.051392
51	0	0	0	0	0	0	0	0	0	0	0.043478	0.043478	0	0.108844	0.101512
52	0	0	0	0	0	0	0	0	0	0	0	0	0.029851	0.074627	0.081731
53	0	0	0	0	0	0	0	0	0	0.052632	0	0.105263	0.016667	0.141667	0.080311
54	0	0	0	0	0	0	0	0	0.5	0	0	0	0.019608	0.098039	0.151261
55	0	0	0	0	0	0	0	0	0	0	0	0.125	0.033708	0.123596	0.137255
56	0	0	0	0	0	0	0	0	0	0	0.214286	0.071429	0	0.144737	0.116541
57	0	0	0	0	0	0	0	0	0	0	0	0.111111	0.046154	0.123077	0.179916
58	0	0	0	0	0	0	0	0	0	0	0	0.125	0.018519	0.203704	0.18593
59	0	0	0	0	0	0	0	0	0	0	0	0.4	0.069767	0.27907	0.323171
60	0	0	0	0	0	0	0	0	0	0	0	0	0	0.428571	0.330435

Table 9: Matrix M with $n = 2000$

Year	1→2	1→3	1→4	1→5	1→6	2→3	2→4	2→5	2→6	3→4	3→5	3→6	4→5	4→6	5→6
1	0	0	0	0	0	0	0	0	0	0	0	0	0	0	0
2	0.023	0	0	0	0	0	0	0	0	0	0	0	0	0	0
3	0.018858	0	0	0	0	0	0	0	0	0	0	0	0	0	0
4	0.027229	0	0	0	0	0	0	0	0	0	0	0	0	0	0
5	0.024698	0	0	0	0	0	0	0	0	0	0	0	0	0	0
6	0.027575	0	0	0	0	0	0	0	0	0	0	0	0	0	0
7	0.03125	0	0	0	0	0	0	0	0	0	0	0	0	0	0
8	0.029869	0	0	0	0	0	0	0	0	0	0	0	0	0	0
9	0.028325	0	0	0	0	0	0	0	0	0	0	0	0	0	0
10	0.031052	0	0	0	0	0	0	0	0	0	0	0	0	0	0
11	0.05036	0	0	0	0	0	0	0	0	0	0	0	0	0	0
12	0.073691	0	0	0	0	0	0	0	0	0	0	0	0	0	0
13	0.070632	0	0	0	0	0	0	0	0	0	0	0	0	0	0
14	0.08	0	0	0	0	0	0	0	0	0	0	0	0	0	0
15	0.091304	0	0	0	0	0	0	0	0	0	0	0	0	0	0
16	0.099522	0	0	0	0	0	0	0	0	0	0	0	0	0	0
17	0.09458	0	0	0	0	0	0	0	0	0	0	0	0	0	0
18	0.103286	0	0	0	0	0	0	0	0	0	0	0	0	0	0
19	0.117801	0	0	0	0	0	0	0	0	0	0	0	0	0	0
20	0.163205	0	0	0	0	0	0	0	0	0	0	0	0	0	0
21	0.095745	0	0	0.014184	0	0	0	0	0	0	0	0	0	0	0
22	0.1	0.056522	0.017391	0.019565	0	0.062777	0.017725	0.023634	0	0.050505	0.020202	0	0.058824	0	0
23	0.127027	0.037838	0.021622	0.010811	0	0.054893	0.025457	0.013524	0	0.029412	0.004902	0	0.011494	0	0
24	0.131313	0.107744	0.020202	0.010101	0	0.060017	0.026205	0.023669	0	0.024735	0.024735	0	0.007576	0	0
25	0.111111	0.083333	0.050926	0.023148	0	0.070513	0.020147	0.022894	0	0.02681	0.018767	0	0.017143	0	0
26	0.14557	0.082278	0.037975	0.044304	0	0.073887	0.033401	0.019231	0	0.028698	0.022075	0	0.02765	0	0
27	0.220183	0.036697	0.036697	0.036697	0	0.090395	0.040678	0.028249	0	0.038685	0.015474	0	0.015209	0	0
28	0.410959	0.041096	0.027397	0.041096	0	0.112565	0.041885	0.018325	0	0.043328	0.032929	0	0.028213	0	0
29	0.371429	0.142857	0.028571	0	0	0.08953	0.040971	0.019727	0	0.040128	0.024077	0	0.013477	0	0
30	0.6875	0.125	0	0	0	0.097391	0.043478	0.026087	0	0.044822	0.032457	0	0.028777	0	0
31	0	0	0	0	0	0	0	0	0	0	0.015244	0.009146	0	0.00655	0.007634
32	0	0	0	0	0	0	0	0	0	0	0.020472	0.011024	0	0.010352	0.018476
33	0	0	0	0	0	0	0	0	0	0	0.027961	0.009868	0	0.011788	0.002212
34	0	0	0	0	0	0.060423	0.036254	0.021148	0.009063	0.040422	0.036907	0.005272	0.02403	0.005545	0.012048
35	0	1	1	0	0	0.055363	0.051903	0.020761	0.00692	0.049815	0.035055	0.012915	0.025	0.008929	0.007505
36	0	0	0	0	0	0.052632	0.05668	0.05668	0.012146	0.057087	0.047244	0.005906	0.034247	0.013699	0.007042
37	0	0	0	0	0	0.057971	0.062802	0.019324	0.009662	0.064516	0.023656	0.012903	0.053512	0.010033	0.008078
38	0	0	0	0	0	0.056818	0.056818	0.034091	0.022727	0.037209	0.037209	0.009302	0.041391	0.011589	0.012121
39	0	0	0	0	0	0.06	0.086667	0.02	0	0.099256	0.057072	0.004963	0.028476	0.0067	0.015782
40	0	0	0	0	0	0.032258	0.080645	0.080645	0.008065	0.075145	0.049133	0.017341	0.033281	0.004754	0.010974
41	0	0	0	0	0	0	0	0	0	0	0.05	0.033333	0	0.026398	0.024707
42	0	0	0	0	0	0.101266	0.088608	0.050633	0.037975	0.062271	0.032967	0.03663	0.057471	0.036125	0.032298
43	0	0	0	0	0	0	0	0	0	0	0.069388	0.028571	0	0.04007	0.026538
44	0	0	0	0	0	0	0	0	0	0	0.061321	0.033019	0	0.020561	0.031653
45	0	0	0	0	0	0.051282	0.051282	0.102564	0	0.036842	0.063158	0.047368	0.07014	0.016032	0.035348
46	0	0	0	0	0	0.125	0.0625	0.1875	0.0625	0.042683	0.067073	0.042683	0.090129	0.045064	0.034637
47	0	0	0	0	0	0.157895	0.157895	0.105263	0	0.028369	0.099291	0.014184	0.079518	0.028916	0.046688
48	0	0	0	0	0	0	0	0	0	0	0.072581	0.024194	0	0.031915	0.038919
49	0	0	0	0	0	0.444444	0.111111	0.111111	0	0.066667	0.066667	0.057143	0.080357	0.050595	0.028785
50	0	0	0	0	0	0	0.75	0	0	0.066667	0.066667	0.033333	0.083893	0.033557	0.05074
51	0	0	0	0	0	0	0	0	0	0	0.026667	0.066667	0	0.076642	0.075594
52	0	0	0	0	0	0	0	0	0	0.014925	0.014925	0.104478	0.008032	0.076305	0.085747
53	0	0	0	0	0	0	1	0	0	0.017544	0.035088	0.070175	0.02193	0.078947	0.119647
54	0	0	0	0	0	0	1	0	1	0.041667	0.020833	0.125	0.02439	0.092683	0.108604
55	0	0	0	0	0	0	0	0	0	0.026316	0	0.131579	0.038251	0.103825	0.118936
56	0	0	0	0	0	0	0	0	0	0	0	0.09375	0.037736	0.194969	0.13181
57	0	0	0	0	0	0	0	0	0	0	0	0.16	0.024	0.168	0.193613
58	0	0	0	0	0	0	0	0	0	0	0	0.15	0	0.188119	0.240196
59	0	0	0	0	0	0	0	0	0	0	0	0.235294	0.02439	0.256098	0.274194
60	0	0	0	0	0	0	0	0	0	0.166667	0	0.25	0.033333	0.283333	0.352423